Platinum group metal coordination complexes of ferrocenyl N-donor ligands and their potential application in catalysis and medicinal chemistry

A thesis submitted to the

University of Cape Town

In fulfilment of the requirements for the degree of

Doctor of Philosophy

by

Jaisheila Rajput

BSc (Hons) (Cape Town)

MSc (Port Elizabeth)

Department of Chemistry

University of Cape Town

Rondebosch, 7701

South Africa

January 2003

Abstract

In this project a series of multinuclear complexes were successfully prepared and characterised using an array of analytical techniques. The use of nitrogen-donor ligands, in particular pyridine and ferrocenyl derivatives thereof was examined. Two main approaches were taken in the preparation of the ferrocenylpyridines:

i. The ferrocenylpyridines were systematically studied by varying the position of substituents along the pyridyl ring in the 4-, 3- and 2-positions.
ii. The effect of placing spacer groups between the ferrocenyl group and the pendant pyridine was examined.
iii. The ligands were prepared with a system of conjugated π bonds, allowing for an electronic pathway within the ligand.

Coordination studies of the substituted pyridines (L), were carried out with rhodium, iridium, platinum and palladium with the preparation of the following types of complexes:

- $[MCl(CO)_2(L)]$ and $[M(COD)(L_2)]ClO_4$ where M = Rh or Ir, COD = 1,5-cyclooctadiene.
- $[M'Cl_2(L)_2]$ where M' = Pt or Pd

These complexes were characterised using several analytical techniques such as NMR, IR and electronic spectroscopy. The electrochemical behaviour of the complexes was of particular interest and was examined using cyclic voltammetry. Additionally, the X-ray crystal structures of several rhodium complexes $[RhCl(CO)_2((C_5H_5)Fe(C_5H_4)C_6H_4N{=}Cpy)]$, [RhCl(COD)(3-Fcpy)] and $[RhCl(COD)(3\text{-}Fc(C_6H_4)py)]$, and a palladium complex, $[PdCl_2(3\text{-}Fcpy)_2]$, was determined.

The properties and some potential applications of these complexes was further demonstrated by preliminary investigations into their catalytic activity through several test reactions.

- The polymerisation of phenylacetylene was studied with rhodium complexes of the type [RhCl(COD)L] and $[Rh(COD)L_2]ClO_4$. A trend was observed between the structure of the catalyst and its activity. Polymers with improved yields, molecular weight and thermal stability were prepared.
- The carbonylation of nitrobenzene with palladium complexes, $[PdCl_2L_2]$ where L = 4-phenylpyridine and 2-, 3- and 4-ferrocenylpyridines. The derivatised pyridyl complexes exhibited greater selectivity and a higher activity relative to similar complexes reported.

- The hydrogenation of cyclohexene and 1-hexene with rhodium and iridium complexes, $[M(COD)L_2]ClO_4$, where L = pyridine, 4-ferrocenylpyridine and 4-ferrocenylphenyl-4'-pyridine.

A preliminary cytotoxic screening of several complexes was also carried out based on the reported anticancer activity of platinum group metal complexes.

Presentations and Publications

Publications

- The synthesis and catalytic properties of rhodium and iridium complexes containing ferrocenyl nitrogen donor ligands, Alan T. Hutton, Christopher Imrie, John R. Moss and Jaisheila Rajput, *Organometallics* (in submission), 2003
- The preparation and anti-cancer properties of complexes formed between the platinum group metals and ferrocenyl nitrogen donor ligands, Christopher Imrie, Jaisheila Rajput, Alan T. Hutton and John R. Moss, *J. Organomet. Chem.*, (in submission), 2003

Conference proceedings

- Preparation and properties of conjugated ferrocene-containing ligand systems, Jaisheila Rajput, Christopher Imrie, John R. Moss and Alan T. Hutton, *34th International Conference on Coordination Chemistry* (ICCC34), University of Edinburgh, Edinburgh, Scotland, July 2000
- Preparation and properties of conjugated ferrocene-containing ligand systems, Jaisheila Rajput, Christopher Imrie, John R. Moss and Alan T. Hutton, *Conference on Catalysis and Inorganic Chemistry*, Bakgatla Resort Pilansberg Game Reserve, South Africa, November 2001
- Preparation and properties of multimetallic complexes, Jaisheila Rajput, John R. Moss, Christopher Imrie and Alan T. Hutton, *36th Convention of the South African Chemical Institute* (SACI), Port Elizabeth, South Africa, July 2002
- The synthesis and properties of a novel series of complexes formed between ferrocenyl nitrogen donor ligands and the platinum group metals, Christopher Imrie, Jaisheila Rajput, Alan T. Hutton and John R. Moss, *XVth FECHEM Conference on Organometallic Chemistry*, University of Zurich, August 2003

Glossary of numbered compounds

[1.1] 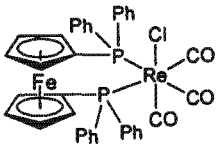

[1.2] 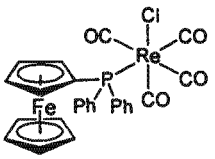

[1.3] 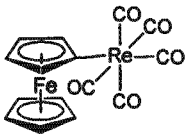

[1.4] 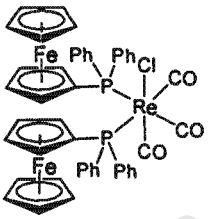

[1.5] 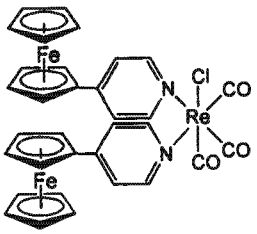

[1.6] 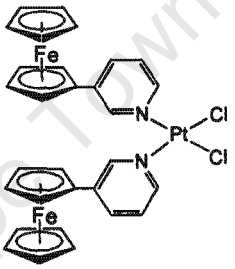

[1.7] 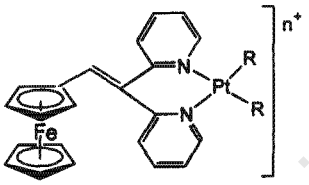

a: R = Cl⁻, n = 0
b: R = py, n = 2

[1.8] 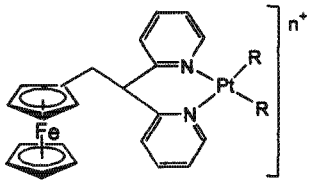

a: R = Cl⁻, n = 0
b: R = py, n = 2

[1.9] 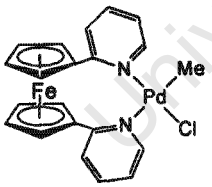

[1.10] 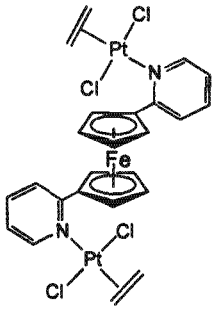

[1.11] 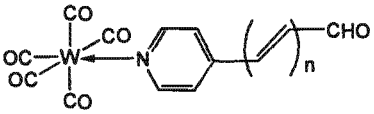

a: n = 0
b: n = 1
c: n = 2

[1.12] 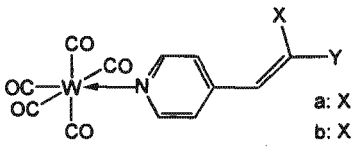

a: X = Y = COOMe
b: X = CN, Y = COOMe
c: X = Y = CN

[2.1] 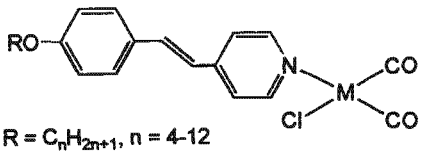

$R = C_nH_{2n+1}$, n = 4-12

M = Rh, Ir

[2.2] 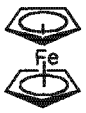

[2.3] 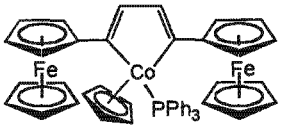

[2.4] 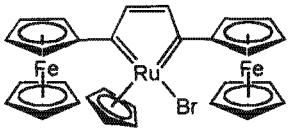

[2.5] 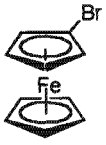

[2.6] 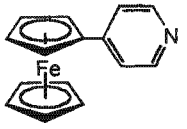

[2.7] 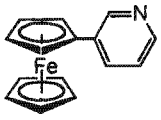

[2.8] 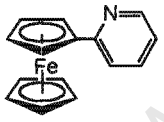

[2.9] 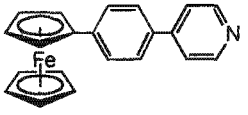

[2.10] 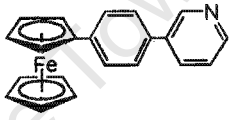

[2.11] 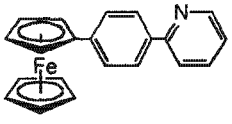

[2.12] 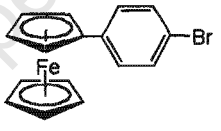

[2.13] 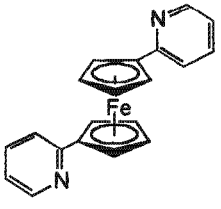

[2.14] 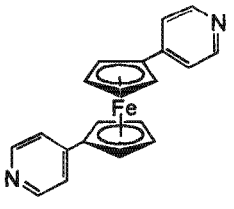

[2.15] 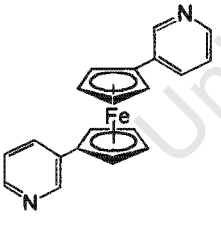

[2.16] 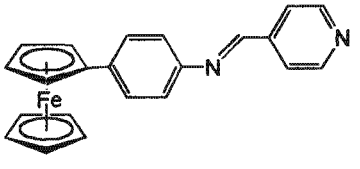

[2.17] 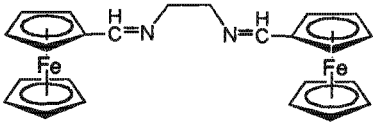

[2.18] 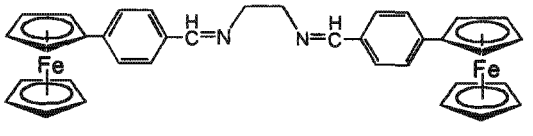

[2.19] 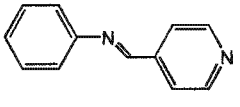

[2.20] 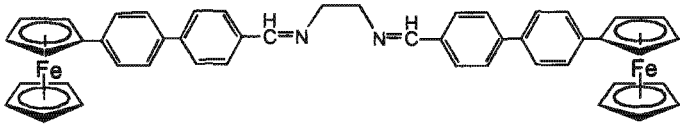

[2.21] 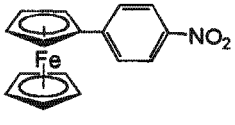

[2.22] 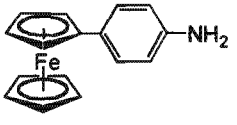

[2.23] 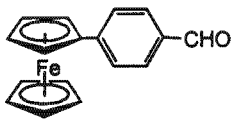

[2.24] 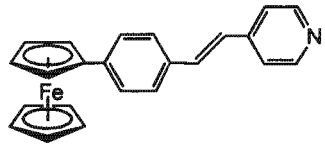

[2.25] 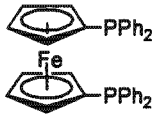

[2.26] 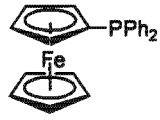

[2.27] 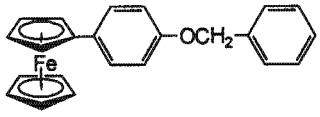

[3.1] 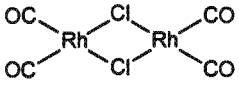

[3.2]-[3.6] 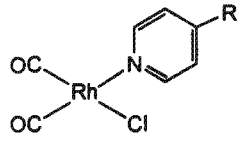

[3.2]: R = H
[3.3]: R = NH_2
[3.4]: R = Fc
[3.5]: R = (C=N)-Ph
[3.6]: R = (C=N)(C_6H_4)Fc

[3.7] 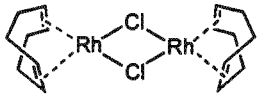

[3.8]-[3.11] 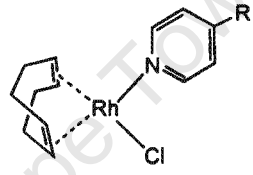

[3.8]: R = H
[3.9]: R = Ph
[3.10]: R = (C=N)-Ph
[3.11]: R = (C=C)(C_6H_4)-OC_8H_{17}

[3.12]-[3.14] 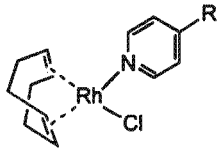

[3.12]: R = Fc
[3.13]: R = (C_6H_4)Fc
[3.14]: R = (C=N)(C_6H_4)Fc

[3.15]-[3.16] 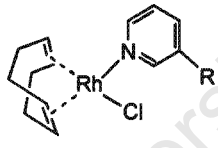

[3.15]: R = Fc
[3.16]: R = (C_6H_4)Fc

[3.17]-[3.18] 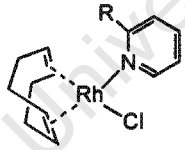

[3.17]: R = Fc
[3.18]: R = (C_6H_4)Fc

[3.19] 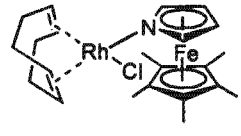

[3.20] 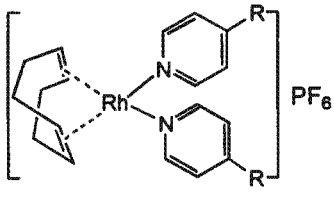

[3.21]-[3.26] 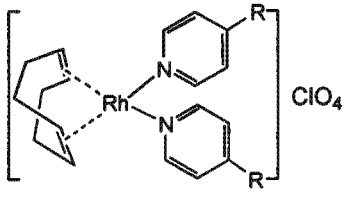

[3.21]: R = H
[3.22]: R = Ph
[3.23]: R = (C=N)-Ph
[3.24]: R = Fc
[3.25]: R = (C_6H_4)Fc
[3.26]: R = (C=N)(C_6H_4)Fc

[3.27] 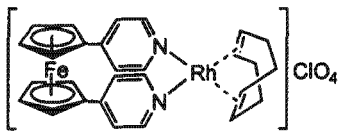

[3.28] 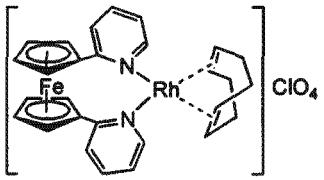

[3.29] 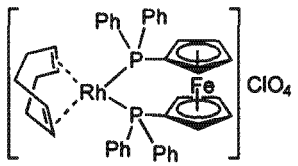

[3.30] 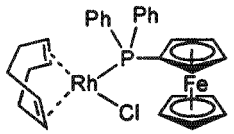

[3.31] 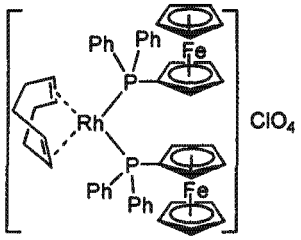

[3.32] 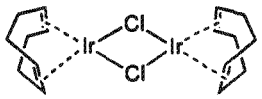

[3.33]-[3.36] 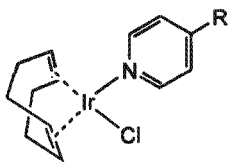

[3.33]: R = H
[3.34]: R = Ph
[3.35]: R = (C=N)-Ph
[3.36]: R = Fc

[3.37] 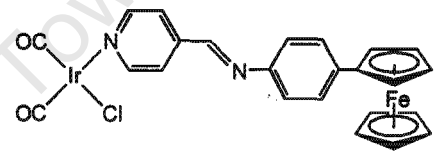

[3.38]-[3.39] 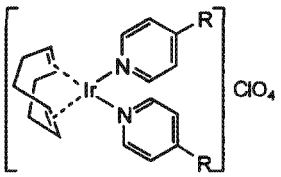

[3.38]: R = H
[3.39]: R = Fc

[3.40]-[3.43] 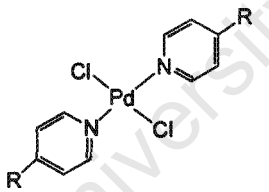

[3.40]: R = H
[3.41]: R = Ph
[3.42]: R = Fc
[3.43]: R = $(C_6H_4)Fc$

[3.44] 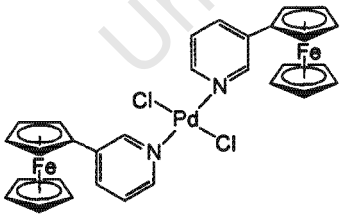

[3.45] 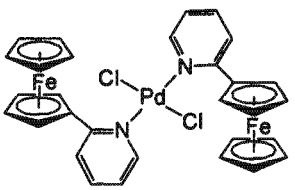

[3.46]-[3.50] 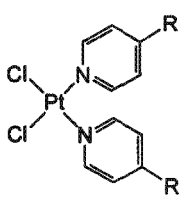

[3.46]: R = H
[3.47]: R = Ph
[3.48]: R = (C=N)-Ph
[3.49]: R = Fc
[3.50]: R = $(C_6H_4)Fc$

[3.51] 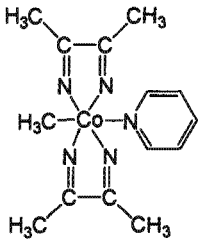

[3.52] 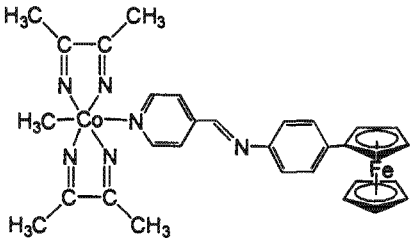

Contents

Chapter 3: Preparation of Multinuclear Complexes

Chapter 4: Some Catalytic Applications of Multimetallic Complexes

Abbreviations

Å	Angstrom
Cp	cyclopentadienyl, C_5H_5
COD	1,5-cyclooctadiene
°	degree
DSC	differential scanning calorimetry
DMSO	dimethyl sulfoxide
ε	Extinction coefficient
EI	electron impact
FAB	fast atom bombardment
Fc	$(C_5H_4)Fe(C_5H_5)$
Fcpy	ferrocenylpyridine
J	coupling constant
Lit.	literature
M	parent molecular ion
MeCN	acetonitrile
MeOH	methanol
mp	melting point
NMR	Nuclear magnetic resonance
Ph	Phenyl
ppm	parts per million
py	pyridyl
TBAP	tetrabutylammonium perchlorate
TGA	thermogravimetric analysis
THF	tetrahydrofuran

Chapter 1: Introduction

Historically, the synthesis and study of transition metal complexes has featured prominently in chemistry, in particular through applications in the fields of catalysis, materials chemistry and even medicinal chemistry. One of the first stable transition metal complexes, Zeise's salt $K[PtCl_3(C_2H_4)]$, was prepared as early as 1827 by a Danish pharmacist, Zeise. It took, however, at least 125 years to understand the true nature of the chemical bonding of ethene to platinum in the complex.[1]

The development of complexes containing transition metals for use in catalysis is closely linked to three major industrial processes developed between 1930 to 1950[2]; the carbonylation of alkenes and alkynes using iron catalysts in the Fischer-Tropsch process[3], preparation of ethene and propene polymers with Ziegler-Natta catalysts[4] and the production of acetaldehyde from ethene by the Wacker process using palladium and copper catalysts.[5]

The hydroformylation or oxo process was also developed during this time. Currently, the hydroformylation of alkenes is the largest industrial-scale reaction that is catalysed homogeneously.[6] Roelen discovered the reaction in 1938 and prepared propionaldehyde from ethene and synthesis gas by means of a cobalt catalyst (see *Equation 1.1*).[6]

$$H_2C{=}CH_2 + CO + H_2 \xrightarrow[\substack{90\text{-}150\ ^\circ C \\ 100\text{-}400\ bar}]{Co_2(CO)_8} CH_3CH_2\overset{\overset{O}{\|}}{C}H \qquad \textbf{Equation 1.1}$$

C_3–C_{15} aldehydes are produced by hydroformylation and converted to amines, carboxylic acids and primary alcohols using mainly cobalt and rhodium catalysts.[6] One of the current objectives in this reaction is to produce linear products selectively. The use of rhodium catalysts with bulky phosphane ligands has been reported to increase the ratio of linear to branched products relative to the cobalt catalysts.[6]

The activity of rhodium catalysts for a variety of reactions is well-known. Wilkinson first prepared $RhCl(PPh_3)_3$ in 1965 when its activity was first noted as an efficient homogeneous catalyst for the hydrogenation of alkenes.

A number of areas of chemistry have evolved from the discovery of certain key complexes. The first carbene complex, $W(CO)_5\{C(Me)OMe\}$ was discovered in 1964 and the first carbyne

complex, $Cr(CO)_4(CR)I$ in 1973.[7] Carbene complexes are intermediates in olefin metathesis and have even been used in a model reaction for the degradation of chlorohydrocarbons in the liver.[6] Olefin metathesis can be used for the catalytic conversion of propene to ethene and 1-butene for the preparation of C_5 aldehyde *via* the hydroformylation reaction. Several types of transition metal catalysts are available for olefin metathesis.[6] These include *Black Box* heterogeneous catalysts with high valent transition metal halides, oxides or oxo-halides with an alkylating zinc or aluminium cocatalyst on an aluminium or silicon support, titanocene-based catalysts, Shrock catalysts with tungsten, molybdenum and rhenium[8] and Grubbs ruthenium catalysts[9] (see *Figure 1.1* for examples of Shrock and Grubbs' catalysts).

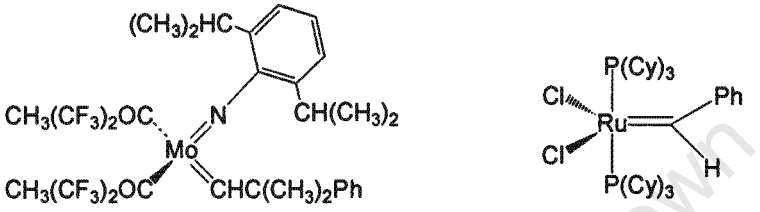

Schrock's catalyst **Grubbs catalyst**

Figure 1.1: Examples of olefin metathesis catalysts[8,9]

Similarly, the discovery of the first sandwich complex, ferrocene,[10] in 1951 led to the preparation of numerous other metallocenes.[11] Ferrocenyl derivatives have found application in several areas of chemistry.[6,12] Monosubstituted and 1,1'-disubstituted ferrocenes are the most frequently studied type of ferrocenyl compounds. The ferrocenyl group has been incorporated into a range of conjugated systems and is able to be coordinated to other metals, due mainly to its unique chemistry. The study of ferrocene and determination of its relative stability led to investigations into compounds with larger ring stack arrays. The first triple-decker sandwich complex, $[Ni(C_5H_5)_3]^+$ was prepared by Werner in 1972.[6]

More recently, the study of transition metals in catalysis and combinatorial chemistry has taken a shift in the development of green chemistry. There is a general move in chemistry in recent times towards clean and sustainable technology that eliminates waste and avoids the use of toxic reagents and solvents in the manufacture and utilisation of chemical products. Rhodium complexes of ferrocenylphosphines, for example, have been useful in this regard as hydrogenation catalysts immobilised on alumina or silica.[13] The catalyst is very active, selective toward a range of substrates and stable to leaching.

Many important transition metal complexes contain phosphine donor ligands. This thesis, however, looks at the role of nitrogen donor ligands and their influence on the development of transition metal chemistry.

1.1 Nitrogen donor coordination complexes

Nitrogen-donor ligands have played a notable role in the development of coordination chemistry. Ligands with sp^2-hybridised nitrogen atoms, such as pyridine, have a significant coordination chemistry.[14] Pyridine could easily be regarded as one of the best-known heterocyclic nitrogen donor ligands. Pyridine is a particularly good ligand as it contains a nitrogen donor ring atom with a localised pair of electrons available for binding.

When considering the uses of these ligands, it is worth noting the differences in coordination behaviour between the nitrogen donor ligands and the well-studied phosphorus ligands as well as the properties of the nitrogen donor ligands.[14]

(i) The nitrogen atoms in donor ligands are known to bond strongly to metal centres where the strength of the bond is dependant on their σ covalency.

(ii) Nitrogen donor ligands generally show only a limited π back-bonding ability, making these ligands unsuitable for the stabilization of low oxidation state transition metals. However, sp^2 hybridised nitrogen donors such as pyridine, have been known to show some π interactions and π back-bonding effects between the nitrogen heterocycle and the metal centre.[15,16]

(iii) These ligands exert a very small *trans* effect in comparison to other ligands used in organometallic chemistry, resulting in a fast rate for substitution reactions.

(iv) The observed reactivity of nitrogen donors is generally high, particularly with alkyl complexes of transition metals containing these ligands.

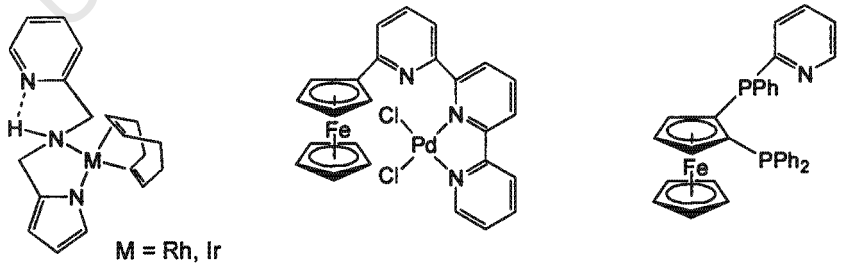

Figure 1.2: Examples of nitrogen donor ligands complexed to palladium, rhodium and iridium[18,17]

In contrast to the widespread use of phosphine donor coordination complexes in catalysis, nitrogen donor complexes are not as well studied. Recently, however, there has been a shift

towards the preparation of mixed ligand systems incorporating nitrogen donor atoms into these systems as well as the preparation of novel nitrogen donor ligand systems for a variety of applications (see for example *Figure 1.2*).[14,18] P,N chelating ligands have been observed to show similar reactivity to complexes containing P,P chelating ligands.

The chemistry of vitamin B_{12}, its coenzyme and the cobalamines are interesting examples of nitrogen donor complexes. The chemistry of vitamin B_{12} has been studied extensively,[19] particularly through simple cobaloxime model compounds (see *Figure 1.3*). The study of these cobaloxime complexes has further application in the catalysis of organic systems.[14,20] Of particular significance is the mode of cleavage of the Co-R bonds in these types of complexes as well as the oxidation state of the cobalt atom with reference to the study of electron transfer processes.[21]

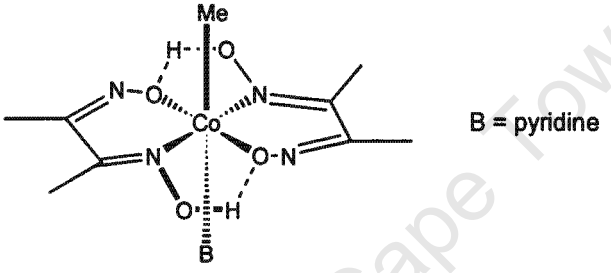

Figure 1.3: Cobaloxime, a model for the vitamin B_{12} system where B is, for example, pyridine

The use of nitrogen donor ligands has featured more significantly in materials chemistry. With an increasing demand for new materials with novel properties, there has been a move in polymer research towards the preparation of materials with a highly controlled architecture.[22] The emphasis in the study of dendrimers or starburst polymers, has been the development of new materials with novel properties that are fundamentally different from the linear polymers. There has been a steadily growing interest in the preparation of dendrimers containing transition metals. The metal centres may be incorporated either at the core, throughout the structure, or at the periphery (see *Figures 1.4* and *1.5*).[23,24,25] The incorporation of nitrogen donor ligands such as pyridyl and bipyridyl groups is advantageous as these groups can be readily derivatised, leading to the development of a supramolecular architecture.

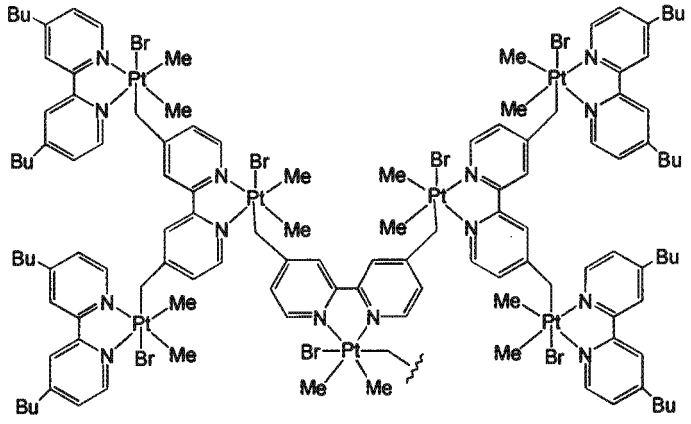

Figure 1.4: Platinum bipyridyl dendrimer[24]

The majority of iron dendrimers reported have involved the inclusion of ferrocenyl groups. The incorporation of redox-active ferrocenyl groups into the dendritic architecture has been studied mainly with the aim of establishing electronic communication between the metal sites.[26] These polymers may be useful as biosensors and as catalysts for the modification of electrodes.[27] *Figure 1.5* shows the first heterometallic dendrimer with different transition metals in different layers.[25]

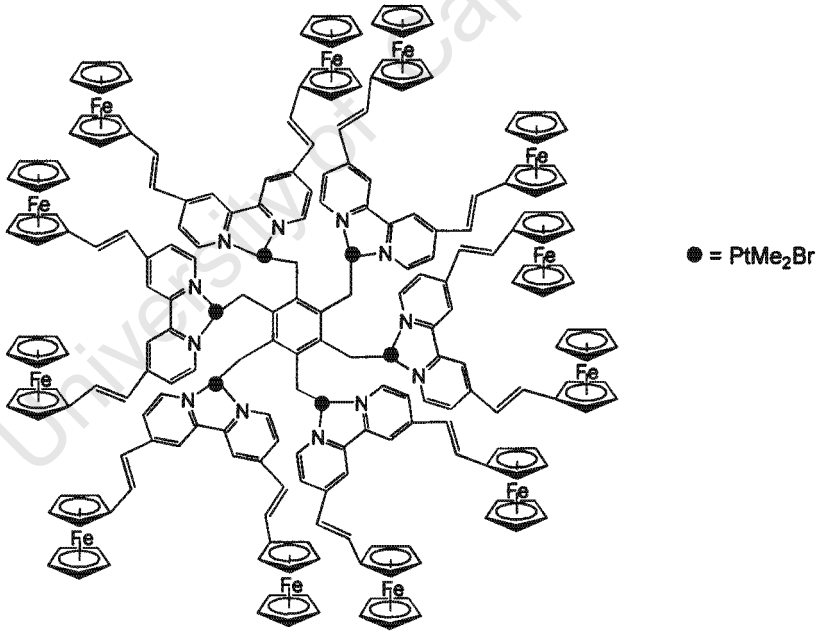

Figure 1.5: Heterometallic dendrimer with platinum and ferrocenyl centres[25]

1.2 Ferrocenyl-containing nitrogen donor coordination complexes

Recently, the study of novel multiple metal-containing complexes has reached prominence with the metals connected through a system of conjugated pathways, sometimes in the form

of polymers. It is anticipated that these complexes will have additional properties that are significantly different from similar organic compounds. The types of anticipated properties include electrical conductivity, magnetic behaviour,[28] enhanced thermal stability, non-linear optical effects[67] and superconductivity.

The preparation of polypyridyl transition metal complexes with electronically coupled photo- or redox-active sensors is currently of interest for a number of potential applications. Comparatively simple ruthenium, osmium and rhenium complexes of 2,2'-bipyridine,[29] for example, exhibit properties related to redox electrocatalysis and solar energy conversion.[30] Although oligopyridyl complexes with redox-active centres are known, until recently, there were few examples reported in which these centres were covalently coupled.[31] The existence of covalent pathways is of interest as electron transfer processes are usually facilitated by the presence of these through-bond pathways.[31] Oligopyridyl ligands are beneficial for the development of metallosupramolecular chemistry and have provided new avenues in the search for new topological molecular systems.[32]

Figure 1.6 shows examples of polynuclear redox-active ferrocenyloligopyridyl complexes. These supramolecular complexes may be assembled either as a single chelating ligand or through coordination of several nitrogen donor ligands.[31,33]

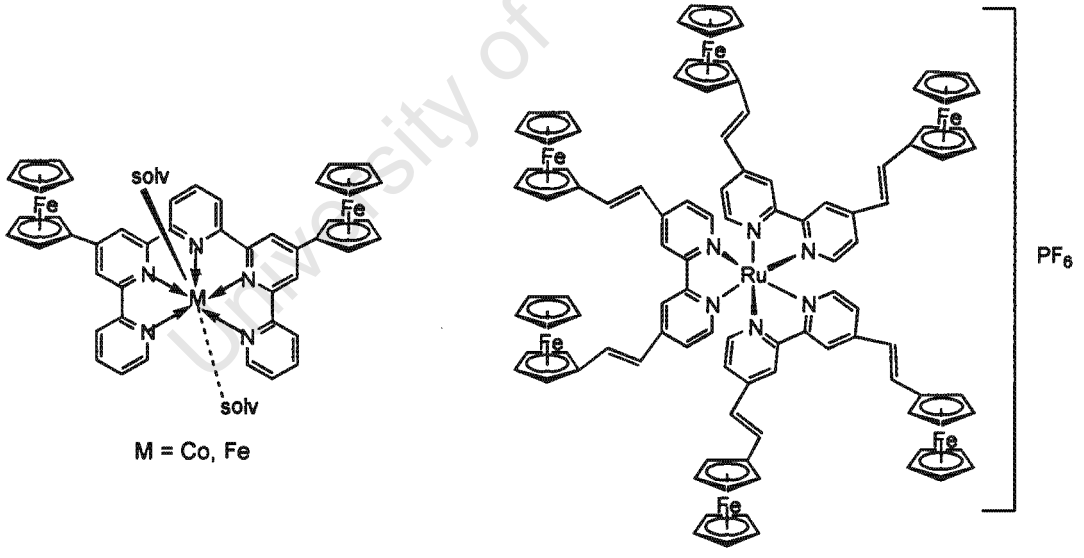

Figure 1.6: Ferrocenyloligopyridyl transition metal coordination complexes[31,33]

The use of ferrocenyl nitrogen donor ligands is further observed in the preparation of ferrocenylimines. The study of ferrocenylimine complexes follows a similar trend to the ferrocenyloligopyridyl complexes where electronic interactions between the metal centres are

of interest.[34] The ligands are often prepared as unsaturated oligomers or polymers. However, one of the disadvantages of aromatic polyimines is their relative insolubility in a range of common organic solvents.

The preparation of 4-ferrocenylpyridine, as well as the 3- and 2-substituted analogues, was reported several years ago.[35,36] However, only a limited number of coordination studies have been carried out with these ligands. The most notable of these described a novel synthetic route for the preparation of 4-ferrocenylpyridine using a nickel-catalysed Grignard reaction. The ferrocenyl ligand was coordinated to a rhenium metal centre, complex **[1.5]**. The complex was further compared to a series of rhenium-ferrocenyl and ferrocenylphosphine coordination complexes, **[1.1]-[1.4]**. Of primary interest in this work was the preparation of a series of organometallic complexes with pendant redox-active ligands (see *Figure 1.7*). The complexes were investigated to determine whether changes in the oxidation state of the ligand would result in changes in the spectroscopic properties and reactivity of the rhenium metal centre, essentially without changing the coordination sphere of the rhenium metal. Rhenium complexes were specifically chosen as rhenium-centred oxidations are generally difficult and these complexes are usually substitutionally inert. Spectroscopic changes were used to monitor redox changes in the ferrocenyl ligand.

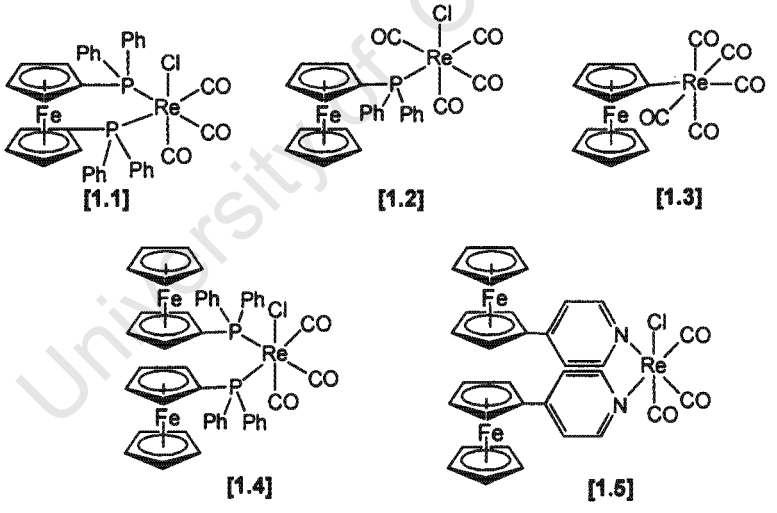

Figure 1.7: Ferrocenyl-rhenium coordination complexes[35]

A series of shifts to higher energy was observed in the infrared carbonyl stretching frequency upon oxidation of the rhenium complexes. This corresponded to a lowered electron density at the rhenium metal centre. The extent of shift was found to be dependant on the number of bonds separating the rhenium metal centre and the ferrocenyl group. It was concluded that

the electron density at a metal centre could be predetermined and adjusted upon oxidation of the ligand redox centre.[35]

The preparation of a platinum complex of 3-ferrocenylpyridine together with the electrochemistry of the complex **[1.6]** was later described (see *Figure 1.8*).[37] A platinum(II) metal centre was chosen as nitrogen-donor complexes of the metal are known to be both thermodynamically and kinetically stable. It is interesting to note that, as with the complexes in *Figure 1.7*, both the ligand and the coordination complex exhibited redox activity.

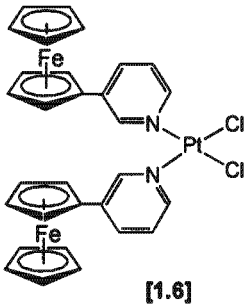

[1.6]

Figure 1.8: Platinum-ferrocenylpyridine complex[37]

Of particular interest was the specific role of platinum as a linker between the ferrocenyl ligands. A single redox wave was observed for complex **[1.6]**, corresponding to a two-electron oxidation at the platinum electrode rather than two separate consecutive one-electron oxidations, indicating little or no communication between the respective ferrocenyl groups. It would appear that the platinum metal centre inhibited electronic communication between the ligands in complex **[1.6]**. Another factor worth considering is the role played by the pyridyl ligand toward effective electronic communication. It was unclear as to which factor in particular contributed to the observed redox behaviour. The complex was simply viewed as a reducing agent able to release two electrons at a time.

Considering the specific contribution various donor atoms make to electronic communication, it is worth taking a second look at the complexes in *Figure 1.7*.[35] The phosphine-donor complex **[1.4]** showed a two-electron oxidation process in the form of two separate one-electron oxidations separated by 100 mV. This indicated significant coupling between the ferrocenyl fragments. It would appear that the rhenium metal centre did not oppose electrochemical communication. However, a single two-electron oxidation was observed for complex **[1.5]**. The specific factor contributing to this observed effect was unclear. A further area for study would be examination of the specific role the pyridyl rings in electrochemical communication.

The complexes described above for the most part contain systems in which the metals are connected through conjugated pathways. This provides an avenue for through-bond electronic communication. This type of communication is expected to predominate in linear conjugated systems but may be diluted in complexes containing relatively long conjugated spacers between the metal centres.[38] Furthermore, electronic communication through space may occur provided the metal centres are within very close proximity to allow this. The significance of a conjugated system has been illustrated in complexes **[1.7]** and **[1.8]** (see *Figure 1.9*).[39]

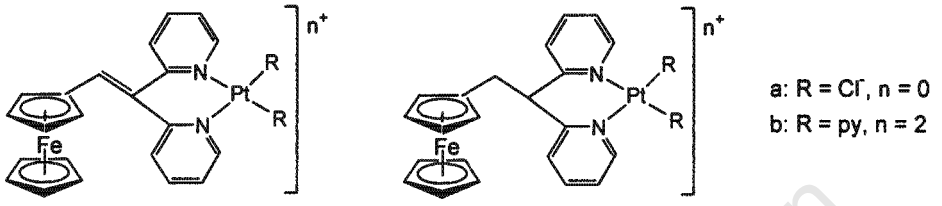

[1.7a], [1.7b] **[1.8a], [1.8b]**

Figure 1.9: Platinum dipyridyl-ferrocene complexes used to illustrate the role of conjugated ligand systems on electrochemical communication[39]

Investigation of the redox behaviour of complexes **[1.7]** and **[1.8]** revealed that the nature of the spacer between the redox active site and the dipyridyl metal-binding sites strongly influenced both the redox and spectroscopic properties of these complexes. The redox behaviour of the ferrocenyl ligands of complexes **[1.7]** and **[1.8]** were fairly similar but differed significantly upon complexation to the platinum metal centre. Comparison of oxidation shifts showed a dramatic difference between the free ligand and coordinated complex, with a shift of at least +150 mV in the case of the conjugated system of complex **[1.7]**, compared to +30 mV in the unconjugated system of complex **[1.8]**. This difference in redox behaviour can be attributed to the conjugated system allowing through-bond communication between the metals. Hence, the electron-withdrawing nature of the bound platinum metal centre makes the ferrocene group harder to oxidise, accounting for the larger oxidation shift.

1.3 Application of transition metals in catalysis

The use of transition metal complexes in both heterogeneous and homogeneous catalysis is commonplace. Although the majority of catalytic synthetic processes occur by means of heterogeneous catalysis in industry, homogeneous catalysis is favoured academically. One of the chief advantages of homogeneous catalysis is the ability to monitor the reaction progress through examination of catalytically active species and catalytic sites. This provides an insight

into the catalytic synthetic process, often leading to the ability to improve reaction conditions, yields and selectivity. A comparison between these types of catalysis is made in *Table 1.1*.

Table 1.1: Comparison of the properties of homogeneous versus heterogeneous catalysts

Homogeneous catalysts	Heterogeneous catalysts
Difficult separation	Easy separation
High selectivity	Low selectivity
Low thermal stability	High thermal stability
High activity	Lower activity
Well-defined catalyst	Poorly defined catalyst
No diffusion limitation	Limited by diffusion processes

The homogeneous and heterogeneous catalytic application of rhodium complexes, for example, is widespread (see for example *Figure 1.10*). The literature abounds with applications of highly active complexes containing this metal centre.[6,40] Wilkinson's catalyst, $[RhCl(PPh_3)_3]$, is the best known of these with simple hydrogenation reactions taking place at ambient temperature and atmospheric pressure. Modifications of this catalyst include $[Rh(CO)H(PPh_3)_3]$, which is the active catalyst formed under hydroformylation conditions.[41] Hydroformylation is an industrially relevant and significant process that is responsible for the preparation of several million tons of aldehydes and alcohols annually.[6] This complex is one of the most active homogeneous hydroformylation catalysts and is used in industrial processes.

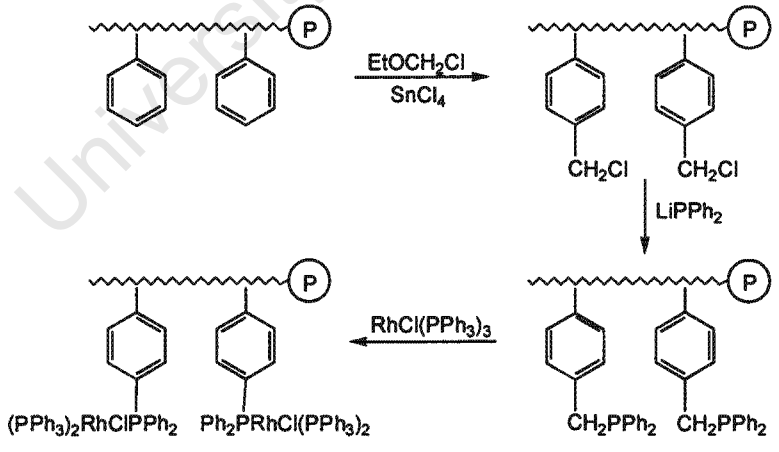

Figure 1.10: Example of Wilkinson's catalyst on a polymeric support[6]

Other interesting rhodium complexes are of the type $[Rh(\beta\text{-diketonate})L_2]$ (where β-diketonate = acetylacetonate, trifluoroacetylacetonate or hexafluoroacetylacetonate and L = alkene,

phosphine or phosphite). These rhodium complexes serve as catalyst precursors for a range of reactions such as alkene hydroboration and diboration, carbon dioxide hydrogenation, hydroformylation and addition of arylboronic acids to aldehydes.[42]

The catalytic study of iridium complexes has similarly been investigated, most notably as homogeneous hydrogenation catalysts. Iridium is usually considered the least catalytically active of the platinum group metals. In the highly coordinatively unsaturated form, however, certain iridium complexes such as the catalyst precursor, Crabtree's catalyst $[Ir(COD)L(py)]PF_6$ (where COD = 1,5-cyclooctadiene, L = phosphine and py = pyridine) may behave as highly active hydrogenation catalysts even for sterically hindered alkenes (see for example *Figure 1.11*).[43] In the development of this catalyst, the presence of the coordinated phosphine-donor ligand was a disadvantage, as the ligand did not readily dissociate to allow coordination of the alkene substrate. Modification of the iridium catalyst led to the introduction of cyclooctadiene (see *Figure 1.11*).[44] The labile ligand readily dissociated for coordination of the alkene.

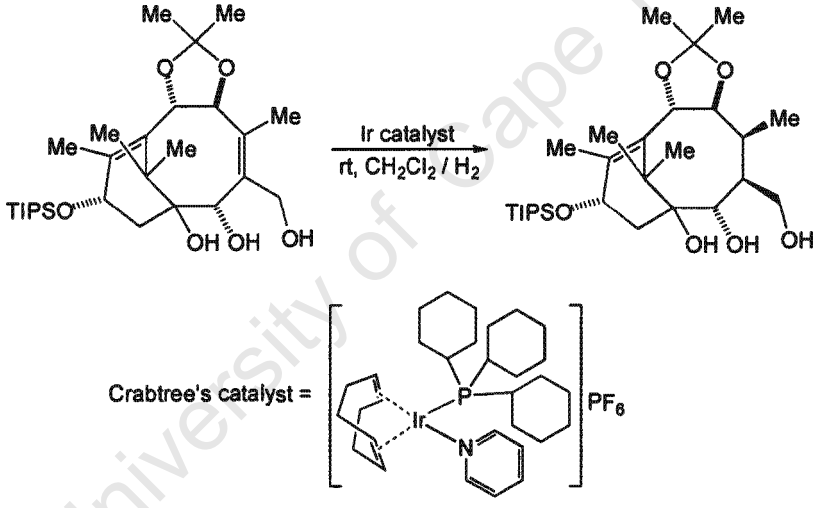

Figure 1.11: Iridium hydrogenation catalyst and an example of a hydrogenation reaction with this catalyst[43,44,45]

A further consideration is the solvent of reaction. The solvent may bind tightly to the metal centre, leading to hindered coordination of the olefin. This was overcome through the use of weakly- or non-coordinating solvents.[44] Catalyst development has reached the stage where these complexes have been used as catalyst precursors for the hydrogenation of imines,[46] a range of steroids[43] and as transfer hydrogenation catalysts from 2-propanol to a range of unsaturated substrates.[47]

Aside from the importance of the metal centre in the observed catalytic activity of various transition metal complexes, the coordinated ligands warrant some consideration. Ferrocenyl phosphine donor ligands, for example, are well-known, with numerous reports of coordination complexes.[12] 1,1'-Bis(diphenylphosphino)ferrocene (abbreviated as dppf), prepared in 1965, was the first example of a ferrocenyl-based phosphine ligand (see *Figure 1.12*).[48] Ferrocenyl phosphine ligands have shown increased popularity since the 1980s with various academic and industrial catalytic applications currently cited, where the activity of the complexes has been associated with the bite size and angle of the ligand.[49]

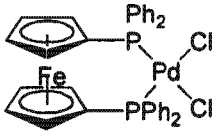

***Figure 1.12*:** Palladium coordination complex of 1,1'-bis(diphenylphosphino)ferrocene[50]

The Kumada-Hayashi coupling reaction, for example,[50] successfully uses $PdCl_2$(dppf) in the formation of a nearly quantitative yield of the desired carbon-carbon coupled product, with good selectivity.[50] The activity of this complex by far exceeds the activity of monodentate as well as some bidentate phosphine-based catalysts. Further examples of reactions where the use of complexes of these ligands results in increased activity, include the Suzuki coupling reaction,[51] the Heck coupling reaction[52] and the Stille coupling reaction[53] with palladium, rhodium and nickel complexes of dppf.

Since the discovery of dppf, a variety of other ferrocenylphosphine complexes have been prepared as well as ferrocenes with both phosphine and nitrogen donor groups. There are several synthetic routes to the preparation of these non-racemic ferrocenyls, a number of which have applications in asymmetric synthesis.[54]

The redox behaviour of ferrocenyl complexes of molybdenum, tungsten, palladium and platinum metal centres has also been studied using cyclic voltammetry.[55] No significant changes were observed between ligand and complex in the case of the molybdenum and tungsten complexes while anodic shifts in the redox wave were observed for the other metals.[56] The study of the electrochemical behaviour of dppf has led to attempts to increase the stability of the ferrocenium monocation, which is known to form during the electrochemical process.[56] Isolation of the various complexes formed during the electrochemical process would lead to a better understanding of this process and potentially allow for electrochemical systems to be tuned for specific needs. The investigation was carried out by examining the electrochemical behaviour of a range of 1,1'-bis(diphenylphosphino)ferrocenes bearing

substituents with a range of electronic properties. Results indicated that substituents with higher electron donating ability lead to the formation of the corresponding ferrocenium monocations with a longer lifetime. Despite this, a stable ferrocenium cation could not be isolated for separate examination.[56]

Quite often the coordination chemistry of transition metal complexes is considered prior to examination of the role of the complex as a potential catalyst. A series of related ligands may be prepared followed by determination of their coordination chemistry with several metal ions. An example is the disubstituted ferrocenyl ligand, 1,1'-bis(2-pyridyl)ferrocene, which although known for some years,[57] has had few coordination complexes reported. Earlier work described the preparation of rhodium and silver complexes of this ligand but studies were limited simply to the preparation of these complexes and a crystal structure of the silver complex.[58]

Since then, platinum and palladium complexes of this ligand (see *Figure 1.13*) have been prepared and their reactivity studied with regard to carbonyl insertion reactions.[59] This reaction forms an important part in the copolymerisation of alkenes and carbon monoxide.[59] The bidentate ligand has been reported to increase the rate of carbonyl insertion reactions. Structural factors, such as its conformational flexibility, as well as the tendency to coordinate with a large bite angle were considered in investigations of the reactivity of complexes of this ligand.[59]

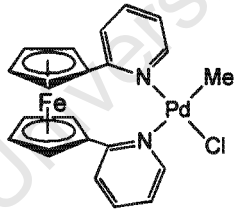

[1.9]

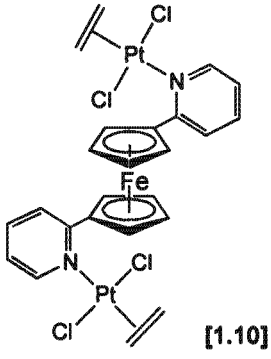

[1.10]

***Figure 1.13*:** Palladium and platinum complexes of 1,1'-bis(2-pyridyl)ferrocene[59]

It is known that complexation of the late transition metals with phosphorus ligands results in the formation of robust complexes. Due to the harder Lewis nature of nitrogen ligands, the analogous complexes were not expected to be as stable. Results however, indicated that the insertion of carbon monoxide into the palladium–methyl bond of complex **[1.9]** occurred rapidly, compared to phosphine-donor ligands. Results have been reported for both flexible

bidentate nitrogen ligands, as well as rigid bidentate nitrogen ligands with small bite angles. The 1,1'-bis(2-pyridyl)ferrocene ligand is flexible and has been known to coordinate with a large bite angle, evidenced by the silver complex of this ligand, $[Ag(L)ClO_4]_2$ (where L = 1,1'-bis(2-pyridyl)ferrocene).[58] Despite the increased carbon monoxide insertion rate due to the presence of the ligand, the group was only weakly bound to the metal centre, preventing detailed kinetic studies of the reaction.[59]

Modifications to systems of this type through changes in the donor atom allows for systematic study of this type of complex and may provide a deeper insight into the mode of reactivity of these and similar complexes.

1.4 Medicinal chemistry

Biomedical inorganic chemistry is a rapidly expanding area of chemistry. A number of the compounds investigated in this field have potential applications in medicine and by extension, offer real possibilities for the pharmaceutical industry, where traditionally organic chemistry has dominated. Some of the key areas of medicinal inorganic chemistry are highlighted in *Figure 1.14*.[60]

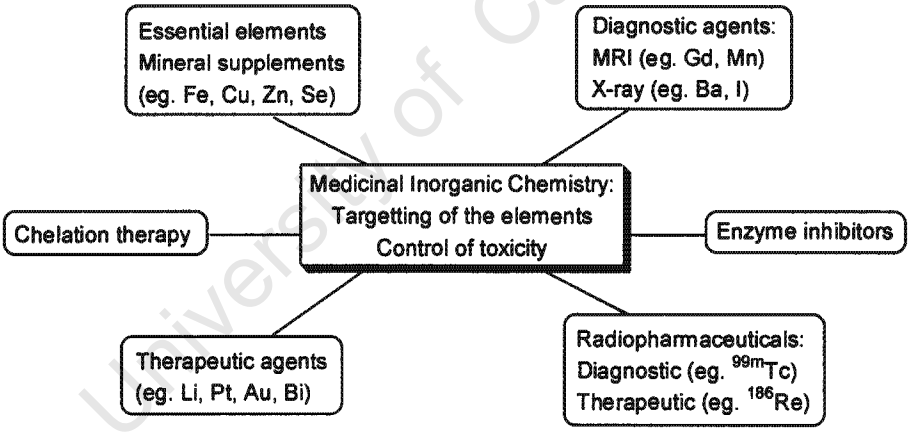

Figure 1.14: Some of the key areas of medicinal inorganic chemistry[60]

The use of transition metals in medicinal chemistry has rapidly developed with the discovery of the antitumour properties of cisplatin.[61] It is interesting to note that despite the range of transition metal complexes prepared and studied for their antitumour activity, only very few have proceeded to clinical phase trials.[62] Due to the observed antitumour activity of cisplatin, numerous platinum complexes with similar geometry have been prepared. Several metallocenes, including ferrocene and titanocene complexes have been investigated for their potential biological activity, although the study of ferrocene has been hampered by its

insolubility in aqueous systems.[62] The insolubility of ferrocene has been overcome to some extent by preparation of the ferrocenium cation[63] or through preparation of ferrocenyl inclusion complexes with cyclodextrin.

Ferrocenyl derivatives have also shown some use as antimalarial agents (see *Figure 1.15*).[64] These compounds are based on the antimalarial agent, chloroquine, and are investigated in a bid to find complexes with different structures and mechanisms of action than those currently employed. Recent studies have found metabolites of these complexes to be more active than chloroquine against the virulent causative agent, *Plasmodium falciparum*.[64]

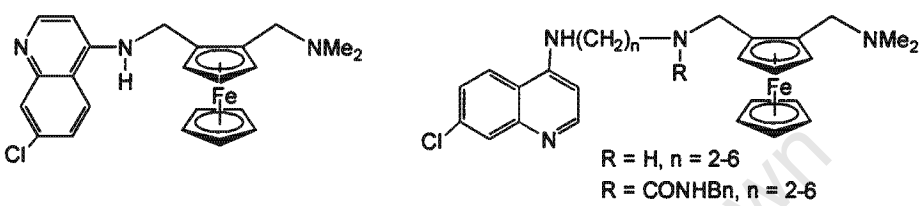

Figure 1.15: Ferrocenyl antimalarial agents[64,65]

1.5 Non-linear optical materials

Ferrocenyl-containing conjugated ligand systems have been extensively studied as non-linear optical materials since the enhanced non-linear optical behaviour of these compounds was first described.[66] Many reports have appeared since then with similar observations on the properties of ferrocenyl-containing systems with high second harmonic generation efficiency.[67]

Reports on the study of non-linear optical properties have resulted from the preparation of multinuclear ferrocene-containing complexes, which tend to satisfy the requirements for non-linear optical behaviour; these include polarizability and crystallisation in a non-centrosymmetric space group.[68] Complexes of this type generally contain metals such as chromium, molybdenum or tungsten as electron accepting groups, while ferrocene serves as an electron donor.[68] These metals appear to enhance the observed non-linear optical properties. Platinum group metals such as rhodium, iridium, platinum and palladium, have largely been ignored for this application due to the observed greater non-linear optical responses from complexes containing chromium, molybdenum or tungsten.[68]

The non-linear optical properties of $W(CO)_5L$ complexes (where L = pyridine or its 4-substituted derivatives), for example, have been well-studied.[69] The activity of complexes of this type with conjugated π substituents has been reported (see *Figure 1.16*).[70] These

complexes were shown to have low energy metal-to-ligand charge transfer bands as well as enhanced solvatochromism, both of which have been linked to enhanced polarisabilities and increased second-order non-linear optical behaviour.

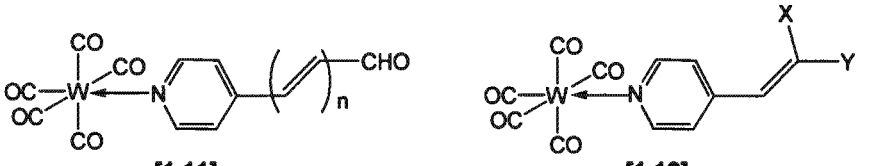

[1.11]

a: n = 0
b: n = 1
c: n = 2

[1.12]

a: X = Y = COOMe
b: X = CN, Y = COOMe
c: X = Y = CN

Figure 1.16: Tungsten pyridyl complexes investigated for non-linear optical properties[70]

1.6 Aims of the project

The above examples serve to illustrate the variety of factors that must be taken into account not only in the preparation of ferrocenyl complexes but also in considering the nature of electrochemical interactions. Accordingly, the ferrocenylpyridines represent an interesting class of compounds due primarily to their redox behaviour. The coordination of a transition metal to a ferrocenylpyridine may be monitored electrochemically due to the presence of the ferrocenyl group.

The current investigation represents a systematic exploration into the preparation of various ferrocenylpyridines and their coordination behaviour with a range of platinum group metals such as rhodium, iridium, palladium and platinum. The motivation for the study of these coordination complexes is to expand the range of applications of these complexes. Investigations include the establishment of synthetic methodologies for the preparation of several transition metal-containing complexes and determination of their respective spectroscopic and redox properties. The study involves the synthesis and examination of the properties of ferrocenyl nitrogen-donor ligands and in particular their metal complexes, an area that has hitherto not been systematically examined. The complexes prepared have been characterised using a wide range of spectroscopic and analytical techniques and the X-ray crystal structures of selected complexes are reported.

Bearing in mind the specific metals that have been targeted as part of this study, an investigation into several potential applications was considered. The incorporation of metals such as rhodium and palladium in particular, allowed for investigation of several catalytic applications of these complexes. Preliminary investigations of the activity of several

complexes prepared in this study have been carried out and comparisons made with related complexes reported in the literature.

A further point of interest in terms of applications of these complexes lies in the study of their biological activity. Since the preparation and antitumour activity of cisplatin, *cis*-diamminedichloroplatinum(II), was first reported, numerous subsequent reports have appeared describing the biological activity of other transition metal complexes. The antitumour activity of several of the complexes prepared in this study was considered in a preliminary investigation.

This thesis addresses the preparation and determination of the physico-chemical properties of novel platinum group metal complexes containing nitrogen-donor groups, such as pyridine bonded to ferrocene. The effect of derivatising the pyridyl group is considered with a view to the determination of resulting effects on spectroscopic and electronic properties of these complexes. The applications of complexes of this type are also examined in several preliminary studies in the areas of catalysis and medicinal chemistry.

References:

1. M. J. S. Dewar, *Bull. Soc. Chim. Fr.*, 1951, C79; J. Chatt and L. A. Duncanson, *J. Chem. Soc.*, 1953, 2939; F. Basolo, *Modern Coordination Chemistry, The Legacy of Joseph Chatt*, eds. G. J. Leigh and N. Winterton, The Royal Society of Chemistry, Cambridge, UK, 2002.
2. J. Tsuji, *Transition Metal Reagents and Catalysts, Innovations in Organic Synthesis*, John Wiley and Sons, Chichester, 2000.
3. C. Masters, *Adv. Organomet. Chem.*, 1979, **17**, 61; R. L. Pruett, *Adv. Organomet. Chem.*, 1979, **17**, 1; L. Mond, C. Langer and F. Quincke, *J. Organomet. Chem.*, 1990, **383**, 1; B. Cornils, W. A. Hermann and M. Basch, *Angew. Chem. Int. Ed. Engl.*, 1994, **33**, 2144.
4. K. Ziegler, H. G. Gellert, E. Holzkamp, G. Wilke, E. W. Duck and W. R. Kroll, *Liebigs Ann. Chem.*, 1960, **629**, 172; K. Ziegler and G. Natta, *Angew. Chem. Int. Ed. Engl.*, 1964, **76**, 545.
5. S. C. Ogburn and W. C. Brastow, *J. Am. Chem. Soc.*, 1933, **55**, 1307; J. Smidt, W. Hafner, R. Jira, R. Sieber, J. Sedlmeier and A. Sabel, *Angew. Chem. Int. Ed. Engl.*, 1962, **1**, 80.

6. Ch. Elschenbroich and A. Salzer, *Organometallics – A Concise Introduction*, 2nd Edition, VCH, Weinheim, 1992 and references therein.
7. H. Fischer, F. R. Kreissl, U. Schubert, P. Hofmann, K. H. Dötz and K. Weiss, *Transition Metal Carbene Complexes*, VCH Publishers, Weinheim, 1984.
8. J. S. Murdzek and R. R. Schrock, *Organometallics*, 1987, **6**, 1373; G. C. Bazan, E. Khosravi, R. R. Schrock, W. J. Feast, V. C. Gibson, M. B. O'Regan, J. K. Thomas and W. M. Davis, *J. Am. Chem. Soc.*, 1990, **112**, 8378; W. A. Nugent, J. Feldman and J. C. Calabrese, *Tetrahedron*, 1995, **117**, 8992.
9. S. T. Nguyen, L. K. Johnson and R. H. Grubbs, *J. Am. Chem. Soc.*, 1992, **114**, 3974; P. Schwab, M. B. France, J. W. Ziller and R. H. Grubbs, *Angew. Chem. Int. Ed. Engl.*, 1995, **34**, 2039; E. L. Dias, S. T. Nguyen and R. H. Grubbs, *J. Am. Chem. Soc.*, 1997, **119**, 3887; R. Roy, R. Dominique and S. K. Dais, *J. Org. Chem.*, 1999, **64**, 5408; C. M. Schuch and R. A. Pilli, *Tetrahedron Asymmetry*, 2000, **11**, 753.
10. T. J. Kealy and P. L. Pauson, *Nature*, 1951, **168**, 1039; S. A. Miller, J. A. Tebboth and J. F. Tremaine, *J. Chem. Soc.*, 1952, 632.
11. R. Grimes, *New Scientist*, 1991, **132**, 45.
12. *Ferrocenes: Homogeneous Catalysis, Organic Synthesis, Material Science*, eds. A. Togni and T. Hayashi, VCH, Weinheim, 1995 and references therein.
13. D. Macquarrie, *Green Chemistry*, 2001, **3**, G9.
14. A. Togni and L. M. Venanzi, *Angew. Chem. Int. Ed. Engl.*, 1994, **33**, 497 and references therein.
15. C. Janiak, *J. Chem. Soc., Dalton Trans.*, 2000, 3885.
16. R. Meyer, P. L. Wessels, P. H. van Rooyen and S. Lotz, *Inorg. Chim. Acta*, 1999, **284**, 127.
17. I. R. Butler, *Organometallics*, 1992, **11**, 74.
18. B. de Bruin, R. J. N. A. M. Kicken, N. F. A. Suos, M. P. J. Donners, C. J.den Reijer, A. J. Sandee, R. de Gelder, J. M. M. Smits, A. W. Gal and A. L. Spek, *Eur. J. Inorg. Chem.*, 1999, 1581.
19. B. Kräutler, *Chimia*, 1987, **41**, 277.
20. R. Scheffold, G. Rytz and L. Walder, *Modern Synthetic Methods, vol. 3*, ed. R. Scheffold, Salle and Sauerländer, Frankfurt, 1983.
21. A. Yamamoto, *Organotransition Metal Chemistry*, Wiley, New York, 1986.
22. C. J. Hawker and J. M. J. Fréchet, *J. Am. Chem. Soc.*, 1990, **112**, 7638; K. L. Wooley, C. J. Hawker and J. M. J. Fréchet, *J. Chem. Soc., Perkin Trans. 1*, 1991, 1059; D. A. Tomalia, H. M. Brothers II, L. T. Piehler and Y. Hsu, *Polym. Mater. Sci. Eng.*, 1995, **73**,

75; N. Ardoin and D. Astruc, *Bull. Soc. Chim. Fr.*, 1995, **132**, 875 and references therein; F. Zeng and S. Zimmerman, *Chem. Rev.*, 1997, **97**, 1681 and references therein.

23. M. A. Hearshaw and J. R. Moss, *Chem. Commun.*, 1999, 1 and references therein.
24. S. Achar, J. J. Vittal and R. J. Puddephatt, *Organometallics*, 1996, **15**, 43.
25. S. Achar, C. E. Immoos, M. G. Hill and V. J. Catalano, *Inorg. Chem.*, 1997, **36**, 2314.
26. I. Cuadrado, C. Casado, B. Alonso, M. Morán, J. Losada and V. Belsky, *J. Am. Chem. Soc.*, 1997, **119**, 7613; B. Alonso, M. Morán, C. M. Casado, F. Lobete, J. Losada and I. Cuadrado, *Chem. Mater.*, 1995, **7**, 1440.
27. F. Moulines, L. Djakovitch, R. Boese, B. Gloaguen, W. Thiel, J.-L. Fillaut, M. H. Delville and D. Astruc, *Angew. Chem., Int. Ed. Engl.*, 1993, **32**, 1075; J.-L. Fillaut and D. Astruc, *J. Chem. Soc., Chem. Commun.*, 1993, 1320; J.-L. Fillaut, J. Linares and D. Astruc, *Angew. Chem., Int. Ed. Engl.*, 1994, **33**, 2460.
28. See for example: C. Kollmar, M. Conty and D. Kahn, *J. Am. Chem. Soc.*, 1991, **113**, 7994; E. Coronado, M. Clemente-León, J. R. Galán-Mascarós, C. Giménez-Saiz, C. J. Gómez-Garcia and E. Martínez-Ferrero, *J. Chem. Soc., Dalton Trans.*, 2000, 3955.
29. J. V. Caspar and T. J. Meyer, *J. Phys. Chem.*, 1983, **87**, 952; M. E. Kober, J. V. Caspar, R. S. Lumpkin and T. J. Meyer, *J. Phys. Chem.*, 1986, **90**, 3722, A. Juris, F. Barigelletti, S. Campagna, V. Balzani, P. Belser and A. von Zeleswsky, *Coord. Chem. Rev.*, 1988, **84**, 85; A. Juris, S. Campagna, I. Bidd, J. M. Lehn and R. Ziessel, *Inorg. Chem.*, 1988, **27**, 4007.
30. T. J. Meyer, *Acc. Chem. Res.*, 1989, **22**, 163; J. S. Connolly, *Photochemical Conversion and Storage of Solar Energy*, Academic Press, New York, 1981.
31. E. C. Constable, A. J. Edwards, R. Martinez-Máñez, P. R. Raithby and A. M. W. Cargill Thompson, *J. Chem. Soc., Dalton Trans.*, 1994, 645; E. C. Constable, R. Martinez-Máñez, A. M. W. Cargill Thompson and J. V. Walker, *J. Chem. Soc., Dalton Trans.*, 1994, 1585.
32. E. C. Constable, *Tetrahedron*, 1992, **48**, 10013.
33. P. D. Beer, O. Kocian and R. J. Mortimer, *J. Chem. Soc., Dalton Trans.*, 1990, 3283.
34. C. M. Asselin, G. C. Fraser, H. K. Hall Jr., W. E. Lindsell, A. B. Padias and P. N. Preston, *J. Chem. Soc., Dalton Trans.*, 1997, 3765.
35. T. M. Miller, J. A. Kazi and M. S. Wrighton, *Inorg. Chem.*, 1989, **28**, 2347.
36. A. Kasahara, T. Izumi and M. Maemura, *Bull. Chem. Soc. Jpn.*, 1977, **50**, 1878.
37. O. Carugo, G. De Santis, L. Fabbrizzi, M. Licchelli, A. Monichino and P. Pallavicini, *Inorg. Chem.*, 1992, **31**, 765.
38. D. Osella, L. Milone, C. Nervi and M. Ravera, *J. Organomet. Chem.*, 1995, **488**, 1.

39. J. D. Carr, S. J. Coles, M. B. Hursthouse, M. E. Light, E. L. Munro, J. H. R. Tucker and J. Westwood, *Organometallics*, 2000, **19**, 3312.
40. A. M. Trzeciak and J. J. Ziólkowski, *Coord. Chem. Rev.*, 1999, **190-192**, 883.
41. F. H. Jardine, *Polyhedron*, 1982, **1**, 569.
42. J. M. Burke, R. B. Coapes, A. E. Goeta, J. A. K. Howard, T. B. Marder, E. G. Robins and S. A. Westcott, *J. Organomet. Chem.*, 2002, **649**, 199.
43. R. H. Crabtree, *Platinum Metals Rev.*, 1978, **22**, 126; J. W. Suggs, S. D. Cox, R. H. Crabtree and J. M. Quirk, *Tetrahedron Lett.*, 1981, **22**, 303.
44. J. R. Shapley, R. R. Schrock and J. A. Osborn, *J. Am. Chem. Soc.*, 1969, **91**, 2816.
45. P. A. Wender, N. F. Badham, S. P. Conway, P. E. Floreancig, T. E. Glass, C. Granicher, J. B. Houze, J. Janichen, D. Lee, D. G. Marquess, P. L. McGrane, W. Meng, T. P. Mucciaro, M. Muhlebach, M. G. Natchus, H. Paulsen, D. B. Rawlins, J. Satkofsky, A. J. Shuker, J. C. Sutton, R. E. Taylor and K. Tomooka, *J. Am. Chem. Soc.*, 1997, **119**, 2755.
46. R. B. Bedford, P. A. Chaloner, S. Z. Dewa, G. López, P. B. Hitchcock, F. Momblona and J. L. Serrano, *J. Organomet. Chem.*, 1997, **527**, 75.
47. A. C. Hillier, H. M. Lee, E. D. Stevens and S. P. Nolan, *Organometallics*, 2001, **20**, 4246.
48. G. P. Sollot, J. P. Snead, S. Portnoy, W. R. Peterson and H. E. Mertoy, *Chem. Abstr.*, 1965, **63**, 18147b; J. J. Bishop, A. Davsion, M. L. Katcher, D. W. Lichtenberg, R. E. Merrill and J. C. Smart, *J. Organomet. Chem.*, 1971, **27**, 241.
49. T. J. Colacot, *Platinum Metals Rev.*, 2001, **45**, 22.
50. T. Hayashi, M. Konishi, Y. Kobori, M. Kumada, T. Higuchi and K. Hirotsu, *J. Am. Chem. Soc.*, 1984, **106**, 158.
51. T. Oh-e, N. Miyaura and A. Suzuki, *Synlett*, 1990, 221; T. Oh-e, N. Miyaura and A. Suzuki, *J. Org. Chem.*, 1993, **58**, 2201; V. Percec, J.-Y. Bae and D. H. Hill, *J. Org. Chem.*, 1995, **60**, 1065; S. Saito, S. Oh-tani and N. Miyaura, *J. Org. Chem.*, 1997, **62**, 8024; M. Ueda, A. Saitoh, S. Oh-tani and N. Miyaura, *Tetrahedron*, 1998, **54**, 13079; T. J. Colacot, H. Qian, R. Cea-Olivares and S. Hernandez-Ortega, *J. Organomet. Chem.*, 2001, **637-639**, 691.
52. K. Olofsson, M. Larhed and A. Hallberg, *J. Org. Chem.*, 1998, **63**, 5076; S.-K. Kang, S.-C. Choi, H.-C. Ryu and T. Yamaguchi, *J. Org. Chem.*, 1998, **63**, 5748; F. Ujjainwalla and D. Warner, *Tetrahedron Lett.*, 1998, **39**, 5355; S. Cerezo, J. Cortés, M. Moreno-Mañas, R. Plexixats and A. Roglans, *Tetrahedron*, 1998, **54**, 14869; A. L. Boyes, I. R. Butler and S. C. Quayle, *Tetrahedron Lett.*, 1998, **39**, 7763.
53. A. M. Echavarren and J. K. Stille, *J. Am. Chem. Soc.*, 1988, **110**, 1557.
54. C. J. Richards and A. J. Locke, *Tetrahedron: Asymm.*, 1998, **9**, 2377.

55. J. C. Kotz, C. L. Nivert, J. M. Lieber and R. C. Reed, *J. Organomet. Chem.*, 1975, **91**, 87; G. Pilloni, B. Longato and B. Corain, *J. Organomet. Chem.*, 1991, **420**, 57.
56. P. Zanello, G. Opromolla, G. Giorgi, G. Sasso and A. Togni, *J. Organomet. Chem.*, 1996, **506**, 61.
57. K. Schlögel and M. Fried, *Monatsch. Chem.*, 1963, **94**, 537; M. D. Rausch and D. J. Ciappenelli, *J. Organomet. Chem.*, 1967, **10**, 127.
58. K. Tani, T. Mihana, T. Yamagata and T. Saito, *Chem. Lett.*, 1991, 2047.
59. J. G. P. Delis, P. W. N. M. van Leeuwen, K. Vrieze, N. Veldman, A. L. Spek, J. Fraanje and K. Goubitz, *J. Organomet. Chem.*, 1996, **514**, 125.
60. Z. Guo and P. J. Sadler, *Angew. Chem. Int. Ed.*, 1999, **38**, 1512 and references therein.
61. B. Rosenberg and L. V. Camp, *Nature*, 1965, **205**, 698; B. Rosenberg, L. V. Camp, J. E. Trosko and V. H. Mansour, *Nature*, 1969, **222**, 385; B. Rosenberg and L. V. Camp, *Cancer Res.*, 1970, **30**, 1799.
62. P. Köpf-Maier, *Eur. J. Clin. Pharmacol.*, 1994, **47**, 1 and references therein.
63. D. Osella, M. Ferrali, P. Zanello, F. Laschi, M. Fonatni, C. Nervi and G. Cavigiolio, *Inorg. Chim. Acta*, 2000, **306**, 42.
64. See for example: C. Biot, G. Glorian, L. A. Maciejewski, J. S. Brocard, O. Domarle, G. Blampain, P. Millet, A. J. Georges, H. Abessolo, D. Dive and J. Lebibi, *J. Med. Chem.*, 1997, **40**, 3715; C. Biot, L. Delhaes, H. Abessolo, O. Domarle, L. A. Maciejewski, M. Mortuaire, P. Delcourt, P. Deloron, D. Camus, D. Dive and J. S. Brocard, *J. Organomet. Chem.*, 1999, **589**, 59; C. Biot, L. Delhaes, C. M. N'Diaye, L. Maciejewski, D. Camus, D. Dive and J. S. Brocard, *Bioorg. Med. Chem.*, 1999, **7**, 2843; L. Delhaes, H. Abessolo, C. Biot, L. Berry, P. Delcourt, L. Maciejewski, J. S. Brocard, D. Camus and D. Dive, *Parasitol. Res.*, 2001, **87**, 239.
65. K. Chibale, J. R. Moss, M. Blackie, D. van Schalkwyk and P. J. Smith, *Tetrahedrom Lett.*, 2000, **41**, 6231.
66. M. L. H. Green, S. R. Marder, M. E. Thompson, J. A. Bandy, D. Bloor, P. V. Kolinsky and R. J. Jones, *Nature*, 1987, **330**, 360.
67. See for example: S. R. Marder, J. W. Perry, B. G. Tiemann and W. P. Schaefer, *Organometallics*, 1991, **10**, 1896; J. C. Calabrese, L.-T. Cheng, J. C. Green, S. R. Marder and W. Tam, *J. Am Chem. Soc.*, 1991, **113**, 7227; B. J. Coe, C. J. Jones, J. A. McCleverty, *Polyhedron*, 1992, **11**, 547; A. Togni and G. Rihs, *Organometallics*, 1993, **12**, 3368.
68. M. M. Bhadbhade, A. Das, J. C. Jeffery, J. A. McCleverty, J. A. Navas Badiola and M. D. Ward, *J. Chem. Soc., Dalton Trans.*, 1995, 2769; S. Sakanishi, D. A. Bardwell, S. Couchman, J. C. Jeffer, J. A. McCleverty and M. D. Ward, *J. Organomet. Chem.*, 1997,

528, 35; J. Mata, S. Uriel, E. Peris, R. Llusar, S. Houbrechts and A. Persoons, *J. Organomet. Chem.*, 1998, **562**, 197.

69. See for example: D. R. Kanis, M. A. Ratner and T. J. Marks, *Chem Rev.*, 1994, **94**, 195; N. J. Long, *Angew. Chem. Int. Ed. Engl.*, 1995, **34**, 21; H. L. Bozec and T. Renouard, *Eur. J. Inorg. Chem.*, 2000, 229; S. DiBella, *Chem. Soc. Rev.*, 2001, **30**, 355.
70. A. Hameed, A. Rybarczyk-Pirek and J. Zakrzewski, *J. Organomet. Chem.*, 2002, **656**, 102.

Chapter 2: Synthesis and Study of Substituted Pyridyl Ligands

2.1 Introduction

The past few decades have seen a rapid growth in the systematic study of phosphine-donor ligands and in particular, ferrocenylphosphine ligands for use in a variety of applications, mainly catalysis.[1,2] The use of nitrogen-donor ligands in areas such as catalysis, materials science and medicinal chemistry has not enjoyed much attention and until recently has remained a relatively unexploited area of chemistry.[3] In the current investigation, we are particularly interested in sp^2 hybridised nitrogen donors with specific reference to the behaviour of pyridyl and substituted pyridyl ligands.

Currently, pyridine and bipyridine are viewed as building blocks from which a range of ligand systems can be built.[4] This is largely due to the relative ease of derivatisation of these groups. The redox stability of complexes of this type gains prominence when considering that a large number of complexes are investigated for their electrochemical activity. Transition metal complexes containing these ligands have uses in a variety of applications. Rhodium complexes with pyridyl ligands and ruthenium complexes with bipyridine, for example, are catalysts for the water gas shift reaction in both the homo- and heterogeneous processes.[5] In the heterogeneous process these groups act as linkers to polymer supports, anchoring the catalyst to a solid support. In the homogeneous process the position of substituents on the pyridine and bipyridine ring systems play a significant role in activity of the catalyst.

Many nitrogen donor ligands have gained distinction as optically active molecules upon coordination to both metal and organic groups and are often noted for the brightly coloured complexes obtained. For example, organometallic compounds have been investigated as dyes for the potential rapid screening of catalysts (see *Figure 2.1*).[6]

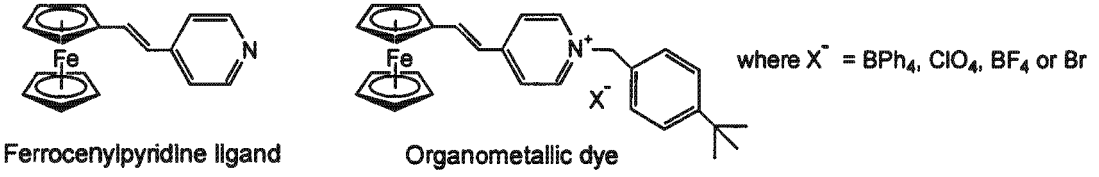

Figure 2.1: Ferrocene ligands with pendant pyridyl groups investigated as dyes for hydrogenation catalyst screening[6]

The dye molecule consists of an electron donor group such as ferrocenyl, linked through a conjugated pathway to an electron acceptor group such as a quarternised pyridinium. These highly conjugated molecules are intensely coloured but if the alkene bond in the ligand is reduced by catalytic hydrogenation, conjugation is lost and the dye bleached. This methodology would allow for the rapid screening of potential hydrogenation catalysts. In practise, the dye was photochemically unstable in solution.[6]

Stilbene and stilbazole ligands, which contain pendant pyridyl groups, have been widely studied for their potential liquid crystalline properties. The incorporation of transition metals into complexes of this type represents an interesting development in terms of including metals in an ordered fluid system.[7] Several nickel,[8] rhodium[9] and iridium complexes have been reported. Initial investigations were into the preparation of rhodium complexes of the type *cis*-[Rh(alkyloxy)Cl(CO)$_2$(cyanobiphenyl)]. These complexes were thermally unstable. The thermal instability was attributed to the presence of a weak rhodium-nitrile bond.

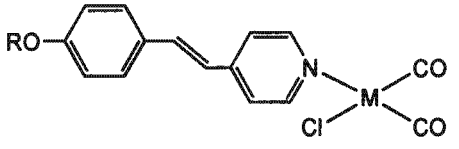

$R = C_nH_{2n+1}$, n = 4-12
M = Rh, Ir

[2.1]

Figure 2.2: Rhodium and iridium complexes prepared with mesogenic ligand, 4-alkyloxy-4'-stilbazole[9]

Rhodium and iridium complexes with mesogenic 4-alkyloxy-4'-stilbazole ligands **[2.1]**, yielded mesomorphic metal-containing complexes showing nematic and smectic A mesophases (see *Figure 2.2*). The preparation of several ferrocenyl-containing mesogens has also been reported in the form of both mono- and bisubstituted ferrocenes.[10] In this instance, a second metal centre is introduced *via* an organometallic group rather than coordination of a given mesogenic ligand to a further metal centre.

Recent developments in the study of nitrogen-containing ligand systems include the preparation of mixed donor systems. These for the most part contain both nitrogen- and phosphine-donor groups (see *Figure 2.3*). Despite the prevalence of phosphine-donor ligands in a number of catalysts, one of the disadvantages of phosphine-donor catalysts is the deactivation of the catalyst under a number of conditions. The inclusion of a nitrogen-donor group into the catalyst together with the phosphine-donor in the form of an *N,P*-chelate, resulted in the preparation of a catalyst with higher stability towards oxidation and consequently, a longer life.[11]

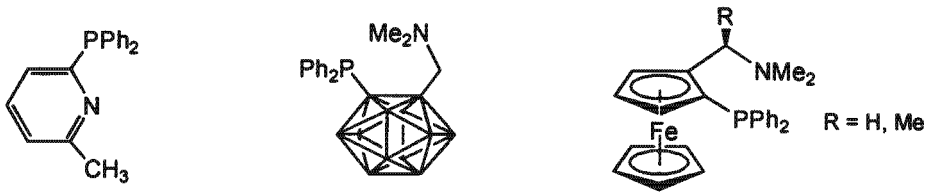

2-pyridylphosphane ligand | *o*-carboranylaminophosphine ligand | 1,2-ferrocenylaminophosphine ligand

Figure 2.3: Chelating ligands containing both *N*- and *P*-donor atoms[11,12,13,14]

Ferrocene chemistry has developed significantly in the fifty-plus years since the preparation of the metallocene was first reported.[15,16] Ferrocene, **[2.2]** is relatively stable and lends itself to derivatisation. The electrochemical behaviour of ferrocene shows a perfectly reversible redox change (see *Figure 2.4*) and is often used as an internal standard and is increasingly being viewed as the nonaqueous counterpart of the standard hydrogen electrode (SHE).[17,18]

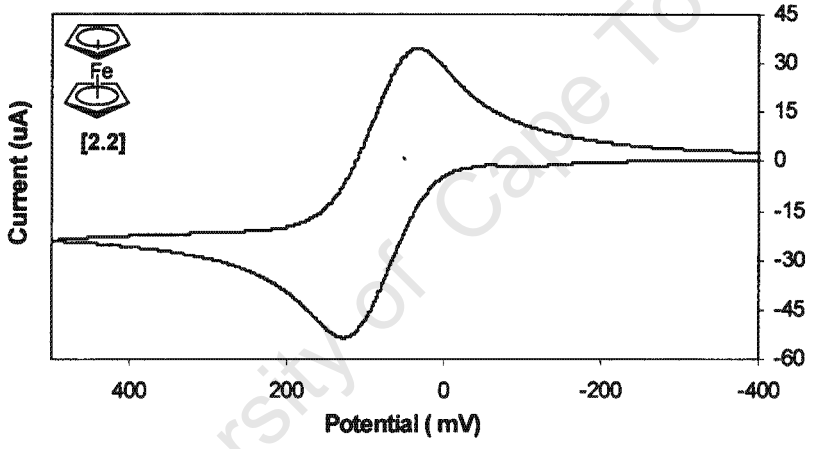

Figure 2.4: Cyclic voltammogram of ferrocene in acetonitrile with 0.1 M TBAP as background electrolyte, $Ag/AgNO_3$ reference electrode, platinum wire auxiliary electrode and platinum disk working electrode

Comparing the redox activity of a substituted ferrocene with ferrocene as a standard can be used to monitor the effect of derivatising the metallocene. The electron-withdrawing or donating effect of the substituent can be readily observed as a change in the position and nature of the ferrocenyl redox wave. The study of the electrochemical behaviour of bisferrocenyl ruthenium and cobalt complexes, for example, monitored the role of the central metal in the electrochemical communication between the ferrocenyl metal centres (see *Figure 2.5*).[19]

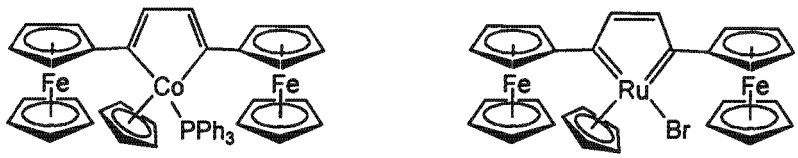

[2.3] [2.4]

Figure 2.5: Bis(ferrocenyl) complexes of cobalt and ruthenium[19]

A study of the electrochemistry of these complexes revealed that the extent of interaction between the ferrocenyl groups of the cobalt complex **[2.3]**, was very similar to that of the free ligand while the ruthenium complex **[2.4]**, showed a marked difference. While complex **[2.3]** showed a single reversible redox wave, complex **[2.4]** showed two separate one electron redox waves, indicating interaction of the ferrocenyl groups through the ruthenium metallacycle. The difference in electrochemical behaviour was thought to be due to differences in the donating ability of the respective metal centres as well as differences in π conjugation within these systems.[19]

The use of ferrocenylpyridines as ligands coordinated to various transition metal ions such as silver,[37] gold,[20] platinum[17] and rhenium[21] has been reported with the primary aim, initially, the preparation of novel coordination complexes. Due to the presence of the ferrocenyl group, the potential electrochemical properties of these transition metal complexes have been studied. These specific ligands are usually conjugated in nature, allowing for an electronic network of communication through a π-electron pathway. *Figure 2.6* for example, shows the electrochemical resonance forms of the 4-ferrocenylphenylpyridine triosmium alkylidene cluster.[22] As illustrated, the *push-pull* interaction in the conjugated ferrocenyl ligand allows electrochemical interaction between the respective metal centres.

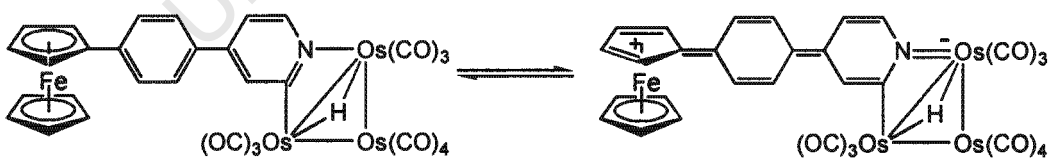

Ground state Excited state

Figure 2.6: Electrochemical flow illustrated in a conjugated ferrocenyl ligand coordinated to a triosmium alkylidyne cluster[22]

The preparation and coordination of ferrocenylpyridine ligands allows for the possibility of electrochemical communication between different metal atoms. This could be of particular

interest for the study of nonlinear optical materials,[23] magnetism,[24] molecular sensors[25] and liquid crystals.[26]

2.2 Types of ligands investigated

The ferrocenyl-containing ligands prepared in this study are for the most part conjugated in nature. They represent a class of ligand that exhibit independent redox activity, in that the redox behaviour of the ligand does not depend on further coordination to a metal ion. These ferrocenyl-based ligands show completely reversible redox activity, allowing them to act potentially as electrochemical switches when coordinated to further metal centres.

Of particular interest would be the ability to tune the electron density of a coordinated metal ion without changing its coordination sphere. This would allow for remote control of reactivity at the coordinated metal centre. Hence, being able to tune the electron density of the coordinated metal ion by oxidation of the pendant ferrocenyl ligand in a system of the type described in *Figure 2.6*, for example, where the coordinated metal ion is represented by the triosmium trialkylidene cluster, would present an alternative to varying the substituents on the coordinated metal centre as well as varying substituents on the cyclopentadienyl rings of the ferrocene or pendant pyridyl group of the ligand.

Several factors were considered in the ligands chosen for this work including steric and electronic factors. Several modes of electrochemical communication are possible. The systems investigated are for the most part connected through conjugated pathways and the primary means of electrochemical communication envisioned is through the π-electron pathway. This is not the only possible mode of communication. It can also occur through space but in order for this to occur, metal centres must be in close proximity to one another. The ligands investigated in this study for their potential electrochemical properties were prepared with this in mind.

The primary aim of this study is the preparation of ferrocenyl-substituted pyridines. Given the possible electrochemical interactions that may be facilitated by these ligands, the effect of positioning substituents on the pyridyl group is of significance. *Figure 2.7* shows a three-dimensional schematic describing various ferrocenylpyridines with the ferrocenyl group as a substituent placed on the 4-, 3- and 2-positions of the pyridyl ring respectively.

I II III

Figure 2.7: Ferrocenylpyridines investigated to determine the effect of substituent position on the pyridyl ring

Given the possible electrochemical pathways with the ligand systems described in *Figure 2.7*, it can be observed that moving the ferrocenyl substituent from the 4-position (I) through to the 2-position (III) not only reduces the number of bonds between the ferrocenyl substituent and the nitrogen donor atom but also creates a bend in the system should a metal ion be coordinated. Hence, a metal ion coordinated to the nitrogen donor atom to a system as described in III, not only allows for a more efficient through–bond electrochemical interaction but also possibly for a through–space interaction.

It should be considered that limitations may arise for systems of the type described by III, these being stereochemical constraints which are dependant on the size of the metal ion and other ligands coordinated to the transition metal centre. The system described by II is a less sterically demanding ligand. The conjugated pathway is slightly reduced from I and depending on the size of the metal ion, through space communication may be a remote possibility.

A further consideration in the preparation of coordination complexes of these ligands is conformational flexibility. The preparation of 1,1'-disubstituted ferrocenylpyridines and comparison of these to the monosubstituted derivatives and their coordination complexes is noteworthy (see *Figure 2.8*).

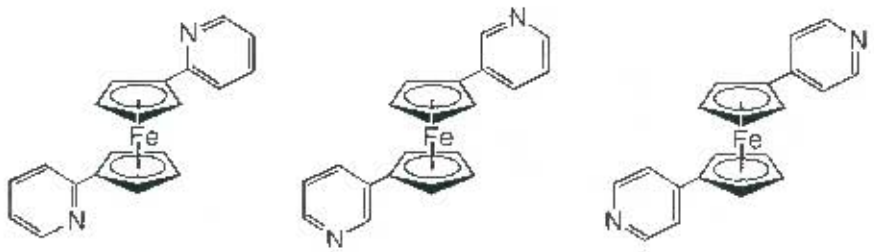

IV V VI

Figure 2.8: 1,1'-disubstituted ferrocenylpyridines

Aside from the position of substituents on the pyridyl ring, the effect of placing various spacers between the ferrocenyl unit and the pendant pyridyl ring was considered. In the ligands investigated, the specific nature of the spacer as well as the distance created between these centres was examined. *Figure 2.9* is a three-dimensional representation of several ferrocenylpyridine ligands with systematic inclusion of various spacers.

I shows no spacer between the ferrocenyl group and pyridyl ring, whereas a phenylene spacer in ligand **VII** separates these groups. A further imine bond was inserted in ligand **VIII**, producing an elongated linear ligand system. The effect of inclusion of spacer groups was evaluated not only with regard to the electrochemical behaviour of the ligands but also the effect on properties and reactivity of these compounds.

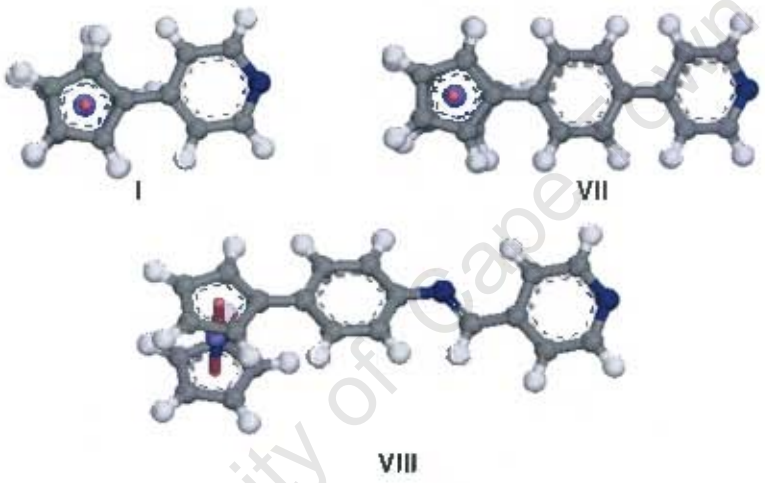

Figure 2.9: Ferrocenylpyridines used to investigate nature of the spacer group

Another interesting factor that has been considered is the aromaticity of ferrocene and to what extent this contributes to the properties and reactivity of the complex.[27] Comparisons have been made with phenylene derivatives, including 4-phenylpyridine.

2.3 Preparation of ligands

2.3.1 Monosubstituted ferrocenylpyridine ligands

One of the main synthetic routes followed for the preparation of the mono-substituted ferrocenylpyridine ligands was *via* the Grignard reaction. This involved a nickel-phosphine catalysed cross-coupling of a Grignard reagent with an aryl halide. The use of the nickel-catalysed Grignard reaction for the coupling of aryl groups has been reported as particularly effective under relatively mild reaction conditions, offering comparatively good yields to other

synthetic routes.[21,28] *Figure 2.10* illustrates the synthetic route to 4-ferrocenylpyridine, **[2.6]**. A similar methodology was applied to the preparation of other ferrocenylpyridine compounds **[2.7]–[2.11]**.

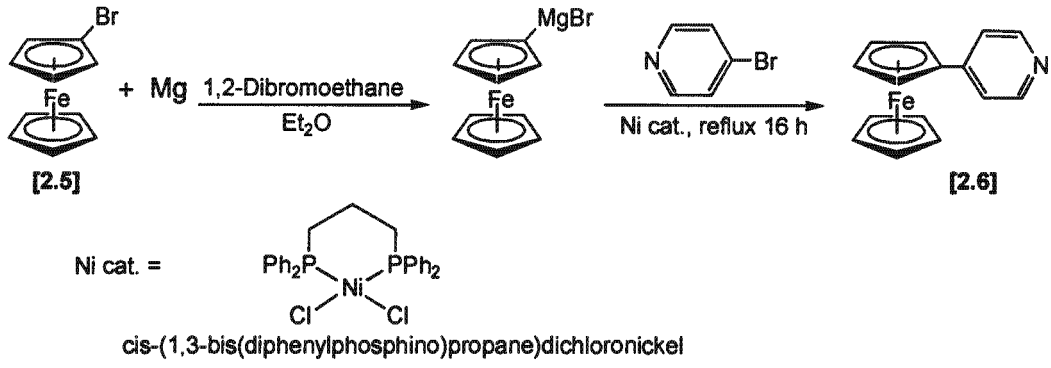

Figure 2.10: Synthesis of 4-ferrocenylpyridine *via* the Grignard reaction

Bromoferrocene, **[2.5]**, was obtained by the bromination of chloromercuriferrocene with *N*-bromosuccinimide.[29] The synthesis of chloromercuriferrocene was achieved through metallation of ferrocene with mercury(II) acetate followed by addition of lithium chloride.[29,30] The metallation of ferrocene in this case yields both mono- and 1,1'-disubstituted chloromercuriferrocene, which were separated by Soxhlet extraction. Unreacted ferrocene was removed by sublimation, yielding the unsublimed portion as chloromercuriferrocene, which was recrystallised to give a fine golden powder.

Ferrocenylmagnesium bromide was formed *in situ* with the magnesium slowly activated by gradual addition of 1,2-dibromoethane in solution with **[2.5]** in diethyl ether. Once the Grignard reagent was generated, a mixture of the halogenated pyridine, together with the nickel catalyst, was added in diethyl ether. The reaction mixture was heated under reflux generating the product **[2.6]**, which was purified by column chromatography. The product was obtained as yellow flakes in good yield and purity.

Using this synthetic route several other ligands were prepared, most notably the ferrocenylpyridines and ferrocenylphenylpyridines shown in *Figures 2.11* and *2.12*. Moving the position of the substituents on the pyridyl ring from the *4-* to the *3-* and finally to the *2-* position was performed with the intention of varying the number of bonds between the ferrocenyl substituent and the nitrogen donor atom, and consequently orientating the metals in the ligand-coordinated transition metal complexes spatially closer together. These types of complexes would allow electrochemical communication to occur both through bond, as well as through space while also considering steric constraints. Compounds **[2.6]-[2.8]** were

similarly obtained from bromoferrocene with the appropriate halogenated pyridines to give the desired isomer.

Although the preparation of **[2.7]** has been reported *via* the diazonium reaction,[17] the Grignard reaction route consistently gave a significantly higher product yield.

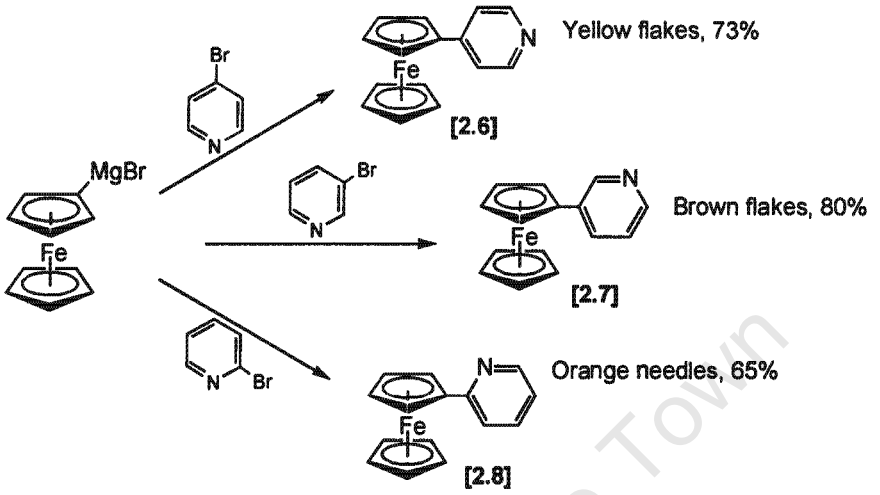

Figure 2.11: Preparation of ferrocenylpyridine ligands *via* a Grignard reaction

The ferrocenylphenylpyridines **[2.9]–[2.11]**, also demonstrate changing positions of substituents on the pyridyl ring but with systems incorporating a phenylene spacer group. The effect of the spacer group is evaluated in coordination studies with various metal ions in *Chapter 3*. It would be of interest to determine the difference in conformational position of the substituent along the pyridyl ring in the presence of the spacer group between the ferrocene and pyridyl groups in comparison to compounds **[2.6]–[2.8]**.

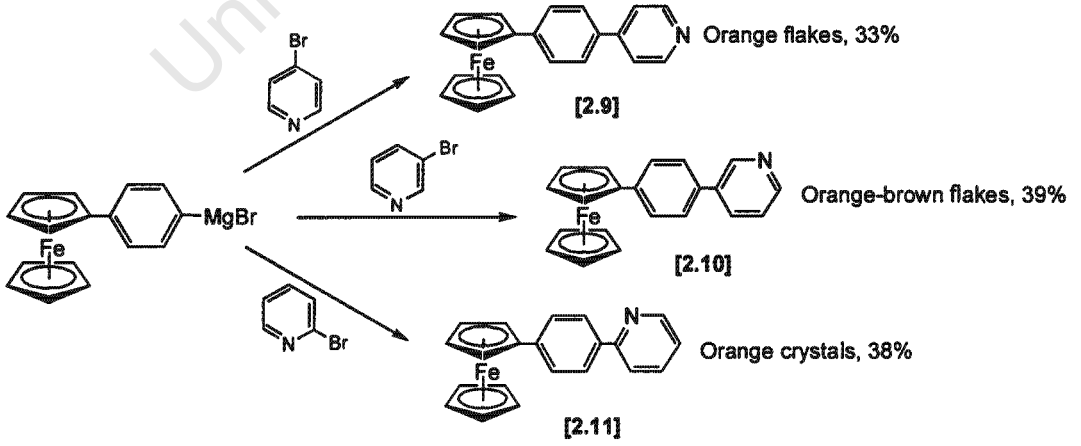

Figure 2.12: Preparation of ferrocenylphenylpyridine ligands *via* a Grignard reaction

The compounds **[2.9]–[2.11]**, were obtained using the same synthetic route as for the preparation of **[2.6]–[2.8]**, starting from 4-bromophenylferrocene. The same high yields obtained for compounds **[2.6]–[2.8]** could not be obtained for compounds **[2.9]–[2.11]**. The exact reason for this is unclear at this stage but may be related to the preparation of ferrocenylphenylmagnesium bromide *in situ*. Although compound **[2.9]** has previously been prepared *via* a palladium-catalysed cross-coupling reaction with an organozinc reagent,[22] the synthetic route described here represents a relatively simple one-pot synthesis.

2.3.2 1,1'-Disubstituted ferrocenylpyridine ligands

The current investigation has predominantly considered the preparation of monosubstituted ferrocenyl ligands with several chelating compounds containing two monosubstituted ferrocenyl groups. Despite the fact that 1,1'-bis(2-pyridyl)ferrocene, **[2.13]** was prepared over three decades ago,[31] the coordination behaviour of the compound has not been extensively investigated.[32,37] Studies have been limited to the preparation and X-ray crystal structure analysis of novel rhodium and silver complexes.[37] Recent work has seen the preparation of palladium and platinum complexes of **[2.13]**. The palladium complex has been further studied in carbonyl insertion reactions.[32] This type of disubstituted ferrocene offers a ligand with a relatively flexible conformation and a large bite angle. A comparison of the properties of the mono- and disubstituted analogues of a given ferrocenylpyridine should be interesting in terms of the properties of the coordinated metal complexes.

These compounds were prepared by a zinc chloride cross-coupling reaction with 1,1'-dilithioferrocene catalysed by a palladium catalyst as shown in *Figure 2.13*. This methodology has been reported for the preparation of **[2.13]**.[32] The dilithioferrocene-TMEDA complex was prepared in *n*-hexane, as this resulted in a higher conversion to the desired dilithiated ferrocene than in the commonly used diethyl ether.[31]

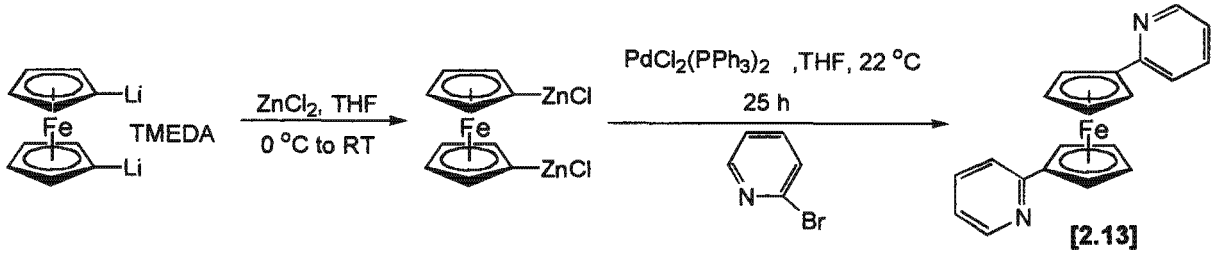

Figure 2.13: Synthetic scheme for the preparation of 1,1'-bis(2-pyridyl)ferrocene, **[2.13]**

This synthetic route was applied to the preparation of both 1,1'-bis(2-pyridyl)ferrocene, **[2.13]**, and 1,1'-bis(4-pyridyl)ferrocene, **[2.14]** (see *Figure 2.14*). The lower isolated yield for **[2.14]**

may be due to some product decomposition in solution. The compound appeared to be relatively unstable in chlorinated solvents in particular, compared to **[2.13]**. Overall the product yields were low with a significant amount of monosubstituted compound obtained in both cases. The higher yield of monosubstituted compound in both cases was attributed to the formation of a mixture of mono- and dilithioferrocenyl species in the initial stage of the reaction.

[2.13]: Pink-red powder; 10% **[2.14]**: Orange-brown powder; 15%

Figure 2.14: 1,1'-Disubstituted ferrocenylpyridine ligands prepared, **[2.13]** and **[2.14]**

The preparation of 1,1'-bis(3-pyridyl)ferrocene **[2.15]**, was also attempted by this method without success. Only the monosubstituted 3-ferrocenylpyridine was obtained. The preparation of the disubstituted ferrocenes **[2.13]**-**[2.15]** was also attempted using the Stille cross-coupling reaction with tributyltin chloride in place of zinc chloride (see *Figure 2.15*).[33,34] The Stille reaction has recently seen a resurgence with the synthesis of several ferrocenyl compounds reported using this synthetic route.[35] The Stille route initially appeared to be more successful for the preparation of these compounds. However, separation of the product from the tin by-products proved to be problematic.

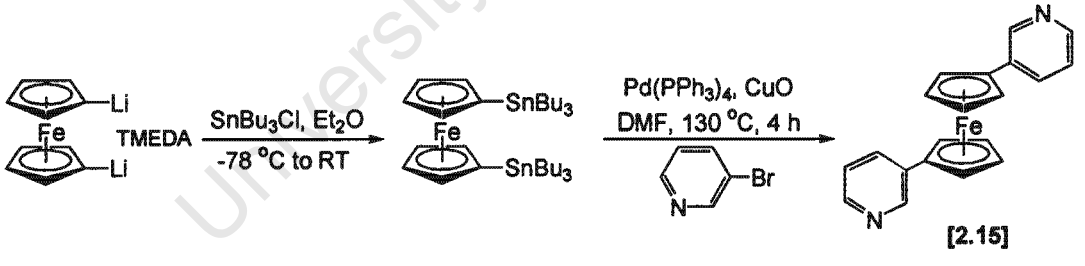

Figure 2.15: Preparation of a 1,1'-disubstituted ferrocenylpyridine *via* a Stille cross-coupling reaction[36]

Although the coordination behaviour of 1,1'-bis(2-pyridyl)ferrocene **[2.13]** has been studied to a limited extent, a rhodium complex of compound **[2.13]** has been prepared which shows coordination of the rhodium metal ion not only through the nitrogen donor atom but also the α-proton of the ferrocenyl cyclopentadienyl group (see *Figure 2.16*).[37] The effect was observed though temperature-controlled NMR studies of the complex in solution. This type of interaction has been noted in some recently prepared palladium and platinum complexes.[32] It

would be interesting to establish whether the monosubstituted 2-ferrocenylpyridine **[2.8]**, would exhibit similar coordination behaviour as well.

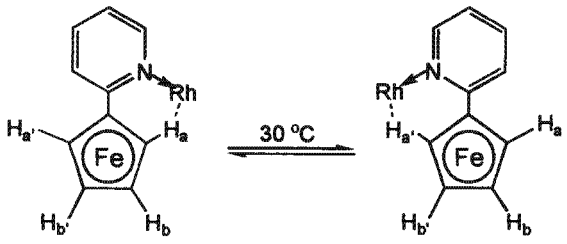

Figure 2.16: The coordination behaviour of 1,1'-bis(2-pyridyl)ferrocene with a rhodium metal centre

2.3.3 Monosubstituted Schiff-base ligands

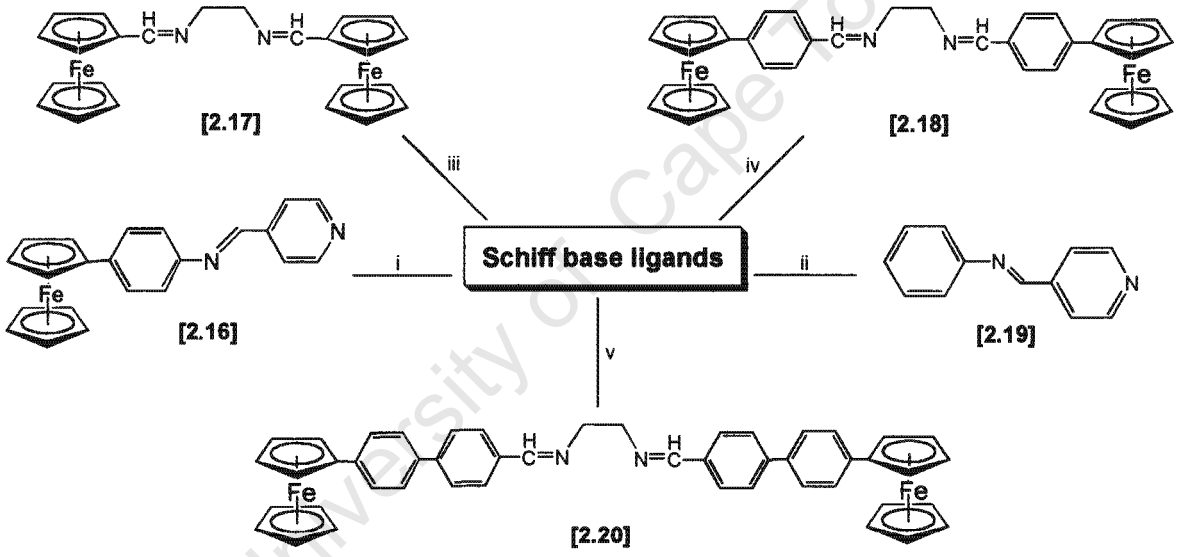

i. 4-Aminophenylferrocene, pyridine-4-carboxaldehyde, 4Å molecular sieves in MeOH; reflux 12 h; maroon flakes 90%

ii. Aniline, pyridine-4-carboxaldehyde, 4Å molecular sieves in MeOH; reflux 12 h; cream flakes 77%

iii. Formylferrocene, ethylenediamine, anhyd. $MgSO_4$ in diethyl ether; stir 24 h at 25 °C; yellow crystals 67%

iv. 4-Formylphenylferrocene, ethylenediamine, anhyd. $MgSO_4$ in Et_2O, stir 4 days at 25 °C; orange powder 18%

v. 4-Formyl-4-biphenylferrocene, ethylenediamine, anhyd. $MgSO_4$ in Et_2O, stir 4 days at 25 °C; orange powder 15%

Figure 2.17: Description of ligands prepared using Schiff base condensation reaction

The Schiff base condensation reaction provided a convenient synthetic route for the preparation of several compounds containing imine bonds, **[2.16]-[2.20]**. It should be noted that although this synthetic route has been well-established for the preparation of the type of compounds shown in *Figure 2.17*, there are associated complications that must be taken into account due to the nature of the reaction. To ensure formation of the desired product, an

efficient dehydrating agent was added to remove water formed during the reaction. This established a shift in the equilibrium reaction, resulting in preparation of the compounds in good yields in some cases. The lower yields observed for **[2.18]** and **[2.20]** were thought to be mainly due to solubility of either the starting material, as was the case for **[2.20]**, or solubility of the product and further separation from the starting material, as in the case for **[2.18]**, rather than choice of dehydrating reagent.

Compound **[2.16]** comprises a phenylene group and imine bond as spacer unit between the ferrocenyl group and pyridyl ring, allowing for study of an extended linear system between these terminal groups. Compound **[2.16]** has been synthesised and coordinated to various metal ions such as tungsten, molybdenum and osmium.[38] As with most ligands investigated here, a conjugated pathway exists within the compound. The ferrocenyl group was observed to behave as an electron donor whereas a further coordinated metal ion may behave as an electron acceptor in a *push-pull* type interaction.[22] Furthermore, the behaviour of complexes containing this ligand for non-linear optical materials has been investigated,[39,40] thus establishing a precedent for study of complexes of this type.

Figure 2.18 shows the preparation of compound **[2.16]**. 4-Nitrophenylferrocene **[2.21]**, was prepared using the diazonium reaction and reduced by catalytic hydrogenation in a Parr hydrogenation reactor, yielding 4-aminophenylferrocene, **[2.22]** in good yield.

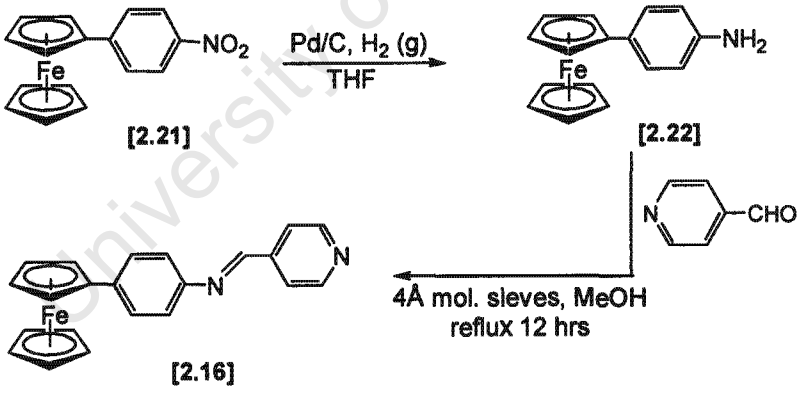

Figure 2.18: Preparation 4-phenylferrocenylimidopyridine *via* a Schiff-base condensation reaction[39]

Compound **[2.16]** was readily isolated in good yield by concentration of the reaction mixture and cooling for at least 5 hours, after which time a further crop of product was obtained from the mother liquor. Dark maroon crystalline flakes were obtained on recrystallising the product from dichloromethane-hexane.

Further variations on **[2.16]** include 4-ferrocenylphenylvinylpyridine, **[2.24]** (see *Figure 2.19*). This particular compound varies from **[2.16]** by a slight variation in the spacer group. An alkene bond replaced the imine bond.

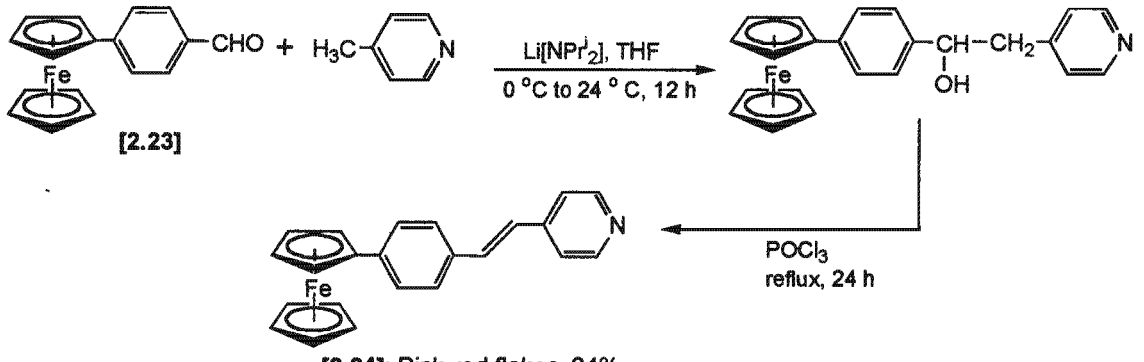

[2.23]

[2.24]: Pink-red flakes, 24%

Figure 2.19: Synthesis of 4-ferrocenylvinylpyridine, **[2.24]**[39]

A specific interest in this study is the role played by the ferrocenyl group. Compound **[2.19]**, was prepared with this in mind, representing the spacer portion of compound **[2.16]**. The study of compound **[2.19]** would enable the determination and to some extent the contribution specific spacers play in the behaviour or activity of the ligand.

Although most ligands investigated are conjugated, allowing for a π-electron pathway, compounds **[2.17]**, **[2.18]** and **[2.20]** are not. Instead, communication between the ferrocenyl groups of the ligand would not readily occur through bond. Compound **[2.17]** can act as a bidentate chelating ligand and would potentially allow for an investigation into the specific role played by the coordinated metal ion. Coordination of a metal ion would result in the formation of a five-membered metallacyle as shown in *Figure 2.20*. Consequently, a pathway for communication between the ferrocenyl groups through the coordinated metal centre could occur, where the nature of communication would depend on the specific metal ion investigated. In addition, ligands **[2.18]** and **[2.10]** have been prepared with additional phenyl groups as spacers. This would allow for further investigations into the nature of spacer groups, particularly in an extended system such as **[2.20]**.

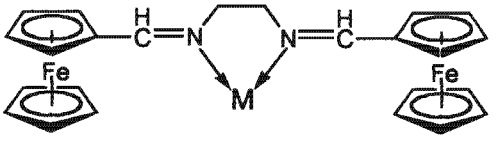

Figure 2.20: Anticipated metal ion coordination to ligand **[2.17]**

The synthesis of compound **[2.17]** has been reported and investigated as a ligand coordinated to both rhodium and iridium metal centres. These complexes were reported as catalysts for the polymerisation of phenylacetylene.[41] However, attempts at repetition of the synthesis of the rhodium complex proved unsuccessful under the reported reaction conditions. The reaction intermediates appeared to be unstable under the reported conditions and were observed to rapidly decompose in solution. Attempted modifications of the synthetic route did not yield the desired product. Further attempts to form coordination complexes with this ligand were not undertaken. Compounds **[2.18]** and **[2.20]** were not investigated further due to their relative insolubility in a range of common organic solvents.

2.3.4 Ferrocenylphosphine ligands

Given the predominance of phosphine donor-ligands and in particular ferrocenylphosphine-donor ligands, two ferrocenylphosphines were included in this study for comparison in terms of reactivity to the ferrocenylpyridine ligands. The commercially available and well-studied 1,1'-bis(diphenylphosphino)ferrocene, **[2.25]** and ferrocenyldiphenylphosphine, the monosubstituted analogue, **[2.26]** were chosen for further complexation studies. Ferrocenyldiphenylphosphine[42] was prepared using the Friedel-Crafts reaction according to the reaction scheme described in *Figure 2.21*. The preparation and activity of rhodium complexes of these ligands is described later with comparisons made to ferrocenylpyridine complexes.

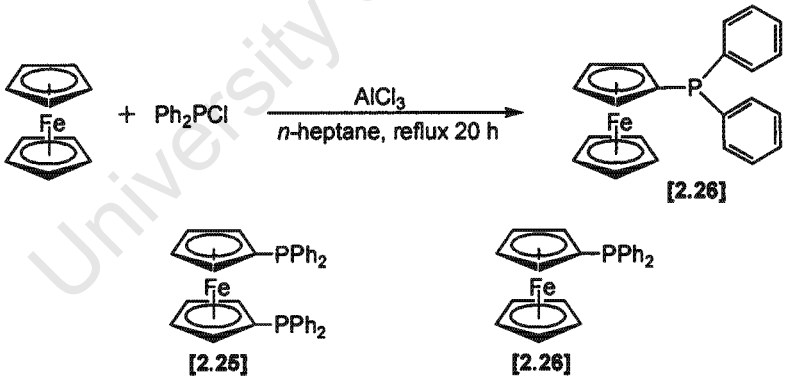

Figure 2.21: Preparation of ferrocenyldiphenylphosphine, **[2.26]**[42]

The conformational flexibility and catalytic activity of 1,1'-bis(diphenylphosphino)ferrocene **[2.25]**, has been studied extensively. A number of metal complexes on coordination to compound **[2.25]**, have shown catalytic activity for a variety of applications. Electrochemical studies of ferrocenylphosphine ligands are, however, somewhat complicated. The redox behaviour of the compound shows the phosphine undergoing a quasi-reversible one-electron

oxidation process based on the ferrocenyl unit, followed by a chemical reaction involving the phosphorus substituent.[43] This is often further complicated by the presence of a coordinated transition metal centre.

The preparation and study of ligands **[2.25]** and **[2.26]**, allows for not only an investigation into the properties of the donor atom but also conformational-activity studies once the ligands are coordinated to various metal ions. A complexed **[2.25]**, for example, would have a relatively rigid conformation with a set bite angle and steric requirements, dictating the reactivity of the complex in turn. It has been described that the bite size and angle of the ligand play a role in its catalytic activity.[44] A complexed **[2.26]** would, however, allow for some freedom of movement within the complex itself, as described in *Figure 2.22*, with however, greater steric hindrance. These factors were taken into account when selecting these ligands for further investigation.

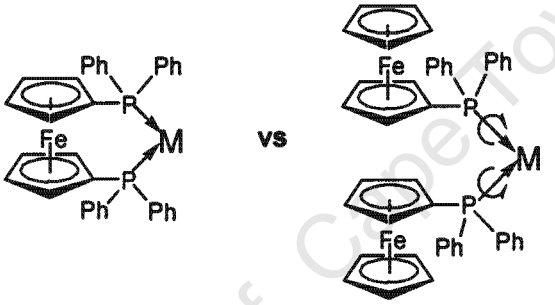

Figure 2.22: Comparison of coordination behaviour of **[2.25]** and **[2.26]**

2.4 Spectroscopic properties

2.4.1 Infrared spectroscopy

Certain characteristic stretching frequencies were observed in all ferrocenyl compounds prepared. Bands at 1110 and 1005 cm^{-1} were observed in most cases and are characteristic of ferrocene. Furthermore a ferrocene C–H stretch and C–C stretch was usually found at 3060-3100 cm^{-1} and 1410-1430 cm^{-1} respectively. An out-of-plane C–H bending band was also observed in the region 810-830 cm^{-1}. Bands due to C–N stretches in pyridine derivatives were observed in the region 1360-1250 cm^{-1} and 1620-1510 cm^{-1} depending on the nature of substituents on the pyridyl ring, while compounds containing imine bonds generally showed stretches in the region 1660-1590 cm^{-1}. The phosphine-donor complexes generally showed absorptions in the region 1310-1320 cm^{-1} that have been assigned to the ferrocenyl-phosphorus group.[42]

2.4.2 NMR spectroscopy

The NMR spectra of the compounds in this study are of interest not only for their identification but also for insight into the electronic contribution of substituents. The ^{1}H NMR spectra provide significant information with regard to the interactions of protons within the pyridyl ring and between the pyridyl protons and the protons of the cyclopentadienyl rings of the ferrocene substituent.

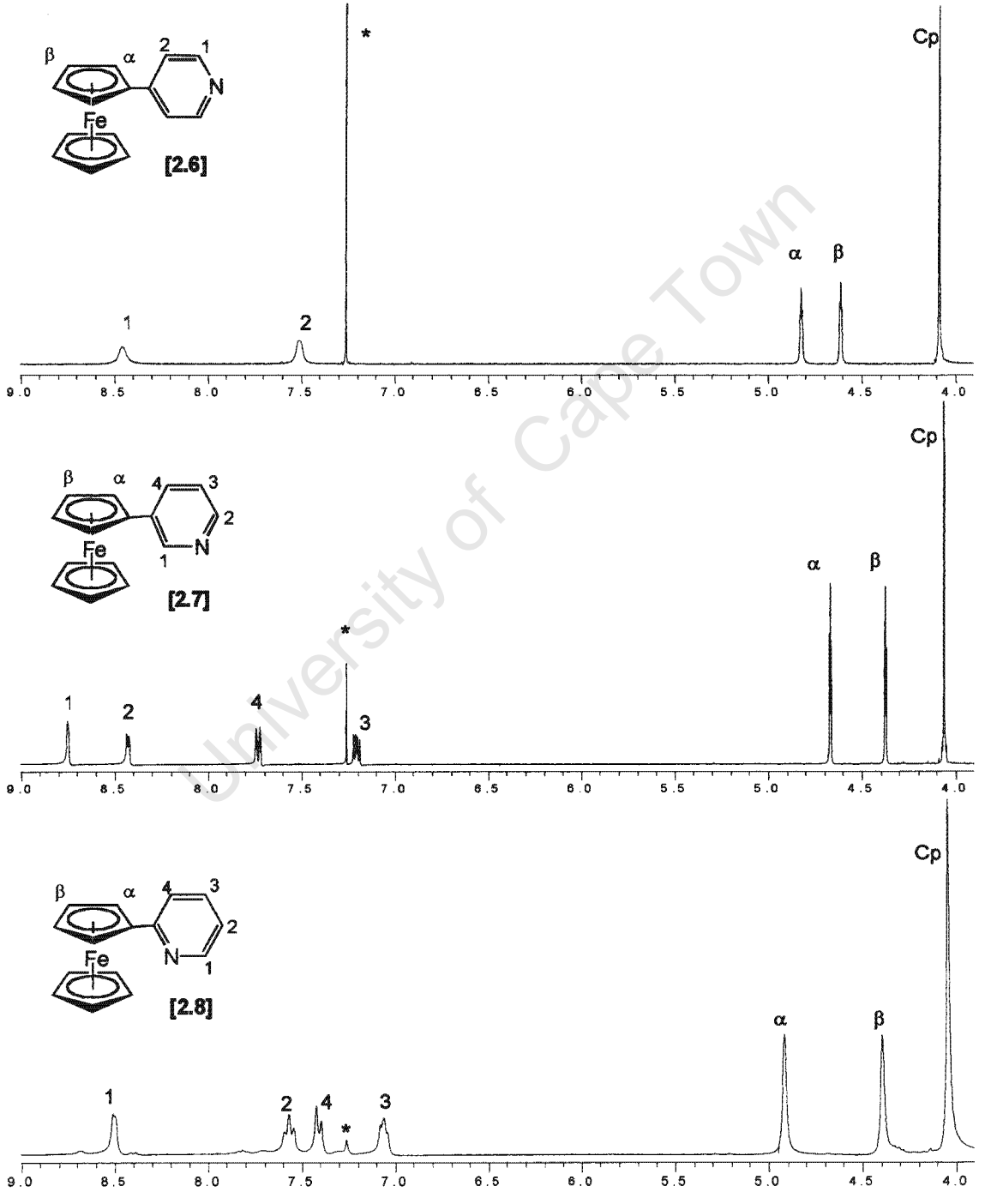

Figure 2.23: ^{1}H NMR spectra of compounds **[2.6]-[2.8]** in $CDCl_3$ (* residual solvent peak)

Figure 2.23 compares the ^{1}H NMR spectra for compounds **[2.6]-[2.8]**. The individual proton resonances have been identified and in particular the ferrocenyl resonances indicated where α and β refer to the respective equivalent protons on the derivatised cyclopentadienyl ring and Cp refers to the unsubstituted cyclopentadienyl ring. The protons occurring on the pyridyl ring have been directly indicated on the respective ^{1}H NMR spectra.

The chemical shift of the unsubstituted cyclopentadienyl ring remains for the most part unchanged, demonstrating that no or limited interaction between the pyridyl ring and unsubstituted cyclopentadienyl ring occur. However, changing the position of the susbstituent on the pyridyl ring has an effect on the electronic shielding of the α and β ferrocenyl protons (these shifts are summarised in *Figure 2.24*). Moving the ferrocenyl substituent along the pyridyl ring from the 4-, 3- and 2-positions results in chemical shifts of 4.61, 4.37 and 4.39 respectively in the case of the β protons and 4.82, 4.67 and 4.92 respectively in the case of the α protons.

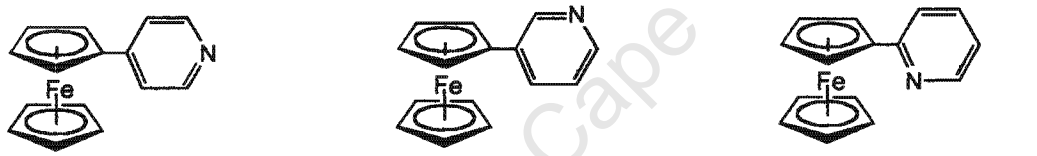

[2.6] α: 4.82, β: 4.61, Cp: 4.08

[2.7] α: 4.67, β: 4.37, Cp: 4.06

[2.8] α: 4.92, β: 4.39, Cp: 4.05

Figure 2.24: Comparison of ferrocenyl chemical shifts for **[2.6]-[2.8]**

The α protons of 2-ferrocenylpyridine show a sharp downfield shift, indicating more strongly deshielded protons, most likely due to the proximity of the electronegative nitrogen atom. Additionally, it is speculated that some interaction may be occurring between the α protons (shown as H_a and $H_{a'}$ in *Figure 2.25*) and the nitrogen-donor atom. Only a single peak has been observed for the α protons, H_a and $H_{a'}$ and they are considered to be equivalent with a situation as described in *Figure 2.25* the most likely scenario. This could be determined through temperature-controlled NMR experiments.

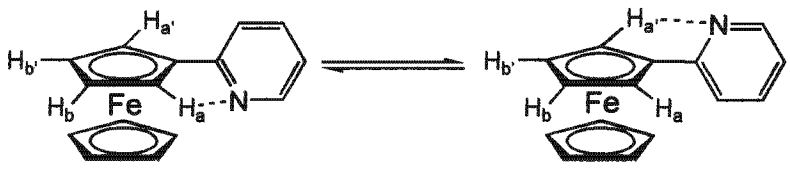

Figure 2.25: Proton interactions in 2-ferrocenylpyridine

Furthermore, the pyridyl protons of **[2.7]** and **[2.8]** show individual resonances for the respective protons due to the position of substitution on the pyridyl ring. Based on the peak assignments in *Figure 2.23*, none of the protons on the pyridyl ring of these compounds are equivalent with proton resonances observed due to the environment of the specific proton.

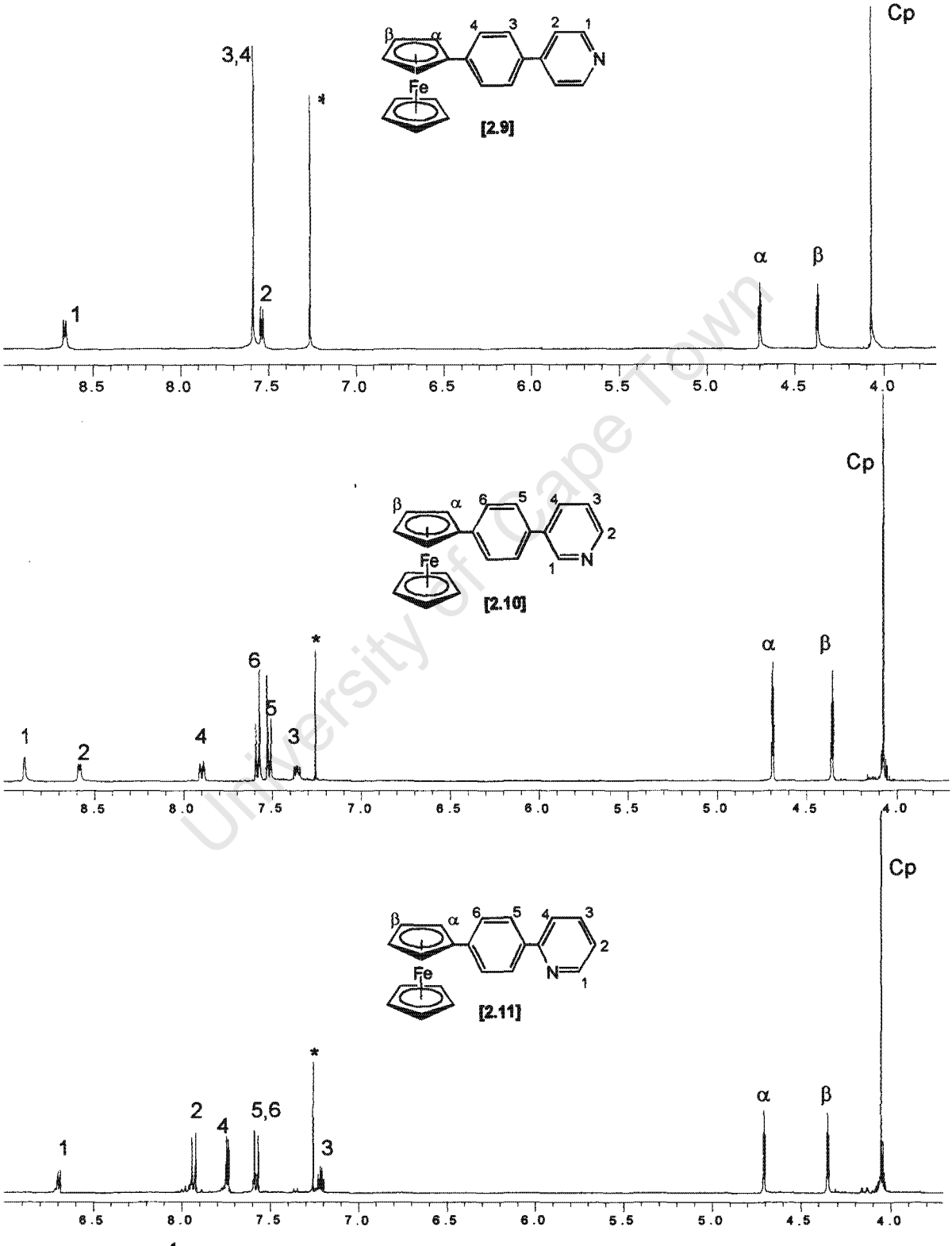

Figure 2.26: ^{1}H NMR of compounds **[2.9]-[2.11]** in $CDCl_3$ (* residual solvent peak)

^{1}H NMR spectra of **[2.9]-[2.11]** have similarly been compared in *Figure 2.26* with the various proton resonances assigned to the respective protons as indicated.

Proton resonances in the ^{1}H NMR spectra of **[2.9]-[2.11]** have similarly been compared in *Figure 2.27* with specific reference to the position of the ferrocenyl protons.

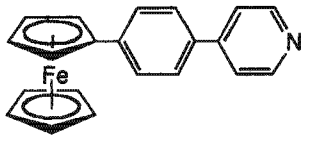

[2.9]

α: 4.70, β: 4.37, Cp 4.07

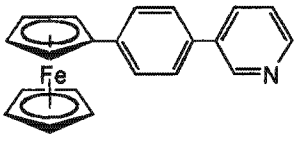

[2.10]

α: 4.69, β: 4.36, Cp 4.07

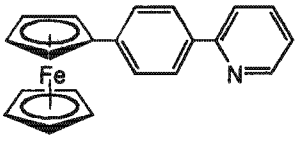

[2.11]

α: 4.71, β: 4.35, Cp 4.05

Figure 2.27: Comparison of ferrocenyl chemical shifts for **[2.9]-[2.11]**

No significant differences in the respective ferrocenyl protons were observed on comparison of compounds **[2.9]-[2.11]**. This is in contrast with the observed shifts in the similar compounds **[2.6]-[2.8]**. The presence of the phenylene spacer group appears to limit the extent of electrostatic interaction between the pyridyl protons and hence, nitrogen donor atom with that of the ferrocenyl protons, despite a conjugated system existing to connect these centres.

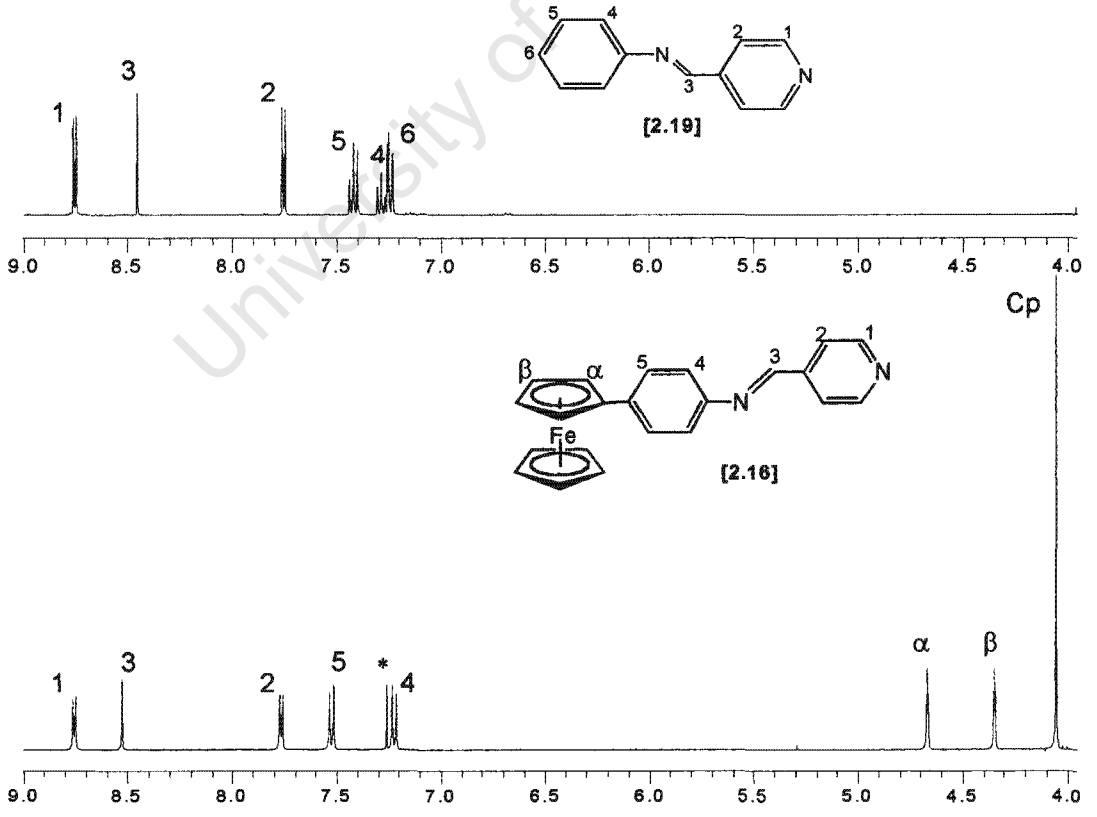

Figure 2.28: ^{1}H NMR of compounds **[2.19]** and **[2.16]** in $CDCl_3$ (* residual solvent peak)

Figure 2.28 compares the ^{1}H NMR spectra of the related compounds **[2.19]** and **[2.16]**. Chemical shifts of the various protons are considered upon introduction of ferrocene in **[2.16]** with peak shifts summarised in *Table 2.1*. These shifts provide some insight into the nature of electrostatic interactions on introduction of ferrocene. On comparison of proton resonances, phenylene protons *5* and *4* show the greatest shifts as expected, while only minor shifts are observed for the pyridyl protons, *1* and *2*. The conjugated nature of the compound is clearly demonstrated through the significant shift observed due to the imine proton, *3*, which was shifted downfield and deshielded due to the presence of the ferrocene group. This effect is also observed on comparison of the imine stretching frequencies of the compounds in the infrared spectra. A shift from 1595 cm^{-1} in **[2.19]** to 1623 cm^{-1} in **[2.16]** on introduction of the ferrocenyl group was observed.

Table 2.1: Comparison of chemical shifts for **[2.19]** and **[2.16]**

	1	3	2	5	4	6	α	β	Cp
[2.19]	8.74	8.44	7.75	7.42	7.31	7.25	–	–	–
[2.16]	8.77	8.54	7.79	7.55	7.22	–	4.68	4.36	4.06

2.5 Cyclic Voltammetry

The redox behaviour of various ferrocenyl compounds prepared in this study was evaluated using cyclic voltammetry. The observed redox behaviour of the respective complexes are all reported with regard to the reversible redox wave of unsubstituted ferrocene, which showed an $E_{½}$ at +75.5 mV under the given conditions in acetonitrile with tetrabutylammonium perchlorate as background electrolyte. Measurements were conducted under an inert atmosphere using a platinum disk working electrode, platinum wire auxiliary electrode and $Ag/AgNO_3$ reference electrode.

Some typical cyclic voltammograms are shown in *Figure 2.29*. Overall, a reversible redox wave similar to the unsubstituted ferrocene was observed for all compounds. However, derivatisation of ferrocene gave a positive shift for all compounds studied, indicating that placing a substituent on the cyclopentadienyl ring of ferrocene made the ferrocene group harder to oxidise. The extent of shift, however, was dependant on the nature of the substituent. Half-wave potentials for several ferrocenyl compounds are listed in *Table 2.2*.

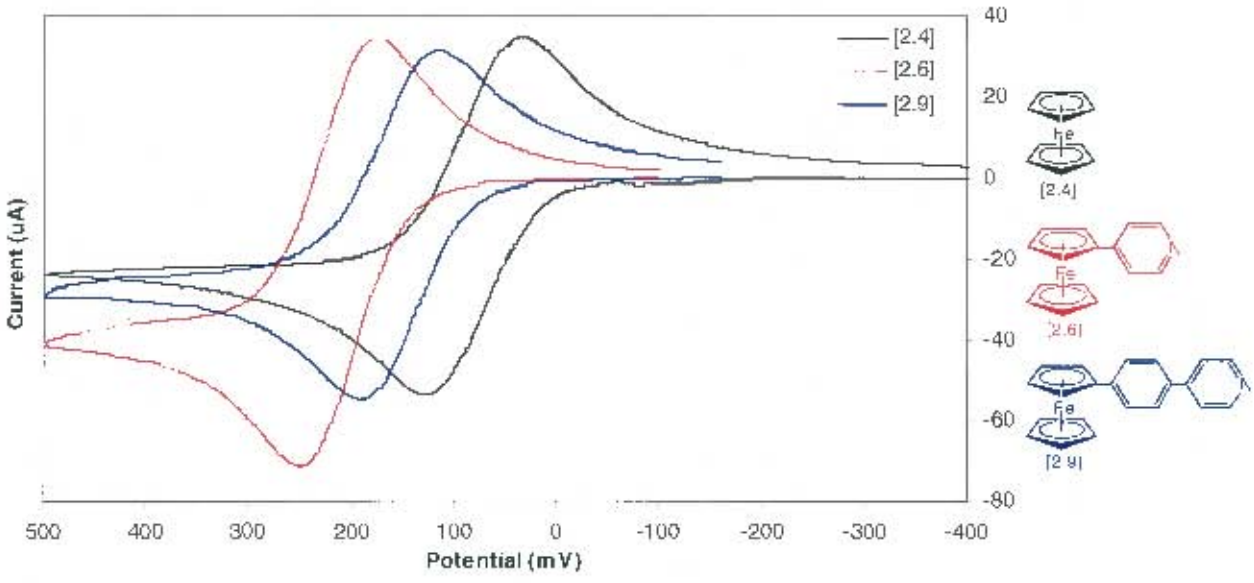

Figure 2.29: Comparison of cyclic voltammograms of ferrocenyl compounds **[2.6]** and **[2.9]** with ferrocene, [**2.4**]

Table 2.2: Half-wave potentials of various ferrocenyl compounds in acetonitrile

Compound number	Compound	E_{pa} / mV	E_{pc} / mV	$E_{½}$ / mv
[2.4]	Ferrocene	+120	+31	+75.5
[2.8]	2-Fcpy	+188	+121	+154.5
[2.7]	3-Fcpy	+204	+131	+167.5
[2.6]	4-Fcpy	+242	+169	+205.5
[2.11]	2-Fc(C_6H_4)py	+161	+92	+126.5
[2.10]	3-Fc(C_6H_4)py	+189	+76	+132.5
[2.9]	4-Fc(C_6H_4)py	+182	+85	+133.5
[2.16]	Fc(C_6H_4)NCpy	+147	+79	+113
[2.27]	Fc(C_6H_4)OCH_2Ph	+112	+39	+75.5

A ferrocenyl compound not previously described has been included in *Table 2.2*. Compound **[2.27]**, unlike the other ferrocenyl compounds in *Table 2.2*, does not have a conjugated network. In addition, compound **[2.27]** does not have a pendant pyridyl group. The effect of the electron-withdrawing pendant pyridyl can be clearly observed as **[2.27]** shows a half-wave potential comparable to ferrocene. Compound **[2.6]** showed the greatest positive shift in half-wave potential with the effect of the pyridyl group clearly demonstrated. Comparison of compounds **[2.6]**, **[2.9]** and **[2.16]** further demonstrated the effect on the electrochemical behaviour of the compound by placing spacer groups between the ferrocenyl group and pyridyl ring. Systematic inclusion of spacer groups showed a half wave potential gradually

closer to that of unsubstituted ferrocene. This indicated that the electron-withdrawing effect became less pronounced with the inclusion of the spacer groups. This effect is also observed on comparison of **[2.7]** and **[2.10]**, as well as **[2.8]** and **[2.11]**.

2.6 Electronic Spectroscopy

The electronic spectra of some of the ferrocenyl compounds prepared were obtained in a dichloromethane solution. Spectral comparisons were made with unsubstituted ferrocene. Ferrocene exhibits two bands at 328 and 443 nm, which have been assigned to $^1A_{2g} \rightarrow {}^1E_{2g}$ and $^1A_{1g} \rightarrow {}^1E_{1g}$ ligand field d-d transitions. Typical electronic spectra obtained are shown in *Figure 2.30*.

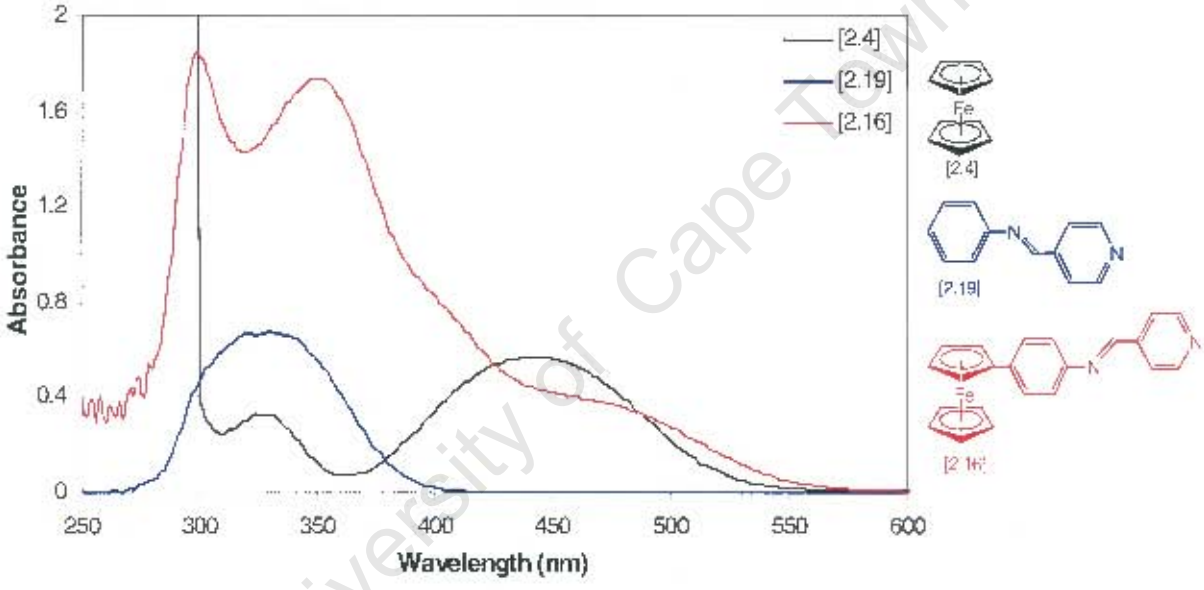

Figure 2.30: Electronic spectra of ferrocene, **[2.4]** with **[2.19]** and **[2.16]** in dichloromethane

In most cases, on substitution of the cyclopentadienyl ring of ferrocene with conjugated substituents, a shift to lower energy in the cyclopentadienyl orbitals was anticipated. An increased mixing of ligand orbitals with metal d orbitals was found. An additional band occurs around 300 nm in the pyridyl ligands with a $\pi \rightarrow \pi^*$ transition due to the conjugated pyridyl substituent.

Comparison of the major bands in the electronic spectra for various ferrocenyl and nitrogen-donor complexes in dichloromethane is summarised in *Table 2.3*. The extinction coefficients are also reported. In most cases, although the weak transition at approximately 450-500 nm due to the ferrocene d-d transition is observed, this band is weak and tends to overlap with

the other ferrocene d-d transition band and was observed as a shoulder. Thus, only two transitions are reported for the high energy $\pi \rightarrow \pi^*$ transition, due to the conjugated pyridyl substituent and for one of the ferrocene d-d transitions. Overall the remaining bands show a bathochromic shift.

Table 2.3: Electronic spectroscopy data for various ferrocenyl and nitrogen donor compounds in dichloromethane

Compound number	Compound	λ_{max} / nm [ε_{max} / mol^{-1}.dm^3.cm^{-1}]	
[2.4]		443 [101]	328 [60]
[2.27]	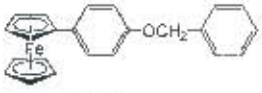	448 [336]	310 [2570]
[2.22]	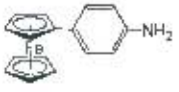	449 [333]	–
[2.16]	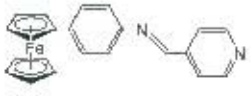	353 [12109]	287 [18113]
[2.19]	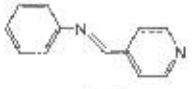	–	330 [3532]
[2.8]	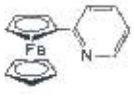	452 [384]	332 [1559]
[2.7]	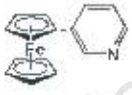	448 [381]	332 [1530]
[2.6]	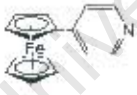	454 [481]	342 [1470]

Further discussion with regard to relative shift of transitions is made later with discussion of complexes of several of the ferrocenyl compounds prepared here.

2.7 Concluding remarks

A series of ferrocenylpyridine ligands were successfully prepared using the synthetic routes described above. The properties of these compounds were further investigated using several spectroscopic techniques. Some of the compounds described above were further examined in coordination studies with rhodium, iridium, palladium and platinum, the results of which are described in *Chapter 3*.

References:

1. *Ferrocenes: Homogeneous Catalysis, Organic Synthesis, Material Science*, eds. A. Togni and T. Hayashi, VCH, Weinheim, 1995 and references therein.
2. T. Hayashi, A. Katsumura, M. Konishi and M. Kumada, *Tetrahedron Lett.*, 1979, 425; W. R. Cullen, F. W. B. Einstein, T. Jones and T. J. Kim, *Organometallics*, 1983, **2**, 741; M. Kitamura, M. Tokunaga, T. Ohkuma and R. Noyori, *Org. Synth.*, 1993, **71**, 1; M. J. Burk, A. Gerlach and D. Semmeril, *J. Org. Chem.*, 2000, **65**, 8933.
3. A. Togni and L. M. Venanzi, *Angew. Chem. Int. Ed. Engl.*, 1994, **33**, 497.
4. P. D. Beer, O. Kocian and R. J. Mortimer, *J. Chem. Soc., Dalton Trans.*, 1990, 3283; C. Kaes, A. Katz and M. W. Hosseini, *Chem. Rev.*, 2000, **100**, 3553; T-J. J. Kinnunen, M. Haukka and T. A. Pakkanen, *J. Organomet. Chem.*, 2002, **654**, 8.
5. D. Choudhury and D. J. Cole-Hamilton, *J. Chem. Soc., Dalton Trans.*, 1982, 1885; K. Toyohara, H. Nagao, T. Adachi, T. Yoshida and K. Tanaka, *Chem. Lett.*, 1996, 27; A. J. Pardey, M. Fernández, J. Alvarez, C. Urbina, D. Moronta, V. Leon, M. Haukka and T. A. Pakkanen, *Appl. Catal. A: General*, 2000, **199**, 275.
6. M. Diéguez, M.-N. Collomb and R. H. Crabtree, *J. Organomet. Chem.*, 2000, **608**, 146.
7. H. Adams, N. A. Bailey, D. W. Bruce, R. Dhillon, D. A. Dunmur, S. E. Hunt, E. Lalinde, A. A. Maggs, R. Orr, P. Styring, M. S. Wragg and P. M. Maitlis, *Polyhedron*, 1988, **7**, 1861; P. Espinet, E. Lalinde, M. Marcos, J. Perez and J. L. Serrano, *Organometallics*, 1990, **9**, 555.
8. A-M. Groud-Godquin, J.-C. Marchon, D. Guillon and A. Skoulios, *J. Phys. Chem.*, 1986, **90**, 5502.
9. D. W. Bruce, E. Lalinde, P. Styring, D. A. Dunmur and P. M. Maitlis, *J. Chem. Soc., Chem. Commun.*, 1985, 581; D. W. Bruce, D. A. Dunmur, M. A. Esteruelas, S. E. Hunt, R. Le Lagadec, P. M. Maitlis, J. R. Marsden, E. Sola and J. M. Stacey, *J. Mater. Chem.*, 1991, **1**, 251.
10. J. Malthête and J. Billard, *Mol. Cryst. Liq., Cryst.*, 1976, **34**, 117; J. Bhatt, B. M. Fung, K. M. Nicholas and C.-D. Poon, *J. Chem. Soc., Chem. Commun.*, 1988, 1439; C. Loubser, C. Imrie and P. H. van Rooyen, *Adv. Mater.*, 1993, **5**, 45; C. Imrie, P. Engelbrecht, C. Loubser and C. W. McCleland, *Appl. Organomet. Chem.*, 2001, **15**, 1.
11. J. A. Casares, P. Espinet, J. M. Martin-Alvarez, G. Espino, M. Pérez-Manrique and F. Vattier, *Eur. J. Inorg. Chem.*, 2001, 289.
12. H.-S. Lee, J.-Y. Bae, J. Ko, Y. S. Kang, H. S. Kim, S.-J. Kim, J.-H. Chung and S. O. Kang, *J. Organomet. Chem.*, 2000, **614-615**, 83.
13. W. A. Herrmann and B. Cornils, *Angew. Chem. Int. Ed. Engl.*, 1997, **36**, 1048.

14. T.-J. Kim, D.-H. Kim, S.-C. Shim and J.-H. Jeong, *Bull. Korean Chem. Soc.*, 1995, **16**, 1126.
15. T. J. Kealy and P. L. Pauson, *Nature*, 1951, **168**, 1039.
16. S. A. Miller, J. A. Tebboth and J. F. Tremaine, *J. Chem. Soc.*, 1952, 632.
17. O. Carugo, G. De Santis, L. Fabbrizzi, M. Licchelli, A. Monichino and P. Pallavicini, *Inorg. Chem.*, 1992, **31**, 765; K. Schlögl and M. Fried, *Monatsh. Chem.*, 1963, **94**, 537.
18. G. Gritzner and J. Küta, *J. Pure Appl. Chem.*, 1984, **56**, 462.
19. Y. Yamada, J. Mizutani, M. Kurihara and H. Nishihara, *J. Organomet. Chem.*, 2001, **637-639**, 80.
20. E. M. Barranco, O. Crespo, M. C. Gimeno, P. G. Jones, A. Laguna and M. D. Villacampa, *J. Organomet. Chem.*, 1999, **592**, 258.
21. T. M. Miller, K. J. Ahmed and M. S. Wrighton, *Inorg. Chem.*, 1989, **28**, 2347.
22. W.-Y. Wong, W.-T. Wong and K.-K. Cheung, *J. Chem. Soc., Dalton Trans.*, 1995, 1379; W.-Y. Wong and W.-T. Wong, *J. Chem. Soc., Dalton Trans.*, 1996, 3209.
23. J. C. Calabrese, L.-T. Cheng, J. C. Green, S. R. Marder and W. Tam, *J. Am. Chem. Soc.*, 1991, **113**, 7227.
24. C. Kollmar, M. Conty and D. Kahn, *J. Am. Chem. Soc.*, 1991, **113**, 7994; E. Coronado, M. Clemente-León, J. R. Galán-Mascarós, C. Giménez-Saiz, C. J. Gómez-Garcia and E. Martínez-Ferrero, *J. Chem. Soc., Dalton Trans.*, 2000, 3955.
25. E. C. Constable, *Angew. Chem. Int. Ed. Engl.*, 1991, **30**, 407.
26. M. A. Esteruelas, E. Sola, L. A. Oro, M. B. Ros, M. Marcos and J. L. Serrano, *J. Organomet. Chem.*, 1990, **387**, 103.
27. M. Laskoski, W. Steffen, M. D. Smith and U. H. F. Bunz, *J. Chem. Soc., Chem. Commun.*, 2001, 691.
28. K. Tamao, K. Sumitani, Y. Kiso, M. Zembayashi, A. Fujioka, S-I. Kodama, I. Nakajima, A. Minato and M. Kumada, *Bull. Chem. Soc. Jpn.*, 1976, **49**, 1958.
29. R. W. Fish and M. Rosenblum, *J. Org. Chem.*, 1965, **30**, 1253.
30. Y.-H. Han, M. J. Heeg and C. H. Winter, *Organometallics*, 1994, **13**, 3009.
31. M. D. Rausch and D. J. Ciappenelli, *J. Organomet. Chem.*, 1967, **10**, 127.
32. J. G. P. Delis, P. W. N. M. van Leeuwen, K. Vrieze, N. Veldman, A. L. Spek, J. Fraanje and K. Goubitz, *J. Organomet. Chem.*, 1996, **514**, 125.
33. T. Sammakia and H. A. Latham, *J. Org. Chem.*, 1996, **61**, 1629.
34. D. R. Coulson, *Inorg. Synth.*, 1972, **13**, 121.
35. M. E. Wright, *Organometallics*, 1990, **9**, 853; R. Sanders, U. T. Mueller-Westerhoff, *J. Organomet. Chem.*, 1996, **512**, 219; T. Sammakia and H. A. Latham, *J. Org. Chem.*, 1996, **61**, 1629; C.-M. Liu, S.-J. Lou and Y.-M. Liang, *Synth. Commun.*, 1998, **28**, 2271;

C.-M. Liu, B.-H. Chen, W.-Y. Liu, X.-L. Wu and Y.-X. Ma, *J. Organomet. Chem.*, 2000, **598**, 348; C.-M. Liu, Y.-L. Guo, X.-L. Wu, Y.-M. Liang and Y.-X. Ma, *J. Organomet. Chem.*, 2000, **612**, 172.

36. C.-M. Liu, S.-J. Lou and Y.-M. Liang, *Synth. Commun.*, 1998, **28**, 2271.
37. K. Tani, T. Mihana, T. Yamagata and T. Saito, *Chem. Lett.*, 1991, 2047.
38. H. Kersten and P. Boldt, *J. Chem. Research (S)*, 1994, 366.
39. M. M. Bhadbhade, A. Das, J. C. Jeffery, J. A. McCleverty, J. A. N. Badiola and M. D. Ward, *J. Chem. Soc., Dalton Trans.*, 1995, 2769.
40. S. Sakanishi, D. A. Bardwell, S. Couchman, J. C. Jeffery, J. A. McCleverty and M. D. Ward, *J. Organomet. Chem.*, 1997, **528**, 35.
41. S.-I. Lee, S.-C. Shim and T.-J. Kim, *J. Polym. Sci.: Part A: Polym. Chem.*, 1996, **34**, 2377.
42. G. P. Sollot, H. E. Mertwoy, S. Portnoy and J. L. Snead, *J. Org. Chem.*, 1963, **28**, 1090.
43. E. M. Barranco, O. Crespo, M. C. Gimeno and A. Laguna, *Inorg. Chem.*, 2000, **39**, 680.
44. J.-F. Ma and Y. Yamamoto, *J. Organomet. Chem.*, 1999, **574**, 148.

Chapter 3: Preparation of Multinuclear Complexes

3.1 Introduction

Transition metal complexes, particularly those containing redox-active fragments such as the ferrocenyl group are increasingly being investigated for a variety of potential uses such as those in the fields of catalysis and materials science.[1] These complexes, principally those linked through conjugated pathways, can exhibit electrochemical behaviour that has been associated with unusual catalytic activity due to the availability of several different metal sites.[2]

The possibility exists of generating chemical and physico-chemical variations in the coordination properties of the transition metal ion by making redox changes in attached redox-active fragments such as a ferrocenyl group. The tuning of electron density in the transition metal without changing its actual coordination sphere potentially provides an avenue to control reactivity at this centre.[3] This premise has largely formed the basis for the study of the electrochemical behaviour of multimetallic complexes. Electronic interactions are generally studied in systems containing metals separated through a system of conjugated bonds, since this has been shown to facilitate interaction of the respective metal centres.[4]

Currently, applications of these electronic interactions are largely in the field of materials chemistry and have provided materials with non-linear optical properties and materials that can act as redox switches and redox active sensors.[4,5] Several novel bis(ferrocenyl) ligands have been prepared and studied as metal cation sensors.[5] These complexes showed shifts in the redox potential of the ferrocenyl group on binding of various cations to the receptor site. These complexes are reported to be selective for magnesium and zinc cations.

There are several different methodologies available for the study of redox-active complexes.[4] In this investigation several pyridyl ligands have been prepared with variations in substituent on the pyridyl ring as well as variation in position of substitution on the ring. Electronic interactions between the pyridyl ligand and coordinated metal centre can be monitored by looking at changes in chemical shift values for the free ligand and coordinated complex in the NMR spectra. These shifts can be correlated to the specific coordinated metal ion and the the substituent on the pyridyl ring. Furthermore, the effect of incorporating spacer groups in

systems containing ferrocenylpyridine ligands can be evaluated on the basis of considering changes in the chemical shifts of the ferrocenyl cyclopentadienyl protons.

A further means of examining these complexes is through the use of electronic spectroscopy and electrochemistry. Due to the conjugated nature of the systems under investigation, study of their intermolecular interactions is possible using electronic spectroscopy. A comparison of the complexes in terms of variation in wavelength shift and extinction coefficient can be made. This information can be considered in terms of ligand variation in systems with a given metal centre. Cyclic voltammetry is particularly useful in evaluating systems containing redox-active groups such as ferrocene. Provided single crystals can be obtained, X-ray crystallography is a particularly useful technique for the examination and comparison of the investigated complexes.

Considering the properties of the investigated ferrocenylpyridine compounds, a series of multinuclear complexes were prepared with several transition metal centres. The properties of these complexes were further evaluated in terms of electronic interactions. The crystal structure analysis of several of these complexes was considered and the effect of substituents on the pyridyl ring evaluated in terms of bond lengths and angles.

3.2 Preparation and properties of rhodium complexes

Rhodium(I) is known to readily form coordination complexes with π acceptor ligands. Most complexes are of the square planar type, although some five-coordinate species are known. Many of the square planar rhodium complexes have high catalytic activity due mainly to the metal being able to increase its coordination number by accepting ligands in the apical sites.[6] This behaviour of rhodium(I) complexes has led to an extensive systematic study of phosphine-donor complexes of the metal.

This has changed to some extent over recent years since pyridines and bipyridines have been actively sought as linkers to solid polymer supports in a bid to bridge the divide between homogeneous and heterogeneous catalysis. An example of this includes catalysis of the water-gas shift reaction. This reaction usually produces hydrogen and carbon dioxide from gaseous water and carbon monoxide over a solid metal oxide catalyst at high temperatures.[7] Initial investigations were reported as under homogeneous conditions with a lower thermal environment and the use of liquid water. This allowed a mechanistic study of the reaction and hence, led to greater catalyst efficiency.[8] Once the efficiency of the rhodium pyridine-containing systems was established, further comparisons with heterogeneous counterparts

using *cis*-$[Rh(CO)_2(amine)_2]PF_6$ complexes (where amine = 4-picoline, 2-picoline, pyridine or 2,6-lutidine) linked to 4-vinylpyridine polymer supports were carried out leading to the application of this work to several other reactions such as a catalytic reduction of nitrobenzene to aniline, under water-gas shift reaction conditions.[9]

3.2.1 Rhodium carbonyl complexes

The rhodium(I) carbonyl dimer, dichlorotetracarbonyldirhodium **[3.1]**, represents a convenient and readily obtained starting material for the preparation of numerous monomeric rhodium complexes. The type of complex formed from **[3.1]** is dependant on the nature of the ligand being complexed, the ratio of the metal-to-ligand and the solvent in which the reaction is performed. The dimer is readily prepared from the reaction of carbon monoxide with rhodium trichloride trihydrate[10] and was first reported in 1925[11] but only correctly identified in 1943.[12] Since then, the dimer has been reacted with several nitrogen-donor ligands[13] as well as ligands containing other donor atoms *via* a bridge-splitting reaction. The preparation of complexes retaining some carbonyl groups allows for their study using a number of physical methods. The position of carbonyl stretching frequencies in the infrared spectrum for example, provides significant information about the electron density of the rhodium metal centre. These properties facilitate the study of rhodium(I) carbonyl complexes. These complexes have a variety of catalytic applications[14] and have interesting biological activity.[15]

The rhodium(I) carbonyl monosubstituted pyridyl coordination complexes in this study were prepared through a bridge-splitting reaction of the rhodium carbonyl dimer, **[3.1]**. The complexes were prepared using the synthetic route shown in *Figure 3.1*. A bridge-splitting reaction of the dimer was carried out in a low coordinating solvent with solvation of the monosubstituted rhodium leading to the formation of a monomeric species. This was followed by addition of the ligand with the product formed by displacement of the solvent molecule.

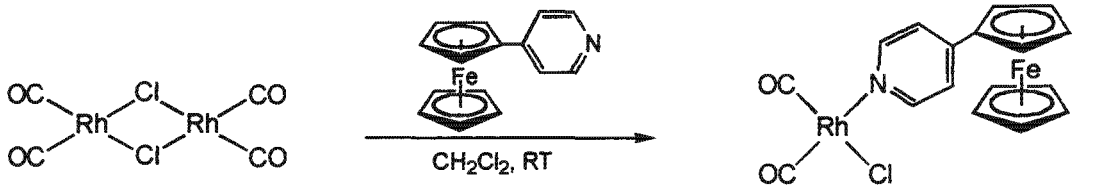

[3.1] **[3.4]**: Red microcrystals, 69%

Figure 3.1: Synthetic route for the preparation of **[3.4]**

An alternative synthetic route is also available. The rhodium carbonyl dimer may be substituted for the related cyclooctadienyl dimer **[3.7]** and this leads to the formation of the analogous cyclooctadienyl complexes. The carbonyl complexes may be obtained by bubbling

a solution of the cyclooctadienyl complex with carbon monoxide gas. The labile cyclooctadienyl group is displaced by the carbonyl ligands. Due to the obvious safety disadvantages, the use of the rhodium carbonyl dimer provides a more convenient method for the preparation of the rhodium carbonyl complexes.

The complexes **[3.2]**-**[3.6]** (see *Figure 3.2*) were prepared using the synthetic route shown in *Figure 3.1*. It was found that in some cases the intermediates formed in the reaction were unstable in solvents such as dichloromethane. Accordingly, reactions were carried out in pentane, as for the preparation of compound **[3.2]**.

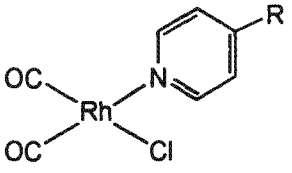

[3.2]: R = H; orange powder, 81%

[3.3]: R = NH_2; dark yellow powder, 64%

[3.4]: R = Fc; red microcrystals, 69%

[3.5]: R = (CH=N)-Ph; yellow crystals, 63%

[3.6]: R = (CH=N)(C_6H_4)Fc; maroon needles, 61%

Figure 3.2: Rhodium carbonyl complexes **[3.2]**-**[3.6]** prepared

Complexes **[3.2]**-**[3.6]** were obtained in good yield. The effect of derivatising the pyridyl ligand as well as the effect of the substituent on the electron density at the rhodium metal centre was reflected in shifts in the carbonyl stretching frequencies in the infrared spectrum. Infrared spectra were all recorded as potassium bromide pellets with strong bands obtained at 2091 and 2016 cm^{-1} for complex **[3.2]** assigned to the carbonyl stretching frequencies of the *cis*-isomer. The introduction of the amine group in **[3.3]** showed a shift in the bands to 2076 and 2012 cm^{-1} while substitution of a ferrocenyl group in complex **[3.4]**, showed shifts to 2086 and 2011 cm^{-1}. The presence of the elongated ligands in **[3.5]** and **[3.6]** resulted in shifts of 2088 and 2013 cm^{-1} as well as 2080 and 2003 cm^{-1} respectively. Comparison of shifts in the carbonyl stretching frequency of **[3.2]** with **[3.3]**-**[3.6]** showed a shift to lower energy. This corresponded to an increased electron density at the rhodium metal centre. The extent of shift appeared to depend on the nature of the substituent on the pyridyl ring.

A further comparison can be made between the free ligand and complex in both **[3.5]** and **[3.6]** by evaluating the imine stretching frequency. A stretching frequency of 1595 cm^{-1} was obtained for the free ligand in **[3.5]**. This shifted to 1605 cm^{-1} on complexation to the rhodium metal centre. Similarly, a shift from 1623 cm^{-1} to 1643 cm^{-1} was observed on complexation in **[3.6]**. This was attributed to a lowering in energy on coordination of the ligand to the rhodium metal centre.

Comparison of carbonyl chemical shifts in the ^{13}C NMR proved difficult as in most cases the peaks observed were very broad and of low intensity. In some instances, they were not observed at all. The carbonyl stretching frequencies observed in the infrared spectrum conversely, were all intense, facilitating the type of comparison described above. Minor chemical shifts in the ^{1}H NMR between the free ligand and coordinated complex were observed mainly on the α-proton adjacent to the nitrogen-donor atom on the pyridyl ring. Shifts in the position of the imine bond proton in **[3.5]** and **[3.6]** were also observed on comparison of the free ligand with complex, with downfield shifts of 8.44 to 8.81 ppm and 8.54 to 8.57 ppm respectively. This indicated a deshielding of these protons on complexation.

Comparing the cyclopentadienyl ^{1}H NMR chemical shifts of the ferrocenyl groups of **[3.4]** and **[3.6]** as well as relative to the free respective ligands, assisted in the evaluation of the effect of the spacer group. Furthermore, the effect of coordinating the rhodium metal centre could be determined on comparison of the free ligand and complex NMR spectra (see *Figure 3.3*).

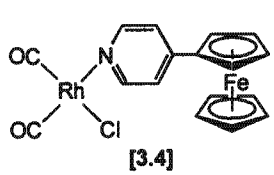

[3.4]

α-H: 4.76; β-H: 4.56; Cp: 4.08 **[3.4]**

α-H: 4.82; β-H: 4.61; Cp: 4.08 **(ligand)**

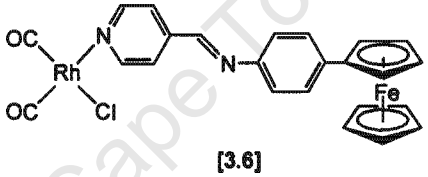

[3.6]

α-H: 4.68; β-H: 4.36; Cp: 4.06 **[3.6]**

α-H: 4.68; β-H: 4.36; Cp: 4.06 **(ligand)**

***Figure 3.3*:** Comparison of ^{1}H NMR chemical shifts (ppm) for the ferrocenyl substituents of **[3.4]** and **[3.6]** respectively

The difference in chemical shift values due to the presence of spacer groups has been noted on comparison of the free ligands, accounting for the differences in shifts between the α-H and β-H in **[3.4]** and **[3.6]**. On comparing the shifts due to the complex with that of the free ligand, no significant differences could be established between these specific chemical shifts in **[3.6]**. It would appear that the long-range conjugative effect between the rhodium metal centre and the ferrocenyl group was reduced by the presence of the spacer, despite a conjugated system of bonds between the two. This proposal is leant some validity when comparing the differences between the free ligand and complex for **[3.4]**.

3.2.2 Rhodium cyclooctadiene complexes

The development of rhodium(I) cyclooctadienyl ligand complexes has been observed since the preparation of the rhodium cyclooctadienyl dimer, chloro(l,5-cyclooctadiene)rhodium(I) **[3.7]**, was first reported.[16] The dimer can be readily prepared by the reaction of excess

cyclooctadiene and rhodium trichloride trihydrate. The cyclooctadienyl dimer is known to readily undergo a bridge-splitting reaction on addition of an uncharged monodentate ligand. These types of monomeric complexes have been studied for their catalytic properties.[14,17] The presence of the labile cyclooctadienyl ligand appears to promote catalytic activity by readily dissociating as part of the catalytic cycle. Some investigations have also been carried out on the potential application of these complexes as bacteriocidal, viricidal and anti-neoplastic agents.[18]

3.2.2.1 Rhodium complexes with a single N-donor ligand [RhCl(COD)L]

Several nitrogen-donor ligands were coordinated to the rhodium metal centre using a bridge split in the rhodium dimer followed by addition of the ligand (see *Figure 3.4*).

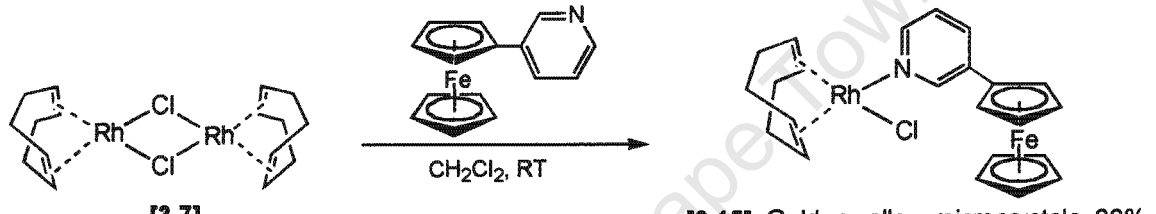

[3.7] **[3.15]**: Golden yellow microcrystals, 88%

Figure 3.4: Synthetic scheme for the preparation of rhodium cyclooctadiene complexes

Using this synthetic route, a series of complexes shown in *Figures 3.5* and *3.6* were prepared. Complexes **[3.8]**-**[3.11]** compare the effect of derivatising the pyridyl ligand with a set of conjugated substituents of increasing length. They also contain ligands that are representative of the spacer portion of several ferrocenyl ligands.

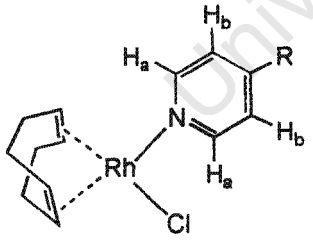

[3.8]: R = H; bright yellow crystals, 62%

[3.9]: R = Ph; bright yellow crystals, 80%

[3.10]: R = (CH=N)-Ph; fine yellow crystals, 83%

[3.11]: R = (CH=CH)(C_6H_4)-OC_8H_{17}; light yellow powder, 67%

Figure 3.5: Rhodium cyclooctadiene pyridyl complexes **[3.8]**-**[3.11]**

Changes in the pyridyl proton chemical shift values were observed on variation of the substituent on the pyridyl ring (indicated as H_a and H_b in *Figure 3.5*). More pronounced shifts in H_a proton values were observed. Complex **[3.8]** showed chemical shifts at 8.76 and 7.32 ppm while introduction of the phenylene substituent in **[3.9]**, showed a shift of these peaks to 8.75 and 7.57 ppm for H_a and H_b respectively. Complex **[3.10]** showed a more pronounced shift of 8.88 and 7.46 ppm for H_a and H_b. A slight shift in the imine proton peak position to from 8.44 to 8.47 ppm was observed on complexation for complex **[3.10]**. This was also

compared to the related carbonyl complex, **[3.5]** where an imine peak was observed at 8.81 ppm. Complex **[3.11]** showed shifts in both sets of pyridyl ring protons to 8.60 and 7.30 ppm respectively.

The direction of shifts in peak positions on comparison of free ligand and complex are similar for both the carbonyl and cyclooctadienyl complexes. The positional shifts were overall more pronounced in the carbonyl complexes. This may be accounted for by considering the synergistic effect of the carbonyl groups on the metal through significant π back-bonding interaction.

Complexes **[3.12]**-**[3.18]** include ferrocenyl substituents on the pyridyl ring. These complexes were prepared in relatively good yield using the general synthetic route described in *Figure 3.4*. Several structural comparsions can be made between these complexes and the effect considered in terms their impact on the rhodium metal centre. Complex **[3.19]** is a pyrrole with the nitrogen donor atom occurring on the cyclopentadienyl ring of the 1',2',3',4',5'-pentamethylazaferrocene compound.

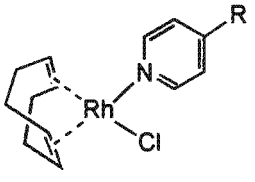

[3.12]: R = Fc; orange solid, 78%

[3.13]: R = (C_6H_4)Fc; dark red powder, 70%

[3.14]: R = $(CH{=}N)(C_6H_4)$Fc; red crystalline flakes, 75%

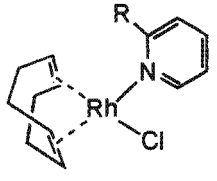

[3.17]: R = Fc;orange-brown powder, 31%

[3.18]: R = (C_6H_4)Fc; orange powder, 40%

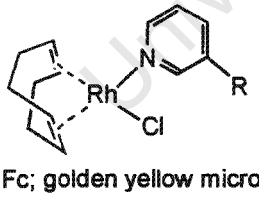

[3.15]: R = Fc; golden yellow microcrystals, 88%

[3.16]: R = (C_6H_4)Fc; orange-mustard powder, 69%

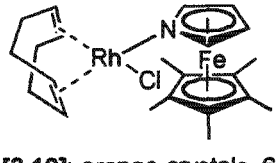

[3.19]: orange crystals, 62%

Figure 3.6: Rhodium complexes with ferrocenyl nitrogen donor ligands **[3.12]**-**[3.19]**

The ^{1}H NMR chemical shifts of the ferrocenyl cyclopentadienyl protons serve as a good indication of the nature of electrostatic interactions within the complex, particularly when comparing those of the free ligand with that of the rhodium complex. A comparison of cyclopentadienyl chemical shifts for selected complexes is shown in *Figure 3.7*, where the extent of shifts varies with the gradual inclusion of spacer groups in the ferrocenyl ligand.

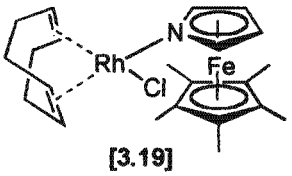

[3.19]

α-H: 5.33, β-H: 4.53 **[3.19]**

α-H: 4.36, β-H: 3.98 **(Ligand)**

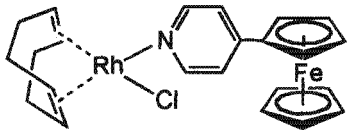

[3.12]

α-H: 4.69, β-H: 4.47, Cp: 4.04 **[3.12]**

α-H: 4.82, β-H: 4.61, Cp: 4.08 **(Ligand)**

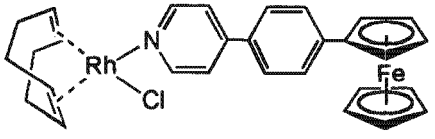

[3.13]

α-H: 4.68, β-H: 4.37, Cp: 4.05 **[3.13]**

α-H: 4.70, β-H: 4.37, Cp: 4.07 **(Ligand)**

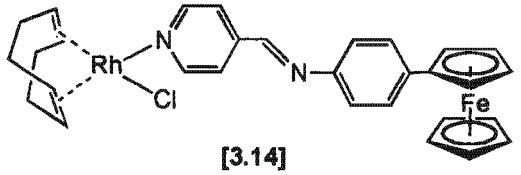

[3.14]

α-H: 4.66, β-H: 4.35, Cp: 4.03 **[3.14]**

α-H: 4.68, β-H: 4.36, Cp: 4.06 **(Ligand)**

Figure 3.7: Comparison of ^{1}H NMR chemical shifts (ppm) for ferrocenyl substituents of **[3.19]** and **[3.12]**-**[3.14]** respectively

The cyclopentadienyl protons for complexes **[3.12]**-**[3.14]** showed similar chemical shift values, while only **[3.12]** showed significant differences on comparison of the free ligand and complex. The α-H and β-H in **[3.12]** showed upfield shifts relative to the free ligand, indicating shielding of these protons on coordination of the rhodium metal centre, similar to the related carbonyl complex, **[3.4]**. The comparable chemical shifts obtained for the free ligand and complex for both **[3.13]** and **[3.14]** indicated a reduced conjugative effect between the ferrocenyl group and rhodium metal centre due to the presence of the spacer groups. Complex **[3.19]**, contrary to complex **[3.12]**, showed significant downfield shift on complexation of the rhodium metal centre. This indicated deshielding of these protons. The complex was paramagnetic with broad signals obtained in the ^{1}H NMR.

The H_a pyridyl protons shifted downfield for complexes **[3.12]**-**[3.14]** and were thus deshielded on complexation to the rhodium metal centre. The imine bond proton in **[3.14]** showed an upfield shift on complexation of the rhodium metal centre. The H_b pyridyl protons showed upfield shifts on complexation to an extent dependant on the substituent on the pyridyl ring for these complexes.

Comparison of ferrocenyl proton chemical shifts for complexes **[3.15]**-**[3.18]** showed no significant differences between the free ligand and complex (see *Figure 3.8*). In general, the α-H's of the respective complexes were significantly downfield to suggest some deshielding due to the presence of the nitrogen-donor atom. The pyridyl protons for each of the complexes showed a downfield shift, indicating deshielding of these protons on coordination of the rhodium metal centre.

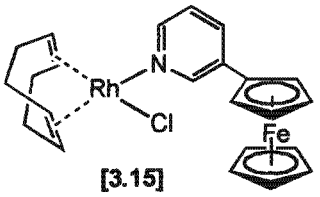

[3.15]

α-H: 4.66, β-H: 4.40, Cp: 4.08 **[3.15]**

α-H: 4.67, β-H: 4.37, Cp: 4.06 **(ligand)**

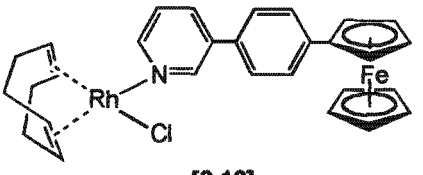

[3.16]

α-H: 4.69, β-H: 4.37, Cp: 4.07 **[3.16]**

α-H: 4.69, β-H: 4.36, Cp: 4.07 **(ligand)**

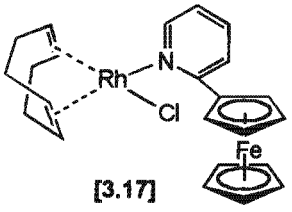

[3.17]

α-H: 4.92, β-H: 4.39, Cp: 4.05 **[3.17]**

α-H: 4.92, β-H: 4.36, Cp: 4.05 **(ligand)**

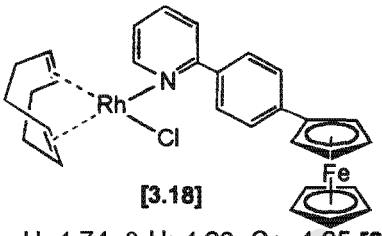

[3.18]

α-H: 4.74, β-H: 4.23, Cp: 4.05 **[3.18]**

α-H: 4.71, β-H: 4.35, Cp: 4.05 **(ligand)**

Figure 3.8: Comparison of ^{1}H NMR chemical shifts (ppm) for ferrocenyl substituents of **[3.15]**-**[3.18]**

3.2.2.2 Cationic rhodium complexes $[Rh(COD)L_2]ClO_4$

As part of the investigation into the preparation of novel metal-containing complexes and the determination of electrochemical communication between these metal centres, square planar rhodium(I) cationic complexes were also prepared. Cationic rhodium complexes are well-known primarily for their application in the field of catalysis. The complexes examined in this study include two pyridyl ligands and in the case of ferrocenyl ligands, would constitute the preparation of a trimetallic complex. The role of the rhodium metal centre can be established in electronic communication by determining the extent of communication between the ferrocenyl groups.

The cationic rhodium(I) complexes were prepared using the general synthetic route described in *Figure 3.9*. Silver perchlorate was added to a solution of the rhodium dimer in acetone, yielding a solvated complex of general formula $[Rh(COD)(Me_2CO)_x]ClO_4$. The addition of a nitrogen-donor ligand to this complex produced a cationic complex by displacement of the solvent from the rhodium coordination sphere.

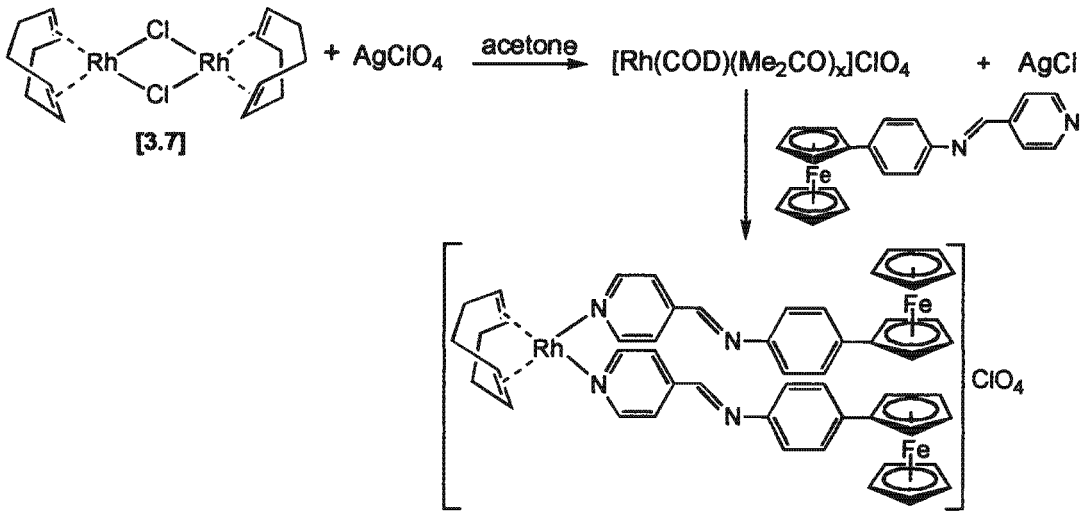

[3.26]: Dark maroon powder, 81%

Figure 3.9: Synthetic scheme for the preparation of rhodium complexes with two pyridyl ligands

These complexes can also be prepared by replacing the counter ion present. A variation on the preparation of complex **[3.21]** (see *Figure 3.10*) included preparation of the complex with a hexafluorophosphate counter ion. The synthesis of this complex, $[Rh(COD)L_2]PF_6$ **[3.20]** involved the addition of excess pyridine to the rhodium dimer in ethanol, followed by addition of a concentrated aqueous solution of ammonium hexafluorophosphate. The product was obtained as a precipitate that was collected by vacuum filtration. The preparation of further complexes with this counter ion was not carried out as complex **[3.20]** showed similar properties to that of complex **[3.21]**.

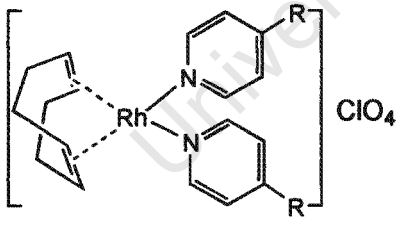

[3.21]: R = H; yellow crystals, 87%

[3.22]: R = Ph; light yellow powder, 59%

[3.23]: R = (CH=N)-Ph; yellow powder, 59%

[3.24]: R = Fc; red-brown crystals, 96%

[3.25]: R = (C_6H_4)Fc, dark red crystals, 83%

[3.26]: R = (CH=N)(C_6H_4)Fc; maroon-red powder, 89%

Figure 3.10: Cationic rhodium complexes **[3.21]**-**[3.26]**

Using the synthetic route described in *Figure 3.9*, a series of cationic rhodium complexes were prepared (see *Figure 3.10*). Complexes were obtained in good yield through concentration of the reaction mixture followed by addition of solvents such as diethyl ether or pentane to precipitate the product. The products were purified by recrystallisation. Selected ^{1}H NMR data for complexes **[3.24]**-**[3.26]** is summarised in *Figure 3.11*.

Little change was observed in the chemical shifts of the ferrocenyl protons for complex **[3.26]** on comparison of the free ligand **[2.16]** and the neutral complex **[3.14]**. The pyridyl protons in

complex **[3.26]** were shifted downfield on coordination of the rhodium metal while the imine protons were shifted upfield on complexation. Similar trends were observed for complex **[3.23]** but with larger shifts. Complex **[3.24]** showed upfield shifts in the ferrocenyl protons with a similar trend to the neutral complex **[3.12]**.

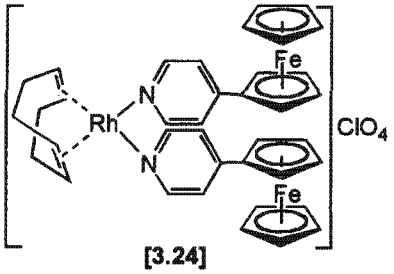

[3.24]

α: 4.68, β: 4.45, Cp: 3.98 **[3.24]**

α: 4.82, β: 4.61, Cp: 4.08 **(ligand)**

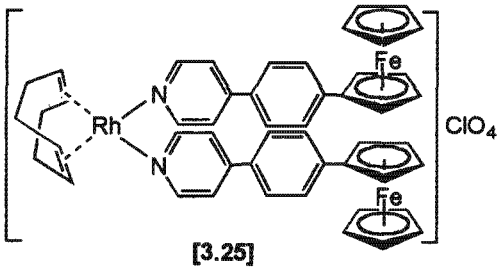

[3.25]

α: 4.80, β: 4.50, Cp: 4.14 **[3.25]**

α: 4.70, β: 4.37, Cp: 4.07 **(ligand)**

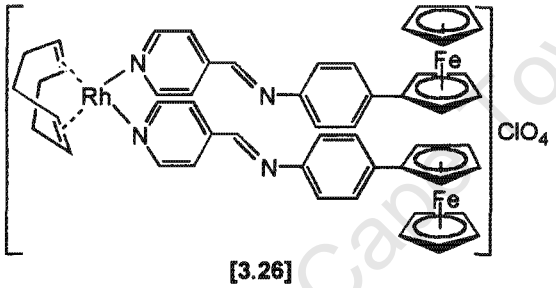

[3.26]

α: 4.67, β: 4.36, Cp: 4.05 **[3.26]**

α: 4.68, β: 4.36, Cp: 4.06 **(ligand)**

Figure 3.11: Comparison of ^{1}H NMR chemical shifts (ppm) for ferrocenyl substituents of **[3.24]**-**[3.26]**

Contrary to the observations so far, a downfield shift in the ferrocenyl protons of complex **[3.25]** was observed. This was regarded in contrast to the neutral complex **[3.13]** and the free ligand **[2.9]**, where no shift in these protons was observed. The similarity in the ferrocenyl chemical shifts for the free ligand **[2.9]** and complex **[3.13]** was attributed to the presence of the phenylene spacer group. The observed effects in **[3.25]** could be due to resonance effects that were amplified due to the presence of two ferrocenyl ligands in the complex.

3.2.2.3 Chelating 1,1'-dipyridylferrocene ligand complexes

The rhodium complexes prepared so far have contained monosubstituted ferrocenyl ligands. Selected 1,1'-disubstituted ferrocenylpyridines have been prepared and these complexed to a rhodium metal centre using a similar synthetic route to that described in *Figure 3.9*. The preparation of complex **[3.28]** has been reported using this synthetic route[19]. Complex **[3.27]** was prepared using the same synthetic route but the solvent substituted for ethanol since some decomposition was observed when the reaction was performed in acetone.

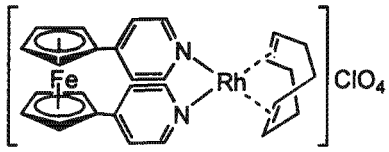

[3.27]: Dark red crystals, 67%

α: 4.85 and β: 4.52 **[3.27]**

α: 4.55 and β: 4.34 **(ligand)**

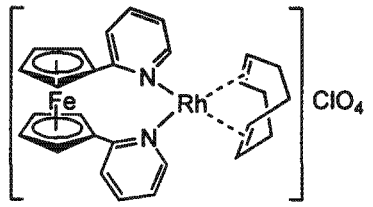

[3.28]: Orange-red crystals, 65%

α: 4.91 and β: 4.36 **[3.28]**

α: 4.91 and β: 4.36 **(ligand)**

Figure 3.12: Comparison of ^{1}H NMR chemical shifts for rhodium 1,1'-dipyridylferrocene complexes **[3.27]**-**[3.28]**

A downfield shift was observed for the ferrocenyl protons of complex **[3.27]** on complexation of the rhodium metal centre, in contrast to complex **[3.28]** where no difference was observed. The minimal difference in ferrocenyl chemical shifts observed for complex **[3.28]** was in line with those observed with the monosubstituted complex **[3.17]**. The downfield shifts observed in the ferrocenyl protons for complex **[3.27]** were contrary to the upfield shifts observed for the monosubstituted neutral **[3.12]** and cationic **[3.24]** complexes. Assuming that the effect of coordination of the rhodium metal centre is felt through the conjugative system of bonds through the resonance stabilising effect, it would appear that these effects differ in the disubstituted complexes.

3.2.3 Phosphine-donor complexes

Although the majority of ligands investigated in this study were nitrogen-donor, some phosphine-donor ligands were investigated in order to draw comparisons between the ligand systems and their metal complexes. Some rhodium complexes were prepared with the mono- and bidentate ligands ferrocenyldiphenylphosphine and 1,1'-bis(diphenylphosphino)ferrocene, respectively (see *Figure 3.13*).

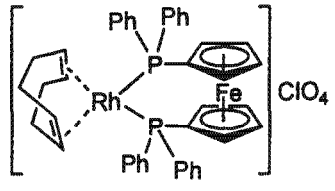

[3.29]: Orange-gold powder, 81%

α: 4.34, β: 4.28 **[3.29]**

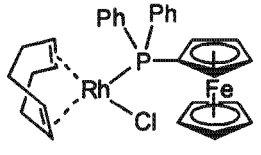

[3.30]: Mustard-yellow powder, 65%

α: 4.89, β: 4.14, cp: 4.31 **[3.30]**

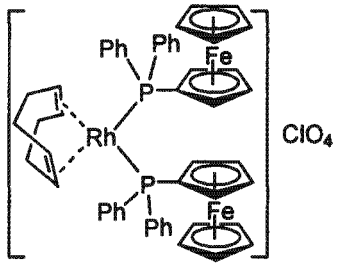

[3.31]: Brown crystalline solid, 99%

α: 4.29, β: 4.13, cp: 4.04 **[3.31]**

Figure 3.13 Comparison of ^{1}H NMR chemical shifts for rhodium phosphine complexes **[3.29]**-**[3.31]**

Complexes **[3.29]**-**[3.31]** were prepared using a similar synthetic route to the rhodium complexes with nitrogen-donor ligands (see *Figures 3.4* and *3.9*) and were obtained in good yield.

The ^{1}H NMR spectrum of complex **[3.29]** was obtained in deuterated chloroform while complexes **[3.30]**-**[3.31]** were obtained in deuterated benzene. Due to solvent effects, chemical shifts for **[3.30]** and **[3.31]** were obtained further downfield than normally expected.[20] However, comparison of chemical shifts for the ferrocenyl protons in complexes **[3.30]** and **[3.31]** clearly showed the significant downfield shift of these protons in complex **[3.30]**. This is consistent with effects observed for neutral and cationic nitrogen donor complexes, for example, complexes **[3.12]** and **[3.24]**.

3.2.4 Crystal structure analysis

X-ray crystallographic data can provide insight into the molecular structure and interactions of molecules within a crystal. Bond lengths and bond angles are obtained which can be used in conjunction with spectroscopic data to account for interactions within a molecule.

The crystal structure of complex **[3.2]** has been reported[21] and is presented below as a model complex (see *Figure 3.14* and *Table 3.1*). The complex has been reported as crystallising with a triclinic space group *P*-1 containing two molecules in an asymmetric unit with no internal coordination. The geometry around the rhodium metal centre is square planar.

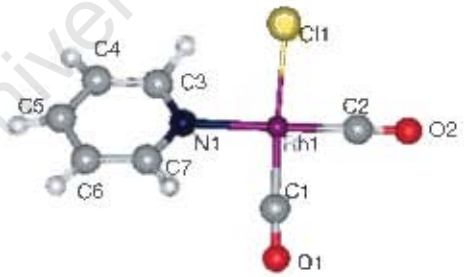

Figure 3.14: Molecular structure with labelled molecule for complex **[3.2]**, hydrogen atom labels omitted. Structure obtained courtesy of *Cambridge crystallographic database*[22]

obtained for each of the molecules. The pyridyl and phenylene rings were confirmed as delocalised.

Table 3.2: Selected bond lengths (Å) and angles (°) for the two molecules in asymmetric unit of **[3.6]**

Molecule 1		Molecule 2	
Rh(1)-Cl(1)	2.357(1)	Rh(2)-Cl(2)	2.353(1)
Rh(1)-N(1)	2.108(4)	Rh(2)-N(5)	2.115(4)
Rh(1)-C(1)	1.852(5)	Rh(2)-C(28)	1.862(6)
Rh(1)-C(2)	1.857(6)	Rh(2)-C(29)	1.850(5)
O(1)-C(1)	1.133(6)	O(3)-C(28)	1.098(6)
O(2)-C(2)	1.111(6)	O(4)-C(29)	1.128(6)
N(2)-C(9)	1.415(6)	N(38)-C(39)	1.416(6)
N(2)-C(8)	1.265(6)	C(37)-N(38)	1.271(6)
C(7)-C(8)	1.467(6)	C(34)-C(37)	1.478(6)
N(1)-C(5)	1.333(4)	N(5)-C(32)	1.345(4)
C(5)-C(6)	1.374(5)	C(32)-C(33)	1.367(5)
C(6)-C(7)	1.388(5)	C(33)-C(34)	1.387(5)
C(9)-C(12)	1.386(5)	C(39)-C(42)	1.395(5)
C(12)-C(13)	1.377(5)	C(42)-C(43)	1.371(5)
C(13)-C(14)	1.395(5)	C(43)-C(44)	1.387(5)
C(14)-C(15)	1.478(5)	C(44)-C(45)	1.474(5)
Cl(1)-Rh(1)-N(1)	90.20(8)	Cl(2)-Rh(2)-N(5)	91.22(8)
N(1)-Rh(1)-C(1)	176.22(14)	N(5)-Rh(2)-C(29)	177.96(15)
C(1)-Rh(1)-C(2)	89.09(16)	C(28)-Rh(2)-C(29)	88.67(16)
Cl(1)-Rh(1)-C(2)	179.14(13)	Cl(2)-Rh(2)-C(29)	90.20(11)
Cl(1)-Rh(1)-C(1)	90.62(11)	Cl(2)-Rh(2)-C(28)	176.53(13)

Relevant bond lengths and angles for complex **[3.6]** were fairly similar to that of complex **[3.2]**. Both the spectroscopic data and crystal structure analysis of the complex suggested that despite the existence of a conjugated network between the respective metals in complex **[3.6]**, the extended spacer group between these centres resulted in a diminished interaction.

In both molecules the cyclopentadienyl ferrocene rings were planar. The rings showed a marginal tilt towards each other with angles of 0.73° (0.27) and 1.93° (0.29) for the molecules. The cyclopentadienyl rings were not completely eclipsed in the ferrocenyl group but were rotated away from each other by an angle of 7.8° and 3.0° in each of the molecules. This degree of rotation has been related to monosubstitution of the ferrocenyl group and to the nature of the substituent. The phenylene ring showed a 26.7° rotation relative to the plane of the adjacent cyclopentadienyl ring of the ferrocenyl group.

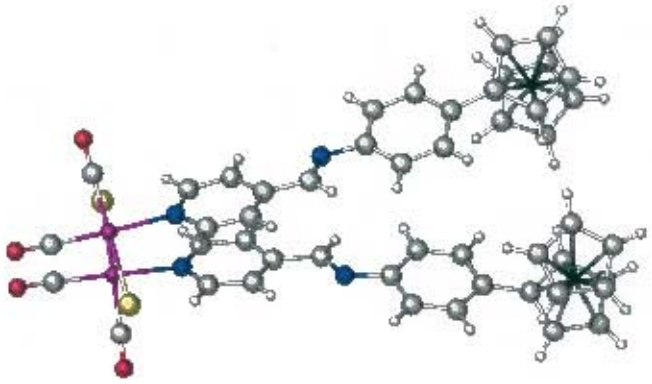

Figure 3.16: Perspective view of two molecules of complex [**3.6**] in the asymmetric unit

The molecules are packed in a tail-to-tail conformation in the unit cell. Despite the presence of two molecules in the asymmetric unit and the elongated nature of the complex, there appears to be some order within the crystal structure (see *Figure 3.17*). Despite the apparent proximity of molecules to each other, no significant intermolecular interactions were observed.

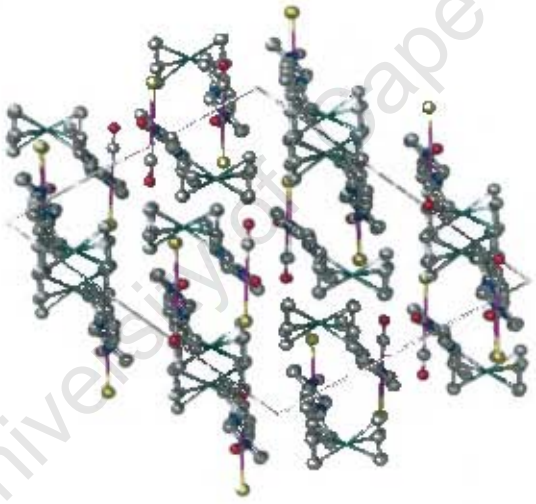

Figure 3.17: View of molecular packing diagram for complex **[3.6]** along the *b* axis of the unit cell

Table 3.3: Crystal and structure refinement data for compound **[3.6]**

	[3.6]	
Empirical formula	$C_{24}H_{18}ClFeN_2O_2Rh$	
Formula weight	560.61	
Crystal size	0.25 x 0.09 x 0.07 mm^3	
Temperature	173(2) K	
Crystal system	Monoclinic	
Space group	$P2_1/c$	
Unit cell dimensions	a = 14.480(1) Å	$\alpha = 90^o$
	b = 18.790(1) Å	$\beta = 111.507(1)^o$
	c = 17.116(1) Å	$\gamma = 90^o$
Volume	4332.7(5) $Å^3$	
μ (Mo-Kα) / mm^{-1}	1.579 mm^{-1}	
Z	8	
Reflections collected / unique	23441 / 9672 [R(int) = 0.0513]	
Goodness-of-fit on F^2	1.008	
Final R indices [I>2sigma(I)]	R1 = 0.0430, wR2 = 0.0725	
R indices (all data)	R1 = 0.1013, wR2 = 0.0857	

The crystal structure of complex **[3.15]** was obtained from single crystals grown from a mixture of dichloromethane and pentane (see *Figure 3.18*). The complex was observed to crystallise in the triclinic space group *P*-1. Least squares refinement of the structure gave a final R factor of 0.0308. Details of crystal and structure refinement data are summarised in *Table 3.5* with selected bond lengths and angles listed in *Table 3.4*.

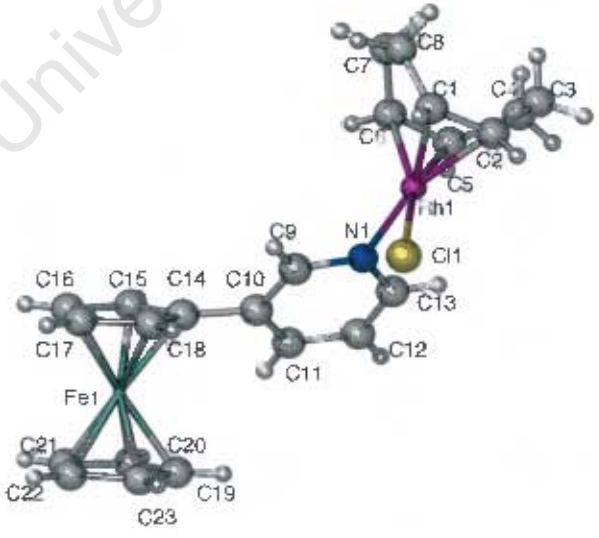

Figure 3.18: Labelled perspective view of molecular structure of complex **[3.15]**, hydrogen atom labels omitted

The coordination geometry around the rhodium metal centre in complex **[3.15]** is square planar. A torsion angle of 129° was obtained between the pyridyl ring and the adjacent cyclopentadienyl ring. The cyclopentadienyl rings are planar with a 1.6° angle of tilt. The rings are not completely eclipsed having a rotation angle of 5.6°. The Rh-N bond length is 2.109 Å, which is in accordance with observed bond lengths of similar complexes reported in the literature.[23]

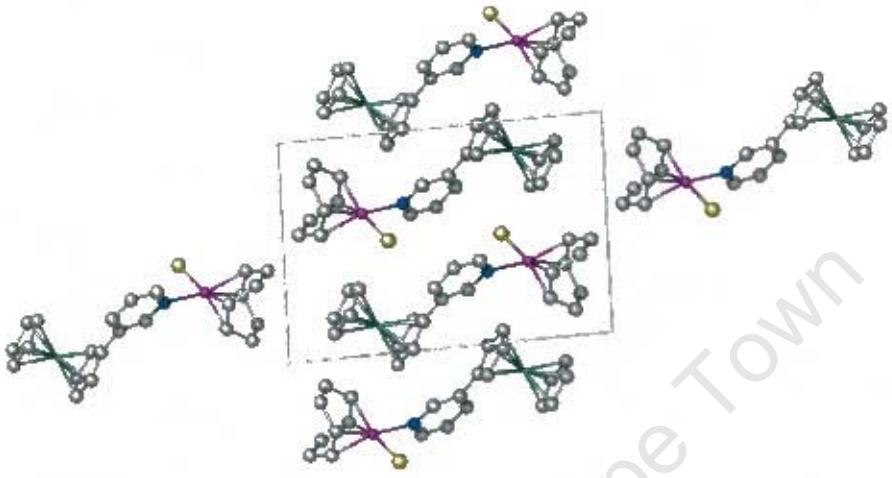

Figure 3.19: View of molecular packing diagram of **[3.15]**

The packing diagram for the crystal structure of complex **[3.15]** (see *Figure 3.19*) showed an ordered unit cell with molecules packing in a head-to-tail arrangement. No significant intermolecular contacts were observed between the molecules in the unit cell.

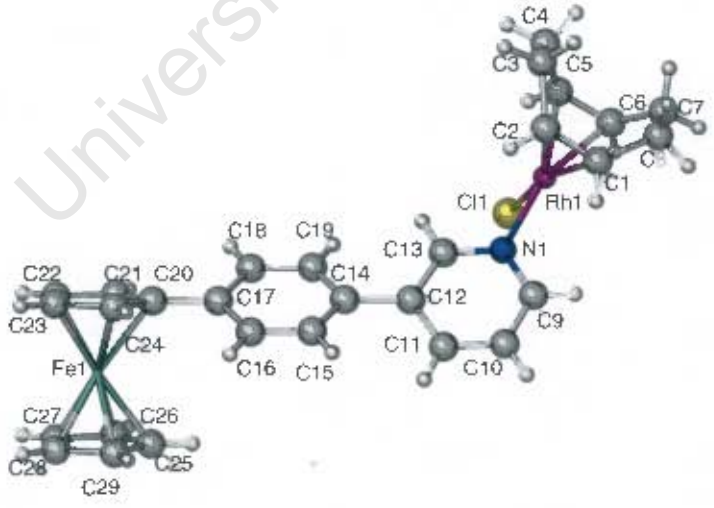

Figure 3.20: Labelled perspective view of molecular structure for complex **[3.16]**, hydrogen atoms labels omitted

The crystal structure of **[3.16]** was obtained from single crystals grown in a mixture of dichloromethane and pentane (see *Figure 3.20*). The complex was observed to crystallise in the triclinic space group *P*-1. Least squares refinement of the structure gave a final R factor of

0.0289. Details of crystal and structure refinement data are summarised in *Table 3.5* with selected bond lengths and angles listed in *Table 3.4*.

Table 3.4: Selected bond lengths (Å) and angles (°) for complexes **[3.15]** and **[3.16]**

[3.15]		**[3.16]**	
Rh(1)-Cl(1)	2.3585(10)	Rh(1)-Cl(1)	2.3719(11)
Rh(1)-N(1)	2.109(2)	Rh(1)-N(1)	2.1031(9)
Rh(1)-C(1)	2.130(3)	Rh(1)-C(1)	2.118(3)
Rh(1)-C(2)	2.124(3)	Rh(1)-C(2)	2.109(3)
Rh(1)-C(5)	2.104(3)	Rh(1)-C(5)	2.131(2)
Rh(1)-C(6)	2.104(3)	Rh(1)-C(6)	2.138(2)
N(1)-C(9)	1.340(3)	N(1)-C(13)	1.340(3)
C(9)-C(10)	1.380(3)	C(13)-C(12)	1.389(3)
N(1)-C(13)	1.343(3)	N(1)-C(9)	1.343(3)
C(13)-C(12)	1.366(4)	C(9)-C(10)	1.376(3)
C(12)-C(11)	1.373(4)	C(11)-C(10)	1.371(4)
C(11)-C(10)	1.387(4)	C(12)-C(11)	1.397(3)
C(10)-C(14)	1.481(4)	C(12)-C(14)	1.482(3)
C(2)-Rh(1)-C(1)	37.84(12)	C(14)-C(19)	1.390(3)
N(1)-Rh(1)-Cl(1)	88.26(6)	C(14)-C(15)	1.385(3)
C(2)-Rh(1)-Cl(1)	90.19(9)	C(19)-C(18)	1.381(3)
C(9)-N(1)-Rh(1)	119.70(17)	C(15)-C(16)	1.375(4)
C(11)-C(10)-C(14)-C(15)	133.8(3)	C(18)-C(17)	1.389(3)
		C(16)-C(17)	1.384(4)
		C(17)-C(20)	1.474(3)
		C(2)-Rh(1)-C(1)	38.48(11)
		N(1)-Rh(1)-Cl(1)	86.88(6)
		C(2)-Rh(1)-Cl(1)	158.17(8)
		C(9)-N(1)-Rh(1)	122.98(16)
		C(19)-C(14)-C(12)-C(13)	26.2(4)
		C(24)-C(20)-C(17)-C(16)	29.8(4)

The structure of complex **[3.16]** showed many similarities to complex **[3.15]**. The rhodium metal centre is square planar and the angle of rotation between the plane of the pyridyl and phenylene rings was 26°. The cyclopentadienyl rings were found to be almost parallel to one another with an angle of 3.11° between the respective planes. Unlike the previous rhodium structures, the cyclopentadienyl rings were eclipsed with only a 1° angle of rotation. The pyridyl and phenylene rings were confirmed as delocalised.

The crystal structure packing diagram for complex **[3.16]** revealed that the molecules pack in a highly ordered fashion adopting a head-to-tail conformation similar to that of complex **[3.15]** (see *Figure 3.21*). No significant intermolecular interactions were observed between the respective molecules in the unit cell.

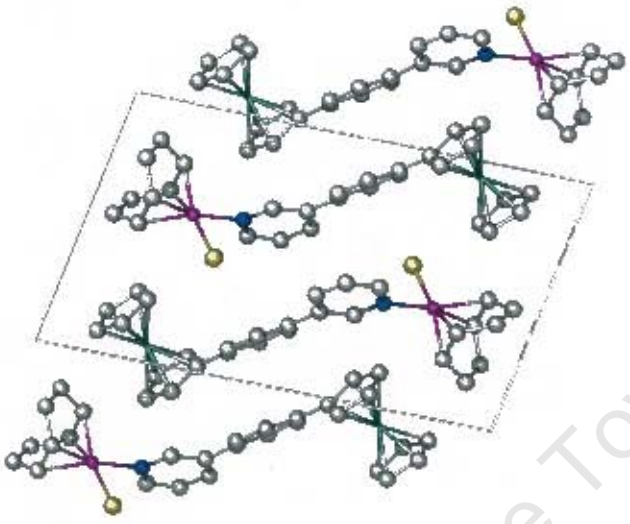

Figure 3.21: View of molecular packing diagram for **[3.16]**

Table 3.5: Crystal and structure refinement data for compounds **[3.15]** and **[3.16]**

	[3.15]		**[3.16]**	
Empirical formula	$C_{24}H_{25}ClFeNRh$		$C_{29}H_{29}ClFeNRh$	
Formula weight	509.65		585.74	
Crystal size	0.30 x 0.07 x 0.04 mm		0.12 x 0.10 x 0.03 mm	
Temperature	298(2) K		298(2) K	
Crystal system	Triclinic		Triclinic	
Space group	*P*-1		*P*-1	
Unit cell dimensions	a = 6.946(1) Å	α = 91.38(3)°	a = 7.003(1) Å	α = 78.60(3)°
	b = 9.999(2) Å	β = 99.30(3)°	b = 10.026(2) Å	β = 80.79(3)°
	c = 14.789(3) Å	γ = 97.11(3)°	c = 17.609(4) Å	γ = 85.92(3)°
Volume	1004.8(4) $Å^3$		1195.5(4) $Å^3$	
μ (Mo-Kα) / mm^{-1}	1.683 mm^{-1}		1.427 mm^{-1}	
Z	2		2	
Reflections collected / unique	8208 / 4397 [R(int) = 0.0315]		34055 / 5459 [R(int) = 0.0465]	
Goodness-of-fit on F^2	1.019		1.025	
Final R indices [I>2sigma(I)]	R1 = 0.0308, wR2 = 0.0568		R1 = 0.0289, wR2 = 0.0657	
R indices (all data)	R1 = 0.0586, wR2 = 0.0627		R1 = 0.0405, wR2 = 0.0698	

The crystal structures of complexes **[3.15]** and **[3.16]** show similarities in their space groups, unit cell dimensions and molecular packing. Complex **[3.16]** has a longer *c*-axis to compensate for the added phenylene space group.

3.2.5 Electrochemical study of rhodium complexes

The study of transition metal complexes using electrochemistry has gained increasing popularity. A considerable amount of information is known about reactive paramagnetic complexes generated by electrochemical methods.[24] Cyclic voltammetry as well as chronoamperometry are ideally suited to study the reactivity of electrogenerated species.[24] These techniques have become popular for the study of organometallic catalytic cycles, modified electrodes and biochemical, macromolecular and photoelectrochemical devices.[24]

The cyclic voltammogram for the rhodium complex **[3.14]**, is shown with three key areas highlighted (*Figure 3.22*). *Peak 1* is an irreversible wave due to the oxidation of rhodium(I) and is often very broad. It is only occasionally observed. *Peak 2* is a typical reversible ferrocenyl redox wave. Shifts in the position of this wave can be related to substituents on the ferrocenyl group and to the presence of coordinated transition metals. An irreversible wave occasionally occurs at the potential indicated by the brace labelled *Peak 3* and has been identified as being due to the reduction of rhodium(I), when rhodium metal is deposited on the electrode surface.

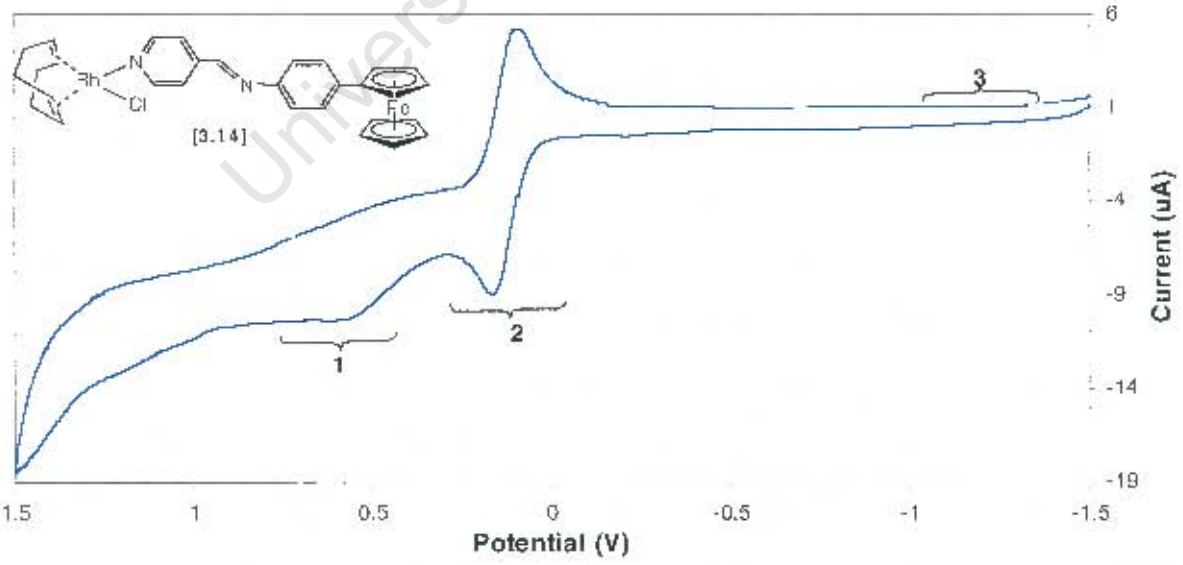

Figure 3.22: Cyclic voltammogram for rhodium ferrocenyl complex **[3.14]**

The broadness of *Peak 1* makes it difficult to use this to monitor changes in the rhodium complexes. Most of the discussion in this section thus involves a comparison of shifts in half-

wave potential of *Peak 2* relative to ferrocene **[2.2]**. *Figure 3.23* displays the reversible ferrocenyl redox waves obtained for complexes **[3.16]** and **[3.13]**

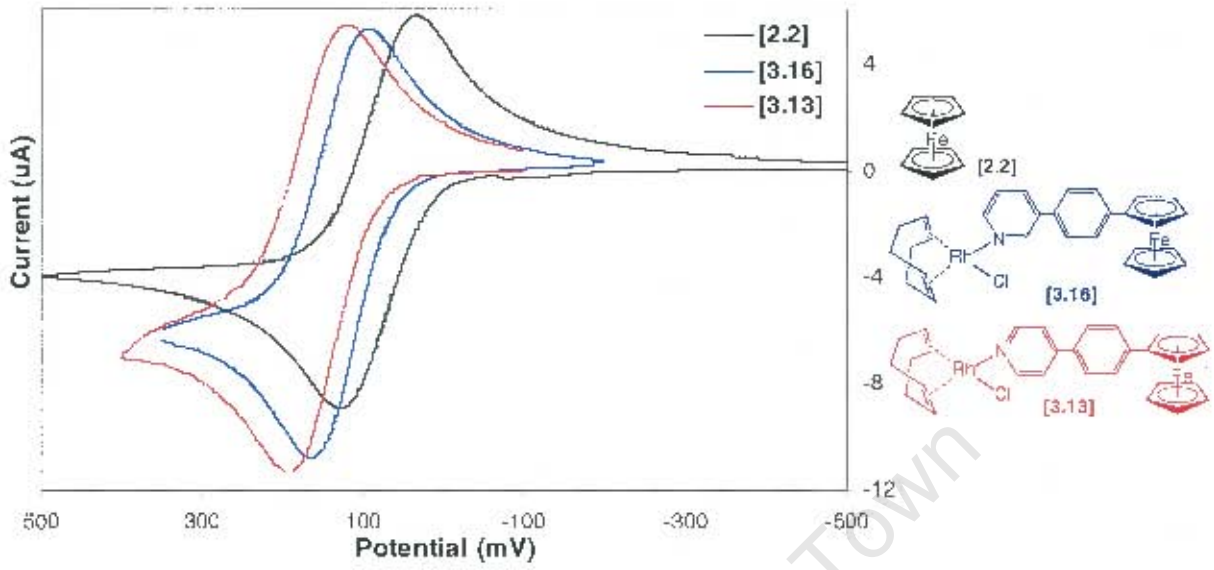

Figure 3.23: Overlay of cyclic voltammograms for ferrocene **[2.2]** and complexes **[3.16]** and **[3.13]**

Reversible redox waves were observed for all rhodium ferrocenyl complexes examined. *Table 3.7* lists the half-wave potential, $E_{½}$, and corresponding anodic E_{pa} (2), and cathodic E_{pc}, peak potentials. Where possible, the irreversible anodic peak potential, E_{pa} (1) corresponding to rhodium(I) oxidation was recorded.

Table 3.6: Electrochemical data for several rhodium(I) complexes in acetonitrile

Complex number	Complex type	Ligand	E_{pa} (1) (mV)	E_{pa} (2) (mV)	E_{pc} (mV)	$E_{½}$ (mV)
[2.2]	Ferrocene	--	--	+120	+31	+75.5
[3.7]	$[Rh(COD)Cl]_2$	–	+446	–	–	--
[3.8]	RhCl(COD)L	py	+529	–	–	–
[3.12]		4-Fcpy	–	+377	+240	+308.5
[3.15]		3-Fcpy	–	+223	+148	+185.5
[3.17]		2-Fcpy	–	+192	+118	+155
[3.13]		4-Fc(C_5H_4)py	+612	+194	+125	+159.5
[3.16]		3-Fc(C_6H_4)py	–	+165	+96	+130.5
[3.18]		2-Fc(C_6H_4)py	–	+165	+89	+127
[3.10]		Ph(NC)py	+632	–	–	–
[3.14]		Fc(C_6H_4)NCpy	+616	+161	+91	+126
[3.6]	$RhCl(CO)_2L$	Fc(C_6H_4)NCpy	–	+145	+82	+113.5
[3.23]	$[Rh(COD)L_2]ClO_4$	4-Fcpy	–	+270	+179	+224.5
[3.25]		Fc(C_6H_4)NCpy	–	+160	+83	+121.5

The resonance effect in the conjugated rhodium complexes was demonstrated by the decreased positive shift in the half-wave potential observed on comparison of complexes **[3.12]**, **[3.15]** and **[3.17]**, which was consistent with spectroscopic trends. This trend was further observed in the related complexes **[3.13]**, **[3.16]** and **[3.18]** with phenylene spacer groups. The effect of the spacer groups was clearly demonstrated on comparison of complexes **[3.12]**, **[3.13]** and **[3.14]** where a gradual decrease in $E_{½}$ value was observed. Changes in the spectator ligands did not appear to play a significant role on electronic interactions as complexes **[3.6]** and **[3.14]** displayed similar $E_{½}$ values.

The single reversible peak obtained for the cyclic voltammograms of complexes **[3.24]** and **[3.25]** indicated that no electrochemical communication occurred between the ferrocenyl groups of these trinuclear complexes through the rhodium metal centre. Furthermore, the electronic interaction was reduced compared to that of the neutral complexes **[3.12]** and **[3.13]**. These effects were attributed to the resonance effect in the conjugated complexes.

3.2.6 Electronic spectroscopy of rhodium complexes

The electronic spectra of the rhodium complexes were obtained in dichloromethane. While the bands due to transitions in the ferrocenyl and pyridyl groups were still found, a d–d transition due to the presence of the rhodium metal centre transpired. This rhodium $\rightarrow$ligand π^* metal-to-ligand charge transfer band occurred in the range of 350 to 550 nm, depending on the specific ligand. Electronic spectra of similar complexes in dichloromethane show two strong bands at approximately 300 and 400 nm with an extinction coefficient of the order of 10^4 $mol^{-1}.dm^3.cm^{-1}$ and a weaker band near 500 nm, which is sometimes discernible as a shoulder only.[25]

A comparison of the major bands together with extinction coefficients in electronic spectra for selected rhodium complexes in dichloromethane is summarised in *Tables 3.8* and *3.9*. Interesting comparisons can be made between the single and bi-ligand complexes **[3.12]** and **[3.24]** as well as complexes **[3.13]** and **[3.24]**. In each of these cases, a shift in the transitions to a longer wavelength and larger extinction coefficient was found on incorporation of an additional ligand.

Table 3.7: Electronic spectral bands and extinction coefficients for a range of rhodium cyclooctadienyl complexes

Complex number		Wavelength / nm [Extinction coefficient / $mol^{-1}.dm^3.cm^{-1}$]		
[3.8]	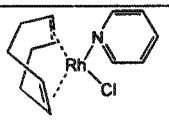	–	366 [1 634]	298 [4 210]
[3.15]	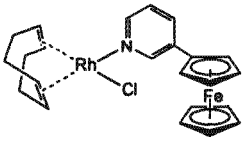	450 [593]	358 [2 474]	308 [4 344]
[3.12]	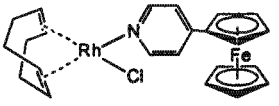	466 [1 811]	360 [5 670]	308 [14 712]
[3.24]	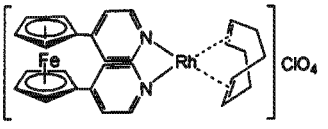	482 [2 760]	370 [4 880]	314 [17 249]
[3.16]	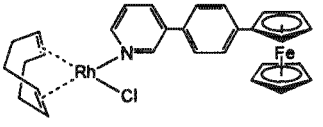	452 [1 050]	362 [4 333]	322 [5 076]
[3.13]	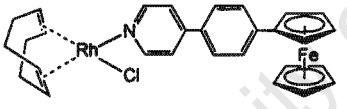	460 [1 755]	376 [6 095]	318 [8 122]
[3.24]	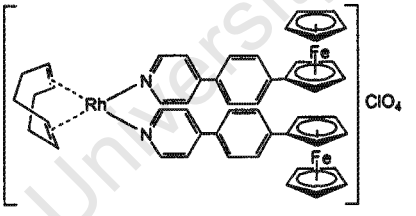	472 [4 887]	384 [10 080]	314 [16 192]

The highly conjugated complexes **[3.10]**, **[3.14]**, **[3.25]** and **[3.26]** in *Table 3.9* all show relatively large extinction coefficients for each of the transitions. A comparison of complexes **[3.14]** and **[3.6]** showed a variation in the middle band, with complex **[3.6]** exhibiting a more intense transition and increased extinction coefficient with a bathochromic shift relative to complex **[3.14]**. This band also became more intense for complex **[3.25]**.

Table 3.8: Electronic spectral band positions and extinction coefficients for a range of rhodium complexes

Complex number		Wavelength / nm [Extinction coefficient / $mol^{-1}.dm^3.cm^{-1}$]		
[3.10]	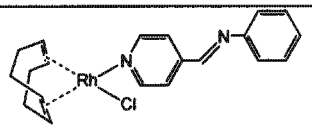	–	354 [11 644]	336 [12 405]
[3.14]	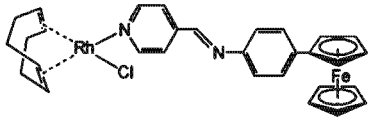	488 [1 998]	358 [9 459]	298 [9 701]
[3.25]	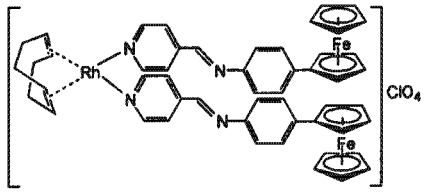	504 [7 895]	364 [14 296]	302 [13 328]
[3.6]	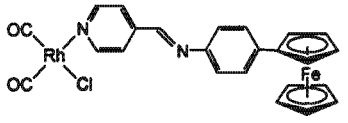	500 [3 621]	374 [13 318]	300 [9 518]

3.3 Preparation and properties of iridium complexes

The chemistry of iridium(I) complexes is known to be similar to that of rhodium(I). In this investigation a series of iridium(I) square planar complexes were prepared. Iridium(I) complexes are generally regarded as less catalytically active. However, intensive investigation of iridium(I) complexes as hydrogenation catalysts have led to their use in the reduction of sterically hindered olefins.[26]

3.3.1 Iridium complexes with a single N-donor ligand [IrCl(COD)L]

Iridium complexes containing a single nitrogen donor ligand were prepared from $[IrCl(COD)]_2$ **[3.32]** using a similar synthetic route to the synthesis of the rhodium cyclooctadiene complexes (see *Figure 3.4*). A series of iridium complexes were prepared with systematic changes in the ligands from a simple unsubstituted pyridyl ligand **[3.33]**, to ferrocenyl ligands, **[3.36]**-**[3.37]** (see *Figure 3.24*).

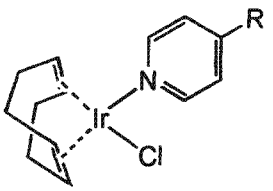

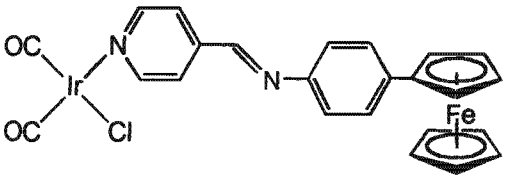

[3.33]: R = H; bright yellow powder, 77%

[3.34]: R = Ph; yellow crystalline solid, 75%

[3.35]: R = (CH=N)-Ph; orange powder, 57%

[3.36]: R = Fc; orange-brown solid, 51%

[3.37]: Maroon powder, 52%

Figure 3.24: Iridium pyridyl complexes **[3.33]**-**[3.37]**

In complex **[3.37]**, the labile cyclooctadiene ligand was displaced with carbonyl groups by bubbling carbon monoxide gas through a solution of the cyclooctadienyl complex. Comparing the ferrocenyl proton chemical shifts of the iridium complex **[3.37]**, the related rhodium complex **[3.6]** and the free ligand **[2.16]**, showed no significant changes. This is in accordance with complexes containing extended ligand systems. The imine bond proton for complex **[3.37]** showed a slight shift on coordination of the iridium metal. A similar shift was observed in complex **[3.6]**. Some differences were observed in the carbonyl stretching frequencies of complexes **[3.37]** and **[3.6]** (see *Figure 3.25*).

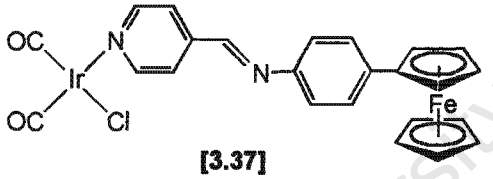

[3.37]

α: 4.69, β 4.38, Cp: 4.06; ν CO: 2067, 1991 **[3.37]**

α: 4.68, β 4.36, Cp: 4.06; ν CO: 2080, 2013 **[3.6]**

α: 4.68, β 4.36, Cp: 4.06 **[ligand]**

Figure 3.25: Comparison of ^{1}H NMR (ppm) and IR stretches (cm^{-1}) for complexes **[3.37]** and **[3.6]**

The majority of iridium complexes decomposed or tended to show line broadening when NMR spectra were obtained in deuterated chloroform. The ^{1}H NMR of complexes **[3.33]**, **[3.34]** and **[3.36]** were obtained in deuterated benzene. Comparing the pyridyl proton chemical shifts of complexes **[3.33]**, **[3.34]** and **[3.36]**, showed deshielding of the H_a proton on derivatising the pyridyl ligand. Complex **[3.36]** displayed a relatively large upfield shift in the Cp protons. This was due to solvent effects rather than interaction of the protons with the iridium metal centre. The pyridyl proton chemical shifts for complex **[3.35]** displayed deshielding of the H_a protons on complexation of the iridium metal while the imine proton chemical shift remained unchanged, relative to the free ligand **[2.19]**.

3.3.2 Cationic iridium complexes $[Ir(COD)L_2]ClO_4$

The preparation of iridium complexes containing two nitrogen donor ligands followed a similar synthetic route to the related rhodium complexes (see *Figure 3.26*).

The coordinating solvent, ethanol, was found to be ideal for this reaction and no decomposition was observed. Furthermore, the products were obtained in high yield. These complexes allowed for simple comparison of the effect of placing a ferrocenyl substituent on the pyridyl ring of an iridium complex **[3.38]**.

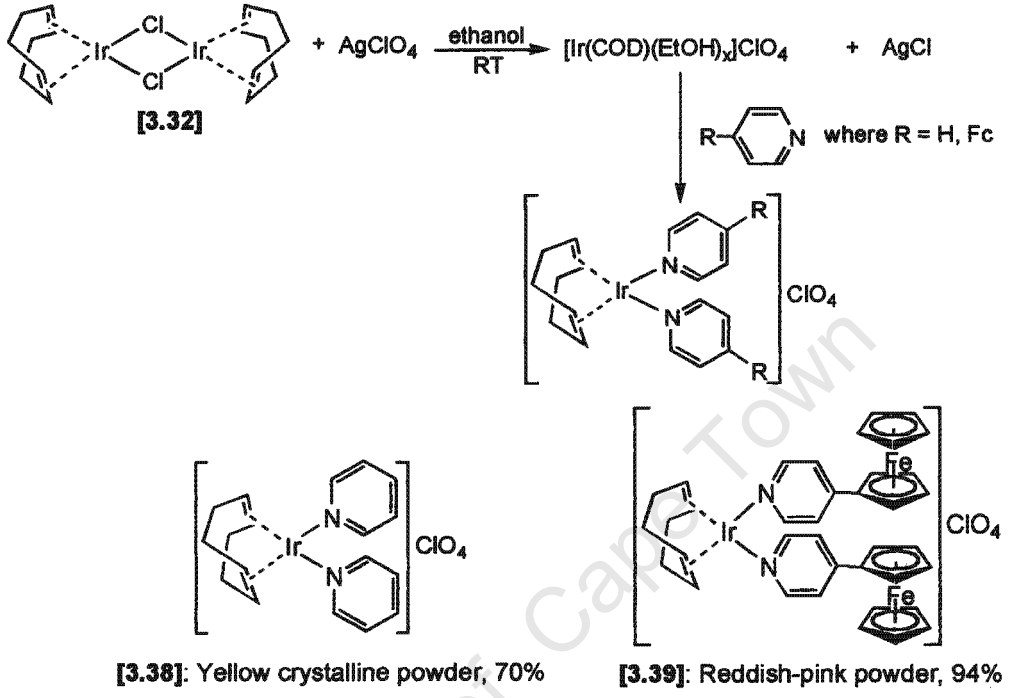

[3.38]: Yellow crystalline powder, 70% **[3.39]**: Reddish-pink powder, 94%

Figure 3.26: Cationic iridium cationic complexes **[3.38]** and **[3.39]**

Both the pyridyl and ferrocenyl protons of complex **[3.39]** shifted downfield on complexation of the iridium metal. The pyridyl shifts were more pronounced than in the related rhodium complex **[3.24]**. Furthermore the downfield ferrocenyl chemical shifts were contrary to the related rhodium complex **[3.24]**, which displayed upfield shifts relative to the free ligand **[2.6]**.

3.3.3 Electrochemical behaviour of iridium complexes

The iridium complexes all display reversible ferrocenyl redox waves (see for example *Figure 3.27*). Results are reported relative to the half-wave potentials of ferrocene in acetonitrile ($E_{½}$ +75.5 mV) (see *Table 3.9*).

Positive shifts in half-wave potential relative to ferrocene and the free ligands were observed for all the iridium ferrocenyl complexes (see *Table 3.9*). The single reversible redox wave in the cyclic voltammogram for complex **[3.39]** indicated that no communication occurred between the ferrocenyl ligands through the iridium metal centre, as with the related rhodium complex **[3.24]**. The relative shift in $E_{½}$ value for complex **[3.36]** was less pronounced than for the related rhodium complex **[3.12]** while complexes **[3.39]** and **[3.37]** displayed more

significant shifts than their rhodium counterparts **[3.24]** and **[3.6]**. This may be due to the resonance conjugative effect and the electron density of the metals.

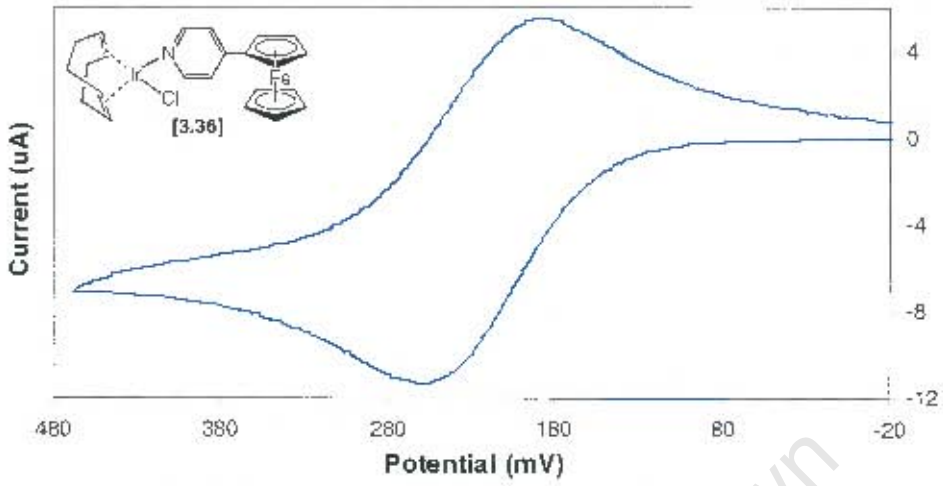

Figure 3.27: Cyclic voltammogram for iridium complex **[3.36]** in acetonitrile

Table 3.9: Electrochemical data for ferrocenyl iridium complexes in acetonitrile

Complex number	Complex type	Ligand	E_{pa} (mV)	E_{pc} (mV)	Complex $E_{1/2}$ (mV)	Ligand $E_{1/2}$ (mV)
[3.36]	IrCl(COD)L	4-Fcpy	+253	+187	+220	+205.5
[3.39]	$[Ir(COD)L_2]ClO_4$	4-Fcpy	+306	+219	+262.5	+205.5
[3.37]	$IrCl(CO)_2L$	$Fc(C_6H_4)NCpy$	+164	+90	+127	+113

3.3.4 Electronic spectroscopy of iridium complexes

The electronic spectra of selected iridium complexes were recorded in dichloromethane. The description of electronic transitions made for the rhodium complexes holds true for the iridium complexes as well, with the high energy transition at approximately 300 nm due to the pyridyl substituent and the low energy transition at approximately 450-500 nm due to the ferrocenyl d-d transition. The remaining band was assigned to an overlap of ferrocenyl as well as metal-to-ligand charge transfer from the iridium metal centre.

The electronic transitions for the ferrocenyl iridium complexes occur at similar positions to the related rhodium complexes **[3.12]**, **[3.24]** and **[3.6]** (see *Tables 3.7* and *3.8*). The extinction coefficients for the complexes **[3.39]** and **[3.37]**, are significantly higher than that for the related rhodium complexes. Since similar ligands are used in both the rhodium and iridium complexes, this difference could be due to the presence of the iridium metal.

Table 3.10: Electronic spectral band positions and extinction coefficients for ferrocenyl iridium complexes in dichloromethane

Complex number	Compound	Wavelength / nm [Extinction coefficient / $mol^{-1}.dm^3.cm^{-1}$]		
[3.36]	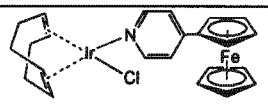	466 [1 870]	370 [5 978]	306 [9 436]
[3.39]	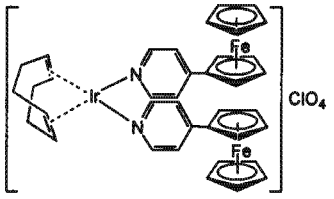	488 [5 149]	366 [9 500]	312 [28 371]
[3.37]	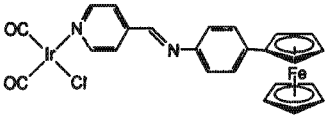	514 [4 433]	378 [14 877]	255 [23 121]

3.4 Preparation and properties of palladium complexes

The preparation of complex **[3.40]** has been reported using the synthetic route described in *Figure 3.28*.[27] This synthetic route has been reported as giving the *trans* isomer of the palladium complexes.

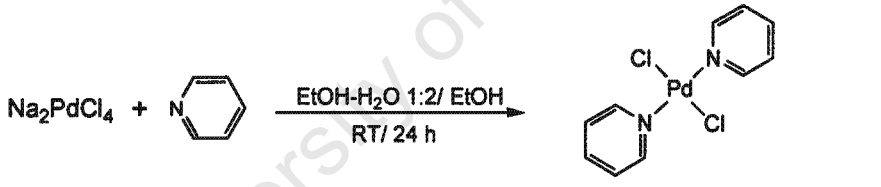

[3.40]: Light yellow powder, 77%

Figure 3.28: Synthesis of palladium complex **[3.40]**[27]

The synthetic route in *Figure 3.28* is, however, limited by the solubility of the ligands and the duration of reaction time (at least 24 hours). To overcome these shortcomings, an alternative biphasic synthetic strategy was devised (see *Figure 3.29*).

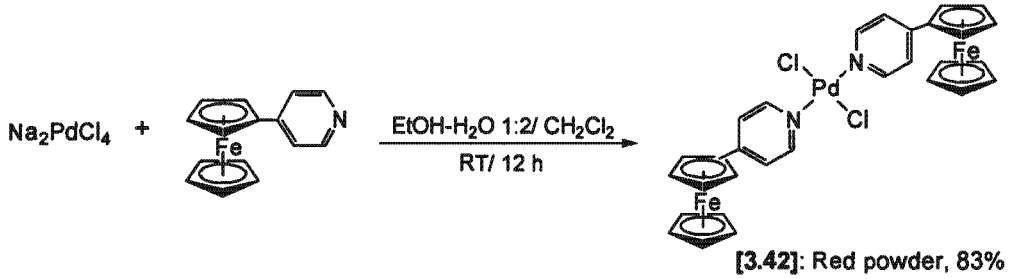

[3.42]: Red powder, 83%

Figure 3.29: Synthetic route for the preparation of complex **[3.42]**

The ligands investigated were soluble in dichloromethane, whereas the palladium starting material was not. The palladium complexes were prepared using a biphasic system with the ligands in a dichloromethane solution and the palladium starting material in an ethanol-water mixture. The reaction mixture was stirred vigorously at room temperature to increase the interface of reaction between the solvent layers. A phase-transfer reaction was established between the layers, where the palladium product formed was found to be either soluble in the dichloromethane phase or formed as an insoluble precipitate. The reaction could be monitored as the palladium layer was observed to lighten from dark brown to colourless.

The use of this synthetic route gave a substantial decrease in reaction time, with the longest reaction time being 10 hours; this constitutes a decrease of more than half the reaction time when compared to the synthetic route described in *Figure 3.28*. Complexes **[3.41]**-**[3.45]** were prepared using this synthetic route and were obtained in high yield (see *Figure 3.30*).

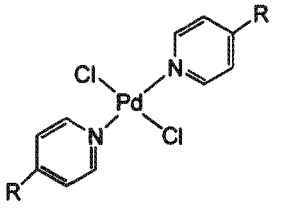

[3.41]: R = Ph; light yellow powder, 83%

[3.42]: R = Fc; red powder, 84%

[3.43]: R = $(C_6H_4)Fc$; maroon-brown powder, 82%

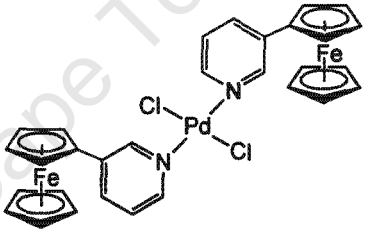

[3.44]: Mustard microcrystals, 84%

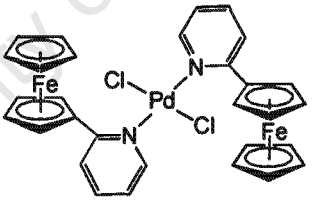

[3.45]: Dark red microcrystals, 78%

Figure 3.30: Palladium complexes **[3.41]**-**[3.45]** prepared using the biphasic synthetic route

The pyridyl proton chemical shifts for all complexes display downfield shifts on complexation of the palladium metal centre. The proton attached to the carbon adjacent to the nitrogen donor atom, H_a, showed the largest shift on complexation of the palladium metal for complex **[3.45]**, contrary to the observed ferrocenyl shifts where very little difference was observed between the free ligand and complex. Complexes **[3.43]** and **[3.44]** showed downfield shifts for both α-H and β-H on complexation to the palladium metal centre (see *Figure 3.31*), contrary to trends observed with the rhodium complexes. Complex **[3.42]**, was the only complex that displayed upfield shifts on complexation while complex **[3.45]** showed no difference between the free ligand and coordinated complex.

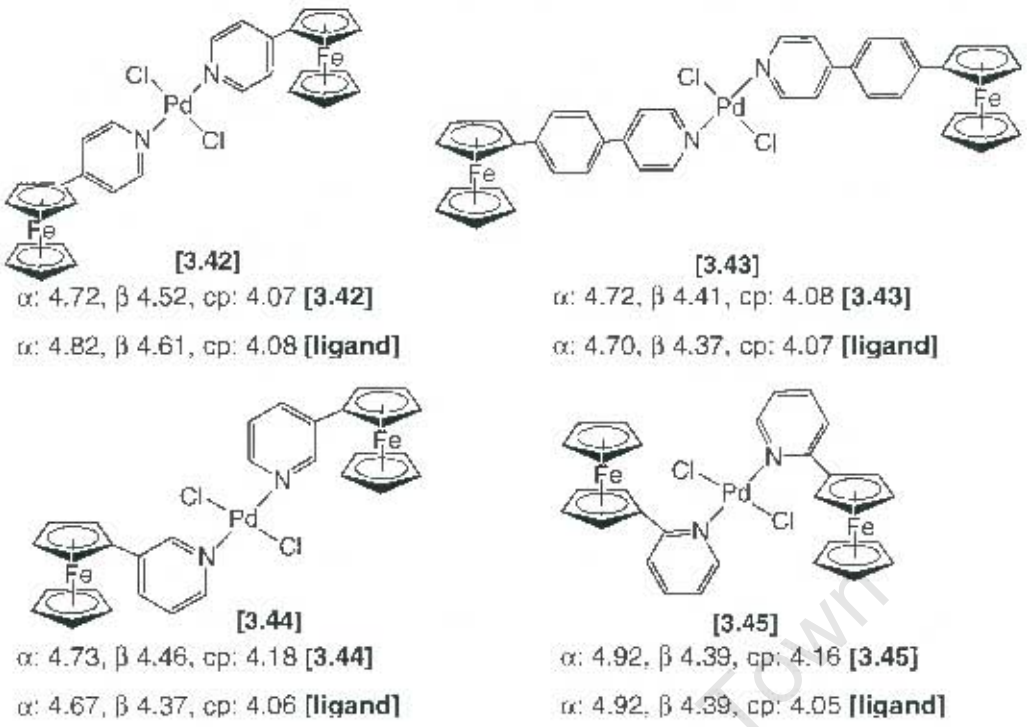

Figure 3.31: Comparison of ^{1}H NMR chemical shifts (ppm) for complexes **[3.42]-[3.45]**

The spectroscopic results indicate that the conjugative resonance effects differ in the palladium complexes to the rhodium complexes with the same ligands. The unusual behaviour may be related to the difference in geometry between these complexes with the trans effect potentially playing a role in the spectroscopy of the palladium complexes.

3.4.1 Crystal structure analysis of palladium complex

The crystal structure of the palladium complex **[3.44]** has been obtained. As with the rhodium crystal structures, the X-ray crystallographic data of this palladium complex was used to provide insight into the molecular structure and interactions of molecules within the crystal structure. Reference is made to the reported structure of complex **[3.40]**[28] and selected bond lengths and angles are reported (see *Figure 3.32* and *Table 3.11*). Complex **[3.40]** crystallises in the monoclinic space group *C2/c*.

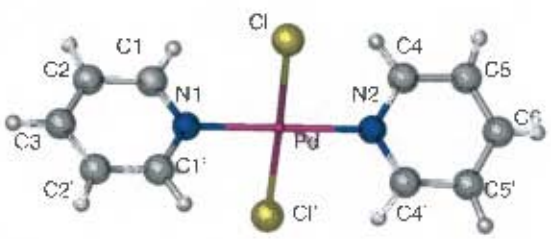

Figure 3.32: Labelled perspective view of complex **[3.40]**, hydrogen atom labels omitted.[28] Structure obtained courtesy of *Cambridge crystallographic database*[22]

Table 3.11: Selected bond lengths (Å) and angles (°) of complex **[3.40]**[28]

Pd-Cl	2.297(1)	Pd-N(1)	2.024(6)	Pd-N(2)	2.023(6)
N(1)-C(1)	1.356(6)	N(2)-C(4)	1.336(6)	N(2)-Pd-Cl	89.17(7)
Cl-Pd-Cl'	178.3(1)	N(1)-Pd-Cl	90.83(7)	C(4)-N(2)-C(4')	119.4(7)
C(1)-N(1)-C(1')	118.3(7)	C(1)-N(1)-Pd	120.8(3)	C(5)-C(4)-N(2)	121.1(6)
C(2)-C(1)-N(1)	121.9(6)	C(4)-N(2)-Pd	120.3(3)		

The crystal structure of complex **[3.44]** was obtained with single crystals grown from a mixture of dichloromethane and pentane. The complex was observed to crystallise in the monoclinic space group *C2/c* (see *Figure 3.33* for molecular structure).

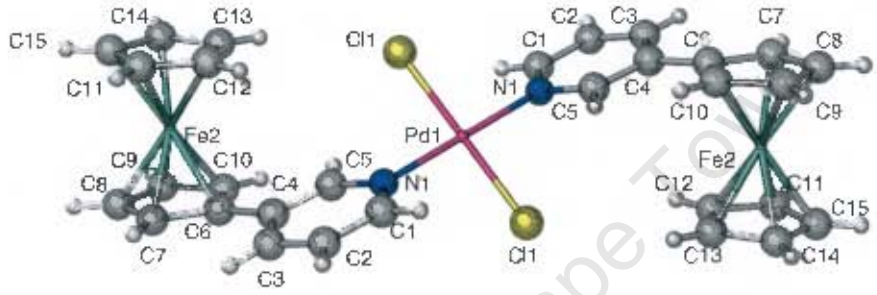

Figure 3.33: Labelled perspective view of molecular structure for complex **[3.44]**, hydrogen atom labels omitted

Table 3.12: Selected bond lengths (Å) and angles (°) for **[3.44]**

Pd(1)-Cl(1)	2.3053(9)	N(1)-Pd(1)-N'(1)	180.00(14)
Pd(1)-N(1)	2.022(2)	Cl(1)-Pd(1)-N(1)	89.82(6)
N(1)-C(5)	1.343(3)	Pd(1)-N(1)-C(1)	122.01(17)
N(1)-C(1)	1.347(3)	Pd(1)-N(1)-C(5)	119.05(18)
C(5)-C(4)	1.390(4)	C(3)-C(4)-C(6)-C(7)	15.7(4)
C(1)-C(2)	1.380(4)	C(5)-C(4)-C(6)-C(10)	12.5(4)
C(2)-C(3)	1.384(4)		
C(3)-C(4)	1.392(4)		
C(4)-C(6)	1.464(3)		

The 3-ferrocenylpyridine ligands are equivalent from a crystallographic point of view, indicating a completely symmetrical structure. Selected bond lengths and angles are listed in *Table 3.12*. The observed bond lengths and angles around the palladium metal centre are similar to that of complex **[3.40]**, with no particularly unusual characteristics observed in the molecular structure of complex **[3.44]**. A dihedral angle between the plane of the palladium metal centre and pyridyl ring of 131° was obtained. As with the rhodium complexes, the degree of tilt of the ferrocenyl cyclopentadienyl rings was determined. The planar rings were

observed to tilt toward each other by an angle of 3.1°, which indicated that the rings were planar. The rings were not completely eclipsed and observed to rotate by an angle of 5.7°, akin to the related rhodium complex **[3.15]** containing the same ferrocenyl ligand **[2.7]**. The pyridyl ring was observed to rotate away from the attached cyclopentadienyl ring by an angle of 12.5°.

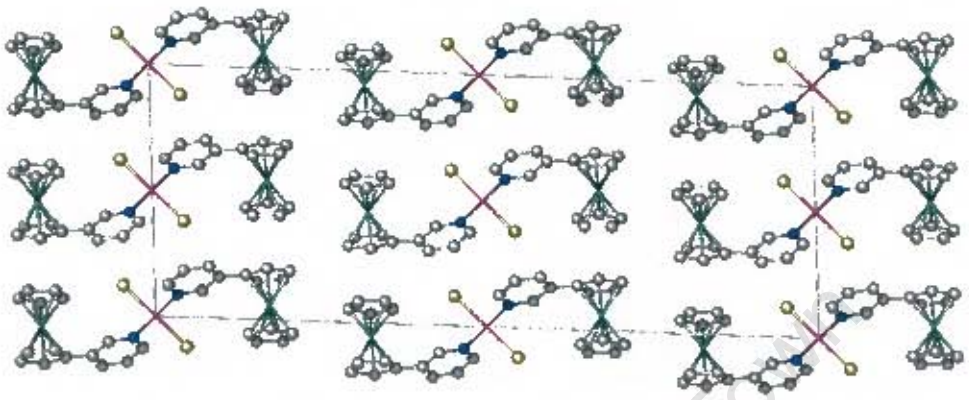

Figure 3.34: View of molecular packing diagram along *b* axis of unit cell for complex **[3.44]**

The packing diagram (see *Figure 3.34*) of complex **[3.44]** showed a highly ordered crystal structure. As with the other crystal structures determined in this study, no significant intermolecular contacts were observed between the molecules in the unit cell.

Table 3.13: Crystal and structure refinement data for complex **[3.44]**

	[3.44]	
Empirical formula	$C_{30}H_{26}Cl_2Fe_2N_2Pd$	
Formula weight	703.53	
Crystal size	0.10 x 0.10 x 0.04 mm	
Temperature	203(2) K	
Crystal system	Monoclinic	
Space group	*C2/c*	
Unit cell dimensions	a = 34.606(7) Å	$\alpha = 90^{\circ}$
	b = 5.674(1) Å	$\beta = 93.52(3)^{\circ}$
	c = 13.126(3) Å	$\gamma = 90^{\circ}$
Volume	2572.8(9) $Å^3$	
μ (Mo-Kα) / mm^{-1}	2.036 mm^{-1}	
Z	4	
Reflections collected / unique	2950 / 2950 [R(int) = 0.0000]	
Goodness-of-fit on F^2	1.091	
Final R indices [I>2sigma(I)]	R1 = 0.0270, wR2 = 0.0537	
R indices (all data)	R1 = 0.0416, wR2 = 0.0641	

3.4.2 Electrochemistry of palladium complexes

Cyclic voltammograms of the palladium complexes were obtained in acetonitrile with tetrabutylammonium perchlorate as background electrolyte and at a platinum disk working electrode (see *Table 3.14*). Data was recorded relative to ferrocene under the same conditions ($E_{½}$ +75.5 mV). A single ferrocenyl wave was observed for all palladium complexes, indicating that no electrochemical communication occurred between the ferrocenyl groups of the complexes through the palladium metal centre.

Table 3.14: Electrochemical data for ferrocenyl palladium complexes **[3.42]**-**[3.45]** in acetonitrile

Complex number	Complex type	Ligand	E_{pa} (mV)	E_{pc} (mV)	Complex $E_{½}$ (mV)	Ligand $E_{½}$ (mV)
[3.42]	$PdCl_2L_2$	4-Fcpy	+253	+187	+220	+205.5
[3.43]		4-Fc(C_6H_4)py	+176	+107	+141.5	+133.5
[3.44]		3-Fcpy	+256	+190	+223	+167.5
[3.45]		2-Fcpy	+136	+32	+84	+154.5

With the exception of complex **[3.45]**, all samples displayed a positive potential shift in $E_{½}$ value indicating that the ferrocenyl group became harder to oxidise on coordination of the palladium metal centre. Complex **[3.44]** offered the largest positive $E_{½}$ value as well as most significant shift on comparison of free ligand **[2.7]** and complex. This is unlike the rhodium complexes, where the rhodium complex with ligand **[2.6]** showed the largest $E_{½}$ shifts. Although the half-wave potential for complex **[3.45]** is puzzling, it is consistent with its spectroscopic properties.

3.5 Preparation and properties of platinum complexes

The preparation of platinum(II) square planar complexes has been well-documented largely owing to the serendipitous discovery of cisplatin, *cis*-diamminedichloroplatinum(II).[29] Since the preparation of cisplatin, a significant number of related platinum complexes have been synthesised in a bid to discover further platinum complexes exhibiting similar or enhanced antitumour activity. Both the *cis* and *trans* isomers of complex **[3.46]** have been prepared and their antitumour activity investigated.[30]

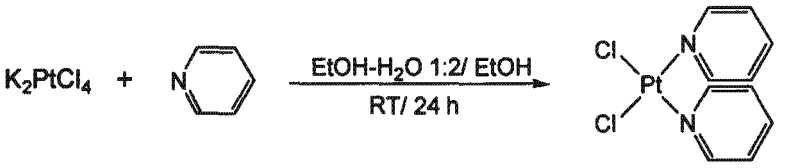

[3.46]: White powder, 72%

Figure 3.35: Synthesis of platinum complex **[3.46]**

The platinum complexes in this study, complexes **[3.46]**-**[3.50]**, were prepared using the synthetic route described in *Figure 3.35*. This methodology is similar to that described for the synthesis of the palladium complex **[3.40]** where the product was formed as a precipitate over time.[31]

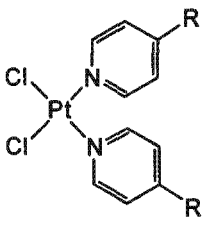

[3.46]: R = H; white powder, 72%

[3.47]: R = Ph; cream powder, 75%

[3.48]: R = (C=N)-Ph; mustard-yellow powder, 70%

[3.49]: R = Fc; orange-red powder, 72%

[3.50]: R = (C_6H_4)Fc; dark red microcrystals, 65%

Figure 3.36: Platinum complexes **[3.46]**-**[3.50]**

The preparation of the ferrocenyl complexes **[3.49]** and **[3.50]** were repeated using the biphasic route devised for the related palladium complexes (see *Figure 3.29*). Both synthetic routes generated the same product with similar yields but with variations in reaction time. On average the biphasic synthetic route proceeded the fastest with reaction times of the order of 5-10 hours, as opposed to 24 hours using the former route.

The complexes were all obtained in good yield. It has been reported that the synthetic route described in *Figure 3.35* produces complexes exclusively in the *cis*-configuration.[31,32] ^{1}H NMR data follow a similar trend to the rhodium complexes. Downfield shifts were observed for the pyridyl protons on complexation of the platinum metal, for all complexes. No shifts were observed in the ferrocenyl protons for complex **[3.50]** while upfield shifts were observed for complex **[3.49]**.

3.6 Preparation and properties of a cobaloxime complex

As a separate point of interest, the preparation of a ferrocenyl cobaloxime complex is reported. The study of cobaloximes is extensive. This class of compound was used as a model for the study of vitamin B_{12} several decades ago.[33] The related pyridine complex, **[3.51]** has previously been prepared. Complex **[3.52]** was prepared through displacement of the pyridyl group in complex **[3.51]** (see *Figure 3.37*).

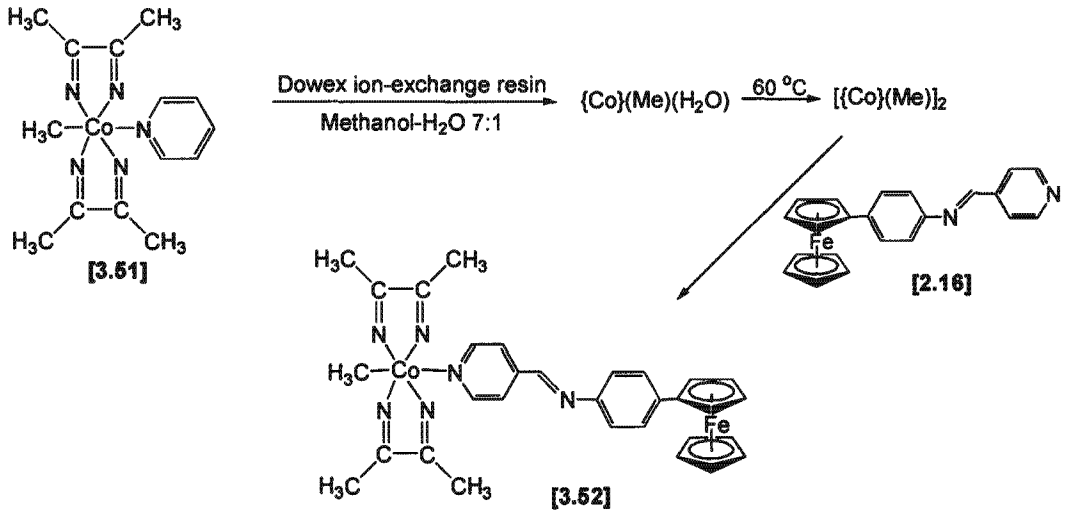

Figure 3.37: Synthesis of cobaloxime complex **[3.52]**

Since both ligands are pyridyl and show similar basicity, a simple displacement of the pyridyl group did not present a feasible route. The pyridyl group in complex **[3.51]** was first removed by displacement with a water molecule with a strongly acidic ion-exchange resin. The water molecule was removed by drying the hydrated compound under vacuum, leading to the formation of a light sensitive dimer. The dimer was reacted with an excess of the ferrocenyl ligand **[2.16]**, in a bridge-splitting reaction to form complex **[3.52]**.

Complex **[3.52]** can be compared to the related rhodium **[3.6]** and iridium **[3.37]** complexes containing the ferrocenyl ligand **[2.16]**. A spectroscopic study of complex **[3.52]** revealed that little to no interaction occurred between the ferrocenyl group and cobalt centre, despite the presence of a conjugated pathway, similar to the rhodium and iridium complexes. Unlike the chemical shifts for the ferrocenyl protons, the pyridyl and imine bond protons did show a slight shift upfield on complexation of the cobalt metal centre, indicating some shielding of these protons on complexation.

The electronic spectra of complexes **[3.6]**, **[3.37]** and **[3.52]** were determined in a range of solvents and shifts in the central metal-to-ligand charge transfer band compared to the free ligand, **[2.16]** (see *Figure 3.38* and *Table 3.15*). Electronic studies of tungsten and molybdenum complexes of ligand **[2.16]** have been reported.[25] These complexes were found to be solvatochromic when comparing electronic spectra recorded in a range of solvents of differing polarity. The most notable differences were recorded in the metal-to-ligand charge transfer band. The results listed in *Table 3.15* reveal that on increasing solvent polarity, small shifts in the metal-to-ligand charge transfer band transpired to a shorter wavelength. These effects were predominantly observed in complex **[3.52]**.

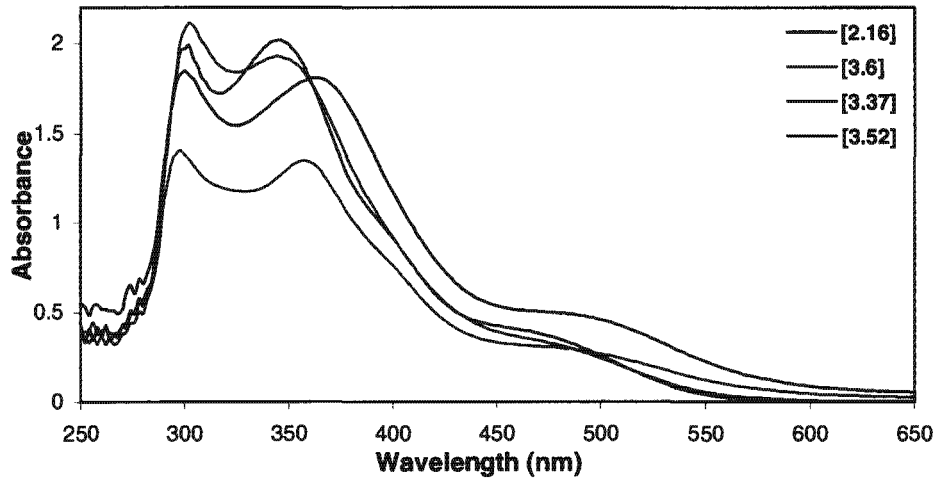

Figure 3.38: Electronic spectra comparing rhodium **[3.6]**, iridium **[3.37]** and cobaloxime **[3.52]** complexes of the ferrocenyl ligand **[2.16]** in acetonitrile

Table 3.15: Solvatochromism of the metal-to-ligand charge transfer band

Complex number		Solvent			
		C_6H_6	THF	MeCN	MeOH
[2.16]	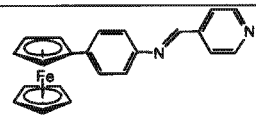	350	350	346	350
[3.6]	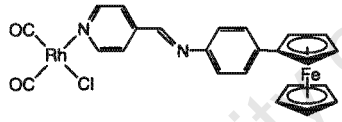	364	364	364	358
[3.37]	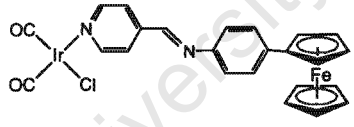	368	370	358	350
[3.52]	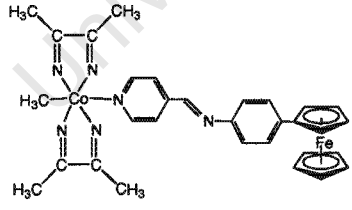	368	360	344	346

The solvatochromic behaviour of transition metal complexes has been linked to their potential non-linear optical properties.[25] Based on the results listed in *Table 3.15*, complex **[3.52]** shows the largest shifts in the metal-to-ligand charge transfer band. Complex **[3.52]** warrants further examination with regard to its potential non-linear optical properties.

References:

1. P. Zanello, *Ferrocenes: Homogeneous Catalysis, Organic Synthesis, Materials Science*, eds. A. Togni and T. Hayashi, VCH, Weinheim, 1995.
2. B. McCulloch, D. L. Ward, J. D. Woolins and C. H. Brubaker Jr., *Organometallics*, 1985, **4**, 1425.
3. T. M. Miller, K. J. Ahmed and M. S. Wrighton, *Inorg. Chem.*, 1989, **28**, 2347.
4. J. D. Carr, S. J. Coles, M. B. Hursthouse, M. E. Light, E. L. Munro, J. H. R. Tucker and J. Westwood, *Organometallics*, 2000, **19**, 3312; J. D. Carr, S. J. Coles, M. B. Hursthouse and J. H. R. Tucker, *J. Organomet. Chem.*, 2001, **637-639**, 304.
5. O. B. Sutcliffe, M. R. Bryce and A. S. Batsanov, *J. Organomet. Chem.*, 2002, **656**, 211.
6. *Comprehensive Inorganic Chemistry*, volume **3**, eds. J. C. Bailar, H. J. Emeléus, R. Nyholm and A. F. Trotman-Dickenson, Pergamon Press, Oxford, 1973.
7. C. L. Thomas, *Catalytic Processes and Proven Catalysts*, Academic Press, New York, 1970.
8. G. Fachinetti, G. Fochi and T. Funaioli, *Inorg. Chem.*, 1994, **33**, 1719.
9. A. J. Pardey, M. Mediavilla, M. Canestrari, C. Urbina, D. Moronta, E. Lujano, P. Baricelli, C. Longo, R. Pastene and S. A. Moya, *Catal. Lett.*, 1998, **56**, 231; A. J. Pardey, M. Fernández, J. Alvarez, C. Urbina, D. Moronta, V. Leon, M. Haukka and T. A. Pakkanen, *Appl. Catal. A: General*, 2000, **199**, 275.
10. J. A. McCleverty and G. Wilkinson, *Inorg. Synth.*, 1966, **8**, 211.
11. W. Manchot and J. König, *Chem. Ber.*, 1925, **58B**, 2173.
12. W. Hieber and H. Lagally, *Z. Anorg. Allg. Chem.*, 1943, **251**, 96.
13. L. Vallarino, *Gazz. Chim. Ital.*, 1959, **89**, 1632.
14. See for example, D. Evans, J. A. Osborn and G. Wilkinson, *J. Chem. Soc.*, 1968, **A**, 3133; A. Spencer, *J. Organomet. Chem.*, 1980, **194**, 113; T. Sakakura and M. Tanaka, *J. Chem. Soc., Chem. Commun.*, 1987, 758; R. B. King, A. D. King and M. Z. Iqbal, *J. Am. Chem. Soc.*, 1979, **101**, 4893.
15. R. D. Gillard, K. Harrison and I. H. Mather, *J. Chem. Soc., Dalton Trans.*, 1975, 133.
16. J. Chatt and L. M. Venanzi, *Nature*, 1956, **177**, 852; J. Chatt and L. M. Venanzi, *J. Chem. Soc.*, 1957, 4735.
17. P. Fougeroux, B. Denise, R. Bonnaire and G. Pannetier, *J. Organomet. Chem.*, 1973, **60**, 375.
18. C. Monti Bragadin, R. H. Dainty, R. D. Gillard and B. T. Heaton, *Nature*, 1969, **223**, 735; T. Giraldi, G. Zassinovich and G. Mestroni, *Chem. Biol. Interactions*, 1974, **9**, 389; G. Zassinovich, G. Mestroni and A. Camus, *J. Organomet. Chem.*, 1975, **91**, 379.

19. K. Tani, T. Mihana, T. Yamagata and T. Saito, *Chem. Lett.*, 1991, 2047.
20. E. M. Barranco, O. Crespo, M. C. Gimeno, A. Laguna, P. G. Jones and B. Ahrens, *Inorg. Chem.*, 2000, **39**, 680.
21. B. T. Heaton, C. Jacob and J. T. Sampanthar, *J. Chem. Soc., Dalton Trans.*, 1998, 1403.
22. *Cambridge Structural Database System*, Version 5.22, Cambridge Crystallographic Data Centre, Cambridge, UK, 2001.
23. A. R. Orpen, L. Brammer, F. A. Allen, O. Kennard, D. G. Watson and R. Taylor, *J. Chem. Soc., Dalton Trans.*, 1989, 51 and references therein.
24. D. Astruc, *Electron Transfer and Radical Processes in Transition-Metal Chemistry*, VCH Publishers Inc., 1995 and references therein.
25. M. M. Bhadbhade, A. Das, J. C. Jeffery, J. A. McCleverty, J. A. Navas Badiola and M. D. Ward, *J. Chem. Soc., Dalton Trans.*, 1995, 2769; S. Sakanishi, D. A. Bardwell, S. Couchman, J. C. Jeffer, J. A. McCleverty and M. D. Ward, *J. Organomet. Chem.*, 1997, **528**, 35.
26. R. B. Bedford, P. A. Chaloner, S. Z. Dewa, G. López, P. B. Hitchcock, F. Momblona and J. L. Serrano, *J. Organomet. Chem.*, 1997, **527**, 75; A. C. Hillier, H. M. Lee, E. D. Stevens and S. P. Nolan, *Organometallics*, 2001, **20**, 4246; J. M. Burke, R. B. Coapes, A. E. Goeta, J. A. K. Howard, T. B. Marder, E. G. Robins and S. A. Westcott, *J. Organomet. Chem.*, 2002, **649**, 199.
27. F. Krauss and B. Brodkor, *Z. Anorg. Allg. Chem.*, 1927, **165**, 73; Y. N. Kukushkin and R. A. Vlasova, *Zh. Obshch. Khim.*, 1983, **53**, 948; B. Viossat, D. Nguyen-Huy, J. C. Lancelot and M. Robba, *Chem. Pharm. Bull.*, 1991, 3023.
28. P. B. Viossat, N-H. Dung and F. Robert, *Acta Cryst.*, 1993, **C49**, 84.
29. B. Rosenberg and L. V. Camp, *Nature*, 1965, **205**, 698; B. Rosenberg, L. V. Camp, J. E. Trosko and V. H. Mansour, *Nature*, 1969, **222**, 385 and B. Rosenberg and L. V. Camp, *Cancer Res.*, 1970, **30**, 1799.
30. N. Farrell, L. R. Kelland, J. D. Roberts and M. Van Beusichem, *Cancer Research*, 1992, **52**, 5065.
31. G. B. Kauffman, *Inorg. Synth.*, 1963, **7**, 249.
32. C. Tessier and F. D. Rochon, *Inorg. Chim. Acta*, 1999, **295**, 25.
33. N. Bresciani-Pahor, M. Forcolin, L. G. Marzilli, L. Randaccio, M. F. Summers and P. J. Toscano, *Coord. Chem. Rev.*, 1985, **63**, 1; B. D. Gupta, R. Yamuna, V. Singh, U. Tiwari, T. Barclay and W. Cordes, *J. Organomet. Chem.*, 2001, **627**, 80.

Chapter 4: Some Catalytic Applications of Multimetallic Complexes

4.1 Introduction

The development of homogeneous catalysis is closely linked to the development of organometallic chemistry, leading to many advances in organic synthesis. The preparation of transition metal complexes has greatly aided in this process with new classes of compounds readily obtained through the use of these catalysts.[1] Transition metal complexes have long been used since the early pioneering work during the 1930 to 1950's. Early applications of these complexes include the carbonylation of alkenes and alkynes by metal carbonyls, polyethene and polypropene preparation by Ziegler-Natta catalysts and acetaldehyde preparation from ethene by the Wacker process using palladium and copper catalysts.[2]

The study of homogeneous catalysis has certain advantages over heterogeneous catalysis. The reactions occur under milder conditions while the selectivity of the catalytic system can be tuned by changes in the ligand or solvent.[3] In theory, designing a homogeneous catalyst for a specific need is possible. Limitations of homogeneous catalysis include separation of the catalyst from the reaction mixture on completion of the reaction and stability of the complexes at extremely high temperatures.[1]

The use of nitrogen donor ligands has received increasing prominence over the past few years but has still not enjoyed the type of systematic investigation that has been done for phosphorus-donors. Nitrogen-donors are often used in chelating ligands containing both phosphorus- and nitrogen–donors in the form of pincer ligands. The P,N-ligands do not differ significantly from the related P,P-ligands. Some differences have been noted in the reactivity of metal complexes containing these ligands.[4] Nitrogen-containing optically active ligands have also made significant contributions to the field of asymmetric catalysis.[5]

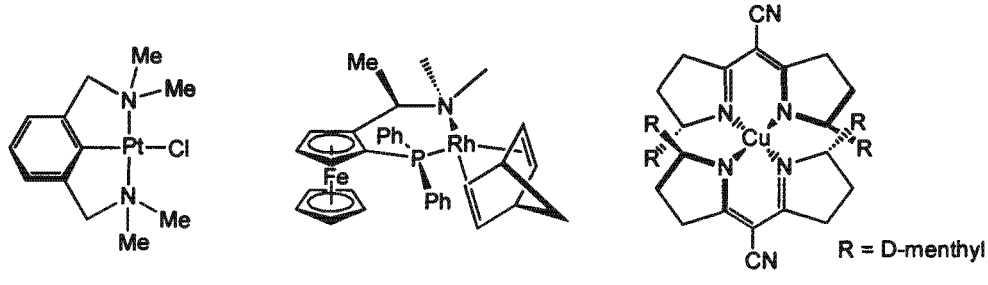

Figure 4.1: Examples of nitrogen donor complexes used as catalysts[5]

Nitrogen-donor ligands have been used in several areas of catalysis, either as solely nitrogen-donor or together with other donor groups such as phosphorus. Several areas of asymmetric catalysis where nitrogen donor complexes have shown activity include hydrogenation and reduction, transfer hydrogenation, hydrosilylation, cyclopropanation, Diels-Alder reactions, aldol condensations, alkylation of aldehydes, conjugate addition reactions, Grignard coupling, allylic alkylation and various oxidation reactions.[5,6,7]

The primary objective of this research was the preparation of novel metal-containing complexes with a view towards investigation of interactions between the metals. Preliminary investigations into the potential catalytic activity of several complexes in this study were carried out. The specific catalytic applications examined were based on the activity of similar complexes reported in the literature.

Three catalytic applications are presented. The polymerisation of phenylacetylene has been reported with rhodium and iridium catalysts. Current investigations include the use ferrocenyl rhodium and iridium catalysts. The study of the ferrocenyl complexes suggests that linear complexes would be better suited to the preparation of high molecular weight polymers. This supposition was investigated through variations in the catalyst ligands. Complexes were examined comparing the activity of catalysts with a systematic increase in the spacer groups. Studies into the carbonylation of nitrobenzene were based on the reported activity of a palladium pyridyl complex, $PdCl_2py_2$. The effect of introducing a substituent on the pyridyl ligand was considered together with the position of the substituent. The contribution of steric and electronic factors on the activity of the catalyst was considered. The activity of rhodium and iridium complexes as hydrogenation catalysts is well-known. The activity of rhodium and iridium pyridyl complexes was examined with variations in the ligand and catalyst ratio.

4.2 Polymerisation of phenylacetylene

4.2.1 Introduction

The examination of polymeric acetylene materials has gained popularity recently due to their electrical conducting properties.[8] The interaction of polymers with small gaseous molecules such as oxygen, nitrogen dioxide and ammonia, have been investigated.[9] It was found that this interaction may result in electrical conductivity. As such, the polymers were investigated for their potential application as sensors and field-effect transistors. Polyphenylacetylene and its derivatives have shown conducting properties and undoped polyphenylacetylene is known to change its conductivity slightly on absorption of gases such as carbon monoxide, carbon

dioxide and methane. The polymer has been further investigated for the potential preparation of humidity sensors.

4.2.2 Polymerisation catalysts for the preparation of polyphenylacetylene

The polymerisation of derivatised acetylenes is reported using a variety of methods such as those incorporating radical, cationic and coordination mechanisms. It was found that transition metal catalysts utilising metals such as chromium, molybdenum and tungsten, polymerise acetylenes mainly through a coordination mechanism.[10,11,12] Initial studies into the polymerisation of acetylenes utilised Ziegler-Natta type catalysts when *trans*-polyacetylene was first prepared by Natta in 1958.[16] Since then, the catalytic activity of other transition metal complexes has been studied. The use of these complexes is not without its disadvantages where low molecular weight (M_w) polymers of the order of 3 000 have been prepared. High reaction temperatures and long reaction times are often required and dimers and cyclic trimers have been known to form as by-products. Despite this, the use of transition metal complexes to catalyse polymerisation reactions still remains popular since these complexes allow an examination of the polymerisation reaction under a host of different conditions including temperature, solvent and catalyst ratio.

The use of tungsten and molybdenum catalysts have been reported, where initial results showed M_w of 5 000-15 000 for polyphenylacetylene.[13] The reaction was optimised by varying the solvent, yielding polymers of up to M_w 100 000.[13] The activity of cationic rhodium complexes of the type $[Rh(COD)(L)]PF_6$ where COD is 1,5-cyclooctadiene and L is 2,2'-bipyridine, 1,10-phenanthroline or 2,9-dimethyl-1,10-phenanthroline has been reported.[9] These catalysts produce highly stereoregular polymers but with low M_w of the order of 9 000. The activity of the zwitterionic complex, $Rh^+(COD)BPh_4^-$ under hydrosilation conditions was reported to yield stereoregular *cis*-polymers with M_w of up to 35 000.[14] The highest reported M_w achieved was of approximately 4.3 x 10^6 with a $[Rh(norbornadiene)Cl]_2$ complex.[15] The use of ferrocenyl rhodium(I) and iridium(I) complexes was also reported (see *Figure 4.2*).[8]

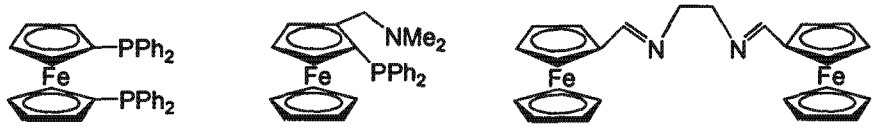

[2.25] FcNP [2.17]

Figure 4.2: Ferrocenyl ligands used in catalytic rhodium and iridium complexes[8]

Cationic and neutral rhodium and iridium ferrocenyl complexes of the type $[M(COD)(LL)]ClO_4$ and $[MCl(LL)]_2$ were reported to be highly effective at producing stereoregular polymers with

M_w of 47 000–95 000.[8] The cationic rhodium complex of **[2.17]** was reported as the most successful overall in terms of yield, *cis* content, molecular weight and polydispersity. However, attempts by us to reproduce the cationic rhodium complex with the ferrocenyl ligand **[2.17]**, were unsuccessful. Comparisons were carried out with the rhodium complex of ferrocenyl ligand **[2.25]**.

4.2.3 Polymer stereochemistry

Three possible stereochemical isomers can be formed in the polymerisation of phenylacetylene (see *Figure 4.3*). These isomers are differentiated by their unique physicochemical and spectroscopic properties, greatly facilitating their identification.[8,16]

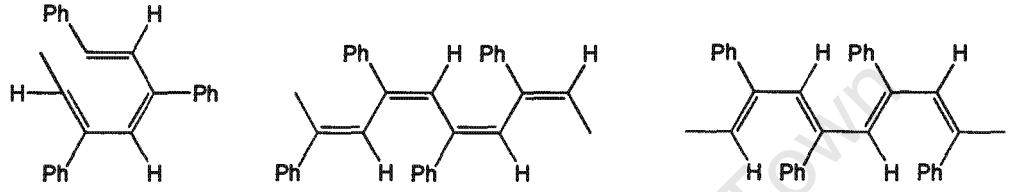

Figure 4.3: Stereochemical isomers of polyphenylacetylene

The *cis-cisoidal* isomer can be differentiated from the remaining two isomers based on its insolubility in benzene; the remaining isomers are completely soluble in the solvent. The *cis-cisoidal* and *cis-transoidal* isomers show similar spectroscopic behaviour in both NMR and infrared spectroscopy, differentiating them from the *trans-cisoidal* isomer.

The *cis-cisoidal* and *cis-transoidal* isomers show a band at 740 cm^{-1} in the infrared spectrum, which is related to the *cis* content of the polymer. The *trans-cisoidal* isomer does not exhibit this band but instead a band is found at 1265 cm^{-1} and 970 cm^{-1}. These bands are due to a *trans* C-H out of plane deformation vibration. A further band occurs at 895 cm^{-1} in the *cis*-isomers and its absorption can be correlated to the 740 cm^{-1} band.

The ratio between the absorption bands at 1500 and 1450 cm^{-1} provides insight into the stereochemistry of the polymer. A ratio of 1.00 or smaller, together with a strong absorption band at 740 cm^{-1} can be correlated to the *cis* content of the polymer, whereas a ratio of greater than 1.00 with no band at 740 cm^{-1} is related to the *trans* content of the polymer. Some polymers with a ratio of greater than 1.00 but weak absorptions at 740 cm^{-1} occur when part of the polymer isomerises to the *trans* conformation.[16]

Similarly, the ^1H NMR spectrum of the polymer allows for differentiation between the respective isomers[8]. ^1H NMR studies have revealed that aside from chemical shift differences in the aromatic protons of the isomers, a peak can be anticipated at approximately 5.82 ppm due to the olefinic proton occurring in the *cis-cisoidal* and *cis-transoidal* isomers. This peak is a characteristic of the *cis* isomer and can be related to the intensity of the 740 cm^{-1} band found in the infrared spectrum. The *trans-cisoidal* polymer has either a small or no 5.82 ppm peak and displays a wide weak resonance in the 3-4 ppm region due to the aliphatic protons.

4.2.4 Catalytic polymerisation studies

The catalytic polymerisation of phenylacetylene was investigated with a series of rhodium complexes (see *Table 4.1*). The catalytic activity of the nitrogen donor complexes was compared to several phosphine donor complexes, **[3.29]**, **[3.30]** and **[3.31]**. The nitrogen donor complexes were selected for a comparison of structural changes in the ligand and to determine its influence on the activity of the catalyst.

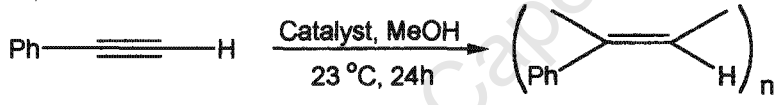

Table 4.1: Comparison of catalytic activity[a]

Complex number	Catalyst	Ligand	Yield[b] (%)	*Cis* content[c] (%)	M_n	M_w	M_w/M_n
[3.8]	RhCl(COD)L	Pyridine	65	99.7	7 591	48 241	6.3
[3.9]		(C_6H_5)py	66	99.3	7 476	48 623	6.5
[3.10]		(C_6H_5)NCpy	65	96.7	7 717	47 113	6.1
[3.14]		Fc(C_6H_4)NCpy	75	99.7	8 673	53 085	6.1
[3.16]		3-Fc(C_6H_4)py	60	96.6	7 044	49 591	7.0
[3.13]		4-Fc(C_6H_4)py	74	93.5	7 831	51 599	6.6
[3.30]		$FcPPh_2$	56	91.3	2 886	27 847	9.6
[3.21]	$[Rh(COD)L_2]ClO_4$	Pyridine	50	100	8 452	47 473	5.6
[3.25]		4-Fc(C_6H_4)py	62	91.3	4 774	45 523	9.5
[3.26]		Fc(C_6H_4)NCpy	64	98.8	11 693	68 415	5.8
[3.31]		$FcPPh_2$	25	84.4	3 364	36 109	10.7
[3.29]	$[Rh(COD)L]ClO_4$	Dppf	62	100	2 903	33 803	11.6

[a] Reaction conditions: 0.3 mol % in MeOH (15 ml); 24 hrs at 23 °C

[b] Isolated yield

[c] Calculated according to reference 16

The yield, *cis* content, number average molecular weight (M_n), weighted average molecular weight (M_w) and the polydispersity (ratio of M_w and M_n) of each polymer sample was determined (see *Table 4.1*).

The activity of the catalysts can be evaluated in terms of,

(i) Polymer yield: Average polymer yields were obtained for all catalysts, with complex **[3.31]** producing very little polymer. The temperature of the reaction played a significant role in the polymer yield. Fluctuations in temperature affected the yield to the point that the temperature was maintained constant with a thermal bath.

(ii) *Cis* content of the polymer: All the rhodium catalysts examined produced polymers with a fairly high *cis* content. Complex **[3.31]** yielded the lowest *cis* content. The spectroscopic data indicated that the polymer was partially isomerised to the *trans* conformation.

(iii) M_w: Complex **[3.26]** produced the largest polymer. The size of the polymer appeared to be related to the length of the catalyst. The more linear extended ferrocenyl rhodium complexes such as complexes **[3.13]** and **[3.14]** produced larger polymers compared to complex **[3.8]**. This was confirmed by comparison of complexes **[3.13]** and **[3.16]**. The rhodium phosphine catalysts produced the smallest polymers.

(iv) Polydispersity: A lower value indicates a more uniform distribution of polymer. The polydispersity values were high for all polymer samples. The polymer was observed to form almost immediately on addition of the catalyst to a solution of the monomer for all catalysts investigated. This rapid formation of polymer was attributed to the elevated polydispersity values. The polydispersity of complex **[3.29]** was significantly higher than reported.[8] This could indicate that the increased values are due to the reaction conditions employed in this study.

(v) Activity of the nitrogen and phosphine donor complexes: The nitrogen donor complexes were significantly more active than the phosphine donor complexes with better yields, M_w values and polydispersity.

4.2.5 Spectroscopic properties

The physico-chemical properties of the polymers carry significant information about the stereochemistry of the isomers. The polymers prepared with the catalysts investigated in this study exhibited similar ^1H and ^{13}C NMR and infrared spectra (see *Figures 4.4* and *4.5*). The ^1H NMR peak distribution indicated mainly *cis*-isomer polymers. In all cases a strong peak was observed at 5.8 ppm in the ^1H NMR spectrum. Two further peaks at 6.9 and 6.6 ppm were observed due to the aromatic protons. The distribution pattern indicated that the

polymers prepared have predominantly *cis-transoidal* character. A similar pattern was observed in the ^{13}C NMR spectrum with a peak due to the olefinic protons observed at 127 ppm and peaks at 139 and 142 ppm due to the aromatic protons.

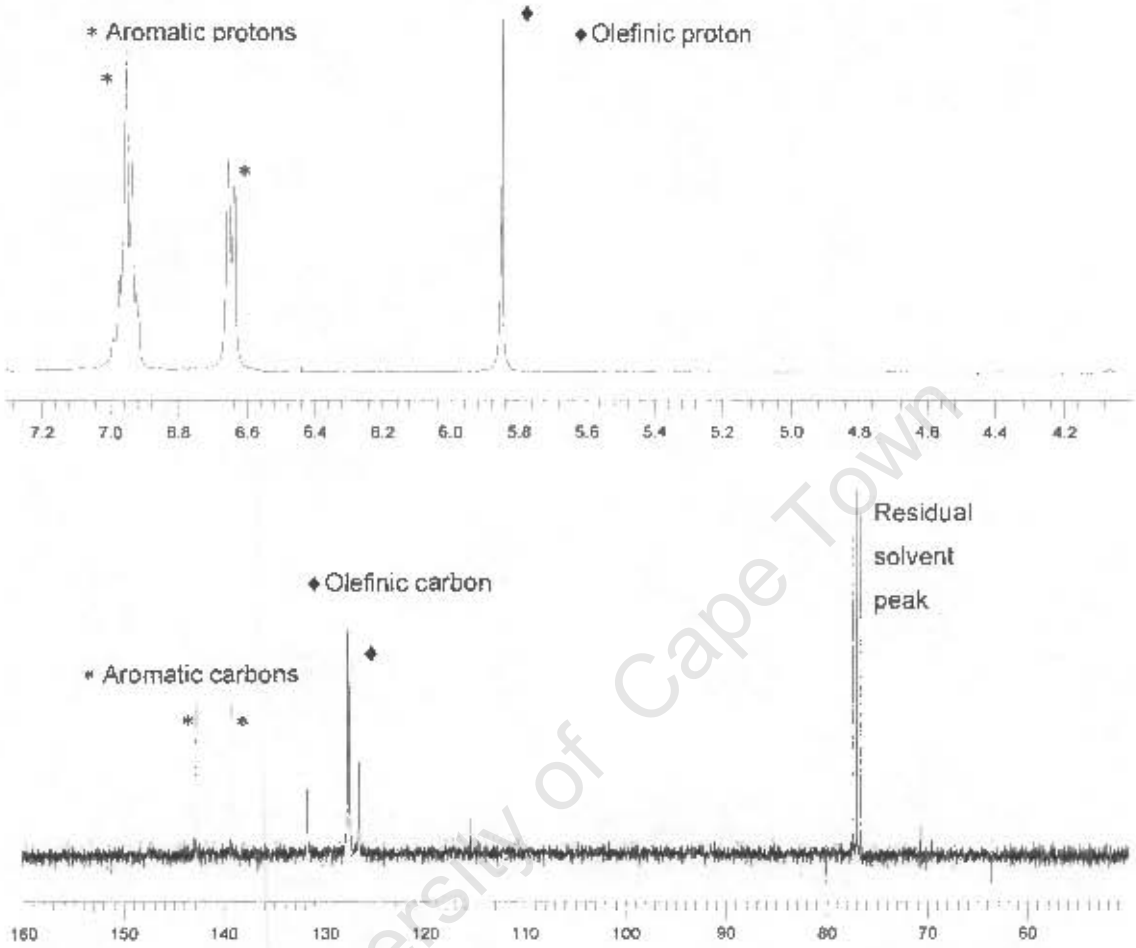

Figure 4.4: ^{1}H and ^{13}C NMR spectra in $CDCl_3$ of polyphenylacetylene, catalysed by RhCl(COD)(4-FcPhpy), complex **[3.13]**

The catalyst was effectively removed from the polymer. No trace of it was detected in the ^{1}H and ^{13}C NMR spectra. All the catalysts and the monomer were completely soluble in methanol while the polymer was not, facilitating separation of the polymer.

A strong absorption band at 740 cm^{-1} was observed in all the polymer samples. Medium to weak bands were observed at 1380 and 895 cm^{-1}. These bands confirmed the *cis* conformation of the polymers. The *trans* conformation bands, in particular 1265 cm^{-1} were absent in the infrared spectra of the polymers.

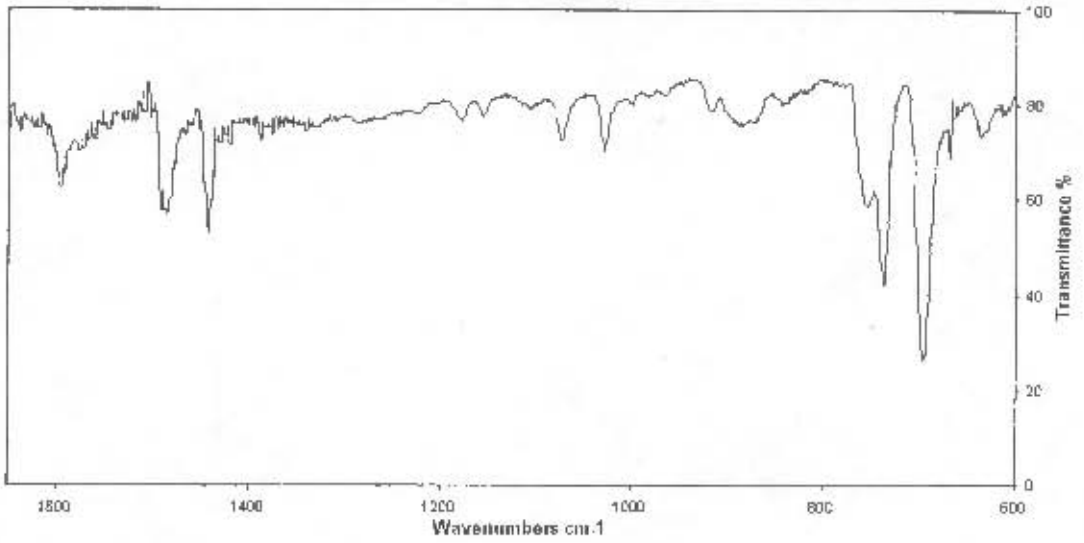

Figure 4.5: IR spectrum of polyphenylacetylene prepared using $[Rh(COD)(py)_2]ClO_4$ as catalyst

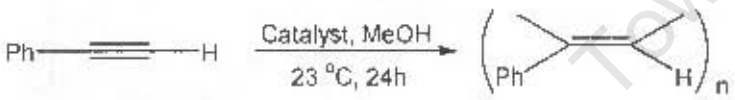

Table 4.2: Determination of the *cis* content of polymers

Complex number	Catalyst	Ligand	1500 vs 1450 ratio (from IR)	% Cis content from NMR[a]	Polymer colour
[3.8]	RhCl(COD)L	Pyridine	1.05	99.7	Yellow
[3.9]		(C_6H_5)py	1.04	99.3	Yellow
[3.10]		(C_6H_5)NCpy	1.05	96.7	Yellow
[3.14]		Fc(C_6H_4)NCpy	1.06	99.7	Yellow
[3.16]		3-Fc(C_6H_4)py	1.09	96.6	Yellow
[3.13]		4-Fc(C_6H_4)py	1.06	93.5	Yellow
[3.30]		$FcPPh_2$	1.02	91.3	Yellow
[3.21]	$[Rh(COD)L_2]ClO_4$	Pyridine	1.08	100	Yellow
[3.25]		4-Fc(C_6H_4)py	1.22	91.3	Yellow-brown
[3.26]		Fc(C_6H_4)NCpy	1.05	98.8	Yellow
[3.31]		$FcPPh_2$	1.03	84.4	Brown
[3.29]	$[Rh(COD)L]ClO_4$	Dppf	1.03	100	Yellow

[a] Calculated according to reference 16

Ratios of approximately 1 were obtained for the 1500 and 1450 cm^{-1} absorbance bands. These values were consistent with the calculated *cis* content of the polymers and their spectroscopic properties. Complex **[3.25]** gave a slightly higher value but this may be related to partial isomerisation of the polymer.

4.2.6 Thermal analysis

The thermal behaviour of the polymers prepared using the catalysts in this study are very similar. The results are all consistent with the predominantly *cis*-conformation of the polymers (see *Figure 4.6*).

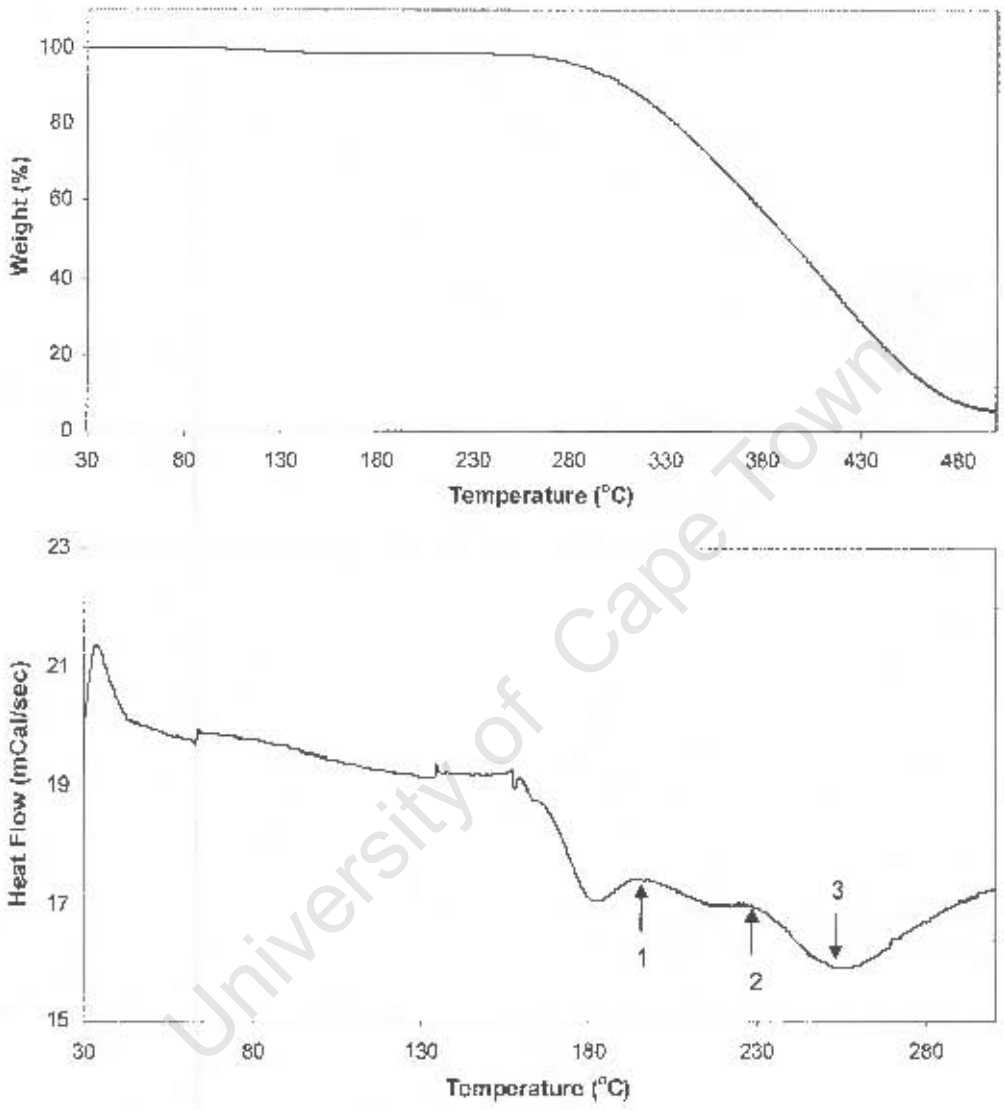

Figure 4.5: TGA and DSC for polyphenylacetylene obtained with RhCl(COD)(4-FcPhpy) as catalyst

The TGA in *Figure 4.6* displays the thermal stability of the polymer. The polymer only starts to decompose from 265 °C. A residual of 5 % is reached at 500 °C. The DSC shows three peaks related to the *cis*-conformation of the polymer. The first two peaks are exotherms at 196 and 226 °C. Peak 1 corresponds to a *cis-trans* isomerisation while peak 2 corresponds to various crystallisation phenomena. No glass transition was observed but this has been noted on

several occasions for this type of polymer.[8,17] The endotherm, peak 3, occurring at 259 °C is characteristic of thermal decomposition of the *cis*-polymer.

The characteristic peaks in the DSC occur in all the polymers prepared. *Table 4.3* lists the exothermic and endothermic temperatures obtained for the polymers. A comparison of the thermal data of these polymers can be used to draw a correlation between the catalyst and the properties of the polymer.

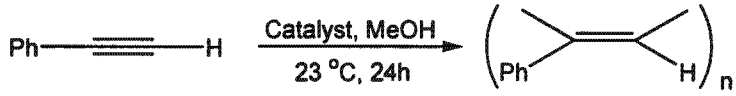

Table 4.3: DSC thermal data for polyphenylacetylenes prepared using rhodium catalysts

Complex number	Catalyst	Ligand	Temperature (°C)		
			Peak 1	Peak 2	Peak 3
[3.8]	RhCl(COD)L	Pyridine	183	203	220
[3.9]		(C_6H_5)py	200	235	255
[3.10]		(C_6H_5)NCpy	163	174	182
[3.14]		Fc(C_6H_4)NCpy	157	220	255
[3.16]		3-Fc(C_6H_4)py	171	236	250
[3.13]		4-Fc(C_6H_4)py	196	226	259
[3.30]		$FcPPh_2$	164	209	261
[3.21]	[Rh(COD)L_2]ClO_4	Pyridine	160	213	250
[3.25]		4-Fc(C_6H_4)py	161	269	280
[3.26]		Fc(C_6H_4)NCpy	160	270	316
[3.31]		$FcPPh_2$	158	182	255
[3.29]	[Rh(COD)L]ClO_4	Dppf	184	222	258

Complex **[3.26]** produced the most thermally stable polymer with the highest onset decomposition temperature recorded. Complex **[3.10]** produced the least thermally stable polymer. The crystallisation and isomerisation temperature vary with the catalyst.

4.2.7 General remarks

Although the mechanism of the polymerisation reaction has not been determined in this work, the most generally accepted mechanisms for the catalytic polymerisation of acetylenes are presented.

The linear polymerisation of phenylacetylene occurs through two main pathways. Firstly, a direct four-centre acetylenic mechanism is possible. This involves a displacement of the

cyclooctadiene by solvent in the catalyst precursor. A species of the type $[Rh(L)_2(solvent)_2]^+$ or $[RhCl(L)(solvent)_2]$ is formed in solution, followed by oxidative addition of phenylacetylene to rhodium, yielding a hydridoacetylenic species. The coordination is followed by a migratory insertion, leading to the formation of a vinylic rhodium intermediate species, ultimately leading to the formation of the polymer (see *Scheme 4.1*). Ziegler-Natta catalysts as well as some nickel and palladium transition metal complexes are known to follow this type of mechanism in their polymerisation reactions.

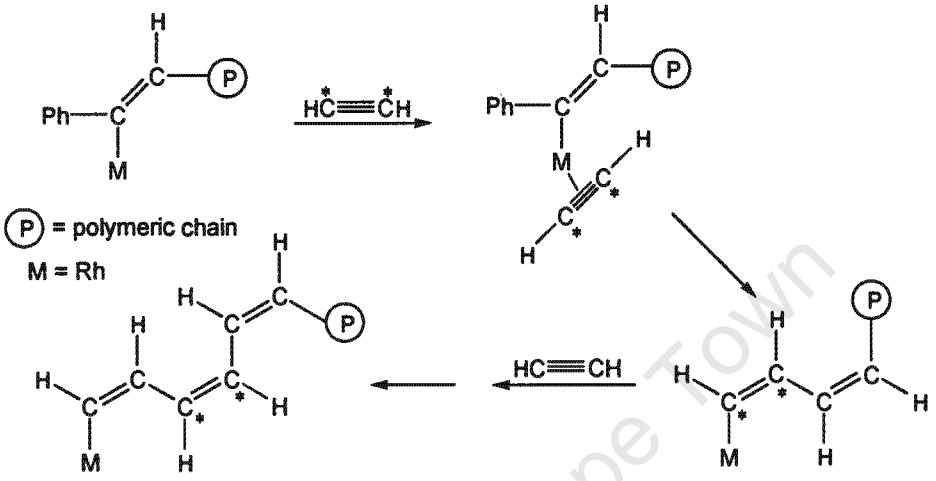

Scheme 4.1: Direct four-centre acetylene insertion mechanism for formation of acetylenic polymer[18]

The second main pathway involves the formation of a metal carbene complex with an intermediate vinylic metallacycle. A key intermediate step involves the rearrangement of a monomer unit within the diacetylenic complex. This is formed by stepwise addition of a second monomer to the metal carbene complex. The metallacycle can be prepared through a 1,2-addition. Repetition of these steps leads to formation of the polymer (see *Scheme 4.2*).

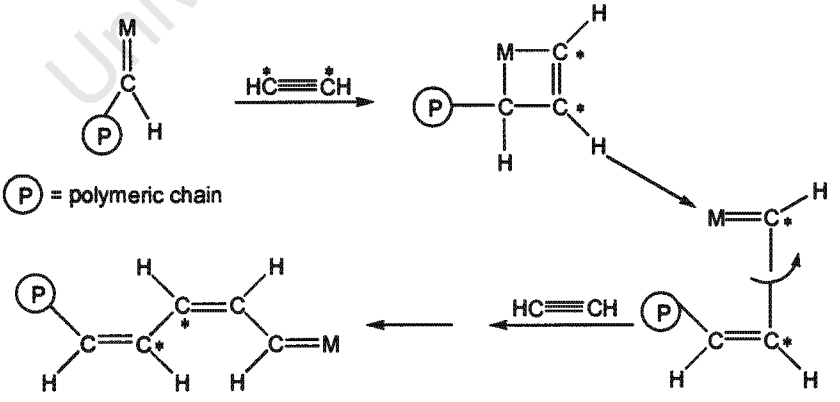

Scheme 4.2: Metallacycle mechanism for formation of acetylenic polymer[18]

In terms of the formation of the polymer, the main difference between the mechanisms involves the carbon bonds of the monomer. The insertion mechanism (*Scheme 4.1*) predicts that the carbon bonds of the monomer will end up doubly bonded to one another while the metallacycle mechanism (*Scheme 4.2*) predicts that although the carbons of the monomer unit end up next to each other, they will be singly bonded to one another.

4.3 Carbonylation of nitrobenzene

4.3.1 Introduction

The range of products formed from the carbonylation of nitrobenzene and other nitro-compounds makes the process of both academic and industrial significance. Isocyanates, carbamates, ureas, azoarenes and azoxyarines, amines, amides, oximes and some heterocyclic compounds represent a range of compounds prepared by this process. Ureas and carbamates are important products and intermediates in the preparation of fertilisers while isocyanates are intermediates in the preparation of polyurethanes, pesticides, synthetic leather, adhesives and coatings.[19] Carbamates and ureas have the most industrial applications as they can be converted to other compounds such as isocyanates. These compounds are readily prepared in carbonylation reactions catalysed by palladium systems.

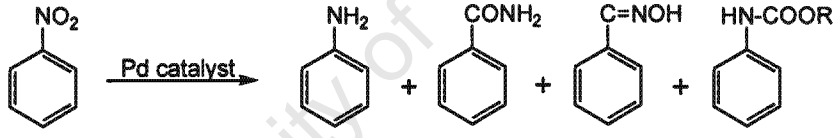

Figure 4.6: Carbonylation of nitrobenzene with selected products listed

4.3.2 Palladium catalysts

Palladium complexes have been reported as among the most active catalysts for the carbonylation of nitrobenzene.[20] These complexes are divided into several categories with reactions involving the addition of a Lewis acid, complexes containing nitrogen-donor ligands and finally phosphine-donor complexes.[20] The former two categories are of relevance to this investigation. The activation of palladium complexes of the type $PdCl_2$ or $PdCl_2py_2$ by a Lewis acid such as a metal oxide or chloride was amongst the first reported. These catalysts produce ureas and carbamates in good yield. However, only limited mechanistic information is available for carbonylation reactions involving palladium complexes. Problems such as reproducibility often arise and may be linked to the corrosive nature of the co-catalysts used. This resulted in significant plating of the palladium metal on the walls of the reaction vessel.[19]

The conditions employed in the current investigation were based on the work of Skupińska and co-workers,[21,22] where the use of the corrosive Lewis acids was replaced with iron and iodine.

The presence of nitrogen-donor ligands such as phenanthroline and pyridine has been credited with promotion of the carbonylation reaction.[19] The addition of excess pyridine, for example, has been reported to stabilise the palladium system against precipitation of the metal while chelating ligands such as 2,2'-bipyridine were reported as deactivating the catalytic system.[19]

4.3.3 Comparison of catalytic activity

The current investigation was based primarily on the work of Skupińska and co-workers.[21,22] A palladium complex of the type $PdCl_2py_2$ was used to catalyse the carbonylation of nitrobenzene. The efficient conversion of nitrobenzene into mainly aniline and ethylphenylcarbamate has been reported, with the carbamate formed in higher yield (see *Figure 4.7*).

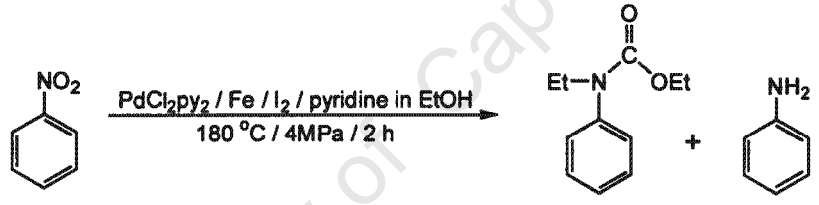

$PdCl_2py_2$ / Fe / I_2 / pyridine: 0.17 / 10 / 0.4 / 6.2 mmol

Figure 4.7: Carbonylation of nitrobenzene with reaction conditions and main products as reported by Skupińska and co-workers[21,22]

Iron powder and iodine were added in place of the corrosive Lewis acid to stabilise the catalyst and minimise plating. The iron was added in as fine a form as possible. The addition of iodine was reported to promote the conversion of amines formed to urea derivatives under relatively mild conditions.[23] Pyridine was added to stabilise the palladium system against precipitation of the metal. Ethanol was used as both a solvent and reagent, acting as a source of hydrogen for the formation of aniline by hydrogenation of nitrobenzene.[24]

The palladium system was reported as extremely active with substrate conversions in the region of 100 % at 180 °C and at least 70 % at 150 °C. The activity of several related palladium complexes in this study was evaluated as carbonylation catalysts (see *Figure 4.8* and *Table 4.4*). The palladium complexes were chosen to compare the effect of derivatising the pyridyl ligands and the effect of the substituent position on the activity of the catalyst.

Examination of the carbonylation reaction with palladium catalysts was specifically chosen for this purpose.

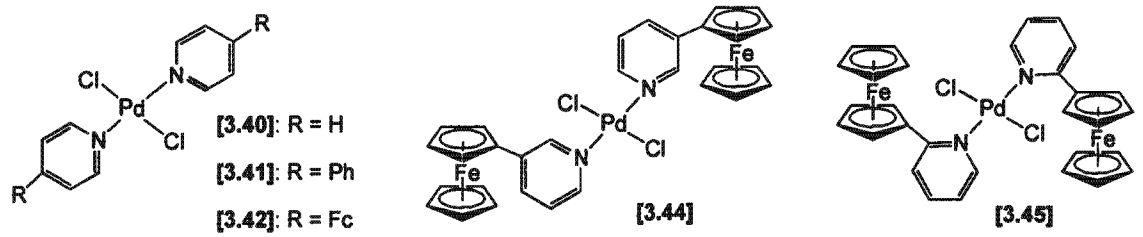

Figure 4.8: Palladium complexes examined as carbonylation catalysts

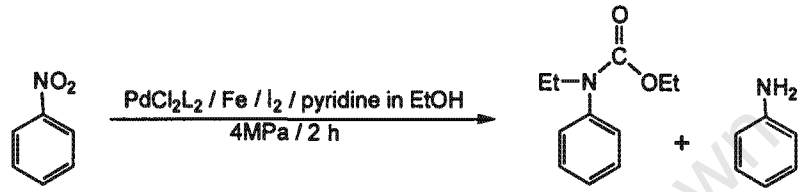

Table 4.4: Summary of carbonylation results catalysed by palladium pyridyl complexes[a]

Entry	Complex number	Catalyst	Ligand	Nitrobenzene conversion (%)[b]	Carbamate formed (%)[b]
1	**[3.40]**	$PdCl_2L_2$	Pyridine[c]	95.6	84.0
2	**[3.40]**		Pyridine	74.8	57.0
3	**[3.41]**		4-Phpy	97.5	94.8
4	**[3.42]**		4-Fcpy	75.4	73.2
5	**[3.44]**		3-Fcpy	96.1	90.4
6	**[3.45]**		2-Fcpy	93.4	90.4

[a] $PdCl_2L_2$/Fe/I_2/pyridine (0.42/25/1/15.5 mmol) in ethanol (50 ml) with nitrobenzene (0.2 mol) for 2 h at 4 MPa and 150 °C

[b] GC determined yields

[c] Reaction temperature 180 °C

The catalyst system with complex **[3.40]**, entry 1, was reported as highly efficient under these conditions with nearly 100% substrate conversion.[22] However, significant plating was observed and the reaction was repeated at 150 °C. Although the plating problem was eliminated, a lower substrate conversion was obtained at this temperature (see entry 2). The subsequent reactions were carried out at 150 °C (see entries 2-6). The modified palladium catalysts were on average more efficient than complex **[3.40]** under similar reaction conditions.

Results for the complexes studied at 150 °C are summarised graphically in *Figure 4.9*. Complexes **[3.41]**, **[3.44]** and **[3.45]** clearly display increased efficiency in formation of the main carbamate product, relative to complex **[3.40]**. It would appear that derivatising the pyridyl ring is linked to the increased activity of the complexes.

The activity of the palladium complexes is due to a combination of steric and electronic effects. The significance of the substituent position on the pyridyl ligand is displayed through comparison of the catalytic efficiency of complexes **[3.42]**, **[3.44]** and **[3.45]**. Complexes **[3.44]** and **[3.45]** were more active than complex **[3.42]**. This result indicates that steric considerations do not play as significant a role.

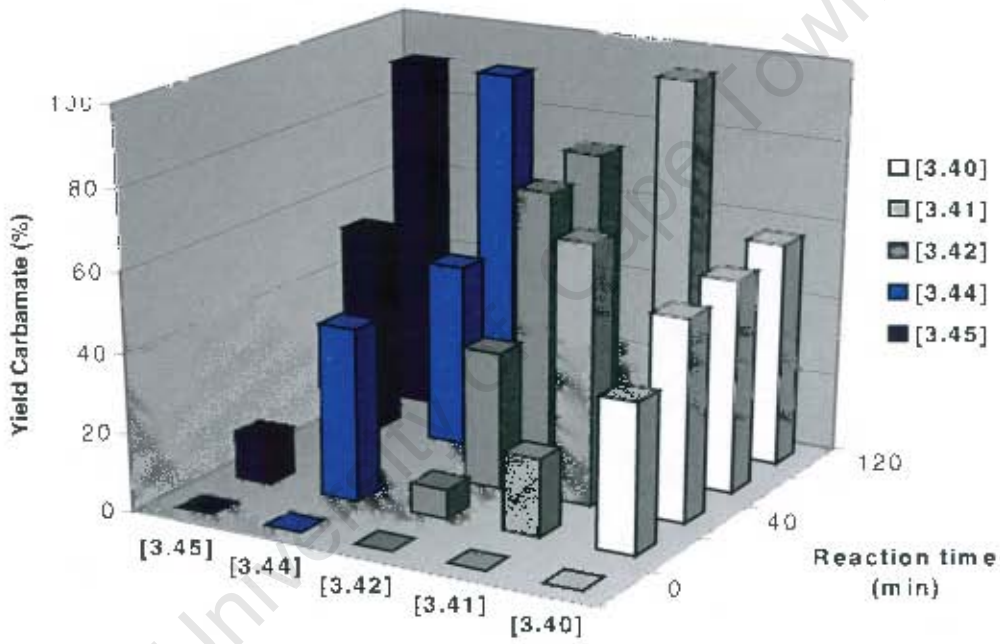

Figure 4.9: Comparison of catalyst activity as a function of product yield over reaction time

The efficiency of the modified palladium complexes was not solely based on the rate of product formation. The reaction was further evaluated with comparisons of substrate conversions and major product formation. A series of graphs are presented in *Figure 4.10* comparing the relative amount of substrate converted to that of major product formed for each of the palladium complexes examined.

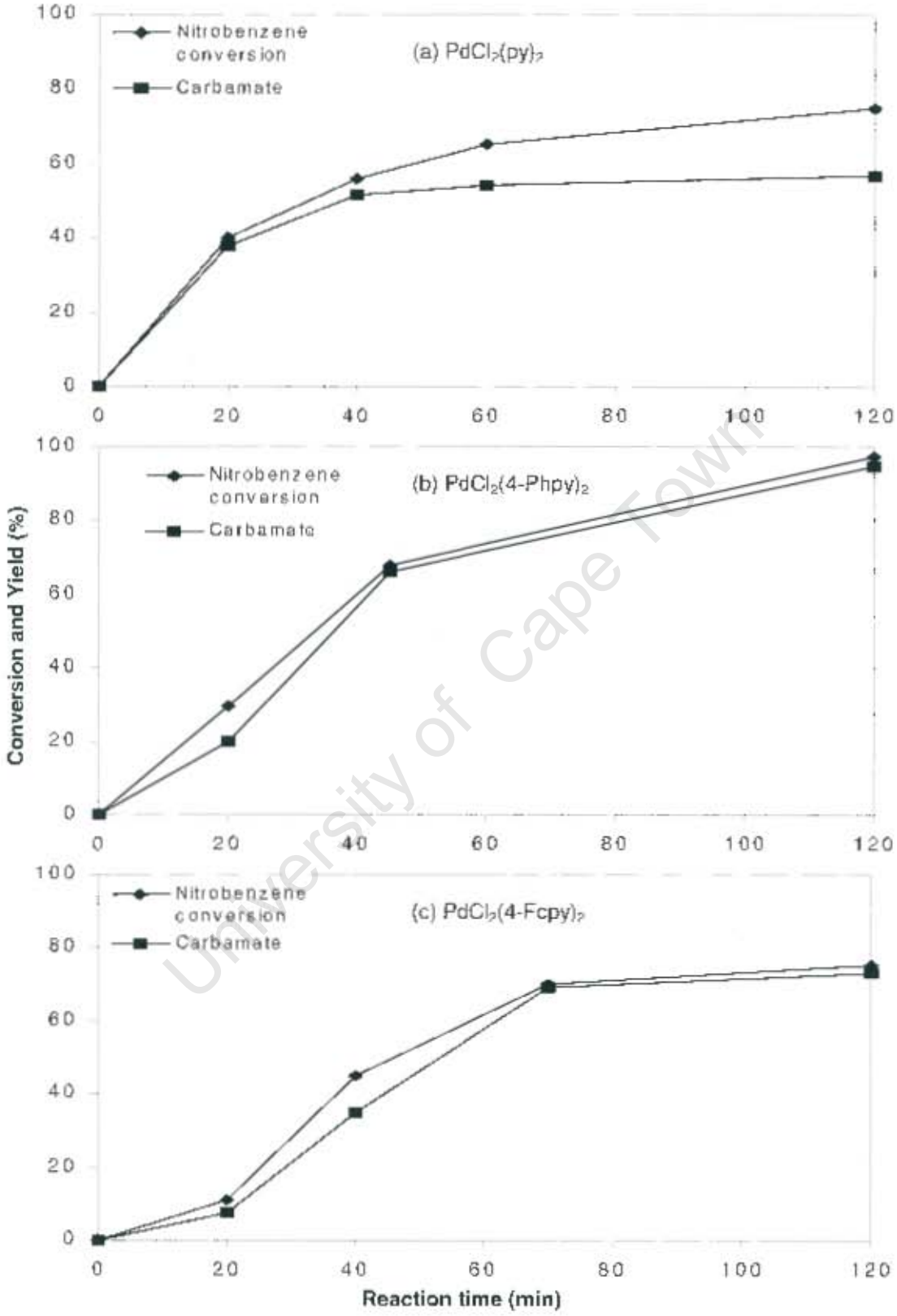

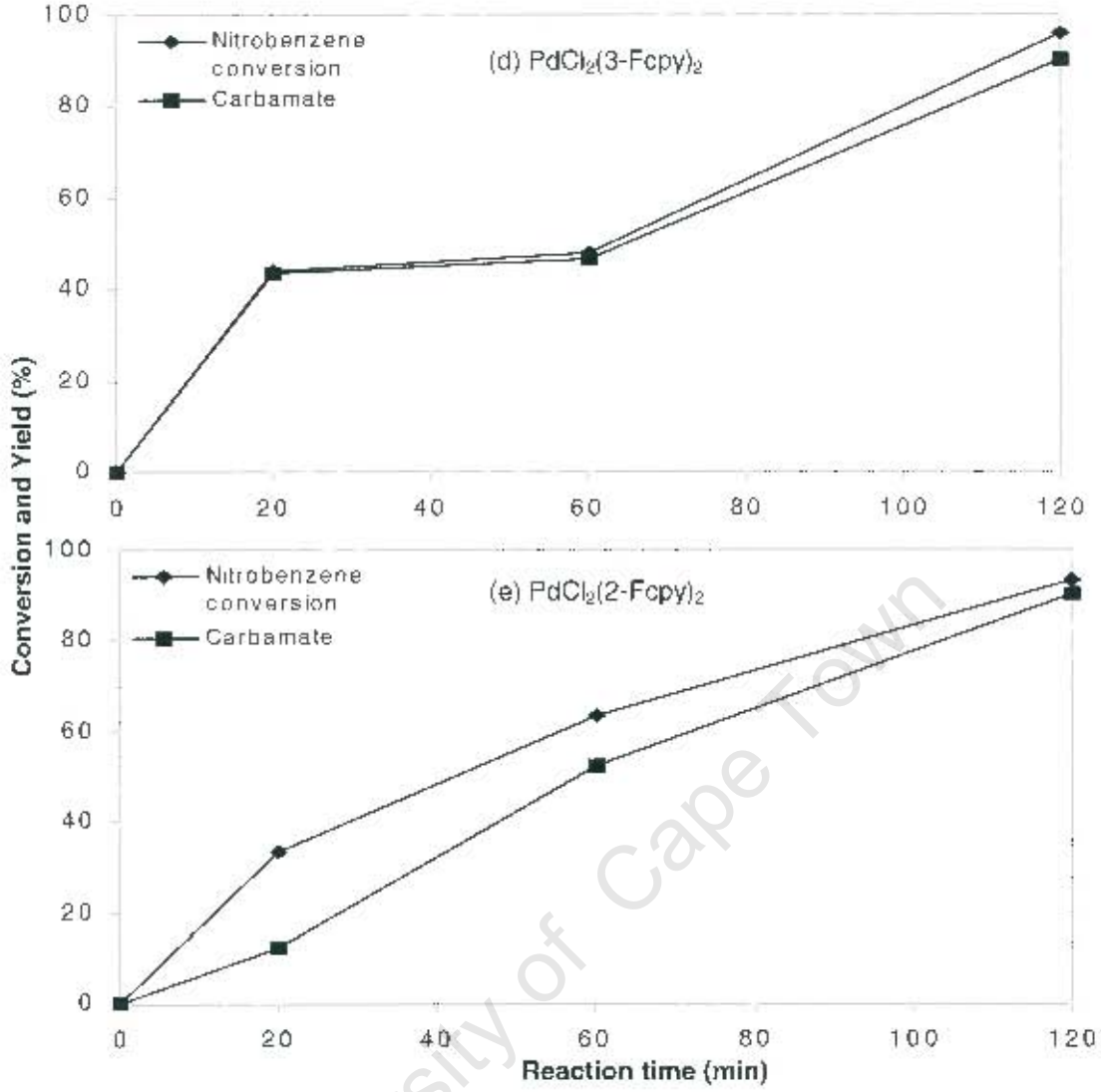

Figure 4.10: (a)-(e) Catalytic activity of various palladium complexes

The carbonylation of nitrobenzene proceeds through the intermediate formation of aniline. The presence of aniline was detected as the reaction progressed in all the catalyst systems examined. However, complex **[3.40]** produced the largest amount of aniline and other minor side-products on termination of the reaction. The remaining palladium complexes efficiently converted the aniline to carbamate, with complex **[3.41]** the most efficient.

4.3.4 General remarks and conclusions

Complex **[3.41]** showed the highest activity and selectivity for carbamate formation with very small amounts of side-products detected. It is difficult at this stage to speculate on the nature of the relationship between the structure and activity of the catalyst, as a clear trend cannot be presented unequivocally. The preliminary results indicated that derivatisation of the pyridyl

ligands enhanced the activity of the catalyst system under less vigorous conditions than reported.[22] More extensive examination of these promising catalytic systems is required.

4.4 Hydrogenation studies of 1-hexene and cyclohexene

4.4.1 Introduction

Hydrogenation, both homogeneous and heterogeneous, is an industrially relevant and significant process. Millions of tons of cyclohexane for example, are obtained annually from the hydrogenation of benzene.[2] Cyclohexane is used for the preparation of nylon. A significant number of other unsaturated compounds such as dehydroamino acids used for the preparation of L-dopa, a drug used for the treatment of Parkinson's disease and (S)-phenylalanine, used for the sweetener aspartame, are produced by catalytic hydrogenation reactions.[2] The hydrogenation reaction, in both homogeneous and heterogeneous versions, forms part of several other important processes such as hydroformylation, hydrogenation of unsaturated fats, liquefaction of coal through arene hydrogenation, hydrogenation of butadiene rubbers and hydrodesulfurisation of crude oil through hydrogenolysis.[7,25]

Rhodium phosphine complexes have long been known for their activity as hydrogenation catalysts.[26] Wilkinson's complex, $RhCl(PPh_3)_3$ is one of the most widely used of these.[25,27] Iridium complexes have also been extensively studied for their activity as hydrogenation catalysts.[28,29,30] Crabtree's catalyst, $[Ir(COD)(py)(PCy_3)]PF_6$,[31,32] where COD = 1,5-cyclooctadiene, py = pyridine and PCy_3 = tricyclohexylphosphine, is one of the best known homogeneous iridium hydrogenation catalysts. Crabtree's catalyst contains both nitrogen- and phosphine-donor ligands; where the activity of the catalyst is considered to arise from the presence of the phosphine ligand in the catalyst.

The preparation and study of homogeneous hydrogenation catalysts containing exclusively nitrogen-donor ligands has, however, only been investigated to a limited extent. The success and development of catalysts containing phosphine-donor ligands has surpassed the development of catalysts containing exclusively nitrogen-donor ligands. Developments in the study of homogeneous catalysts have included the incorporation of nitrogen-donor ligands in a phosphine-ligand complex, as illustrated with Crabtree's catalyst. In most cases the incorporation of the nitrogen-donor group in the catalyst confers stability on the complex whereas the activity of the catalyst is a function of the phosphine-donor group in the catalyst.

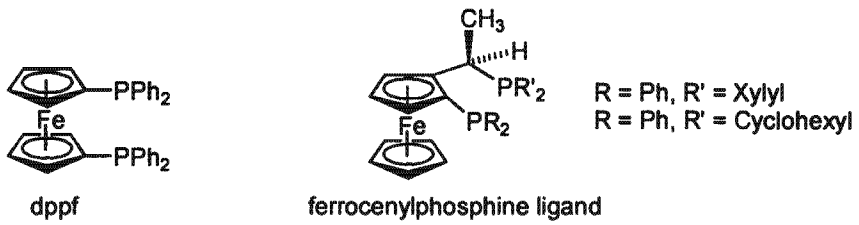

dppf ferrocenylphosphine ligand

Figure 4.11: Ferrocenylphosphine ligands used in various hydrogenation catalysts[34]

The use of ferrocenyl ligands in the preparation of rhodium and iridium hydrogenation catalysts has gained prominence with the preparation of ferrocenyl diphosphine ligands.[33] 1,1'-Bis(diphenylphosphino)ferrocene (abbreviated to dppf) is one of the best known ferrocenyl ligands (see *Figure 4.11*). A relationship exists between the structure and activity of the catalyst where the structure of the ligand may be readily adapted to a specific transformation. In principle, these ligands lend themselves to being tuned to the needs of a specific conversion.[34]

The hydrogenation of unsaturated compounds is a clean reaction where few side products are formed. The hydrogenation of simple alkenes such as 1-hexene and cyclohexene presents a relatively uncomplicated system with which to study and compare the catalytic activity of potential hydrogenation catalysts. The complexes examined are of the type, $[M(COD)L_2]ClO_4$ where M = Rh or Ir, COD = 1,5-cyclooctadiene and L = pyridine or a derivatised pyridyl ligand.

4.4.2 Comparison of catalytic activity

The catalytic activity of several rhodium and iridium complexes was determined as hydrogenation catalysts under a range of conditions by varying the central metal, altering the ligand and changing the catalyst ratio. The activity of the complexes was examined under ambient conditions of room temperature (maintained at 24 °C) and atmospheric pressure.

The hydrogenation of 1-hexene and cyclohexene served as test reactions. These substrates were chosen to compare the activity of the catalysts for terminal and internal alkenes. Catalysis runs were carried out in dichloromethane. The solvent was chosen for its low coordinating ability, limiting competition between the solvent and alkene for coordination to active sites of the metal.[35] The use of dichloromethane as solvent is not entirely usual since the solvent is known to act as a poison, oxidising classical homogeneous catalysts. The solvent was, however, successfully used by Crabtree for iridium(I) hydrogenation catalysts.[3]

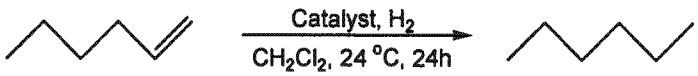

Table 4.5: Effect of catalyst and catalyst ratio on 1-hexene conversion[a]

Entry	Complex number	Catalyst	Ligand	Ratio catalyst to substrate	1-Hexene conversion (%)
1	**[3.21]**	$[Rh(COD)L_2]ClO_4$	Py	1:100	13.3
2	**[3.24]**		4-Fcpy	1:100	8.0
3	**[3.25]**		4-Fc(C_6H_4)py	1:100	2.8
4	**[3.21]**		Py	1:50	26.7
5	**[3.24]**		4-Fcpy	1:50	6.9
6	**[3.38]**	$[Ir(COD)L_2]ClO_4$	py	1:50	48.3
7	**[3.39]**		4-Fcpy	1:50	29.5

[a] Reaction conditions: Solvent = dichloromethane, 24 °C, atmospheric pressure, 24 h

Although the selected complexes were not very active under the chosen reaction conditions, the iridium complexes, particularly complex **[3.38]**, displayed the greatest catalytic activity (see *Table 4.5*). Results indicated that the derivatisation of the pyridyl ligand is linked to a decrease in the activity of the catalyst for both metals.

Studies into the hydrogenation of cyclohexene were carried out under similar reaction conditions, catalyst to substrate ratios and variations on ligands. The results are summarised in *Table 4.6*.

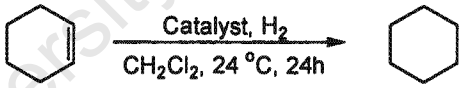

Table 4.6: Effect of catalyst and ratio on cyclohexene conversion[a]

Entry	Complex number	Catalyst	Ligand	Ratio catalyst to substrate	Cyclohexene conversion (%)
8	**[3.21]**	$[Rh(COD)L_2]ClO_4$	Py	1:100	18.0
9	**[3.24]**		4-Fcpy	1:100	6.4
10	**[3.25]**		4-Fc(C_6H_4)py	1:100	2.8
11	**[3.21]**		Py	1:50	4.4
12	**[3.24]**		4-Fcpy	1:50	3.1
13	**[3.38]**	$[Ir(COD)L_2]ClO_4$	py	1:50	2.1
14	**[3.39]**		4-Fcpy	1:50	4.5

[a] Reaction conditions: Solvent = dichloromethane, 24 °C, atmospheric pressure, 24 h

The complexes examined for the hydrogenation of cyclohexene showed very low activity. A significant amount of catalyst was found decomposed and deposited in the reaction mixture for all complexes examined on termination of the experiments.

On comparison of the activity of the catalysts in *Tables 4.5* and *4.6*, it would appear that the iridium complexes are slightly more active catalysts. The catalysts appear to be more suited to the hydrogenation of terminal alkenes, as expected, since terminal alkenes are more easily hydrogenated. The complexes were, however, not very active hydrogenation catalysts under the given reaction conditions.

4.4.3 General remarks

Although mechanistic studies were not carried out, a possible mechanism for the hydrogenation of the alkenes is presented diagrammatically in *Scheme 4.3*. This catalytic cycle is in line with similar complexes[36] where the labile cyclooctadiene in the catalyst precursor dissociates in the initial stages and is hydrogenated, generating the active catalytic species *in situ*.

The mechanism proposes the formation of a dihydride upon oxidative addition of H_2 to the rhodium(I) metal centre. The reaction proceeds by insertion of the alkene to the metal hydride bond with a migratory insertion followed by reductive elimination. The use of a low or non-coordinating solvent eliminates competition between the alkene and solvent for coordination to the metal. Steric effects play a role in the alkene insertion step. Depending on the nature and bulk of the catalyst and its ligands, terminal alkenes are preferentially hydrogenated.

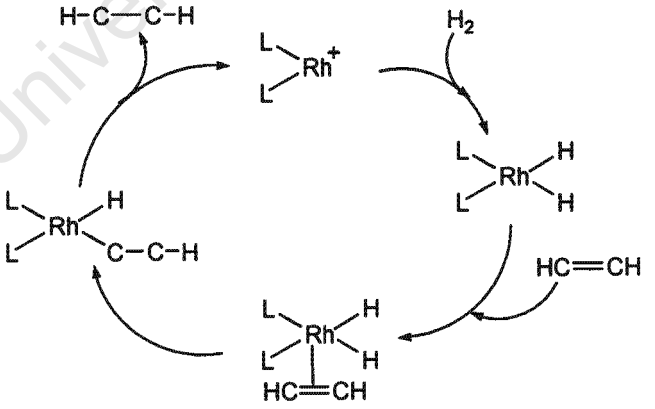

***Scheme 4.3*:** Reaction mechanism for hydrogenation of a simple alkene

Some differences were observed on variation of ligand systems in the complexes examined. This supports the premise that the ligand remains coordinated to the metal rather than dissociates during the course of the catalytic reaction.

4.5 Conclusions

The catalytic activity of several complexes in this study was investigated in three different catalytic applications – the polymerisation of phenylacetylene, carbonylation of nitrobenzene and hydrogenation of 1-hexene and cyclohexene. Where possible, reactions were modelled on the reactivity of similar complexes described in the literature.

The catalytic polymerisation of phenylacetylene was investigated with several rhodium complexes with systematic variation in the ligands of these complexes. This preliminary study indicated the existence of a relationship between the structure of the catalyst, its activity and the physico-chemical properties of the polymers. The results indicated that a linear rhodium catalyst with ferrocenyl ligand leads to the formation of higher molecular weight polymers with greater stability. Further investigations would be needed to optimise the performance of the catalysts to increase the molecular weight of the polymer as well as decrease the polydispersity.

The carbonylation of nitrobenzene was investigated with a series of palladium complexes and the activity of these compared to a similar complex described in the literature. The preliminary study revealed the enhanced activity of the palladium complexes. These complexes displayed greater activity and selectivity for the formation of the major product.

The hydrogenation studies were not as successful under the reaction conditions investigated. Rhodium phosphine complexes are known to be particularly active but this was not the case with the nitrogen-donor complexes examined.

References:

1. W. A. Herrmann and B. Cornils, *Angew. Chem. Int. Ed. Engl.*, 1997, **36**, 1048.
2. J. Tsuji, *Transition Metal Reagents and Catalysts, Innovations in Organic Synthesis*, West Sussex, England, 2000.
3. R. H. Crabtree, *Chemtech*, 1982, **12**, 506.
4. R. Crabtree, *Acc. Chem. Res.*, 1979, **12**, 331.

5. A. Togni and L. M. Venanzi, *Angew. Chem. Int. Ed. Engl.*, 1994, **33**, 497.
6. S. Yamada, T. Mashiko and S. Terashima, *J. Am. Chem. Soc.*, 1977, **99**, 1988; S. Coleman Kammula and E. T. Duim-Koolstra, *J. Organomet. Chem.*, 1983, **246**, 53.
7. H. Brunner, *Applied Homogeneous Catalysis with Organometallic Compounds*, eds. B. Cornils and W. A. Herrmann, Wiley-VCH, Weinheim, 2000.
8. S-I. Lee, S-C. Shim and T-J. Kim, *J. Polym. Sci.: Part A: Polym. Chem.*, 1996, **34**, 2377.
9. A. Furlani, G. Iucci, M. V. Russo, A. Bearzotti and A. D'Amico, *Sensors and Actuators B*, 1992, **7**, 447.
10. P. R. Hein, *J. Polym. Sci.: Polym. Chem. Ed.*, 1973, **11**, 163.
11. P. S. Woon and M. F. Farona, *J. Polym. Sci.: Polym. Chem. Ed.*, 1974, **12**, 1749.
12. T. J. Katz, T. H. Ho, N-Y. Shih, Y-C. Ying and V. I. W. Stuart, *J. Am. Chem. Soc.*, 1984, **106**, 2659.
13. T. Masuda, K. Hasegawa and T. Higashimura, *Macromolecules*, 1974, **8**, 255; T. Masuda, T. Takahasi, K. Yamamoto and T. Higgashimura, *J. Polym. Sci.: Polym. Chem. Ed.*, 1982, **20**, 2603.
14. Y. Goldberg and H. Alper, *J. Chem. Soc., Chem. Commun.*, 1994, 1209.
15. M. Tabata, W. Yang and K. Yokoda, *Polym. J.*, 1990, **20**, 1105; W. Yang, M. Tabata, K. Yokota and A. Shimizu, *Polym. J.*, 1991, **23**, 1135.
16. C. I. Simionescu, V. Percec and S. Dumitrescu, *J. Polym. Sci.: Polym. Chem. Ed.*, 1977, **15**, 2497.
17. F. D. Kleist and N. R. Byrd, *J. Polym. Sci.: Part A-1*, 1969, **7**, 3419.
18. T. C. Clarke, C. S. Yannoni and T. J. Katz, *J. Am. Chem. Soc.*, 1983, **105**, 7787.
19. F. Ragaini and S. Cenini, *J. Mol. Catal A: Chem.*, 2000, **161**, 69.
20. S. Cenini, M. Pizzotti and C. Crotti, *Aspects of Homogeneous Catalysis*, ed. R. Ugo, Reidel, Dordrecht, 1988, vol. **6**.
21. J. Skupińska, G. Smółka, W. Kaźmierowicz and J. Ilmużyńska, *React. Kinet. Catal. Lett.*, 1995, **54**, 59.
22. J. Skupińska and M. Karpińska, *J. Mol. Catal. A: Chem.*, 2000, **161**, 69.
23. I. Pri-Bar and J. Schwartz, *J. Org. Chem.*, 1995, **60**, 8124.
24. C-H. Liu and C-H. Cheng, *J. Organomet. Chem.*, 1991, **420**, 119.
25. B. R. James, *Comprehensive Organometallic Chemistry*, eds. G. Wilkinson, F. G. A. Stone and E. W. Abel, Pergamon, Oxford, 1982.
26. K. E. Koenig, *Asymmetric Synthesis, vol. 5*, ed. J. D. Morrison, Academic Press, USA, 1985.
27. W. A. Herrmann and B. Cornils, *Angew. Chem. Int. Ed. Engl.*, 1997, **36**, 1049.
28. R. H. Crabtree, H. Felkin and G. E. Morris, *J. Organomet. Chem.*, 1977, **135**, 205.

29. R. B. Bedford, P. A. Chaloner, S. Z. Dewa, G. López, P. B. Hitchcock, F. Momblona and J. L. Serrano, *J. Organomet. Chem.*, 1997, **527**, 75.
30. J. W. Suggs, S. D. Cox, R. H. Crabtree and J. M. Quirk, *Tetrahedron Lett.*, 1981, **22**, 303.
31. H. M. Lee, T. Jiang, E. D. Stevens and S. P. Nolan, *Organometallics*, 2001, **20**, 1255.
32. A. Togni, C. Breutel, A. Schnyder, F. Spindler, H. Landert and A. Tijani, *J. Am. Chem. Soc.*, 1994, **116**, 4061.
33. H-U. Blaser, H-P. Buser, R. Häusel, H-P. Jalett and F. Spindler, *J. Organomet. Chem.*, 2001, **621**, 34.
34. R. H. Crabtree, A. Gautier, G. Giordano and T. Khan, *J. Organomet. Chem.*, 1977, **141**, 113.
35. R. R. Schrock and J. A. Osborn, *J. Am. Chem. Soc.*, 1976, **98**, 2134.

Chapter 5: Potential Biological Activity

5.1 Introduction

The use of metals in the treatment of various illnesses dates as far back as between 2500 and 2000 BC with the ancient Chinese using gold medicinally for the treatment of various ailments. The medicinal use of metals has occasionally been observed through time. Paracelsus in the fifteenth century used a variety of metals such as iron, cadmium, mercury, arsenic and antimony to treat various diseases including syphilis and cancer.[1] Lissauer in the nineteenth century gave Fowler's mixture, an arsenic mixture, to patients with leukaemia.[1] Currently, the mercury compound, mercurochrome is still used in first aid.

It was, however, in the twentieth century with the serendipitous discovery of the anti-cancer compound, *cis*-diamminedichloroplatinum(II), also referred to as cisplatin,[2,3,4] that significant developments in the investigation of other types of non-organic cytostatic drugs took place.

The development of medicinal bioinorganic chemistry has been rapid with significant contributions of inorganic compounds to the pharmaceutical industry.[5] The toxicity of metals such as gadolinium,[6] technetium[7] and rhenium,[5] for example, have been adjusted to the point where the metals act as diagnostic agents and radiopharmaceuticals. Designed ligands allow these metals to be targeted to specific organs.

The current investigation involves a preliminary study into the antitumour activity of several of the metal complexes prepared during this study. The complexes investigated were divided on the basis of transition metal centre. Several platinum, palladium, rhodium and iridium complexes comparing the effect of derivatised ligand systems were examined with this purpose in mind.

5.2 Metal complexes in cancer therapy

Some of the metal-containing complexes that have been investigated for their potential anti-tumour activities are shown in *Figure 5.1*.

Metallocene complexes are particularly active against a number of tumours, and some titanocene complexes have reached clinical phase trials.[1] It is interesting to note that despite

the observed anti-cancer properties of the metal complexes in *Figure 5.1*, aside from the platinum complexes, titanocene dichloride is one of the first metal complexes to be tested at the preclinical stage against a range of human carcinomas.

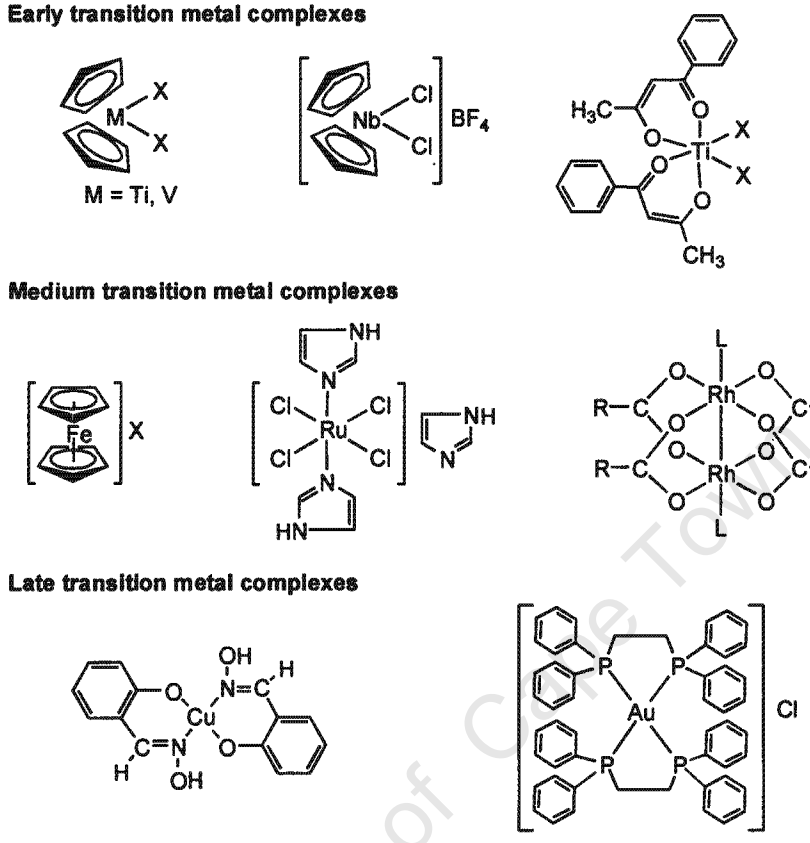

Figure 5.1: Some transition metal complexes proven to be active in experimental tumours[1]

Ferrocene through the ferrocenium cation, is known to exhibit antineoplastic activity against Erlich ascites murine tumour.[8] The radical ferrocenium ion is known to interact readily with radical precursors and a host of biologically important electron donors. As such, several cisplatin-type ferrocenyl platinum complexes have been prepared and their potential antitumour activity investigated (see for example *Figure 5.2*).[9]

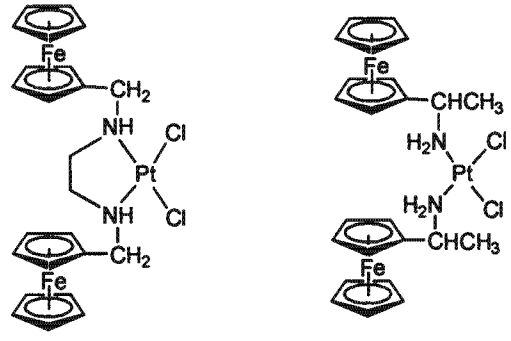

Figure 5.2: Cisplatin-type ferrocenyl platinum complexes[9]

It has been noted that unsubstituted ferrocene, although not displaying any antitumour activity due to its lack of solubility in an aqueous medium, once inserted into a target cell, could be converted into ferrocenium ion. It has been suggested that the ferrocenyl group acts as an iron carrier and the different redox states of the iron are responsible for its anticancer activity through the formation of radical metabolites that are responsible for biological damage in the cancer cell.[10]

5.3 Metal complexes investigated

A preliminary investigation into the antitumour activity of several metal-containing complexes prepared during the course of this study (see *Figure 5.3*) was carried out in the form of cytotoxicity assays on two separate cancer cell lines – human oesophageal (WHCO1) and cervical (ME180) cancer cell lines. Several IC_{50} values are reported.

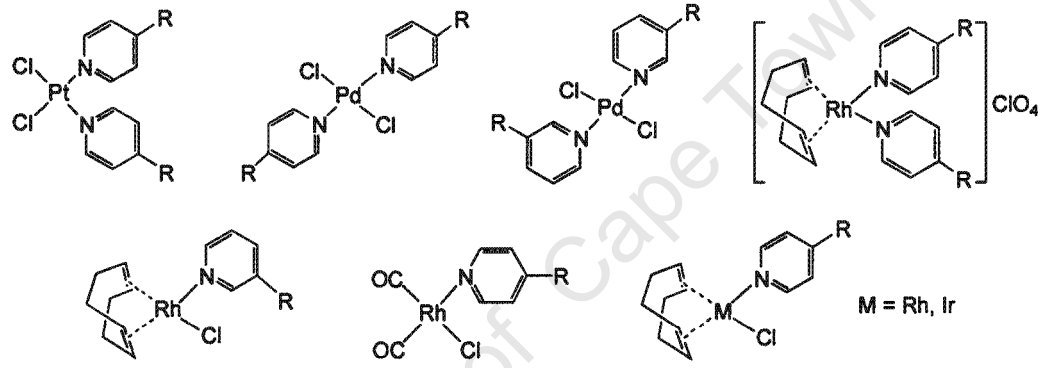

Figure 5.3: Metal complexes examined for antitumour activity

5.3.1 Cytotoxicity determinations

Cytotoxicity determinations can be regarded as an introductory course to anticancer activity. Many platinum group metal complexes are reportedly active against a range of tumours.[1] The complexes investigated in this study were examined for their efficacy against two different cancer cell lines, with comparison of activity for each of the cell lines.

The cytotoxicity results are displayed in bar charts with absorbance readings reported for a range of drug concentrations (0-50 µg/ml). The 0 µg/ml reading corresponds to the blank reading without cells or drug. The optimal situation would be to have a significantly lower absorbance reading at 1 µg/ml, indicating an extremely active compound.

As a guide, changes in the absorbance readings can be attributed to two main factors,

(i) The amount of protein present, which corresponds to the living cell number. This decreases with increasing drug concentration if the complex is cytotoxic, displaying a lowered absorbance reading.

(ii) The solubility of the complex in the aqueous medium. If some crystalline insoluble complex remains in the cell well, interference in the absorbance reading can occur. This would be indicated by an abnormal distribution in the readings.

5.3.1.1 Platinum complexes

The use of platinum in antitumour drugs has been well established and cisplatin is the most prominent member of this class of drugs.[1] Cisplatin is a widely used and effective cytostatic drug for the treatment of solid carcinomas.[11] The drug is known to be 70-90 % effective in cases of testicular cancer and also highly effective against ovarian cancers. It contributes to the treatment of head and neck cancers, bladder cancer and lymphomas. Despite the success of cisplatin, some tumours have developed natural as well as acquired resistance to the drug. Severe side effects such as renal impairment, neurotoxicity and ototoxicity are known to occur with prolonged use of the drug. These effects may only be partially reversed upon termination of treatment.[1]

Since the discovery of cisplatin, numerous platinum-containing compounds have been prepared and their efficacy investigated with a view to the reduction of side effects and toxicity.[9,12,14,17] Carboplatin, diammine(1,1'-cyclobutanedicarboxylato)platinum(II) has shown promise in this regard (see *Figure 5.4*).[13]

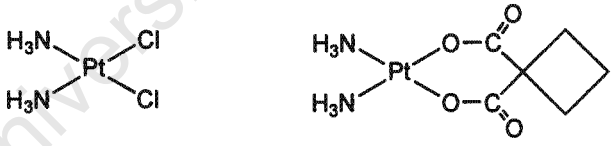

cisplatin carboplatin

Figure 5.4: Platinum-containing anti-cancer drugs

The *trans*-$PtCl_2(py)_2$ complex is reported to be highly active against several carcinomas such as Erlich's murine tumour, while the *cis*-isomer is not.[14] One of the possible reasons cited for this difference is steric constraints where the *cis*-isomer may be too sterically hindered for the complex to bind to DNA.

The cytotoxicity of several pyridyl platinum complexes was examined (see *Figure 5.5*). These complexes are reported as being in the *cis*-conformation based on the reported spectroscopic data for complex **[3.46]**.[15]

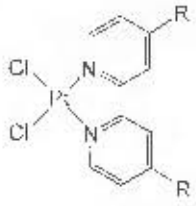

[3.46] R – H

[3.47] R – Ph

[3.49] R = Fc

Figure 5.5: Platinum complexes investigated as antitumour agents

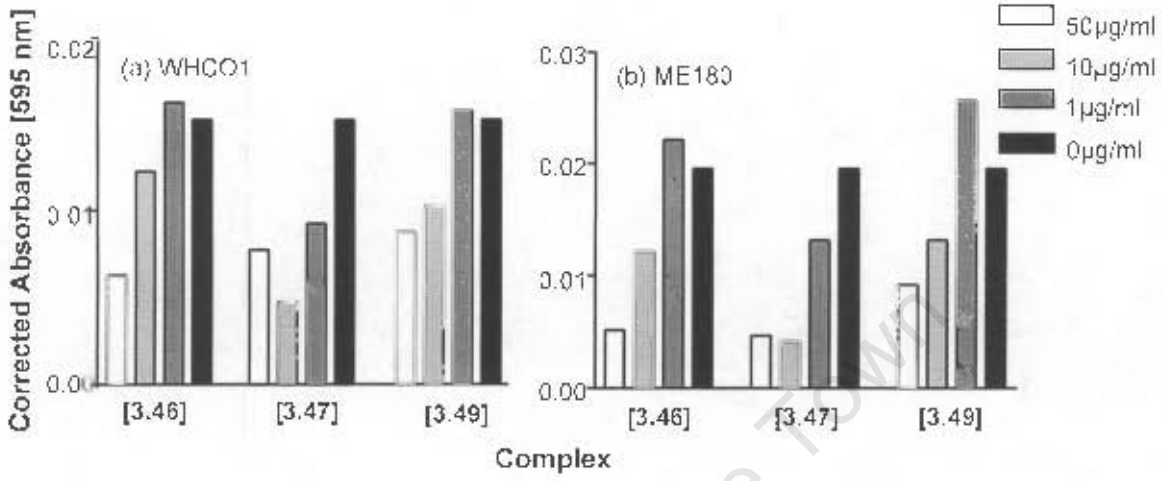

Figure 5.6: Cytotoxicity results for *cis*-platinum complexes **[3.46]** **[3.47]** and **[3.49]** for (a) WHCO1 and (b) ME180

Complex **[3.46]** appeared to show some activity for both cancer cell lines (see *Figure 5.6*). It was considered that although spectroscopic evidence indicated that the complex was in the *cis*-conformation, it could be adopting the *trans*-conformation under certain conditions. All the complexes examined displayed some activity while complex **[3.47]** appeared to be the most active for both cell lines.

5.3.1.2 Palladium complexes

The antitumour activity of several palladium(II) complexes has been reported against Sarcoma 180. The palladium complexes were less active than related platinum complexes under the same conditions.[16,17] These reports show the palladium complexes as having at best marginal success.

Despite this, the cytotoxicity of a series of palladium complexes was determined (see *Figure 5.7*). Complexes were compared with structural differences in the pyridyl ligands. The role played by substituents on the pyridyl ligand was evaluated together with the position of substitution. The complexes are reported in the *trans*-conformation based on reported spectroscopic data for complex **[3.40]**[18] and the crystal structure of complex **[3.44]**.

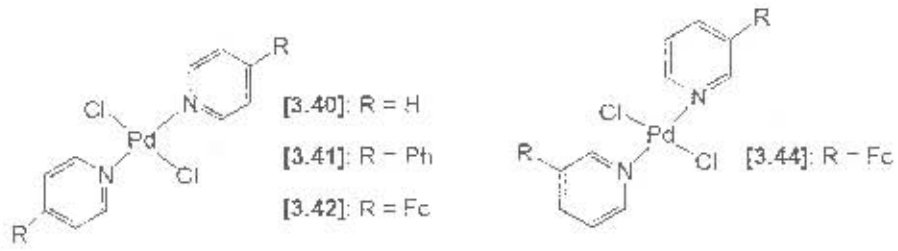

Figure 5.7: Palladium complexes investigated as antitumour agents

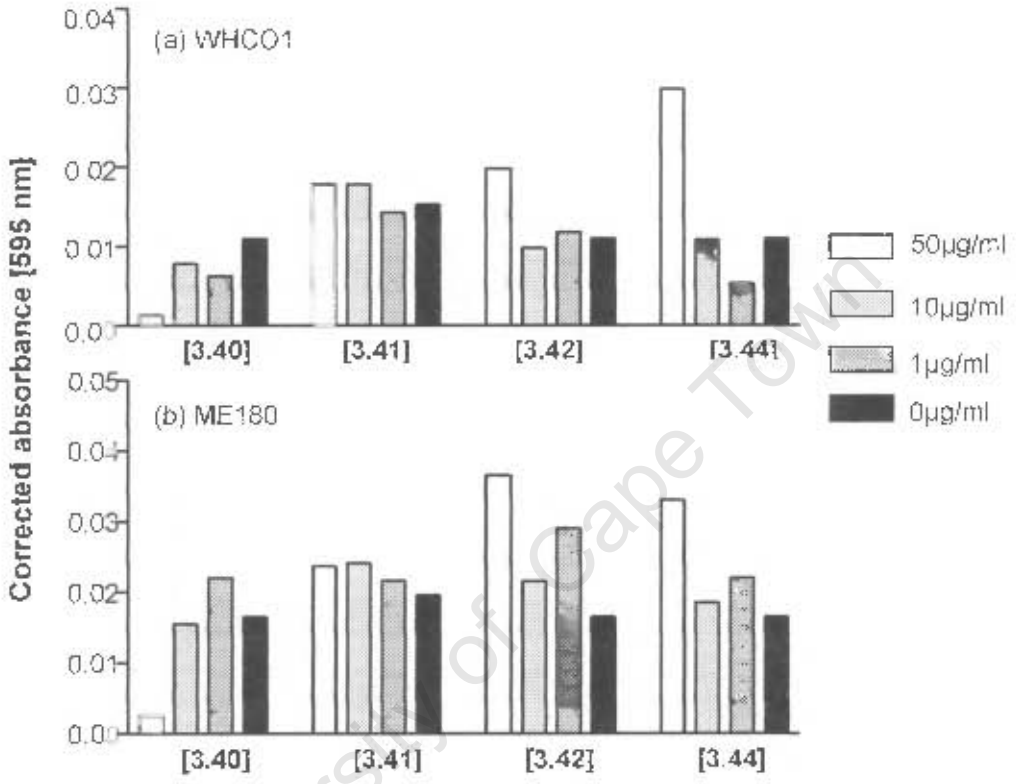

Figure 5.8: Cytotoxicity results for *trans*-palladium complexes **[3.40]–[3.42]**, **[3.44]** for (a) WHCO1 and (b) ME180

The complexes displayed similar distribution patterns for both cell lines (see *Figure 5.8*). Complex **[3.40]** appeared to be the most active by far. The results indicated that derivatising the pyridyl ring leads to a lowered activity in the complex. This could be due to deactivation of the ring due to the presence of the substituents or to steric constraints. The abnormal distribution patterns for complexes **[3.42]** and **[3.44]** was due to the precipitation of the complex in the cell well.

5.3.1.3 Rhodium complexes

The antitumour properties of rhodium(II) complexes in the form of inorganic, binuclear and caged complexes were first discovered in 1975 . These complexes were mainly rhodium(II) carboxylate derivatives, with the butyrate and propionate analogues showing the greatest

inhibition of tumour growth. Rhodium(I) and iridium(I) square planar cyclooctadienyl complexes of the type [RhCl(COD)(NH_3)] and [RhCl(COD)(piperdine)][19] as well as acetylacetonato complexes of the type [M(acac)(COD)] where M = Rh(I) or Ir(I) have also been examined.[20,21] These complexes exhibit antitumour activity against Erlich ascites tumour, leukaemia L1210 and sarcoma 180. Most recently, investigations into rhodium(I) acetylacetonato complexes have gained renewed interest (see *Figure 5.9*).[22]

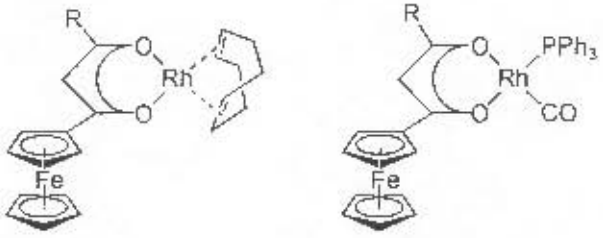

R = CF_3, CCl_3, CH_3, Ph and Fc

Figure 5.9: Rhodium complexes examined as anticancer agents[22]

Rhodium(I) carbonyl complexes of the type [$Rh(CO)_2L$] where L = sulfonamide derivatives have shown some activity. These complexes inhibit the growth of leukaemia P388, Erlich tumour and advanced B16 melanoma.[23] Reports have indicated that despite the heavy-metal character of rhodium, no nephrotoxicity was observed with these complexes.[23,1]

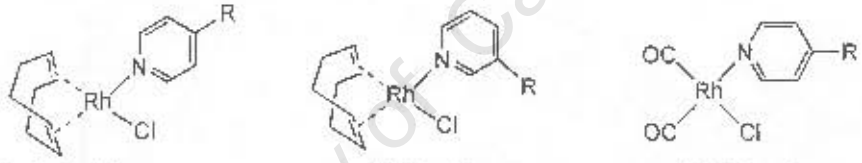

[3.8]: R = H

[3.9]: R = Ph

[3.13]: R = $(C_6H_4)Fc$

[3.14]: R = $(C{=}N)(C_6H_4)Fc$

[3.15]: R = Fc

[3.16]: R = $(C_6H_4)Fc$

[3.4]: R = Fc

Figure 5.10: Rhodium complexes, [RhCl(COD)L] investigated as antitumour agents

The antitumour activity of several rhodium cyclooctadienyl complexes was compared based on structural differences (see *Figure 5.10*). The role played by the position and nature of substituent on the pyridyl ligand was evaluated. A rhodium carbonyl complex was included for examination based on the reported activity of similar complexes.

Several rhodium complexes showed significant activity for both cancer cell lines (see *Figure 5.11*). Complex **[3.15]** seems to be particularly active, while complex **[3.16]** displayed specific activity for WHCO1 and complexes **[3.4]** and **[3.14]** were more active on ME180. Based on the results for complex **[3.8]**, it would appear that derivatisation of the pyridyl ligand is related to enhanced cytotoxic activity.

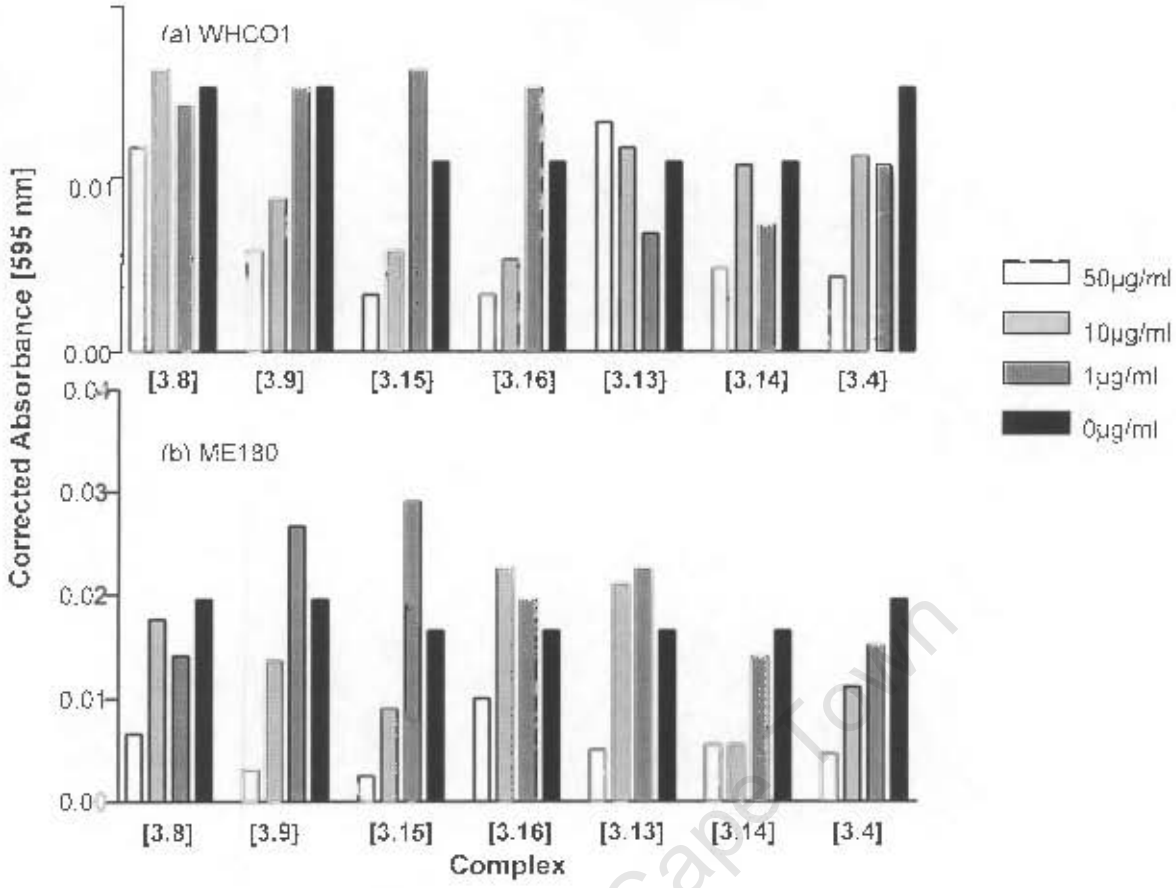

Figure 5.11: Cytotoxicity results of rhodium complexes for (a) WHCO1 and (b) ME180

However, the majority of the rhodium complexes were only partially soluble in the aqueous environment. Cationic rhodium complexes were further examined in an attempt to overcome the problem. Several rhodium cationic complexes were investigated with comparison of the derivatised pyridyl ligands and the effect on the cytotoxicity considered (see *Figure 5.12*).

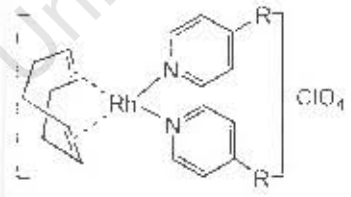

[3.21]: R = H

[3.24]: R = Fc

[3.25]: R = $(C_5H_4)Fc$

[3.26]: R = $(C{=}N)(C_5H_4)Fc$

Figure 5.12: Cationic rhodium complexes, $[Rh(COD)L_2]ClO_4$ investigated as antitumour agents

Complexes **[3.24]** and **[3.26]** displayed the most significant activity for both cancer cell lines while complex **[3.21]** seemed to be inactive (see *Figure 5.13*). This could indicate that placing a (ferrocenyl) substituent on the pyridyl ring leads to enhanced activity of the complexes. The solubility problems were not completely overcome, as the complexes remained partially soluble. The presence of a counterion other than perchlorate could provide a solution.

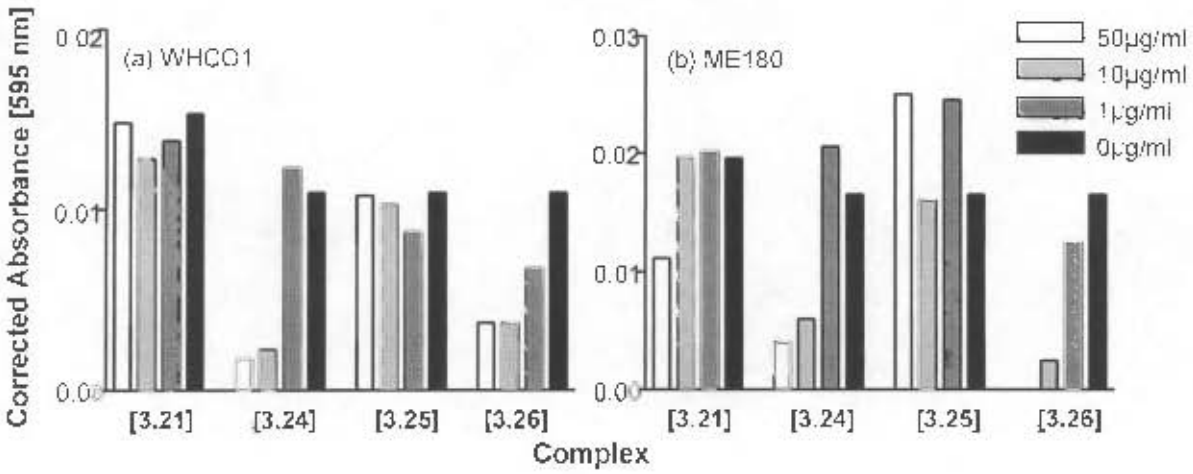

Figure 5.13: Cytotoxicity results for rhodium complexes, $[Rh(COD)L_2]ClO_4$ for (a) WHCO1 and (b) ME180

5.3.1.4 Iridium complexes

The study of the antitumour activity of iridium(I) complexes is closely linked to that of the related rhodium(I) complexes. As with the related rhodium complexes, the metal has been reported as readily undergoing oxidative addition under physiological conditions leading to the formation of an active iridium(III) complex.

Two iridium complexes were examined for their cytotoxic activity with differences in the substituent on the pyridyl ring ligand (see *Figure 5.14*).

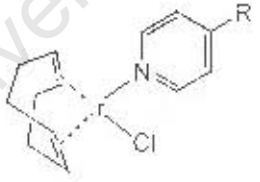

[3.34]: R = Ph

[3.36]: R = Fc

Figure 5.14: Iridium complexes investigated as antitumour agents

A comparison of the cytotoxicity results revealed that neither iridium complex was particularly active against either WHCO1 or ME180 (see *Figure 5.15*).

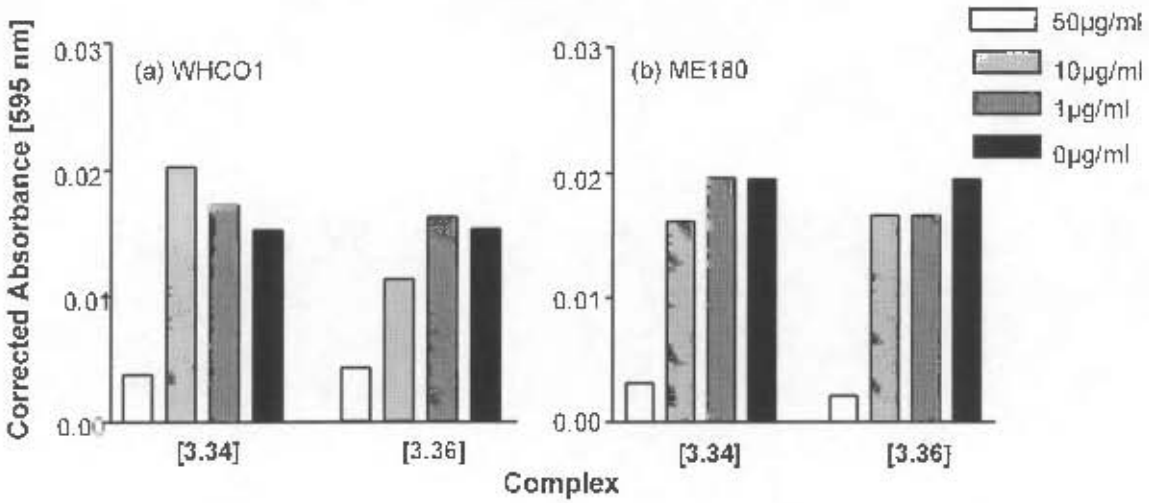

Figure 5.15: Cytotoxicity of iridium complexes, [IrCl(COD)L] for (a) WHCO1 and (b) ME180

5.3.2 Determination of selected IC_{50} values

The IC_{50} values of selected complexes was obtained. The determination of cytotoxicity and the IC_{50} value represents the first screening stage for cancer therapy drugs. The selection of complexes was limited by the solubility of the complex in an aqueous medium. Thus, the IC_{50} values for selected complexes could only be determined as the exact concentration of drug had to be known (see *Table 5.1*).

Table 5.1: IC_{50} values for selected complexes examined[a]

Complex number		IC_{50} value (µg/ml)
[3.46]	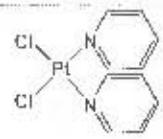	25.00
[3.40]	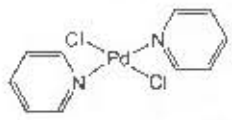	29.43
[3.9]	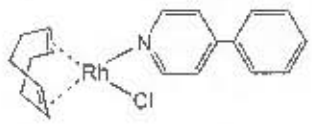	24.99
[3.34]	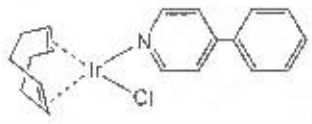	27.71

[a] Values determined using WHCO1 cell line

The determination of IC_{50} values for complexes **[3.14]** and **[3.15]** was attempted due to their significant cytotoxic activity. However, one of the key problems associated with these complexes was solubility in an aqueous medium. Large amounts of precipitate were observed at a range of the concentrations investigated and an endpoint could not be effectively obtained. Despite the potential of several of the ferrocenyl complexes examined, the insolubility of the complexes prevented further examination.

5.4 General remarks and conclusions

One of the key issues described in the literature with reference to the study of metal-containing antitumour agents is the relatively random manner in which complexes are selected for investigation. Attempts were made to compare the activity of complexes displaying structural similarities. The rhodium complexes, for example, displayed enhanced activity for complexes with derivatised pyridyl ring ligands.

One of the chief problems associated with several of the complexes examined, lies in the insolubility of the complexes in an aqueous medium. Given that solutions of the complexes are administered to biological systems, the choice of solvent is limited. Similar problems related to the insolubility of ferrocenyl systems have been reported. The preparation of ferrocenium salts of the complexes or cyclodextrin inclusion complexes could potentially stabilise the complexes and render them soluble in an aqueous medium. The use of cyclodextrins for this purpose has been reported where anticancer studies were conducted with ferrocene.[10] Recently, the preparation of 4-ferrocenylpyridine as well as a rhenium complex thereof, (4-ferrocenylpyridine)methyltrioxorhenium, has been reported as cyclodextrin inclusion complexes.[24]

References:

1. P. Köpf-Maier, *Eur. J. Clin. Pharmacol.*, 1994, **47**, 1 and references therein.
2. B. Rosenberg and L. V. Camp, *Nature*, 1965, **205**, 698.
3. B. Rosenberg, L. V. Camp, J. E. Trosko and V. H. Mansour, *Nature*, 1969, **222**, 385.
4. B. Rosenberg and L. V. Camp, *Cancer Res.*, 1970, **30**, 1799.
5. Z. Guo and P. J. Sadler, *Angew. Chem. Int. Ed.*, 1999, **38**, 1512 and references therein.
6. W. Kuhn, *Angew. Chem. Int. Ed.*, 1990, **29**, 1.

7. J. F. Kronauge, A. S. Leon, E. S. Verdera, H. S. Balter, E. T. Leon, F. Mut, M. C. Oliveira, F. A. Garcia, B. L. Holman, A. Davison and A. G. Jones, *J. Nucl. Med.*, 1992, **33**, 1949.
8. P. Köpf-Maier, H. Köpf and E. W. Neuse, *Angew. Chem.*, 1984, **96**, 446.
9. E. W. Neuse, M. G. Meirim and N. F. Blom, *Organometallics*, 1988, **7**, 2562.
10. D. Osella, M. Ferrali, P. Zanello, F. Laschi, M. Fonatni, C. Nervi and G. Cavigiolio, *Inorg. Chim. Acta*, 2000, **306**, 42.
11. R. B. Weiss and M. C. Christian, *Drugs*, 1993, **46**, 360.
12. *See for example*: S. E. Sherman and S. J. Lippard, *Chem. Rev.*, 1987, **87**, 1153; M. van Beusichem and N. Farrell, *Inorg. Chem.*, 1992, **31**, 634; T. W. Hambley, *Coord. Chem. Rev.*, 1997, **166**, 181; G. B. Onoa, V. Moreno, E. Freisinger and B. Lippert, *J. Inorg. Biochem.*, 2002, **89**, 237.
13. P. C. McGowan, *Education in Chem.*, 2001, 134.
14. N. Farrell, L. R. Kelland, J. D. Roberts and M. Van Beusichem, *Cancer Research*, 1992, **52**, 5065.
15. G. B. Kauffman, *Inorg. Synth.*, 1963, **7**, 249; C. Tessier and F. D. Rochon, *Inorg. Chim. Acta*, 1999, **295**, 25.
16. G. R. Gale, J. A. Howle and A. B. Smith, *Proc. Soc. Exp. Biol. Med.*, 1970, **135**, 690.
17. M. J. Cleare and J. D. Hoeschele, *Platinum Metals Rev.*, 1973, **17**, 2.
18. Y. N. Kukushkin and R. A. Vlasova, *Zh. Obshch. Khim.*, 1983, **53**, 948; B. Viossat, D. Nguyen-Huy, J. C. Lancelot and M. Robba, *Chem. Pharm. Bull.*, 1991, 3023.
19. T. Giraldi, G. Zassinovich and G. Mestroni, *Chem. Biol. Interact.*, 1974, **9**, 389.
20. T. Giraldi, G. Mestroni, G. Zassinovich and D. Stolfa, *Chem. Biol. Interact.*, 1978, **22**, 231.
21. G. Sava, T. Giraldi, G. Mestroni and G. Zassinovich, *Chem. Biol. Interact.*, 1983, **45**, 1.
22. J. C. Swartz, W. C. du Plessis, J. Conradie and T. G. Vosloo, Conference proceedings, *South African Chemical Institute and Catalysis Society of South Africa conference on catalysis and inorganic chemistry*, 2001.
23. G. Craaciunescu, V. Scarcia, A. Furlani, E. P. Iglesias, C. Ghirvu and A. Papaioannou, *Anticancer Res.*, 1989, **9**, 781.
24. L. Cunha-Silva, I. S. Gonçalves, M. Pillinger, W.-M. Xue, J. Rocha, J. J. C. Teixeira-Dias and F. E. Kühn, *J. Organomet. Chem.*, 2002, **656**, 281.

Chapter 6: Conclusions & Future Work

6.1 Project overview

In this project a series of multinuclear complexes were successfully prepared and characterised using an array of analytical techniques. The electronic and electrochemical properties of the complexes were determined and these related to the structure of the complexes. The application of these complexes was further investigated through determination of the anticancer properties and catalytic activity of the complexes. The catalytic activity of the complexes was determined through several test reactions.

In the current investigation into the preparation of novel multinuclear complexes, several approaches were taken.

- A series of pyridyl complexes was successfully prepared. The ligands studied for complexation, were all in the form of derivatised pyridyl ligands where the nature of the substituent was considered together with the position of substitution on the pyridyl ring. The effect of spacer groups between the ferrocenyl group and pyridyl ring was examined. Both monosubstituted and 1,1'-disubstituted ferrocenylpyridines were synthesised.

- Viable synthetic routes for both ligand and complex preparation were studied where these complexes were prepared in good isolated yield. The ligands prepared were complexed to a series of platinum group metals – rhodium, iridium, palladium and platinum, in the form of mono-, bi- and trinuclear complexes. The complexes were fully characterised using NMR, infrared spectroscopy, elemental analysis, mass spectrometry, electronic spectroscopy and cyclic voltammetry. The X-ray crystal structure of selected complexes was determined.

- Electrostatic changes between the free ligand and metal complexes were monitored using a number of spectroscopic techniques and related to the substituent on the pyridyl ring and its positon. The extent of electrochemical interaction in the ferrocenyl complexes was evaluated, where changes in redox potential was reported relative to the standardised ferrocene redox potential.

- Results indicated that the length of spacer group affected the extent of interaction between the metal centres. Extended linear systems showed little to no electrochemical

communication. The most pronounced electrochemical interaction was obtained for the linear rhodium binuclear complex [RhCl(COD)(4-Fcpy)]. The extent of shift of redox potential indicated a strong interaction between the metals in this complex. The interaction was further displayed through the spectroscopic comparison of the free ligand and complex.

- The resonance effect appeared to limit electrochemical interaction in the *ortho* and *meta* ferrocenylpyridine complexes. The electrochemical interactions for these complexes was not as pronounced in these complexes relative to the *para*-substituted ferrocenylpyridines.

6.2 Catalysis

Several catalytic reactions were investigated with the metal complexes prepared in this study. Certain trends were discernible from these investigations. Where possible, the activity of the catalysts was correlated with the structure of the complex taking into account steric and electronic effects.

- The polymerisation of phenylacetylene was investigated with several neutral and cationic rhodium complexes. The activity of nitrogen-donor complexes was compared to several ferrocenylphosphine complexes. The nitrogen-donor ligands were more active, displaying increased polymer yield, polymer molecular weight and thermal stability with comparable polymer isomer formation. Certain structure-activity relationships were speculated since results indicated that catalysts with linear extended ligands showed the best activity in terms of higher molecular weight and more thermally stable polymer. The rhodium catalysts examined gave the *cis*-isomer of the polymer almost exclusively. There is potential for the further investigation of these complexes. Modifications to this type of system would include extension of the linear ligand framework. One of the key areas to be addressed includes the polydispersity.

- The carbonylation of nitrobenzene was catalysed with palladium complexes. Derivatisation of the pyridyl ring in the palladium complex $PdCl_2(py)_2$ lead to enhanced activity under relatively milder reaction conditions than that reported in the literature. The derivatised palladium complexes displayed greater selectivity for the formation of the major product. The results indicated that the position of substitution on the pyridyl ring of the ligand makes a difference to the activity of the complex. The palladium complex, $PdCl_2$(4-Phpy) was the most active.

nitrogen into a glass storage vessel with Teflon stopcock. All other commercial reagents were used as obtained without further purification. 1',2',3',4',5'-Pentamethylazaferrocene was prepared according to the method of Fu[3] and obtained courtesy of Dr P. Beagley, Organometallic Research Group, University of Cape Town.

Rhodium, iridium, platinum, and palladium were obtained as chloride salts on loan from Johnson-Matthey and ferrocene obtained commercially from Sigma Aldrich.

Thin layer chromatography was performed on aluminium backed silica gel or aluminium oxide 60 F_{254} plates in a variety of solvent systems using the ascending technique. Plates were analysed under ultraviolet light. Column chromatography was conducted either on silica gel 60, particle size 0.063 mm – 0.200 mm (70 – 230 mesh ASTM) or neutral alumina, particle size 0.063 mm – 0.200 mm (70 – 230 mesh ASTM). Columns were generally prepared with 1:100 ratio product to chromatographic material.

7.1.1 Instrumentation

Melting points were determined on a Kofler hotstage microscope (Reichart Thermovar). Microanalyses were obtained on a Carlo Erba EA 1108 elemental analyser. Fast atomic bombardment (FAB) and high resolution (EI) mass spectra were recordered on a VG-70SEQ mass spectrometer at the mass spectrometry unit, Cape Technikon. In all cases the isotopic distribution was checked against the theoretical distribution.

Infrared spectra were recorded on a Perkin Elmer Paragon 1000 FT-IR spectrometer, with solid samples prepared as potassium bromide disks and solution samples in sodium chloride solution cells. Thermal analyses were conducted on Perkin Elmer Thermogravimetric analyser TGA7 and Differential Scanning Calorimeter DSC7.

NMR spectra were recorded on either a Varian Unity-400 (^{1}H: 400 MHz; ^{13}C: 100.6 MHz) or Varian Mercury-300 (^{1}H: 300 MHz; ^{13}C: 75.5 MHz) spectrometer at ambient temperatures. ^{1}H NMR spectra were referenced internally using residual protons in the deuterated solvent ($CDCl_3$: δ 7.27; C_6D_6: δ 7.24, CD_3OD: δ 5.84, CD_3COCD_3: δ 2.09) and values reported relative to tetramethylsilane (δ 0.00). ^{13}C NMR spectra were similarly referenced internally to the solvent resonance ($CDCl_3$: δ 77.0; C_6D_6: δ 128.1, CD_3OD: δ 49.1, CD_3COCD_3: δ 30.60 and 205.87) with values reported relative to tetramethylsilane (δ 0.0).

UV-Vis spectra were recordered on a Hewlett Packard 8452A diode array spectrophotometer in a range of solvents. Cyclic voltamograms were obtained on a BAS 100B electrochemical analyser with a one compartment three-electrode system consisting of a $Ag/AgNO_3$ (0.01 M) reference electrode, platinum wire auxiliary electrode and platinum disc working electrode. Samples (1-2 mM) were prepared and run under argon at ambient temperature, in anhydrous acetonitrile with tetrabutylammonium perchlorate (0.1 M) as background electrolyte. Solutions were saturated with argon by bubbling for several minutes prior to each run. The system gave ferrocene $E_{½}$ = +75.5 mV. The platinum disc working electrode was polished between runs.

Gas chromatography was conducted on a Carlo Erba Strumentazione Fractovap 4200 series dual column modular gas chromatograph fitted with a Phenomenex Zebron ZB-1 column. Gel-permeation chromatography was conducted at Stellenbosch University with a Waters 717 autosampler, Waters 619 flow unit, Waters 410 differential refractometer, Waters 600E system controller, Waters 515 HPLC pump, Valveco 8-port switch valves for high and low temperature HPLC applications and Wyatt technology laser photometer. The programme was controlled using Millenium™ software.

X-ray diffraction data was collected at 173 K using Nonius Kappa CCD with 1.5 kW graphite monochromated Mo radiation. The strategy for data collection was evaluated using *COLLECT*.[4] Several sets of data were collected with both a 199° phi scan and omega scans to collect cusp data. The data was scaled and reduced as well as treated for absorption by a semi-empirical method using *DENZO-SMN*.[5] Unit cell dimensions were refined on all data. The structure was solved and refined using *SHELX97*.[6,7] Molecular graphics were generated using *ORTEP-III*,[8] *PLATON*[9] and X-Seed,[10] a graphical interface for the SHELX program.

Biological studies were carried out by Dr D. Hendricks at Medical Biochemistry, University of Cape Town.

Preparation of ferrocenyl precursors, ligands and their coordination complexes

7.2 Synthesis of ligands

7.2.1 Chloromercuriferrocene[11,12]

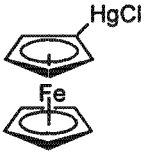

A solution of mercuric acetate (5.26 g, 16.5 mmol) in methanol (45 ml) was added dropwise to a solution of ferrocene (6.25 g, 33.0 mmol) in benzene (30 ml). The reaction mixture was stirred under nitrogen at room temperature for at

least 10 hours. A solution of lithium chloride (1.48 g, 35.0 mmol) in ethanol-water 1:1 (10 ml) was added slowly to the reaction mixture, changing it from dark brown to light orange. Upon further stirring for 2 hours at room temperature, an orange suspension was observed. The reaction mixture was set to reflux for an hour, followed by filtration of the crude residue under vacuum. The residue obtained was purified by Soxhlet extraction with dichloromethane, followed by sublimation to remove unreacted ferrocene. Recrystallisation of the unsublimed portion yielded the product as a fine golden powder (2.92 g, 42%), mp 194-195 °C (dec.) (lit.[13] 194-198 °C dec.). ν_{max} (KBr)/ cm^{-1} 3091, 1653, 1409, 1324, 1105, 1020, 999, 823 and 493; ^1H NMR δ_H (300 MHz; solvent $CDCl_3$): 4.47 (2H, t, *J = 1.7 Hz*, C_5H_4), 4.23 (5H, s, C_5H_5), 4.11 (2H, t, *J = 1.7 Hz*, C_5H_4); ^{13}C NMR δ_C (75 MHz; solvent $CDCl_3$): 73.01 (C_5H_4), 70.38 (C_5H_4) and 68.98 (C_5H_5).

7.2.2 Iodoferrocene[11]

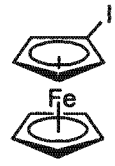

A solution of iodine (4.52 g, 35.6 mmol) in dichloromethane (100 ml) was added slowly to a solution of chloromercuriferrocene (5.00 g, 11.87 mmol) in dichloromethane (300 ml) at room temperature under nitrogen. The reaction mixture was further stirred for several days, concentrated under vacuum and subjected to flash chromatography. The filtrate was washed with sodium thiosulfate (10 % aqueous solution), followed by water. The organic fractions were collected, dried over anhydrous magnesium sulfate and the solvent removed *in vacuo*. The residue obtained was subjected to column chromatography on silica with petroleum ether (40-60 °C) as eluant. The product was obtained as yellow crystals (1.90 g, 51%), mp 44-45 °C (lit.[11] 44-46 °C). ν_{max} (KBr)/ cm^{-1} 3090, 1600-1700, 1412, 1105, 1018, 1000 and 820; ^1H NMR δ_H (300 MHz; solvent $CDCl_3$): 4.35 (2H, t, *J = 1.7 Hz*, C_5H_4), 4.12 (5H, s, C_5H_5), 4.09 (2H, t, *J = 1.8 Hz*, C_5H_4); ^{13}C NMR δ_C (75 MHz; solvent $CDCl_3$): 74.85 (C_5H_4), 71.42 (C_5H_5) and 69.20 (C_5H_4).

7.2.3 Bromoferrocene[11]

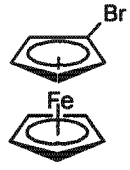

A solution of N-bromosuccinimide (1.10 g, 6.2 mmol) in anhydrous N,N'-dimethylformamide (20 ml) was added slowly to a cold (~0 °C) stirred solution of chloromercuriferrocene (2.10 g, 5.0 mmol) in anhydrous N,N'-dimethylformamide (40 ml), under nitrogen. The reaction mixture was further stirred at this temperature for at least 3 hours. A sodium thiosulfate (10 % aqueous) solution was added to the dark green reaction mixture, forming a lighter green suspension that was poured into 500 ml of cold water. The resulting green solution was extracted several times with hexane. The hexane fractions were collected, washed with water, dried over anhydrous magnesium sulfate

and the solvent removed *in vacuo*. The crude orange residue obtained was subjected to column chromatography on alumina and the product eluted with hexane. The product was observed as orange-yellow crystals (0.79 g, 60%), mp 32-34 °C (lit.[11] 31-32 °C). ^{1}H NMR δ_H (300 MHz; solvent $CDCl_3$): 4.51 (2H, t, *J = 1.8 Hz*, C_5H_4), 4.32 (5H, s, C_5H_5), 4.18 (2H, t, *J = 1.8 Hz*, C_5H_4); ^{13}C NMR δ_C (75 MHz; solvent $CDCl_3$): 75.48 (C_5H_4), 72.32 (C_5H_5) and 69.02 (C_5H_4).

7.2.4 4-Bromophenylferrocene[13,14]

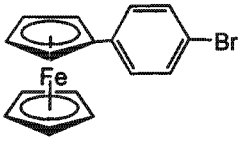

A mixture of 4-bromobenzeneboronic acid (0.64 g, 3.21 mmol), iodoferrocene (0.50 g, 1.60 mmol), barium hydroxide (0.71 g, 2.24 mmol) and palladium acetate (0.12 g, 0.53 mmol) in degassed 90 % ethanol (250 ml) was vigorously shaken for 30 minutes. The mixture was set to reflux while stirring under nitrogen (49 hours). The solvent was then removed in vacuo and the residue taken up in diethyl ether and filtered. The filtrate was washed with water, dried over anhydrous sodium sulfate and the solvent removed *in vacuo*. The residue obtained was purified by column chromatography over silica gel. The product was eluted with hexane-dichloromethane 8:2 and collected as bright red crystals, which were recrystallised from hexane (0.08 g, 15%), mp 122-123 °C (lit.[13] 125 °C); (Found: M^+ 339.9551. $C_{16}H_{13}BrFe$ requires M^+ 339.9550). ν_{max} (KBr)/ cm^{-1} 3086, 3050, 2926, 2853, 1588, 1510, 1446, 1406, 1383, 1279, 1103, 1088, 1067, 1050, 1030, 1001, 884, 819, 712, 644, 516, 498 and 478; ^{1}H NMR δ_H (300 MHz; solvent $CDCl_3$): 7.41 (2H, d, J = 8.5 Hz, C_6H_4), 7.34 (2H, d, J = 8.5 Hz, C_6H_4), 4.62 (2H, t, J = 1.8 Hz, C_5H_4), 4.34 (2H, t, J = 1.7 Hz, C_5H_4), 4.04 (5H, s, C_5H_5); *m/z* (EI) 340 (M^+, 100%), 260 (3), 205 (23), 203 (10), 202 (9).

7.2.5 4-Ferrocenylphenol[15]

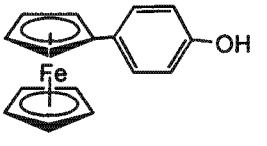

A cold aqueous solution of sodium nitrite (8.01 g, 0.12 mol) was added slowly to a cold (0 °C) solution of dilute hydrochloric acid (60 ml, 2 M) and 4-aminophenol (12.00 g, 0.11 mol) in a 2-necked round-bottom flask. The mixture was stirred at this temperature for at least 30 minutes. The diazonium salt that formed was added to a cold solution of ferrocene (18.60 g, 0.10 mol) in diethyl ether (450 ml). The reaction mixture was gradually warmed to room temperature overnight and nitrogen gas formed as the reaction progressed. The two-layer reaction mixture was poured into a separating funnel and the aqueous layer was extracted with diethyl ether. The organic fractions were combined, washed with water, dried over anhydrous sodium sulfate and the solvent removed *in vacuo*. The crude brown residue

obtained was initially passed over a silica gel flash column to remove decomposed material, followed by column chromatography over silica gel. The product was eluted as a red band with diethyl ether. 4-Ferrocenylphenol was obtained as an orange crystalline solid (8.80 g, 32%), mp 162-164 °C (lit.[15] 164-166 °C); (Found: M^+ 278.0393. $C_{16}H_{14}FeO$ requires M^+ 278.03940). ν_{max} (KBr)/ cm^{-1} 3515, 1651, 1609, 1528, 1269, 1175, 840 and 815; ^1H NMR δ_H (300 MHz; solvent $CDCl_3$): 7.38 (2H, d, *J = 8.5 Hz*, C_6H_4), 6.79 (2H, d, *J = 8.2 Hz*, C_6H_4), 4.76 (1H, s, OH), 4.56 (2H, t, *J = 1.8 Hz*, C_5H_4), 4.27 (2H, t, *J = 1.7 Hz*, C_5H_4), 4.03 (5H, s, C_5H_5); *m/z* (EI) 278 (M^+, 100%), 157 (11) and 121 (10).

7.2.6 4-Benzyloxy-4'-phenylferrocene[16]

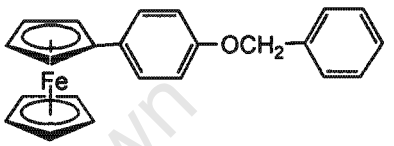

A mixture of 4-hydroxyphenylferrocene (0.30 g, 1.08 mmol), benzyl bromide (0.18 g, 1.08 mmol), potassium carbonate (0.89 g, 6.47 mmol) and sodium iodide (0.97 g, 6.47 mmol) in acetone (50 ml) was heated under reflux while stirring under nitrogen for 46.2 hours. The reaction mixture was then concentrated, washed with water and extracted several times with dichloromethane. The organic fractions were dried over anhydrous sodium sulfate and the solvent removed *in vacuo*. The crude residue obtained was purified by column chromatography on silica gel and the product was eluted with hexane-dichloromethane (7:3). 4-Benzyloxy-4'-phenylferrocene was obtained as golden flakes (0.16 g, 39%), mp 161-162 °C (lit.[16] 164-167 °C); (Found: M^+ 368.0863. $C_{23}H_{20}FeO$ requires M^+ 368.08635). ν_{max} (KBr)/ cm^{-1} 3447, 1653, 1526, 1455, 1384, 1245, 1103, 1029, 828, 753, 701 and 495; ^1H NMR δ_H (300 MHz; solvent $CDCl_3$): 7.47 – 7.28 (7H, m, C_6H_5 and C_6H_4), 6.93 (2H, dd, *J = 8.7 Hz*, C_6H_4), 5.05 (2H, s, OCH_2), 4.57 (2H, t, *J = 1.6 Hz*, C_5H_4), 4.29 (2H, t, *J = 1.6 Hz*, C_5H_4), 4.04 (5H, s, C_5H_5); ^{13}C NMR δ_C (75 MHz; solvent $CDCl_3$): 137.49 (C_6H_4), 131.96 (C_6H_4), 128.98 (C_6H_4), 128.35 (C_6H_4), 127.92 (C_6H_4), 127.60 (C_6H_4), 115.14 (C_6H_4), 96.80 (OCH_2), 70.47 (C_5H_4), 69.94 (C_5H_5), 68.96 (C_5H_4) and 66.56 (C_5H_4); *m/z* (EI) 368 (M^+, 68%), 277 (100), 249 (14), 121 (30), 91 (9) and 56 (6).

7.2.7 4-Nitrophenylferrocene[17]

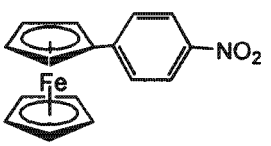

A cold aqueous (50 ml) solution of sodium nitrite (8.01 g, 0.12 mol) was added slowly to a cold (0 °C) solution of dilute hydrochloric acid (100 ml, 2 M) and 4-nitroaniline (15.00 g, 0.11 mol) in a 2-necked round-bottom flask. The mixture was stirred at this temperature for at least 30 minutes. The diazonium salt that formed was added to a cold solution of ferrocene (18.50 g, 0.10 mol) in diethyl ether (500 ml). The reaction mixture was gradually warmed to room temperature

overnight and nitrogen gas was formed as the reaction progressed. The two-layer reaction mixture was then poured into a separating funnel and the aqueous layer was extracted with diethyl ether. The organic fractions were combined, washed with water, dried over anhydrous sodium sulfate and the solvent removed *in vacuo*. The crude dark residue obtained was initially passed over a silica gel flash column to remove decomposed material, followed by column chromatography over deactivated alumina. The product was eluted as a dark red band with diethyl ether. 4-Nitrophenylferrocene was obtained as dark red-black crystals (3.10 g, 21%), mp 108-110 °C (lit.[17] 108-111 °C); (Found: M^+ 307.0293. $C_{16}H_{13}FeNO_2$ requires M^+ 307.0293). ν_{max} (KBr)/ cm^{-1} 3019, 1594, 1509, 1340, 1106, 1003, 847, 816 and 474; ^1H NMR δ_H (300 MHz; solvent $CDCl_3$): 8.14 (2H, d, *J = 8.5 Hz*, C_6H_4), 7.56 (2H, d, *J = 8.5 Hz*, C_6H_4), 4.74 (2H, t, *J = 1.8 Hz*, C_5H_4), 4.47 (2H, t, *J = 1.8 Hz*, C_5H_4), 4.16 (5H, s, C_5H_5); ^{13}C NMR δ_C (75 MHz; solvent $CDCl_3$): 134.97 (C_6H_4), 129.7 (C_6H_4), 126.33 (C_6H_4), 124.22 (C_6H_4), 123.88 (C_6H_4), 71.00 (C_5H_4), 70.44 (C_5H_4) and 68.31 (C_5H_5); *m/z* (EI) 308 (M^+, 20%), 261 (47), 244 (9), 186 (17), 152 (7), 139 (21) and 121 (17).

7.2.8 4-Ferrocenylaniline[18]

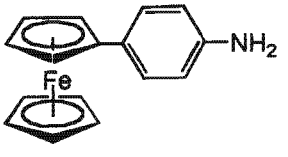

The hydrogenation of 4-nitrophenylferrocene (3.54 g, 11.53 mmol) to 4-aminophenylferrocene was catalysed by 10 % palladium/ carbon (0.15 g) in tetrahydrofuran (200 ml) in a Parr hydrogenation reactor (400 atm). The product was purified by column chromatography on silica gel and eluted with dichloromethane. 4-Ferrocenylaniline was obtained as an orange-brown solid (0.99 g, 31%), mp 157-159 °C (lit. 159-160 °C); (Found: M^+ 277.05682. $C_{16}H_{15}FeN$ requires M^+ 277.05539). ν_{max} (KBr)/ cm^{-1} 3436, 3356, 3102, 1653, 1622, 1529, 1452, 1288, 1103, 1012, 820, 640, 531 and 507; ^1H NMR δ_H (300 MHz; solvent $CDCl_3$): 7.30 (2H, d, *J = 8.5 Hz* C_6H_4), 6.65 (2H, d, *J = 8.5 Hz*, C_6H_4), 4.54 (2H, t, *J = 1.8 Hz*, C_5H_4), 4.24 (2H, t, *J = 1.8 Hz*, C_5H_4), 4.03 (5H, s, C_5H_5), 3.62 (2H, s, NH_2); ^{13}C NMR δ_C (75 MHz; solvent $CDCl_3$): 144.94 (C_6H_4), 129.40 (C_6H_4), 127.54 (C_6H_4), 115.59 (C_6H_4), 96.51 (C_6H_4), 86.95 (C_5H_4), 68.58 (C_5H_4) and 66.20 (C_5H_5); *m/z* (EI) 277 (M^+, 100%), 211 (7), 156 (22) and 121 (8).

7.2.9 4-Phenylimine-4'-pyridine[19,20]

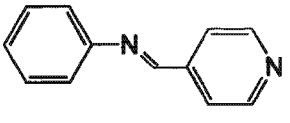

Pyridine-4-carboxaldehyde (1.15 g, 1.10 ml, 10.74 mmol) was added to a solution of aniline (1.0 g, 0.98 ml, 10.74 mmol) in methanol (40 ml) with 4Å molecular sieves (3 g). The reaction mixture was heated under reflux overnight while stirring under nitrogen. The reaction mixture then was filtered and

concentrated. The concentrate was cooled to 0 °C to precipitate the product, which was collected *via* vacuum filtration. The product was obtained as cream crystalline flakes (1.52 g, 77%), mp 60-66 °C. ν_{max} (KBr)/ cm^{-1} 3052, 2883, 1651, 1621, 1595, 1494, 1226, 1186, 1166, 1075, 1023, 1000, 821 and 500;^{1}H NMR δ_H (400 MHz; solvent $CDCl_3$): 8.74 (2H, dd, C_5H_4N), 8.44 (1H, s, N=CH), 7.75 (2H, dd, C_5H_4N), 7.42 (2H, t, C_6H_5), 7.31 (2H, d, C_6H_5), 7.25 (1H, t, C_6H_5); ^{13}C NMR δ_C (101 MHz; solvent $CDCl_3$): 158.12 (N=C), 151.21 (C_5H_4N), 150.81 (C_5H_4N), 143.05 (C_6H_5), 129.51 (C_5H_4N), 127.21 (C_6H_5), 122.47 (C_6H_5) and 121.12 (C_6H_5).

7.2.10 4-Pyridylimine-4'-phenylferrocene[21]

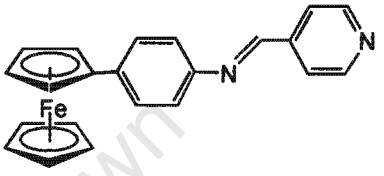

Pyridine-4-carboxaldehyde (0.12 g, 1.08 mmol) was added to a solution of 4-ferrocenylaniline (0.20 g, 0.72 mmol) in methanol (20 ml) with 4Å molecular sieves (1 g). The reaction mixture was heated under reflux overnight. The reaction mixture was then filtered and concentrated. The concentrate was cooled to 0 °C to precipitate the product. The product was collected *via* vacuum filtration and obtained as maroon crystalline flakes (0.24 g, 90%), mp 195-196 °C; (Found: M^+ 366.08140. $C_{22}H_{18}FeN_2$ requires M^+ 366.08194). ν_{max} (KBr)/ cm^{-1} 3506, 1623, 1408, 1105, 846 and 823; ^{1}H NMR δ_H (400 MHz; solvent $CDCl_3$): 8.77 (2H, d, *J = 5.9 Hz*, C_5H_4N), 8.54 (1H, s, N=CH), 7.79 (2H, dd, *J = 5.9 Hz*, C_5H_4N), 7.55 (2H, dd, *J = 6.7 Hz*, C_6H_4), 7.22 (2H, d, *J = 8.5 Hz*, C_6H_4), 4.68 (2H, t, *J = 1.8 Hz*, C_5H_4), 4.36 (2H, t, *J = 1.8 Hz*, C_5H_4), 4.06 (5H, s, C_5H_5); ^{13}C NMR δ_C (101 MHz; solvent $CDCl_3$): 156.71 (N=C), 150.80 (C_5H_4N), 148.61 (C_5H_4N), 143.26 (C_6H_4), 139.07 (C_5H_4N), 127.00 (C_5H_4N), 122.38 (C_5H_4N), 121.48 (C_6H_4), 69.88 (C_5H_5), 69.42 (C_5H_4) and 66.70 (C_5H_4); *m/z* (EI) 366 (M^+, 100%), 301 (8), 245 (9), 139 (8), 121 (8) and 56 (3).

7.2.11 4-Pyridylvinyl-4'-phenylferrocene[21, 22]

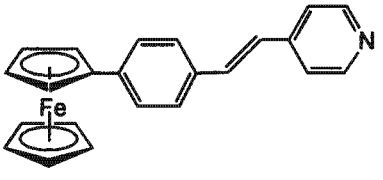

Lithium *n*-diisopropylamide (1.20 mmol) in tetrahydrofuran (30 ml) was prepared *in situ* at –78 °C. A solution of 4-methylpyridine (30.8 mg, 0.03 ml, 0.33 mmol) in tetrahydrofuran (20 ml) was added slowly to the solution, after which the reaction mixture was slightly warmed by replacing the –78 °C cold bath with an ice-bath. The reaction mixture was further stirred at this temperature for an hour. A solution of 4-formylphenylferrocene (80.0 mg, 0.28 mmol) in tetrahydrofuran (10 ml) was slowly added to the reaction mixture, which was then gradually allowed to warm to room temperature overnight. The reaction mixture was concentrated and the residue taken up in chloroform and washed successively with water and brine. The organic fractions were

combined, dried over anhydrous magnesium sulfate and the solvent removed *in vacuo*. The crude intermediate hydroxy species obtained was taken up in toluene (15 ml) and stirred under reflux (23.7 hours) with pyridinium toluene-*p*-sulfonate (27.5 mg, 0.11 mmol) to form the alkene. The reaction mixture was concentrated, the residue taken up in chloroform and washed successively with water and brine. The organic portions were combined, dried over anhydrous magnesium sulfate and the solvent removed *in vacuo*. The crude residue was further purified by column chromatography on silica gel. The product was collected after recrystallisation (dichloromethane-hexane) as pink-red crystalline flakes (23.9 mg, 24%), mp 228-230 °C. ^{1}H NMR δ_H (300 MHz; solvent $CDCl_3$): 8.59 (2H, d, *J = 5.9 Hz*, C_5H_4N), 7.48 (4H, dd, *J = 8.4 Hz*, C_6H_4), 7.36 (1H, d, *J = 16.1 Hz*, CH=CH), 7.26 (2H, d, *J = 5.8 Hz*, C_5H_4N), 7.04 (1H, d, *J = 16.1 Hz*, CH=CH), 4.68 (2H, t, *J = 1.9 Hz*, C_5H_4), 4.36 (2H, t, *J = 1.8 Hz*, C_5H_4), 4.05 (5H, s, C_5H_5); ^{13}C NMR δ_C (75 MHz; solvent $CDCl_3$): 150.21 (C_5H_4N), 133.09 (C_5H_4N), 127.12 (C_6H_4), 126.34 (C_6H_4), 124.98 (C=C), 120.76 (C=C), 69.70 (C_5H_5), 69.32 (C_5H_4) and 66.52 (C_5H_4).

7.2.12 4-Ferrocenylpyridine[23,24]

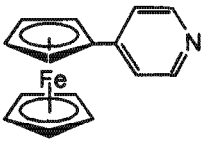

Diethyl ether (5 ml) was added to previously dried and weighed magnesium (396.0 mg, 16.0 mmol) in a two-necked 50 ml round bottom flask fitted with a condenser and dropping funnel. A solution of 1,2-dibromoethane (0.7 ml, 7.9 mmol) and bromoferrocene (792.0 mg, 4.0 mmol) in diethyl ether (10 ml) was added dropwise. On complete addition, two layers were observed with a small amount of unreacted magnesium. A mixture of 4-bromopyridine (462.2 mg, 2.6 mmol) and cis-(1,3-bis(diphenylphosphino)propane)dichloronickel (16.7 mg, 31 μmol) in diethyl ether (10 ml) was added to the freshly prepared Grignard reagent. The reaction mixture was heated under reflux under nitrogen for 23 hours, changing to a deep red solution over time. Upon cooling the reaction mixture, distilled water was added slowly to destroy any active Grignard reagent remaining. The two-layer reaction mixture was poured into a separating funnel and the aqueous layer extracted repeatedly with diethyl ether. The organic fractions were combined, washed with brine, dried over anhydrous magnesium sulfate and the solvent removed *in vacuo* yielding an orange residue. The residue was purified by column chromatography on silica gel. The product was eluted with 5 % methanol in diethyl ether and isolated as golden yellow flakes (450 mg, 73%), mp 137-139 °C (lit.[23] 136-138 °C). ν_{max} (KBr)/ cm^{-1} 3104, 3069, 3033, 3047, 1612, 1569, 1478, 1436, 1348, 1105, 1093, 1033, 823 and 486; ^{1}H NMR δ_H (300 MHz; solvent $CDCl_3$): 8.45 (2H, d, *J = 6.0 Hz*, C_5H_4N), 7.51 (2H, dd, *J = 6.3 Hz*, C_5H_4N), 4.82 (2H, t, *J = 1.8 Hz*, C_5H_4), 4.61 (2H, t, *J = 1.9 Hz*, C_5H_4), 4.08 (5H, s, C_5H_5);

^{13}C NMR δ_C (75 MHz; solvent $CDCl_3$): 150.78 (C_5H_4N), 123.85 (C_5H_4N), 72.02 (C_5H_5), 70.46 (C_5H_4) and 67.96 (C_5H_4).

7.2.13 3-Ferrocenylpyridine[23,25]

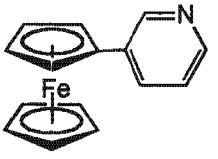

3-Ferrocenylpyridine was prepared according to the general procedure for *7.1.12*. Magnesium (183.7 mg, 7.55 mmol), 4-bromoferrocene (500.0 mg, 1.89 mmol), 1,2-dibromoethane (702.0 mg, 0.32 ml, 3.74 mmol), 3-bromopyridine (194.0 mg, 0.12 ml, 1.23 mmol) and cis-(1,3-bis(diphenylphosphino)propane)dichloronickel (8.0 mg, 14.7 µmol) in diethyl ether (25 ml) was heated under reflux for 19 hours. The product was obtained as large flat brown crystals from dichloromethane-hexane (258.0 mg, 80%), mp 60-62 °C (lit.[26] 57-59 °C). ν_{max} (KBr)/ cm^{-1} 3853, 3743, 1699, 1652, 1569, 1495, 1419, 1305, 1282, 1215, 1103, 1088, 1007, 887, 808, 702, 668, 523, 498 and 404; ^1H NMR δ_H (400 MHz; solvent $CDCl_3$): 8.75 (1H, br s, C_5H_4N), 8.42 (1H, d, *J = 4.3 Hz*, C_5H_4N), 7.73 (1H, dd, *J = 8.0 Hz*, C_5H_4N), 7.21 (1H, dd, *J = 6.3 Hz*, C_5H_4N), 4.67 (2H, t, *J = 1.8 Hz*, C_5H_4), 4.37 (2H, t, *J = 1.8 Hz*, C_5H_4), 4.06 (5H, s, C_5H_5); ^{13}C NMR δ_C (101 MHz; solvent $CDCl_3$): 145.87 (C_5H_4N), 145.40 (C_5H_4N), 131.41 (C_5H_4N), 121.63 (C_5H_4N), 68.05 (C_5H_5), 67.85 (C_5H_4) and 64.87 (C_5H_4).

7.2.14 2-Ferrocenylpyridine[27]

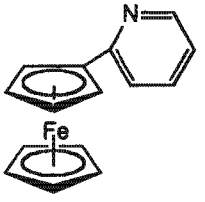

2-Ferrocenylpyridine was prepared by the general procedure *7.1.12* via the Grignard reaction. Magnesium (220.6 mg, 9.06 mmol), bromoferrocene (600.9 mg, 2.26 mmol), 1,2-dibromoethane (840.0 mg, 0.39 ml, 4.48 mmol), 2-bromopyridine (200.0 mg, 0.12 ml, 1.28 mmol) and cis-(1,3-bis(diphenylphosphino)propane)dichloronickel (6.9 mg, 12.8 µmol) in diethyl ether (27 ml) heated under reflux for 44.4 hours. The product was obtained as orange rod-like microcrystals from dichloromethane-hexane (218.9 mg, 65%), mp 85-87 °C (lit.[27] 87-89 °C); (Found: M^+ 263.0. $C_{15}H_{13}FeN$ requires M^+ 263.1). ν_{max} (KBr)/ cm^{-1} 3608, 3565, 2324, 1843, 1767, 1698, 1622, 1587, 1558, 1495, 1423, 1275, 1106, 892, 824, 788, 741, 667, 518, 496, 441 and 403; ^1H NMR δ_H (300 MHz; solvent $CDCl_3$): 8.49 (1H, br s, C_5H_4N), 7.57 (1H, d, C_5H_4N), 7.41 (1H, dd, *J = 7.8 Hz*, C_5H_4N), 7.06 (1H, t, C_5H_4N), 4.92 (2H, t, *J = 1.8 Hz*, C_5H_4), 4.39 (2H, t, *J = 1.8 Hz*, C_5H_4), 4.05 (5H, s, C_5H_5); ^{13}C NMR δ_C (75 MHz; solvent $CDCl_3$): 149.30 (C_5H_4N), 135.87 (C_5H_4N), 120.45 (C_5H_4N), 120.04 (C_5H_4N), 69.87 (C_5H_4), 69.56 (C_5H_5) and 67.23 (C_5H_4); *m/z* (FAB) 264 (58%), 263 (M^+, 100), 198 (M-Cp, 39), 121 (Cp, 5), 56 (Fe, 6).

7.2.15 4-Ferrocenylphenyl-4'-pyridine[28]

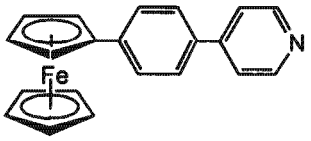

4-Ferrocenylphenyl-4'-pyridine was prepared by the general procedure for *7.1.12* via the Grignard reaction. Magnesium (178.2 mg, 7.33 mmol), 4-bromophenylferrocene (625.4 mg, 1.83 mmol), 1,2-dibromoethane (682.0 mg, 0.31 ml, 3.63 mmol), 4-bromopyridine (188.2 mg, 1.19 mmol) and cis-(1,3-bis(diphenylphosphino)propane)dichloronickel (7.8 mg, 14.3 µmol) in diethyl ether (36 ml) was heated under reflux for 21.8 hours. The product was obtained as an orange powder (134.0 mg, 33%), mp 225-226 °C. ν_{max} (KBr)/ cm^{-1} 3085, 3023, 1645, 1610, 1545, 1500, 1435, 1401, 1105, 1087, 1000, 842, 810, 656, 498 and 409; ^1H NMR δ_H (400 MHz; solvent $CDCl_3$): 8.66 (2H, dd, *J = 5.9 Hz*, C_5H_4N), 7.59 (4H, s, C_6H_4), 7.54 (2H, dd, *J = 6.1 Hz*, C_5H_4N), 4.70 (2H, t, *J = 1.8 Hz*, C_5H_4), 4.37 (2H, t, *J = 1.8 Hz*, C_5H_4), 4.07 (5H, s, C_5H_5); ^{13}C NMR δ_C (101 MHz; solvent $CDCl_3$): 150.45 (C_5H_4N), 127.09 (C_6H_4), 126.86 (C_6H_4), 121.35 (C_5H_4N), 66.83 (C_5H_4), 69.56 (C_5H_4) and 69.92 (C_5H_5).

7.2.16 4-Ferrocenylphenyl-3'-pyridine

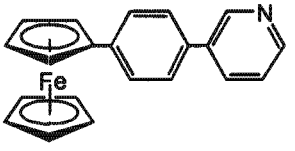

4-Ferrocenylphenyl-3'-pyridine was prepared by the general procedure for *7.1.12* via the Grignard reaction. Diethyl ether (5 ml) was added to previously dried and weighed magnesium (179.4 mg, 7.38 mmol) in a two-necked 50 ml round bottom flask fitted with a condenser and dropping funnel. A solution of 1,2-dibromoethane (682.0 mg, 0.31 ml, 3.63 mmol) and 4-bromophenylferrocene (625.3 mg, 1.83 mmol) in diethyl ether (10 ml) was added dropwise. On complete addition, two layers were observed with a small amount of unreacted magnesium. A mixture of 3-bromopyridine (188.2 mg, 0.11 ml, 1.19 mmol) and cis-(1,3-bis(diphenylphosphino)propane)dichloronickel (7.8 mg, 14.3 µmol) in diethyl ether (15 ml) was added to the freshly prepared Grignard reagent. The reaction mixture was heated under reflux under nitrogen for 20.5 hours, changing to a bright orange solution over time. Upon cooling the reaction mixture, distilled water was added slowly to destroy any active Grignard reagent remaining. The two-layer reaction mixture was poured into a separating funnel and the aqueous layer extracted repeatedly with diethyl ether. The organic fractions were combined, washed with brine, dried over anhydrous magnesium sulfate and the solvent removed *in vacuo* yielding an orange residue, which was subjected to column chromatography on silica gel. The product was eluted with 5 % methanol in diethyl ether and isolated as an orange solid (156.0 mg, 39%), mp 144-147 °C; (Found: C, 74.44 %, H, 5.06, N, 3.79; M^+ 339.1. $C_{21}H_{17}FeN$ requires C, 74.3 %, H, 5.1, N, 4.1; M^+ 339.1) ν_{max} (KBr)/ cm^{-1} 3083, 3022, 2913, 2329, 1645, 1609, 1542, 1498, 1436, 1401, 1105, 1087, 1000, 842, 809,

668, 498 and 409; ^{1}H NMR δ_H (400 MHz; solvent $CDCl_3$): 8.89 (1H, br s, C_5H_4N), 8.58 (1H, d, *J = 4.8 Hz*, C_5H_4N), 7.89 (1H, dt, *J = 1.8 and 11.7 Hz*, C_5H_4N), 7.58 (2H, d, *J = 8.4 Hz*, C_6H_4), 7.52 (2H, d, *J = 8.8 Hz*, C_6H_4), 7.36 (1H, dd, *J = 12.4 Hz*, C_5H_4N), 4.69 (2H, t, *J = 1.8 Hz*, C_5H_4), 4.36 (2H, t, *J = 2.2 Hz*, C_5H_4), 4.07 (5H, s, C_5H_5); ^{13}C NMR δ_C (101 MHz; solvent $CDCl_3$): 148.16 (C_5H_4N), 139.98 (C_5H_4N), 133.81 (C_5H_4N), 126.96 (C_6H_4), 126.65 (C_6H_4), 123.51 (C_5H_4N), 69.61 (C_5H_5), 69.14 (C_5H_4) and 66.51 (C_5H_4); *m/z* (EI) 340 (24%), 339 (M^+, 100), 218 (M^+ - Cp-Fe, 18), 189 (4), 169 (4), 121 (Cp-Fe, 31) and 56 (Fe, 15).

7.2.17 4-Ferrocenylphenyl-2'-pyridine

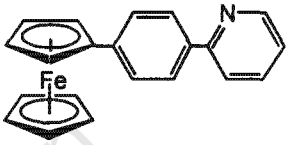

4-Ferrocenylphenyl-2'-pyridine was prepared by the general procedure for *7.1.12* via the Grignard reaction. Diethyl ether (5 ml) was added to previously dried and weighed magnesium (129.0 mg, 5.28 mmol) in a two-necked 50 ml round bottom flask fitted with a condenser and dropping funnel. A solution of 1,2-dibromoethane (490.0 mg, 0.24 ml, 2.61 mmol) and 4-bromophenylferrocene (450.0 mg, 1.32 mmol) in diethyl ether (10 ml) was added dropwise. On complete addition, two layers were observed with a small amount of unreacted magnesium. A mixture of 2-bromopyridine (136.0 mg, 82.0 µl, 0.86 mmol) and cis-(1,3-bis(diphenylphosphino)propane)dichloronickel (5.6 mg, 10.3 µmol) in diethyl ether (16 ml) was added to the freshly prepared Grignard reagent. The reaction mixture was heated under reflux under nitrogen for 20.1 hours, changing to a bright orange-red solution over time. Upon cooling the reaction mixture, distilled water was added slowly to destroy any active Grignard reagent remaining. The two-layer reaction mixture was poured into a separating funnel and the aqueous layer extracted repeatedly with diethyl ether. The organic fractions were combined, washed with brine, dried over anhydrous magnesium sulfate and the solvent removed *in vacuo* yielding an orange residue, which was subjected to column chromatography on silica gel. The product was eluted with 5 % methanol in diethyl ether and isolated as a bright orange-red solid (112.0 mg, 38 %), mp 37-39 °C; (Found: C, 74.54 %, H, 5.25, N, 4.10; M^+ 339.1. $C_{21}H_{17}FeN$ requires C, 74.3 %, H, 5.0, N, 4.1; M^+ 339.1). ν_{max} (KBr)/ cm^{-1} 1585, 1467, 1434, 1105, 818, 782, 492, 441, 418, 411 and 404; ^{1}H NMR δ_H (400 MHz; solvent $CDCl_3$): 8.69 (1H, dd, *J = 4.8 Hz*, C_5H_4N), 7.93 (2H, dd, *J = 8.4 Hz*, C_6H_4), 7.74 (2H, dd, *J = 6.2 Hz*, C_5H_4N), 7.57 (2H, dd, *J = 8.8 Hz*, C_6H_4), 7.21 (1H, dd, *J = 6.6 Hz*, C_5H_4N), 4.71 (2H, t, *J = 1.8 Hz*, C_5H_4), 4.35 (2H, t, *J = 2.2 Hz*, C_5H_4), 4.05 (5H, s, C_5H_5); ^{13}C NMR δ_C (101 MHz; solvent $CDCl_3$): 149.60 (C_5H_4N), 136.58 (C_5H_4N), 126.22 (C_6H_4), 126.77 (C_6H_4), 121.70 (C_5H_4N), 120.05 (C_5H_4N), 69.60 (C_5H_5), 69.12 (C_5H_4) and 66.49 (C_5H_4); *m/z* (FAB) 340 (56%), 339 (M^+, 100), 274 (M-Cp, 5), 121 (Cp, 3), 56 (Fe, 3).

7.2.18 1,1'-Bis(2-pyridyl)ferrocene[29, 30]

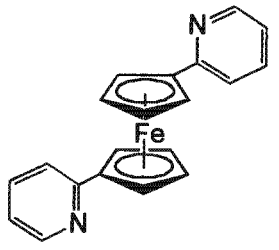

n-Butyllithium (6.23 ml, 9.97 mmol, 1.6 M in hexanes) was added slowly to a solution of N,N,N',N'-tetramethylethylenediamine (1.16 g, 1.50 ml, 9.97 mmol) in hexane (5 ml). The mixture was stirred under nitrogen for at least 10 minutes at room temperature to allow butyllithium-TMEDA to form. A solution of ferrocene (0.743 g, 4.0 mmol) in hexane (35 ml) was added slowly and the mixture further stirred at room temperature for 6 hours. Hexane was then removed and the residue taken up in tetrahydrofuran (30 ml) and cooled to 0 °C. A cold solution of zinc chloride (1.09 g, 8.0 mmol) in tetrahydrofuran (20 ml) was added to the dark solution, which was further stirred at room temperature for at least an hour. Meanwhile Superhydride® (0.40 ml, 0.40 mmol, 1 M in tetrahydrofuran) was added to a suspension of dichlorobis(triphenylphosphine)palladium (0.140 g, 0.20 mmol) in tetrahydrofuran (10 ml), forming a dark solution that was added via cannula to the ferrocene reaction mixture. 2-Bromopyridine (1.58 g, 0.95 ml, 9.97 mmol) was added dropwise to the reaction mixture. An aqueous solution of sodium hydroxide (25 ml, 2.5 M) was added after 25 hours. The two-layer reaction mixture was poured into a separating funnel. The aqueous phase was extracted repeatedly with dichloromethane. The organic fractions were combined and dried over anhydrous magnesium sulfate. The solvent was removed *in vacuo* and the residue further purified by column chromatography on alumina. Elution with diethyl ether yielded a yellow band of 2-ferrocenylpyridine (575.5 mg, 55%). Elution with dichloromethane yielded an orange band of the product. The product was obtained as a pinkish-red powder (114.0 mg, 10%), mp 180-182 °C (lit.[29] 179-180 °C). ν_{max} (KBr)/ cm^{-1} 3568, 2323, 1773, 1700, 1636, 1617, 1586, 1562, 1507, 1457, 1425, 1100, 1025, 984, 668, 420 and 405; ^1H NMR δ_H (300 MHz; solvent $CDCl_3$): 8.35 (2H, d, *J = 5.3 Hz*, C_5H_4N), 7.67 (2H, t, *J = 7.8 Hz*, C_5H_4N), 7.50 (2H, dd, *J = 6.7 Hz*, C_5H_4N), 7.08 (2H, dd, *J = 11.6 Hz*, C_5H_4N), 4.91 (4H, t, *J = 1.8 Hz*, C_5H_4), 4.36 (4H, t, *J = 1.8 Hz*, C_5H_4); ^{13}C NMR δ_C (75 MHz; solvent $CDCl_3$): 156.97 (C_5H_4N), 136.51 (C_5H_4N), 131.90 (C_5H_4N), 128.39 (C_5H_4N), 120.30 (C_5H_4N), 71.48 (C_5H_4) and 68.73 (C_5H_4).

7.2.19 1,1'-Bis(4-pyridyl)ferrocene

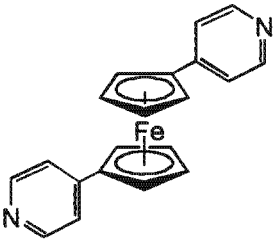

1,1'-Bis(4-pyridyl)ferrocene was prepared according to the general procedure for *7.2.18*. *n*-Butyllithium (6.23 ml, 9.97 mmol, 1.6 M in hexanes) was added slowly to a solution of N,N,N',N'-tetramethylethylenediamine (1.16 g, 1.50 ml, 9.97 mmol) in hexane (5 ml). The mixture was stirred under nitrogen for at least 10 minutes at

room temperature to allow butyllithium-TMEDA to form. A solution of ferrocene (0.742 g, 4.0 mmol) in hexane (35 ml) was added slowly and the mixture further stirred at room temperature for 6 hours. Hexane was then removed and the residue taken up in tetrahydrofuran (30 ml) and cooled to 0 °C. A cold solution of zinc chloride (1.09 g, 8.0 mmol) in tetrahydrofuran (20 ml) was added to the dark solution, which was further stirred at room temperature for at least an hour. Meanwhile Superhydride® (0.40 ml, 0.40 mmol, 1.0 M in tetrahydrofuran) was added to a suspension of chlorobis(triphenylphosphine)palladium (0.140 g, 0.20 mmol) in tetrahydrofuran (10 ml), forming a dark solution that was added via cannula to the ferrocene reaction mixture. 4-Bromopyridine (1.576 g, 9.97 mmol) was added dropwise to the reaction mixture. An aqueous solution of sodium hydroxide (25 ml, 2.5 M) was added after 25 hours. The two-layer reaction mixture was poured into a separating funnel. The aqueous phase was extracted repeatedly with dichloromethane. The organic fractions were combined and dried over anhydrous magnesium sulfate. The solvent was removed *in vacuo* and the residue further purified by column chromatography on alumina. Elution with diethyl ether yielded an orange band of 4-ferrocenylpyridine. Elution with dichloromethane yielded an orange band of the product. The product was obtained as a yellow crystalline material (204.1 mg, 15%). ν_{max} (KBr)/ cm^{-1} 3083, 3029, 2353, 2320, 1941, 1695, 1634, 1606, 1557, 1538, 1505, 1456, 1418, 1284, 1225, 1118, 1091, 1036, 818, 677, 646, 525, 500 and 480; ^{1}H NMR δ_H (400 MHz; solvent $CDCl_3$): 8.39 (4H, d, *J = 6.0 Hz*, C_5H_4N), 7.06 (4H, d, *J = 5.0 Hz*, C_5H_4N), 4.55 (4H, t, *J = 1.8 Hz*, C_5H_4), 4.34 (4H, t, *J = 1.9 Hz*, C_5H_4); ^{13}C NMR δ_C (101 MHz; solvent $CDCl_3$): 149.69 (C_5H_4N), 120.18 (C_5H_4N), 72.24 (C_5H_4) and 68.45 (C_5H_4).

7.2.20 4-Formylphenylferrocene[14]

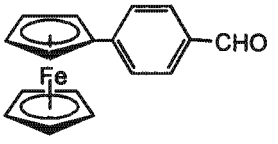

A mixture of iodoferrocene (1.95 g, 6.24 mmol), 4-formylbenzene boronic acid (1.87 g, 12.48 mmol), barium hydroxide (2.76 g, 8.74 mmol) and palladium(II) acetate (0.35 g, 1.56 mmol) in degassed ethanol (90 %, 200 ml) was initially stirred under nitrogen for 10 minutes, followed by vigorous shaking on an automatic shaker for 30 minutes. The reaction mixture was heated under reflux while stirring under nitrogen for 54.3 hours. The reaction mixture was then concentrated and the residue taken up in diethyl ether and washed with water. The combined organic fractions were dried over anhydrous sodium sulfate, the solvent removed *in vacuo* and the crude residue subjected to column chromatography on silica gel. The product was obtained by elution with hexane-dichloromethane (1:1) as a red crystalline solid (0.91 g, 50%), mp 136-137 °C; (Found: M^+ 290.0384. $C_{17}H_{14}FeO$ requires M^+ 290.0393). ν_{max} (KBr)/ cm^{-1} 3096, 2730, 1700, 1653, 1601, 1565, 1520, 1422, 1385, 1304, 1280, 1261, 1214, 1173, 1103, 1081, 1028, 999, 885, 827, 681, 526 and 486; ^{1}H NMR δ_H (300 MHz;

solvent $CDCl_3$): 9.97 (1H, s, CHO), 7.80 (2H, d, *J = 8.4 Hz* C_6H_4), 7.59 (2H, d, *J = 8.2 Hz*, C_6H_4), 4.74 (2H, t, *J = 1.9 Hz*, C_5H_4), 4.44 (2H, t, *J = 1.9 Hz*, C_5H_4), 4.05 (5H, s, C_5H_5); ^{13}C NMR δ_C (75 MHz; solvent $CDCl_3$): 191.71 (CHO), 147.34 (*C*-CHO), 134.02 (Fc-C_6H_4), 129.98 (C_6H_4-CHO), 82.82 (C_5H_4), 70.18 (C_5H_4), 69.93 (C_5H_5) and 67.09 (C_5H_4); *m/z* (EI) 290 (M^+, 100%), 261 (5), 225 (2), 202 (3), 169 (2), 145 (9), 141 (8), 139 (5), 121 (23) and 115 (5).

7.2.21 4-Formyl-4'-biphenylferrocene[31]

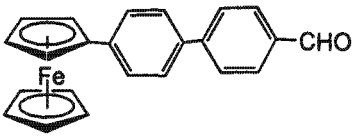

A mixture of 4-bromophenylferrocene (1.00 g, 2.93 mmol), formylbenzene boronic acid (0.88 g, 5.86 mmol), barium hydroxide (1.29 g, 4.10 mmol) and palladium(II) acetate (0.16 g, 0.733 mmol) in degassed ethanol (90 %, 200 ml) was initially stirred at room temperature under nitrogen, followed by vigorous shaking on an automatic shaker for at least 30 minutes. The reaction mixture was heated under reflux while stirring under nitrogen for 33.2 hours. The reaction mixture was filtered, the filtrate concentrated and the crude residue taken up in diethyl ether which was washed several times with distilled water. The organic fractions were combined, washed with water, dried over anhydrous sodium sulfate and the solvent removed *in vacuo*. The crude residue was subjected to column chromatography on silica gel and the product was eluted with dichloromethane-hexane (7:3). The product was obtained as an orange-red crystalline solid (0.45 g, 42%), mp 196-199 °C (lit.[31] 203-204 °C); (Found: C, 75.4 %, H, 5.0; M^+ 366.07002. $C_{23}H_{18}FeO$ requires C, 75.4 %, H, 5.0; M 366.07070). ν_{max} (KBr)/ cm^{-1} 3147, 3000, 2900, 2759, 1698, 1651, 1600, 1520, 1397, 1362, 1326, 1300, 1150, 1097, 1012, 1002, 817, 520 and 486;^1H NMR δ_H (300 MHz; solvent $CDCl_3$): 10.06 (1H, s, C*H*O), 7.96 (2H, d, *J = 8.4 Hz*, Fc-C_6H_4), 7.79 (2H, d, *J = 7.7 Hz*, C_6H_4-CHO), 7.58 (4H, s, C_6H_4), 4.70 (2H, t, *J = 1.8 Hz*, C_5H_4), 4.37 (2H, t, *J = 1.8 Hz*, C_5H_4), 4.07 (5H, s, C_5H_5); ^{13}C NMR δ_C (75 MHz; solvent $CDCl_3$): 191.92 (CHO), 146.93 (*C*-CHO), 140.16 (C_6H_4-CHO), 136.89 (C_6H_4-Fc), 135.00 (Fc-C_6H_4), 130.35 (C_6H_4-CHO), 127.28 (C_6H_4-CHO), 127.20 (Fc-C_6H_4-Ph), 126.61 (Fc-C_6H_4-Ph), 84.33 (C_5H_4), 69.72 (C_5H_5), 69.32 (C_5H_4) and 66.61 (C_5H_4); *m/z* (EI) 367 (36%), 366 (M^+, 100) and 364 (10).

7.2.22 N,N'-Ethylenebis((ferrocenylmethylidene)amine)[32]

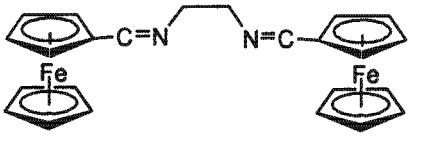

Anhydrous sodium sulfate (276.7 mg, 1.9 mmol) was added to a dark red solution of 4-formylferrocene (429.0 mg, 2.0 mmol) in diethyl ether (10 ml). A solution of ethylenediamine (0.15 g, 0.18ml, 2.5 mmol) in diethyl ether (5 ml) was added slowly to the

reaction mixture, which was further stirred at room temperature for 23 hours. The reaction mixture was filtered, the filtrate concentrated and cooled to 0 °C to precipitate the product. The product was collected as a yellow crystalline solid *via* vacuum filtration (0.61 g, 67%). ν_{max} (KBr)/ cm^{-1} 3072, 2893, 2830, 2322, 1843, 1761, 1717, 1699, 1695, 1668, 1639, 1616, 1575, 1538, 1505, 1471, 1435, 1247, 1104, 1013, 818, 668, 519, 487, 427, 416 and 403; ^1H NMR δ_H (400 MHz; solvent $CDCl_3$): 8.15 (2H, br s, N=CH), 4.61 (4H, t, C_5H_4), 4.32 (4H, t, C_5H_4), 4.14 (10H, s, C_5H_5), 3.75 (4H, s, CH_2); ^{13}C NMR δ_C (101 MHz; solvent $CDCl_3$): 162.38 (C=N), 70.43 (C_5H_4), 69.23 (C_5H_5), 68.58 (C_5H_4), 62.34 (CH_2).

7.2.23 N,N'-Ethylenebis((4-phenylferrocenylmethylidene)amine)

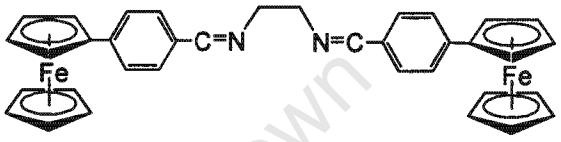

N,N'-Ethylenebis((4-phenylferrocenylmethylidene)amine) was prepared according to the procedure described for *7.1.22*. Anhydrous sodium sulfate (69.6 mg, 0.49 mmol) was added to a solution of 4-formylphenylferrocene (150.7 mg, 0.52 mmol) in diethyl ether (15 ml). A solution of ethylenediamine (40.0 mg, 44 µl, 0.65 mmol) in diethyl ether (5 ml) was added slowly to the reaction mixture, which was then further stirred at room temperature under a nitrogen atmosphere for 4 days. The reaction mixture was then filtered, the filtrate concentrated and cooled to 0 °C to precipitate the product. The product was then collected as an orange powder *via* vacuum filtration (76.3 mg, 23%), mp 212-215 °C; (Found: M^+ 604. $C_{36}H_{32}Fe_2N_2$ requires M^+ 604). ν_{max} (KBr)/ cm^{-1} 3418, 2322, 1644, 1616, 1606, 1575, 1505, 1423, 1362, 1279, 1104, 1017, 820, 667, 604, 594, 507, 458, 439 and 411; ^1H NMR δ_H (400 MHz; solvent $CDCl_3$): 8.28 (2H, s, N=CH), 7.62 (4H, dd, *J = 8.4 Hz*, C_6H_4), 7.48 (4H, dd, *J = 8.4 Hz*, C_6H_4), 4.67 (4H, t, *J = 2.0 Hz*, C_5H_4), 4.35 (4H, t, *J = 1.8 Hz*, C_5H_4), 4.03 (10H, s, C_5H_5), 3.97 (4H, s, CH_2); ^{13}C NMR δ_C (101 MHz; solvent $CDCl_3$): 162.21 (C=N), 128.10 (C_6H_4), 125.93 (C_6H_4), 69.63 (C_5H_5), 69.32 (C_5H_4), 66.58 (C_5H_4), 61.97 (CH_2); *m/z* (FAB) 604 (M^+, 25%), 594 (12), 399 (11), 290 (10), 261 (11), 245 (72), 223 (52), 179 (17), 136 (41) and 120 (18).

7.2.24 N,N'-Ethylenebis((4,4'-diphenylferrocenylmethylidene)amine)

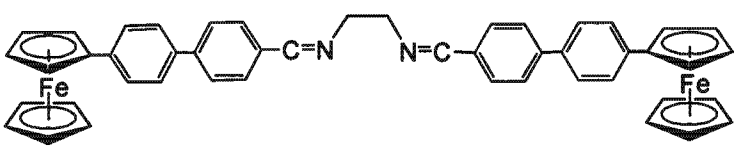

N,N'-Ethylenebis((4,4'-diphenylferrocenylmethylidene) amine) was prepared according to the procedure described for *7.1.22*. Anhydrous sodium sulfate (37.4 mg, 0.26 mmol) was added to a solution of 4-formylbiphenylferrocene (100.4 mg, 0.27 mmol) in diethyl ether (20 ml). A solution of

ethylenediamine (20.0 mg, 23 µl, 0.34 mmol) in diethyl ether (5 ml) was added slowly to the reaction mixture, which was further stirred at room temperature under a nitrogen atmosphere for 4 days. The reaction mixture was filtered, the filtrate concentrated and cooled to 0 °C to precipitate the product. The product was collected as an orange powder *via* vacuum filtration. It should be noted that complete characterisation of this compound proved difficult as it was found to be insoluble in a range of common organic solvents (30.6 mg, 15%), mp 220-222 °C dec.; (Found: M^+ 756. $C_{48}H_{40}Fe_2N_2$ requires M^+ 756). ν_{max} (KBr)/ cm^{-1} 3430, 2845, 2324, 1843, 1642, 1600, 1575, 1569, 1505, 1436, 1403, 1279, 1203, 1104, 1089, 1002, 889, 822, 667, 516, 482, 467, 415 and 404; *m/z* (FAB) 757 (M, 42%), 756 (M^+, 2), 559 (4), 375 (25), 304 (10), 277 (58), 265 (22), 241 (31), 203 (92), 149 (100) and 115 (40).

7.2.25 Ferrocenyldiphenylphosphine[33]

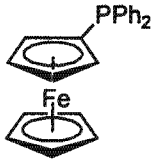

A suspension of ferrocene (1.90 g, 10.2 mmol) and aluminium chloride (1.36 g, 10.2 mmol) in *n*-heptane (20 ml) was heated initially to form a clear solution. A solution of chlorodiphenylphosphine (2.25 g, 1.85 ml, 10.2 mmol) in *n*-heptane (10 ml) was added slowly to the ferrocene solution at room temperature. The reaction mixture was heated under reflux for 20.5 hours. The suspension obtained was cooled to room temperature, the yellow-orange supernatant decanted and concentrated *in vacuo*. The black residue remaining from the reaction mixture was extracted several times with hot *n*-heptane and the extract added to the supernatant concentrate. The black residue was further washed with hot water, yielding an orange solid, which was extracted with hot toluene. Toluene was removed, all fractions combined and extracted with *n*-heptane at room temperature. Removal of *n*-heptane *in vacuo* yielded the product as an orange solid (1.43 g, 47%), mp 120-123 °C (lit.[33] 122-124 °C). ν_{max} (KBr)/ cm^{-1} 3076, 3042, 1476, 1432, 1410, 1325, 1315, 1192, 1182, 1160, 1106, 1019, 1005, 840, 834, 827, 819, 745, 698, 491, 451, 434, 416 and 404; ^{1}H NMR δ_H (300 MHz; solvent $CDCl_3$): 7.38-7.32 (10H, m, C_6H_5), 4.37 (2H, br s, C_5H_4), 4.16 (2H, br s, C_5H_4), 4.08 (5H, s, C_5H_5); ^{13}C NMR δ_C (75 MHz; solvent $CDCl_3$): 133.53 (C_6H_5), 131.72 (C_6H_5), 128.38 (C_6H_5), 128.08 (C_6H_5), 72.90 (C_5H_4), 70.67 (C_5H_4), 69.06 (C_5H_5)

7.3 Rhodium carbonyl complexes

7.3.1 Dichlorotetracarbonyldirhodium[34]

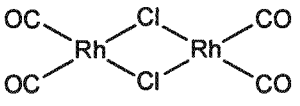

Carbon monoxide was bubbled through a solution of rhodium trichloride (2.00g, 7.59 mmol) in anhydrous ethanol (50 ml) while

heating under reflux for at least 5 hours. The solvent was then removed in vacuo and the residue sublimed. The product was obtained as bright red crystals (0.38 g, 26%), mp 123-125 °C (lit.[34] = 126-127 °C). ν_{max}/cm^{-1} (CH_2Cl_2): 2107m (CO), 2091s (CO), 2035s (CO) and 2003w(CO).

7.3.2 Bis(carbonyl)chloro(pyridine)rhodium[35]

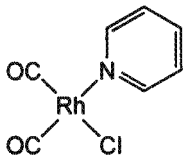

Pyridine (48.8 mg, 50.0 µl, 0.62 mmol) was added slowly to a solution of the rhodium dimer, dichlorotetracarbonyldirhodium (120.0 mg, 0.31 mmol) in pentane (10 ml). An orange suspension was observed to form on gradual addition of the pyridine. The product was collected *via* vacuum filtration as an orange powder (137.2 mg, 81%), mp 60-63 °C (lit.[35] 62-64 °C). ν_{max}/cm^{-1} (KBr): 2359 , 2340, 2253, 2091 (CO), 2016 (CO), 1794, 1653, 1606, 1471, 1381, 1219, 1096, 911, 762, 734, 648, 623 and 485; ^1H NMR δ_H (400 MHz; solvent $CDCl_3$): 8.73 (2H, dd, *J = 8.1 Hz*, C_5H_4N), 7.91 (1H, t, *J = 7.7 Hz*, C_5H_4N), 7.48 (2H, t, *J = 6.2 Hz*, C_5H_4N); ^{13}C NMR δ_C (101 MHz; solvent $CDCl_3$): 152.48 (C_5H_4N), 139.34 (C_5H_4N), and 125.56 (C_5H_4N).

7.3.3 Bis(carbonyl)chloro(4-aminopyridine)rhodium[36]

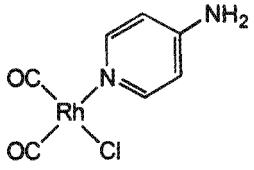

Bis(carbonyl)chloro(4-aminopyridine)rhodium was prepared according to the procedure described for *7.3.2.* 4-Aminopyridine (38.5 mg, 0.33 mmol) was added to a solution of dichlorotetracarbonyldirhodium (80.4 mg, 0.16 mmol) in dichloromethane (20 ml). The reaction mixture was stirred under nitrogen for 20 minutes and then concentrated *in vacuo*. Hexane was added to precipitate the product. The product was collected by vacuum filtration as a dark yellow powder (60.6 mg, 64%), mp 170-172 °C dec. ν_{max}/cm^{-1} (KBr): 3455, 3350, 3218, 2352, 2326, 2076 (CO), 2012 (CO), 1732, 1615, 1575, 1564, 1541, 1509, 1398, 1336, 1291, 1215, 1060, 1031, 820, 675, 653, 617, 500 and 483; ^1H NMR δ_H (solvent $CDCl_3$): 8.19 (2H, d, *J = 6.8 Hz*, C_5H_4N), 6.54 (2H, dd, *J = 6.9 Hz*, C_5H_4N), 4.65 (2H, br s, NH_2); ^{13}C NMR δ_C (75 MHz; solvent $CDCl_3$): 153.24 (C_5H_4N) and 120.65 (C_5H_4N).

7.3.4 Bis(carbonyl)chloro(4-phenylimine-4'-pyridine)rhodium

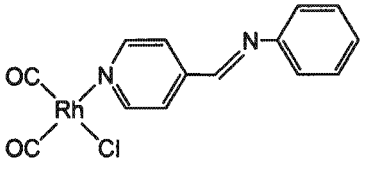

Bis(carbonyl)chloro(4-phenylimine-4'-pyridine)rhodium was prepared according to the procedure described for *7.3.2.* 4-Phenylimine-4'-pyridine (56.2 mg, 0.31 mmol) was added to a solution of dichlorotetracarbonyldirhodium ((60.7 mg, 0.15

mmol) in dichloromethane (10 ml). The reaction mixture was stirred under nitrogen for 20 minutes and then concentrated *in vacuo*. Pentane was added to precipitate the product. The product was collected by vacuum filtration as a yellow crystalline solid (74.0 mg, 63%). ν_{max}/cm^{-1} (KBr): 3040, 2088 (CO), 2013 (CO) and 1605 (C=N); ^1H NMR δ_H (300 MHz; solvent CD_3COCD_3): 8.96 (2H, dd, *J = 6.8 Hz*, C_5H_4N), 8.81 (1H, s, N=CH), 8.16 (2H, dd, *J = 6.8 Hz*, C_5H_4N), 7.51-7.44 (2H, tt, *J = 15.1 Hz*, C_6H_5), 7.41 (2H, d, *J = 1.5 Hz*, C_6H_5), 7.35 (1H, t, *J = 10.6 Hz*, C_6H_5); ^{13}C NMR δ_C (75 MHz; solvent $CDCl_3$): 158.42 (N=C), 154.78 (C_5H_4N), 130.93 (C_6H_5), 129.20 (C_5H_4N), 125.57 (C_6H_5) and 122.94 (C_6H_5).

7.3.5 Bis(carbonyl)chloro(4-pyridylimine-4'-phenylferrocene)rhodium

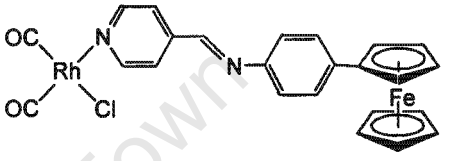

Bis(carbonyl)chloro(4-pyridylimine-4'-phenylferrocene)rhodium was prepared according to the procedure described for *7.3.2.* 4-Pyridylimine-4'-phenylferrocene (120.1 mg, 0.33 mmol) was added to a solution of dichlorotetracarbonyldirhodium (79.9 mg, 0.16 mmol) in dichloromethane (20 ml) and further stirred for 25 minutes. The reaction mixture was concentrated *in vacuo* and hexane was added to precipitate the product. The product was collected by vacuum filtration as small maroon-red rod-shaped crystals (56.0 mg, 61%), mp 165-175 °C; (Found: C, 51.2%, H, 3.1, N, 4.8; M^+ 560.0. $C_{24}H_{18}ClFeN_2O_2Rh$ requires C, 51.4%, H, 3.2, N, 5.0; M^+ 560). ν_{max}/cm^{-1} (KBr): 3054, 2359, 2080, 2003, 1684, 1643, 1589, 1427, 1326, 1280, 1106, 1014, 846, 823, 759, 740, 704, 491 and 414; ^1H NMR δ_H (300 MHz; solvent $CDCl_3$): 8.81 (2H, d, *J = 6.6 Hz*, C_5H_4N), 8.57 (1H, s, N=CH), 7.93 (2H, d, *J = 6.5 Hz*, C_5H_4N), 7.54 (2H, d, *J = 8.5 Hz*, C_6H_4), 7.27 (2H, d, *J = 8.3 Hz*, C_6H_4), 4.68 (2H, t, *J = 1.8 Hz*, C_5H_4), 4.36 (2H, t, *J = 1.8 Hz*, C_5H_4), 4.06 (5H, s, C_5H_5); ^{13}C NMR δ_C (75 MHz; solvent $CDCl_3$): 153.18 (N=C), 152.89 (C_5H_4N), 147.13 (C_6H_4), 145.97 (C_6H_4), 140.34 (C_5H_4N), 126.78 (C_5H_4N), 123.75 (C_6H_4), 121.65 (C_6H_4), 84.01 (C_5H_4), 69.71 (C_5H_5), 69.44 (C_5H_4) and 66.54 (C_5H_4); *m/z* (FAB) 560 (M^+, 8%), 525 (M-Cl, 5), 496 (M-CO, 2), 469 (M-CO, 2), 367 (M-Rh, 50), 366 (M-ligand, 90) and 287 (M-py, 10).

7.3.6 Bis(carbonyl)chloro(4-ferrocenylpyridine)rhodium

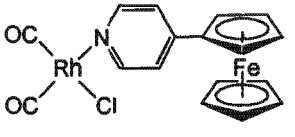

4-Ferrocenylpyridine (94.9 mg, 0.36 mmol) was added to a light yellow solution of dichlorotetracarbonyldirhodium (70.6 mg, 0.18 mmol) in anhydrous pentane (10 ml). A red suspension was observed almost immediately with the supernatant turning to a much lighter, almost clear colour. The product was isolated *via* vacuum filtration as red micro-crystals (113.8 mg, 69%),

mp 128-130 °C; (Found: C, 44.4%, H, 2.6, N, 3.0; M^+ 458.7. $C_{17}H_{13}ClFeNO_2Rh$ requires C, 44.6%, H, 2.7, N, 3.1; M 458.9). ν_{max}/cm^{-1} (KBr): 3020, 2086 (CO), 2011 (CO), 1615, 1522, 1435, 1382, 1107, 1034, 833 and 482; ^1H NMR δ_H (300 MHz; solvent $CDCl_3$): 8.49 (2H, dd, *J* = *6.7 Hz*, C_5H_4N), 7.39 (2H, dd, *J* = *6.7 Hz*, C_5H_4N), 4.76 (2H, t, C_5H_4), 4.56 (2H, t, C_5H_4), 4.08 (5H, s, C_5H_5); ^{13}C NMR δ_C (75 MHz; solvent $CDCl_3$): 151.65 (C_5H_4N), 121.66 (C_5H_4N), 71.68 (C_5H_4), 70.36 (C_5H_5) and 67.45 (C_5H_4); *m/z* (FAB) 459 (M^+, 8%), 424 (M-Cl, 8), 389 (4), 367 (M-2CO, 3), 312 (34), 265 (ligand, 100), 235 (1) and 200 (1).

7.4Rhodium cyclooctadiene complexes

7.4.1 Chloro(l,5-cyclooctadiene)rhodium(l) dimer[37]

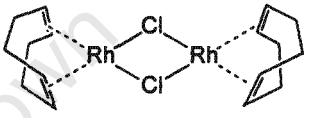

1,5-Cyclooctadiene (2.65 ml, 3.0 ml, 24.5 mmol) was added to a dark red solution of rhodium trichloride trihydrate (2.00 g, 7.6 mmol) in deoxygenated ethanol-water 5:1 (20 ml). The mixture was then heated under reflux overnight while stirring under nitrogen. A yellow suspension formed gradually over time. The reaction mixture was then filtered under vacuum and the precipitate washed with pentane followed by methanol. The product was obtained after recrystallisation as orange-yellow crystals (1.84 g, 49%), mp 142-144 °C dec. (lit.[37] 140-145 °C dec.). ν_{max} (KBr)/ cm^{-1} 3547, 2936, 2359, 1696, 1473, 960, 668, 487 and 449;^1H NMR δ_H (300 MHz; solvent $CDCl_3$): 4.23 (8H, br s, COD-CH), 2.53-2.47 (8H, m, COD-CH_2), 1.75 (8H, d, *J* = *8.3 Hz*, COD-CH_2).

7.4.2 Chloro(1,5-cyclooctadiene)(pyridine)rhodium[38]

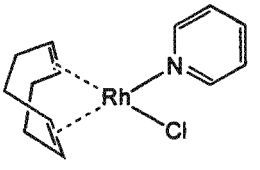

Pyridine (39.55 mg, 42 µl, 0.50 mmol) was added dropwise to an orange-yellow solution of chloro(l,5-cyclooctadiene)rhodium(l) dimer (123.6 mg, 0.25 mmol) in dichloromethane (15 ml). The reaction mixture was then stirred for a further 39 minutes at room temperature under nitrogen. The reaction mixture was then concentrated *in vacuo* and diethyl ether added to precipitate the product. The product was collected by vacuum filtration as bright yellow rod-like crystals (101.0 mg, 62%), mp 230-233 °C (lit.[38] 229-232 °C). ν_{max} (KBr)/ cm^{-1} 3567, 2933, 2359, 1696, 1599, 1484, 1212, 1068, 962, 695, 668, 494, 458 and 431; ^1H NMR δ_H (300 MHz; solvent $CDCl_3$): 8.76 (2H, d, *J* = *5.9 Hz*, C_5H_5N), 7.71 (1H, t, C_5H_5N), 7.32 (2H, t, C_5H_5N), 4.18 (4H,br s, COD-CH), 2.54-2.49 (4H, m, COD-CH_2), 1.85 (4H, d, *J* = *8.1 Hz*, COD-CH_2); ^{13}C NMR δ_C (75 MHz; solvent $CDCl_3$): 150.58 (C_5H_5N), 137.01 (C_5H_5N), 124.54 (C_5H_5N), 78.51 (COD) and 30.61 (COD).

7.4.3 (1,5-Cyclooctadiene)bis(pyridine)rhodium hexafluorophosphate[39]

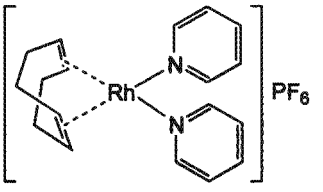

Pyridine (48.0 mg, 49.5 µl, 0.61 mmol) was added slowly to a solution of chloro(l,5-cyclooctadiene)rhodium(I) dimer (50.1 mg, 0.10 mmol) in ethanol (5 ml). After stirring the reaction mixture at room temperature for a further 15 minutes, a concentrated aqueous solution of ammonium hexafluorophosphate was added. A precipitate was observed to form and collected by vacuum filtration as yellow crystals (34.7 mg, 67%). ν_{max} (KBr)/ cm^{-1} 3568, 3004, 1696, 1602, 1445, 1430, 1216, 1068, 698, 668 and 458; ^1H NMR δ_H (300 MHz; solvent $CDCl_3$): 8.79 (4H, dd, *J = 6.1 Hz*, C_5H_5N), 7.70 (2H, t, C_5H_5N), 7.39 (4H, dd, C_5H_5N), 4.10 (4H,s, COD-CH), 2.62 (4H, br s, COD-CH_2), 1.95 (4H, d, *J = 8.1 Hz*, COD-CH_2); ^{13}C NMR δ_C (75 MHz; solvent $CDCl_3$): 150.39 (C_5H_5N), 138.32 (C_5H_5N), 126.01 (C_5H_5N), 85.00 (COD) and 30.55 (COD).

7.4.4 (1,5-Cyclooctadiene)bis(pyridine)rhodium perchlorate[39]

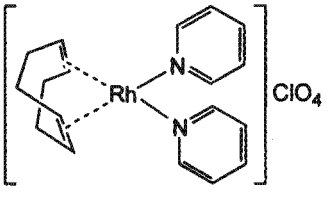

A white precipitate was observed to form immediately on addition of silver perchlorate (51.3 mg, 0.24 mmol) to a solution of chloro(l,5-cyclooctadiene)rhodium(I) dimer (60.0 mg, 0.12 mmol) in acetone (10 ml). Pyridine (38.5 mg, 40.0 µl, 0.49 mmol) was then added slowly to the supernatant, which was stirred at room temperature for a further 20 minutes. The reaction mixture was then concentrated and diethyl ether added to precipitate the product. The product was collected by vacuum filtration as small yellow crystals (49.1 mg, 87%), mp 193-195 °C (lit. 191-195 °C). ν_{max} (KBr)/ cm^{-1} 1692, 1605, 1445, 1430, 1215, 1080, 698, 664 and 457; ^1H NMR δ_H (300 MHz; solvent $CDCl_3$): 8.88 (4H, dd, *J = 6.1 Hz*, C_5H_5N), 7.71 (2H, t, C_5H_5N), 7.41 (4H, dd, C_5H_5N), 4.10 (4H,s, COD-CH), 2.66 (4H, m, COD-CH_2), 1.91 (4H, d, COD-CH_2); ^{13}C NMR δ_C (75 MHz; solvent $CDCl_3$): 150.39 (C_5H_5N), 138.32 (C_5H_5N), 126.01 (C_5H_5N), 84.80 (COD) and 30.56 (COD).

7.4.5 Chloro(1,5-cyclooctadiene)(4-phenylpyridine)rhodium

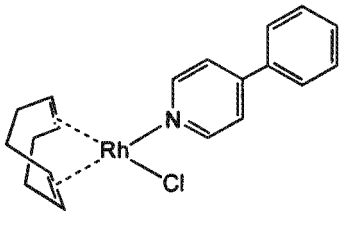

Chloro(1,5-cyclooctadiene)(4-phenylpyridine)rhodium was prepared according to the procedure followed for *7.4.2.* 4-Phenylpyridine (100.8 mg, 0.64 mmol) was added to a solution of chloro(l,5-cyclooctadiene)rhodium(I) dimer (159.0 mg, 0.32 mmol) in dichloromethane (10 ml). The reaction mixture was

stirred for a further 31 minutes. The reaction mixture was then concentrated *in vacuo* and diethyl ether added to precipitate the product. The product was collected *via* vacuum filtration as bright yellow crystals (206.7 mg, 80%); (Found: C, 56.73%, H, 5.15, N, 3.46; M^+ 401.04176. $C_{19}H_{21}ClNRh$ requires C, 56.8%, H, 5.3, N, 3.5; M^+ 401.74272). ν_{max}/cm^{-1} (KBr): 2990, 2931, 2880, 2825, 2367, 2324, 1772, 1674, 1607, 1541, 1471, 1429, 1413, 1333, 1215, 1068, 993, 961, 848, 765, 733, 690, 626, 565, 486 and 480; ^1H NMR δ_H (300 MHz; solvent $CDCl_3$): 8.75 (2H, dd, *J = 6.6 Hz*, C_5H_4N), 7.57 (2H, d, *J = 5.6 Hz*, C_5H_4N), 7.48 (5H, m, C_6H_5), 4.19 (4H, br s, COD-CH), 2.51 (4H, m, COD-CH_2), 1.84 (4H, d, *J = 8.0 Hz*, COD-CH_2);.^{13}C NMR δ_C (75 MHz; solvent $CDCl_3$): 151.03 (C_5H_5N), 149.63 (C_5H_5N), 136.59 (C_6H_5), 129.86 (C_6H_5), 129.29 (C_6H_5), 126.97 (C_6H_5), 122.46 (C_5H_5N), 80.05 (COD) and 30.88 (COD); *m/z* (FAB) 401 (M^+, 13%), 366 (M-Cl, 100), 346 (3), 310 (4), 258 (M-COD, 9), 211 (42), 181 (11), 156 (38), 136 (8), 103 (Rh, 5) and 77 (5).

7.4.6 (1,5-Cyclooctadiene)bis(4-phenylpyridine)rhodium perchlorate

(1,5-Cyclooctadiene)bis(4-phenylpyridine)rhodium perchlorate was prepared according to the procedure for *7.4.4*. A white precipitate was observed to form immediately on addition of silver perchlorate (66.8 mg, 0.32 mmol) to a solution of chloro(l,5-cyclooctadiene)rhodium(I) dimer (79.7 mg, 0.16 mmol) in acetone (20 ml). 4-phenylpyridine (100.1 mg, 0.64 mmol) was then added slowly to the supernatant, which was stirred at room temperature for a further 20 minutes. The reaction mixture was then concentrated and diethyl ether added to precipitate the product. The product was collected by vacuum filtration as a light yellow powder (117.2 mg, 59%); (Found: C, 57.85%, H, 4.92, N, 4.12; M^+ 521.2. $C_{30}H_{30}ClN_2O_4Rh$ requires C, 58.0%, H, 4.9, N, 4.5; M^+ 521.5). ν_{max}/cm^{-1} (KBr): 3056, 2872, 2818, 2370, 2324, 1616, 1575, 1544, 1516, 1483, 1418, 1398, 1221, 1095, 841, 766, 733, 696, 623, 565, 481 and 437; ^1H NMR δ_H (400 MHz; solvent $CDCl_3$): 8.88 (4H, d, *J = 5.9 Hz*, C_5H_4N), 7.62-7.53 (10H, m, C_6H_5), 7.46 (4H, d, *J = 5.8 Hz*, C_5H_4N), 4.14 (4H, br s, COD-CH), 2.69 (4H, m, COD-CH2), 1.99 (4H, d, *J = 10.3 Hz*, COD-CH_2); ^{13}C NMR δ_C (101 MHz; solvent CD_3COCD_3): 153.85 (C_5H_5N), 136.02 (C_5H_5N), 130.43 (C_5H_5N), 129.77 (C_6H_5), 129.58 (C_6H_5), 127.58 (C_6H_5), 127.28 (C_6H_5), 123.54 (C_5H_5N), 85.15 (COD), 30.54 (COD); *m/z* (FAB) 521 (M^+, 10%), 465 (3), 413 (M^+-COD, 11), 398 (6), 366 (90), 258 (29), 218 (7), 211 (37), 156 (100), 136 (17) and 89 (19).

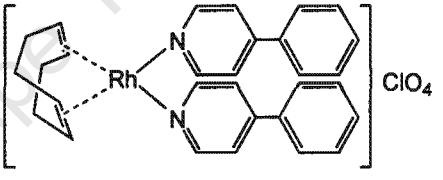

7.4.7 Chloro(1,5-cyclooctadiene)(4-phenylimine-4'-pyridine)rhodium

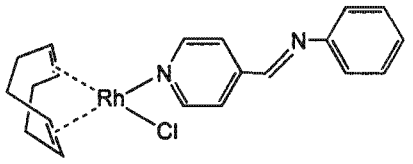

Chloro(1,5-cyclooctadiene)(4-phenylimine-4'-pyridine)rhodium was prepared according to the procedure followed for *7.4.2*. 4-Phenylimine-4'-pyridine (52.4 mg, .29 mmol) was added to a solution of chloro(l,5-cyclooctadiene)rhodium(I) dimer (70.6 mg, 0.14 mmol) in dichloromethane (10 ml). The reaction mixture was stirred for a further 28 minutes. The reaction mixture was then concentrated *in vacuo* and diethyl ether added to precipitate the product. The product was collected *via* vacuum filtration as fine yellow crystals (85.3 mg, 83%); (Found: C, 44.56%, H, 2.69, N, 7.26. $C_{20}H_{22}ClN_2Rh$ requires C, 44.6%, H, 2.7, N, 7.4). ν_{max} (KBr)/ cm^{-1} 3049, 2948, 2873, 2359, 1651, 1608, 1574, 1485, 1191, 1166, 1075, 1055, 961, 818, 668, 481, 459 and 406; ^1H NMR δ_H (300 MHz; solvent $CDCl_3$): 8.89 (2H, dd, C_5H_4N), 8.47 (1H, s, N=CH), 7.88 (2H, d, *J = 6.2 Hz*, C_5H_4N), 7.44 (2H, t, C_6H_5), 7.34 (2H, d, *J = 7.2 Hz*, C_6H_5), 7.26 (1H, t, C_6H_5), 4.21 (4H, br s, COD-CH), 2.54-2.48 (4H, m, COD-CH_2), 1.82 (4H, d, *J = 8.3 Hz*, COD-CH_2); ^{13}C NMR δ_C (75 MHz; solvent $CDCl_3$): 156.85 (N=C), 154.28 (C_5H_4N), 151.89 (C_5H_4N), 144.51 (C_6H_5), 129.38 (C_5H_4N), 127.65 (C_6H_5), 124.24 (C_6H_5) and 122.06 (C_6H_5), 85.42 (COD) and 30.55 (COD).

7.4.8 (1,5-Cyclooctadiene)bis(4-phenylimine-4'-pyridine)rhodium perchlorate

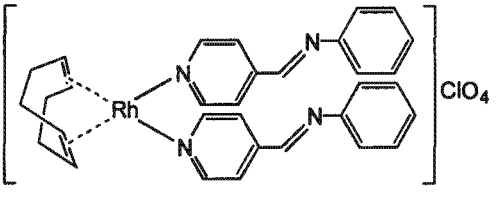

(1,5-Cyclooctadiene)bis(4-phenylimine-4'-pyridine)rhodium perchlorate was prepared according to the procedure for *7.4.4*. A white precipitate was observed to form immediately on addition of silver perchlorate (58.9 mg, 0.28 mmol) to a solution of chloro(l,5-cyclooctadiene)rhodium(I) dimer (70.6 mg, 0.14 mmol) in acetone (15 ml). 4-Phenylimine-4'-pyridine (103.5 mg, 0.57 mmol) was then added slowly to the supernatant, which was stirred at room temperature for a further 20 minutes. The reaction mixture was then concentrated and diethyl ether added to precipitate the product. The product was collected by vacuum filtration as a yellow powder (110.9 mg, 59%), mp = 199 °C dec.; (Found: C, 55.98%, H, 4.63, N, 8.06; M^+ 5751682. $C_{32}H_{32}ClN_4O_4Rh$ requires C, 56.5%, H, 4.8, N, 8.3; M^+ 575.53486). ν_{max} (KBr)/ cm^{-1} 3583, 2339, 1770, 1738, 1622, 1610, 1109, 1086, 833, 552 and 445; ^1H NMR δ_H (300 MHz; solvent $CDCl_3$): 9.01 (4H, d, *J = 5.6 Hz*, C_5H_4N), 8.39 (2H, s, N=CH), 7.86 (4H, d, *J = 5.5 Hz*, C_5H_4N), 7.40 (4H, t, *J = 7.3 Hz*, C_6H_5), 7.28 (2H, t, *J = 7.3 Hz*, C_6H_5), 7.19 (4H, d, *J = 8.0 Hz*, C_6H_5), 4.15 (4H, br s, COD-CH), 2.71 (4H, m, COD-CH_2), 2.00 (4H, d, *J = 8.8 Hz*, COD-CH_2); ^{13}C NMR δ_C (75 MHz; solvent $CDCl_3$):

158.21 (N=C), 151.12 (C_5H_4N), 150.89 (C_5H_4N), 143.15 (C_6H_5), 129.35 (C_5H_4N), 127.74 (C_6H_5), 124.24 (C_6H_5) and 121.06 (C_6H_5), 85.42 (COD) and 30.55 (COD); *m/z* (FAB) 575.2 (M^+, 10%), 546 (4), 532 (2), 492 (2), 471 (4), 439 (4), 409 (5), 393 (100), 364 (4), 350 (8), 284 (8), 211 (47), 183 (37), 136 (12), 89 (17) and 80 (17).

7.4.9 Chloro(1,5-cyclooctadiene)(4-pyridylimine-4'-phenylferrocene)rhodium

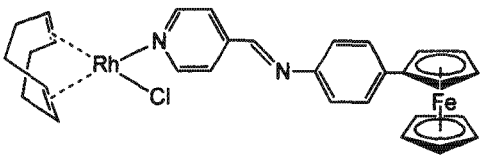

Chloro(1,5-cyclooctadiene(4-pyridylimine-4'-phenylferrocene)rhodium was prepared according to the procedure followed for *7.4.2.* 4-Pyridylimine-4'-phenylferrocene (109.0 mg, 0.29 mmol) was added to a solution of chloro(l,5-cyclooctadiene)rhodium(I) dimer (73.4 mg, 0.15 mmol) in dichloromethane (10 ml). The reaction mixture was stirred for a further 34 minutes. The reaction mixture was then concentrated *in vacuo* and hexane added to precipitate the product. The product was collected *via* vacuum filtration as red crystalline flakes (134.1 mg, 75%), mp 200-202 °C; (Found: C, 58.29%, H, 4.59, N, 4.40; M^+ 612.05019. $C_{30}H_{30}ClFeN_2Rh$ requires C, 58.8%, H, 4.9, N, 4.6; M^+ 612.79361). ν_{max}/cm^{-1} (KBr): 3056, 2954, 2879, 2356, 2329, 2295, 1745, 1731, 1684, 1616, 1609, 1575, 1541, 1514, 1480, 1426, 1392, 1371, 1106, 1004, 977, 950, 841, 814, 807, 672, 638, 543, 495, 481 and 434;^{1}H NMR δ_H (solvent $CDCl_3$): 8.84 (2H, d, *J = 5.9 Hz*, C_5H_4N), 8.48 (1H, s, N=CH), 7.77 (2H, dd, *J = 5.9 Hz*, C_5H_4N), 7.51 (2H, dd, *J = 6.7 Hz*, C_6H_4), 7.22 (2H, d, *J = 8.5 Hz*, C_6H_4), 4.66 (2H, t, *J = 1.8 Hz*, C_5H_4), 4.35 (2H, t, *J = 1.8 Hz*, C_5H_4), 4.19 (4H, br s, COD-CH), 4.03 (5H, s, C_5H_5), 2.52-2.48 (4H, m, COD-CH_2), 1.85 (4H, d, *J = 8.6 Hz*, COD-CH_2); ^{13}C NMR δ_C (solvent $CDCl_3$): 156.02 (N=C), 151.10 (C_5H_4N), 126.83 (C_5H_4N), 124.13 (C_6H_4), 121.55 (C_6H_4), 69.75 (C_5H_5), 69.40 (C_5H_4), 66.58 (C_5H_4), 30.62 (COD); *m/z* (FAB) 612 (M^+, 1%), 532 (2), 519 (3), 382 (5), 366 (Ligand, 100), 305 (26), 289 (41), 277 (41), 229 (9), 176 (27) and 89 (22).

7.4.10 (1,5-Cyclooctadiene)bis(4-pyridylimine-4'-phenylferrocene)rhodium perchlorate

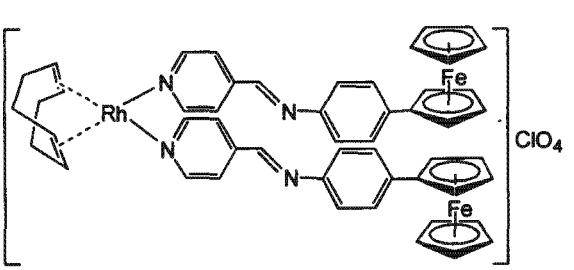

(1,5-Cyclooctadiene)bis(4-pyridylimine-4'-phenylferrocene)rhodium perchlorate was prepared according to the procedure for *7.4.4.* A white precipitate was observed to form immediately on addition of silver perchlorate (22.6 mg, 0.11 mmol) to a solution of chloro(l,5-cyclooctadiene)rhodium(I) dimer (26.9 mg, 0.05 mmol) in acetone (10 ml). 4-

Pyridylimine-4'-phenylferrocene (80.0 mg, 0.22 mmol) was then added slowly to the supernatant, which was stirred at room temperature for a further 30 minutes. The reaction mixture was then concentrated and diethyl ether added to precipitate the product. The product was collected by vacuum filtration as a fine dark maroon-red powder (92.8 mg, 81%), mp 265-268 °C dec.; (Found: C, 65.97%, H, 5.12, N, 5.78; M^+ 943.2. $C_{52}H_{48}Fe_2N_4RhClO_4$ requires C, 66.2%, H, 5.1, N, 5.9; M^+ 943.2). ν_{max}/cm^{-1} (KBr): 3076, 3063, 2363, 2322, 2295, 1738, 1684, 1616, 1575, 1541, 1514, 1487, 1432, 1398, 1120, 1100, 1086, 1065, 998, 963, 889, 841, 821, 760, 726, 678, 617, 549, 501, 481 and 434;^{1}H NMR δ_H (400 MHz; solvent $CDCl_3$): 8.99 (4H, br s, C_5H_4N), 8.47 (2H, s, N=CH), 7.87 (4H, d, *J = 4.4 Hz*, C_5H_4N), 7.49 (4H, d, *J = 8.4 Hz*, C_6H_4), 7.19 (4H, d, *J = 8.1 Hz*, C_6H_4), 4.67 (4H, br s, C_5H_4), 4.36 (4H, br s, C_5H_4), 4.16 (4H, br s, COD-CH), 4.05 (10H, s, C_5H_5), 2.81-2.66 (4H, m, COD-CH_2), 2.02 (4H, d, *J = 8.8 Hz*, COD-CH_2); ^{13}C NMR δ_C (101 MHz; solvent $CDCl_3$): 153.95 (N=C), 129.84 (C_5H_4N), 126.94 (C_5H_4N), 124.25 (C_6H_4), 121.66 (C_6H_4), 80.24 (COD), 69.95 (C_5H_5), 69.58 (C_5H_4), 66.75 (C_5H_4), 30.71 (COD); *m/z* (FAB) 943 (M^+, 4%), 577 (M-ligand, 93), 366 (ligand, 100).

7.4.11 Chloro(1,5-cyclooctadiene)(4-ferrocenylpyridine)rhodium

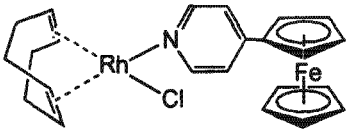

Chloro(1,5-cyclooctadiene(4-ferrocenylpyridine)rhodium was prepared according to the procedure followed for *7.4.2.* 4-Ferrocenylpyridine (74.6 mg, 0.28 mmol) was added to a solution of chloro(I,5-cyclooctadiene)rhodium(I) dimer (69.8 mg, 0.14 mmol) in dichloromethane (10 ml). The reaction mixture was stirred for a further 15 minutes. The reaction mixture was then concentrated *in vacuo* and pentane added to precipitate the product. The product was collected *via* vacuum filtration as an orange solid (111.7 mg, 78%), mp 167-169 °C; (Found: C, 54.2%, H, 4.6, N, 2.7; M^+ 509.0. $C_{23}H_{25}ClFeNRh$ requires C, 54.2%, H, 4.0, N, 2.7; M^+ 509.0). ν_{max}/cm^{-1} (KBr): 3069, 2872, 2832, 2358, 2331, 1739, 1670, 1615, 1568, 1544, 1516, 1475, 1436, 1398, 1338, 1286, 1106, 1031, 963, 825, 809, 674 and 503;^{1}H NMR δ_H (300 MHz; solvent $CDCl_3$): 8.51 (2H, dd, *J = 6.7 Hz*, C_5H_4N), 7.27 (2H, dd, *J = 7.3 Hz*, C_5H_4N), 4.69 (2H, t, C_5H_4), 4.47 (2H, t, C_5H_4), 4.19 (4H, br s, COD-CH), 4.04 (5H, s, C_5H_5), 2.53-2.49 (4H, m, COD-CH_2), 1.84 (4H, d, *J = 8.1 Hz*, COD-CH_2); ^{13}C NMR δ_C (75 MHz; solvent $CDCl_3$): 150.28 (C_5H_4N), 121.19 (C_5H_4N), 79.28 (COD-CH), 70.98 (C_5H_4), 70.14 (C_5H_5), 67.15 (C_5H_4) and 30.90 (COD-CH_2); *m/z* (FAB) 509 (M+, 3%), 312 (32), 265 (58), 167 (17) and 89 (44).

7.4.12 [(1,5-Cyclooctadiene)bis(4-ferrocenylpyridine)rhodium perchlorate

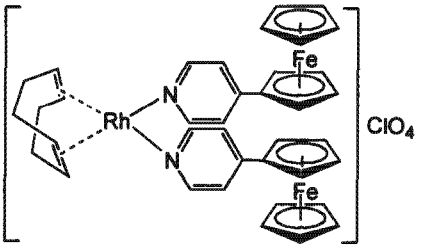

(1,5-Cyclooctadiene)bis(4-ferrocenylpyridine)rhodium perchlorate was prepared according to the procedure for *7.4.4.* A white precipitate was observed to form immediately on addition of silver perchlorate (43.8 mg, 0.20 mmol) to a solution of chloro(l,5-cyclooctadiene)rhodium(I) dimer (50.4 mg, 0.10 mmol) in acetone (15 ml). 4-Ferrocenylpyridine (106.1 mg, 0.40 mmol) was then added slowly to the supernatant, which was stirred at room temperature for a further 21 minutes. The reaction mixture was then concentrated and diethyl ether added to precipitate the product. The product was collected by vacuum filtration as small red-brown crystalline flakes (162.2 mg, 96 %), mp 225 °C dec.; (Found: C, 54.2%, H, 4.6, N, 3.1; M^+ 737.1. $C_{38}H_{38}Fe_2N_2RhClO_4$ requires C, 54.5%, H, 4.6, N, 3.3; M^+ 737.0). ν_{max}/cm^{-1} (KBr): 3069, 2349, 2322, 1684, 1616, 1608, 1575, 1544, 1516, 1429, 1397, 1340, 1217, 1122, 832, 686, 677, 622, 538, 481, 472 and 418;^{1}H NMR δ_H (300 MHz; solvent $CDCl_3$): 8.60 (4H, d, *J = 6.2 Hz*, C_5H_4N), 7.36 (4H, d, *J = 6.4 Hz*, C_5H_4N), 4.68 (4H, br s, C_5H_4), 4.45 (4H, br s, C_5H_4), 4.12 (4H, br s, COD-CH), 3.98 (10H, s, C_5H_5), 2.75-2.68 (4H, m, COD-CH_2) and 1.98 (4H, d, *J = 8.8 Hz*, COD-CH_2); ^{13}C NMR δ_C (75 MHz; solvent $CDCl_3$): 151.78 (C_5H_4N), 122.55 (C_5H_4N), 77.82 (COD-CH), 70.52 (C_5H_5), 70.04 (C_5H_4), 67.36 (C_5H_4) and 30.62 (COD-CH_2); *m/z* (FAB) 737 (M^+, 10%), 476 (30), 312 (19), 265 (97), 155 (67), 137 (56) and 89 (20).

7.4.13 Chloro(1,5-cyclooctadiene)(3-ferrocenylpyridine)rhodium

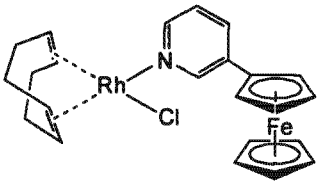

Chloro(1,5-cyclooctadiene(3-ferrocenylpyridine)rhodium was prepared according to the procedure followed for *7.4.2.* 3-Ferrocenylpyridine (78.3 mg, 0.30 mmol) was added to a solution of chloro(l,5-cyclooctadiene)rhodium(I) dimer (73.4 mg, 0.15 mmol) in dichloromethane (15 ml). The reaction mixture was stirred for a further 35 minutes. The reaction mixture was then concentrated *in vacuo* and pentane added to precipitate the product. The product was collected *via* vacuum filtration as golden yellow microcrystals (134.5 mg, 88%), mp 162-164 °C; (Found: C, 54.20%, H, 4.76, N, 2.68; M^+ 509.00799. $C_{23}H_{25}ClFeNRh$ requires C, 54.2%, H, 4.9, N, 2.7; M^+ 509.65806). ν_{max} (KBr)/ cm^{-1} 3616, 3584, 2830, 2349, 1798, 1703, 1634, 1615, 1422, 1105, 814, 667, 439 and 408; ^{1}H NMR δ_H (400 MHz; solvent $CDCl_3$): 8.80 (1H, br s, C_5H_4N), 8.52 (1H, dd, *J = 6.6 Hz*, C_5H_4N), 7.70 (1H, dt, *J = 8.1 Hz*, C_5H_4N), 7.18 (1H, dd, *J = 5.5 Hz*, C_5H_4N), 4.66 (2H, t, *J = 1.8 Hz*, C_5H_4), 4.40 (2H, t, *J = 1.8 Hz*, C_5H_4), 4.22 (4H, br s, COD-CH), 4.08 (5H, s, C_5H_5), 2.51 (4H, m, COD-

CH_2), 1.85 (4H, d, *J = 8.0 Hz*, COD-CH_2); ^{13}C NMR δ_C (101 MHz; solvent $CDCl_3$): 148.41 (C_5H_4N), 147.52 (C_5H_4N), 133.89 (C_5H_4N), 124.01 (C_5H_4N), 80.00 (COD), 69.91 (C_5H_4), 69.81 (C_5H_5), 66.70 (C_5H_4), 30.82 (COD); *m/z* (FAB) 509 (M^+, 3%), 474 (M-Cl, 41), 365 (M-COD, 4), 350 (6), 310 (18), 263 (ligand, 100), 211 (M-ligand, 18), 154 (6) and 136 (6).

7.4.14 Chloro(1,5-cyclooctadiene)(2-ferrocenylpyridine)rhodium

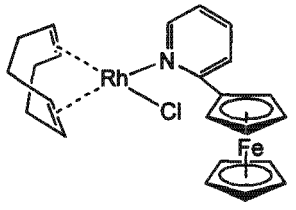

Chloro(1,5-cyclooctadiene(2-ferrocenylpyridine)rhodium was prepared according to the procedure followed for *7.4.2.* 2-Ferrocenylpyridine (45.0 mg, 0.17 mmol) was added to a solution of chloro(I,5-cyclooctadiene)rhodium(I) dimer (42.2 mg, 0.08 mmol) in dichloromethane (10 ml). The reaction mixture was stirred for a further 25 minutes. The reaction mixture was then concentrated *in vacuo* and pentane added to precipitate the product. The product was collected *via* vacuum filtration as an orange-brown powder (26.6 mg, 31%), mp 123-125 °C; (Found: C, 54.48%, H, 4.72, N, 2.48; M^+ 509. $C_{23}H_{25}ClFeNRh$ requires C, 54.2%, H, 4.9, N, 2.7; M^+ 509). ν_{max} (KBr)/ cm^{-1} 3616, 3584, 2830, 2349, 1798, 1703, 1634, 1615, 1598, 1495, 1422, 1386, 1105, 817, 457 and 408; ^1H NMR δ_H (400 MHz; solvent $CDCl_3$): 8.50 (1H, d, *J = 4.8 Hz*, C_5H_4N), 7.57 (1H, t, *J = 7.7 Hz*, C_5H_4N), 7.41 (1H, d, *J = 8.1 Hz*, C_5H_4N), 7.06 (1H, t, *J = 4.8 Hz*, C_5H_4N), 4.92 (2H, t, *J = 1.8 Hz*, C_5H_4), 4.39 (2H, t, *J = 1.8 Hz*, C_5H_4), 4.23 (4H, s, COD-CH), 4.05 (5H, s, C_5H_5), 2.49 (4H, m, COD-CH_2), 1.74 (4H, d, *J = 8.4 Hz*, COD-CH_2); ^{13}C NMR δ_C (101 MHz; solvent $CDCl_3$): 149.25 (C_5H_4N), 145.18 (C_5H_4N), 136.51 (C_5H_4N), 120.36 (C_5H_4N), 120.04 (C_5H_4N), 78.66 (COD), 69.78 (C_5H_4), 68.48 (C_5H_5), 67.16 (C_5H_4), 30.79 (COD); *m/z* (FAB) 510 (M, 9%), 509 (M^+, 1), 473 (M^+-Cl), 365 (M-COD, 13), 303 (7), 263 (2-Fcpy, 2), 185 (100) and 115 (20).

7.4.15 Chloro(1,5-cyclooctadiene)(4-ferrocenylphenyl-4'-pyridine)rhodium

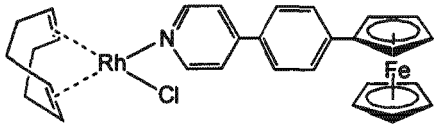

Chloro(1,5-cyclooctadiene(4-ferrocenylphenyl-4'-pyridine)rhodium was prepared according to the procedure followed for *7.4.2.* 4-Ferrocenylphenyl-4'-pyridine (50.0 mg, 0.15 mmol) was added to a solution of chloro(I,5-cyclooctadiene)rhodium(I) dimer (36.3 mg, 0.07 mmol) in dichloromethane (7 ml). The reaction mixture was stirred for a further 20 minutes. The reaction mixture was then concentrated *in vacuo* and diethyl ether added to precipitate the product. The product was collected *via* vacuum filtration as a dark red powder (59.9 mg, 70%), mp 213 °C dec.; (Found: C, 59.62%, H, 5.12, N, 2.48; M^+ 585. $C_{29}H_{29}ClFeNRh$ requires C, 59.4%, H, 5.0, N, 2.4; M^+ 585). ν_{max}/cm^{-1} (KBr): 3069, 2356, 2322, 2295, 1682, 1616, 1593, 1569, 1544, 1516, 1489,

1432, 1398, 1338, 1283, 1222, 1106, 1079, 1032, 998, 964, 814, 719, 698, 644, 597, 502, 475 and 441;^{1}H NMR δ_H (300 MHz; solvent $CDCl_3$): 8.72 (2H, dd, *J = 6.6 Hz*, C_5H_4N), 7.59-7.50 (6H, m, C_6H_4 and C_5H_4N), 4.68 (2H, t, *J = 1.8 Hz*, C_5H_4), 4.37 (2H, t, *J = 1.8 Hz*, C_5H_4), 4.18 (4H, br s, COD-CH), 4.05 (5H, s, C_5H_5), 2.54-2.49 (4H, m, COD-CH_2), 1.84 (4H, d, *J = 7.9 Hz*, COD-CH_2); ^{13}C NMR δ_C (75 MHz; solvent $CDCl_3$): 150.97 (C_5H_4N), 149.25 (C_5H_4N), 142.02 (C_6H_4), 133.56 (C_6H_4), 126.92 (C_6H_4), 126.73 (C_6H_4), 121.89 (C_5H_4N), 83.65 (COD-CH), 69.73 (C_5H_5), 69.55 (C_5H4_5), 66.66 (C_5H_4) and 30.90 (COD-CH_2); *m/z* (FAB) 585 (M^+, 1%), 574 (23), 387 (4-Fc(C_6H_4)py, 3), 339 (3), 273 (2), 241 (24), 185 (100) and 115 (10).

7.4.16 (1,5-Cyclooctadiene)bis(4-ferrocenylphenyl-4'-pyridine)rhodium perchlorate

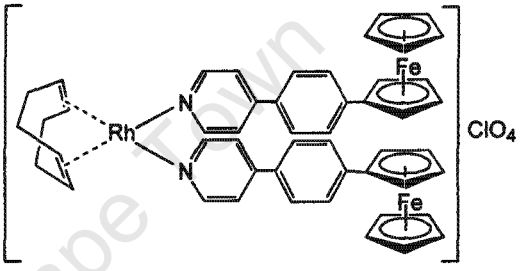

(1,5-Cyclooctadiene)bis(4-ferrocenylphenyl-4'-pyridine)rhodium perchlorate was prepared according to the procedure for *7.4.4.* A white precipitate was observed to form immediately on addition of silver perchlorate (42.0 mg, 0.20 mmol) to a solution of chloro(l,5-cyclooctadiene)rhodium(I) dimer (50.0 mg, 0.10 mmol) in acetone (15 ml). 4-Ferrocenylphenyl-4'-pyridine (106.1 mg, 0.40 mmol) was then added slowly to the supernatant, which was stirred at room temperature for a further 46 minutes. The reaction mixture was then concentrated and diethyl ether added to precipitate the product. The product was collected by vacuum filtration as small dark red crystals (164.6 mg, 83%) mp 110-112 °C; (Found: C, 60.32%, H, 4.72, N, 2.59; M^+ 988. $C_{50}H_{46}ClFe_2N_2O_4Rh$ requires C, 60.7%, H, 4.7, N, 2.8; M^+ 988). ν_{max}/cm^{-1} (KBr): 3069, 2879, 2832, 2356, 2322, 2023, 1772, 1616, 1602, 1589, 1541, 1487, 1432, 1405, 1283, 1215, 1120, 1100, 1004, 889, 814, 760, 726, 624, 509, 481, 475 and 447;^{1}H NMR δ_H (300 MHz; solvent $CDCl_3$): 8.85 (4H, d, *J = 5.0 Hz*, C_5H_4N), 7.87-7.34 (12H, m, C_6H_4 and C_5H_4N), 4.80 (4H, br s, C_5H_4), 4.50 (4H, br s, C_5H_4), 4.31 (4H, br s, COD-CH), 4.14 (10H, s, C_5H_5), 2.89-2.56 (4H, m, COD-CH_2), 2.00 (4H, d, *J = 8.4 Hz*, COD-CH_2); ^{13}C NMR δ_C (75 MHz; solvent $CDCl_3$): 150.50 (C_5H_4N), 142.47 (C_5H_4N), 126.87 (C_6H_4), 126.68 (C_6H_4), 122.88 (C_5H_4N), 84.89 (COD-CH), 70.83 (C_5H_5), 70.56 (C_5H4_5), 67.40 (C_5H_4) and 30.62 (COD-CH_2); *m/z* (FAB) 988 (M^+, 10%), 851 (3), 639 (7), 559 (11), 474 (9), 375 (58), 338 (4-Fc(C_6H_4)py, 7), 277 (100), 258 (20), 186 (100) and 115 (33).

7.4.17 Chloro(1,5-cyclooctadiene)(4-ferrocenylphenyl-3'-pyridine)rhodium

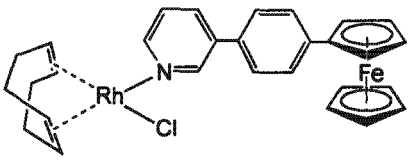

Chloro(1,5-cyclooctadiene(4-ferrocenylphenyl-3'-pyridine)rhodium was prepared according to the procedure followed for *7.4.2.* 4-Ferrocenylphenyl-3'-pyridine (70.0 mg, 0.21 mmol) was added to a solution of chloro(I,5-cyclooctadiene)rhodium(I) dimer (50.9 mg, 0.10 mmol) in dichloromethane (10 ml). The reaction mixture was stirred for a further 31 minutes. The reaction mixture was then concentrated *in vacuo* and diethyl ether added to precipitate the product. The product was collected *via* vacuum filtration as an orange-mustard powder (84.6 mg, 69%), mp 215-217 °C; (Found: C, 59.59%, H, 5.00, N, 2.32; M^+ 585.0. $C_{29}H_{29}ClFeNRh$ requires C, 59.5%, H, 5.0, N, 2.4; M^+ 585). ν_{max} (KBr)/ cm^{-1} 3689, 3671, 2832, 1612, 1395, 1104, 803, 700, 531, 442, 430, 406 and 404; ^1H NMR δ_H (400 MHz; solvent $CDCl_3$): 8.98 (1H, br s, C_5H_4N), 8.68 (1H, dd, *J = 6.6 Hz*, C_5H_4N), 7.88 (1H, dt, *J = 7.3 Hz*, C_5H_4N), 7.58 (2H, d, *J = 8.4 Hz*, C_6H_4), 7.49 (2H, d, *J = 8.4 Hz*, C_6H_4), 7.37 (1H, dd, *J = 5.9 Hz*, C_5H_4N), 4.69 (2H, t, *J = 1.8 Hz*, C_5H_4), 4.37 (2H, t, *J = 1.8 Hz*, C_5H_4), 4.22 (4H, br s, COD-CH) 4.07 (5H, s, C_5H_5), 2.52 (4H, m, COD-CH_2), 1.86 (4H, d, *J = 8.1 Hz*, COD-CH_2); ^{13}C NMR δ_C (101 MHz; solvent $CDCl_3$): 147.45 (C_5H_4N), 147.26 (C_5H_4N), 133.25 (C_5H_4N), 125.50 (C_6H_4), 125.15 (C_6H_4), 122.77 (C_5H_4N), 82.26 (COD), 68.11 (C_5H_5), 67.74 (C_5H_4), 65.00 (C_5H_4) and 29.25 (COD); *m/z* (FAB) 585 (M^+, 1%), 550 (M-Cl, 28), 386 (21), 339 (3-Fc(C_6H_4)py, 100), 274 (6), 238 (50) and 211 (17).

7.4.18 Chloro(1,5-cyclooctadiene)(4-ferrocenylphenyl-2'-pyridine)rhodium

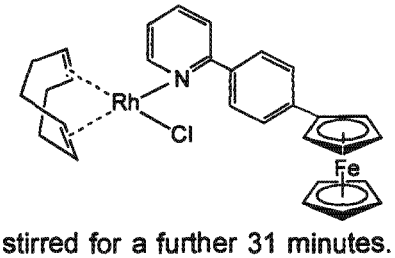

Chloro(1,5-cyclooctadiene(4-ferrocenylphenyl-2'-pyridine)rhodium was prepared according to the procedure followed for *7.4.2.* 4-Ferrocenylphenyl-2'-pyridine (60.0 mg, 0.18 mmol) was added to a solution of chloro(I,5-cyclooctadiene)rhodium(I) dimer 43.6 mg, 0.09 mmol) in dichloromethane (10 ml). The reaction mixture was stirred for a further 31 minutes. The reaction mixture was then concentrated *in vacuo* and diethyl ether added to precipitate the product. The product was collected *via* vacuum filtration as an orange powder (42.6 mg, 40%), mp 90-92 °C; (Found: C, 59.42%, H, 5.12, N, 2.32; M^+ 585. $C_{29}H_{29}ClFeNRh$ requires C, 59.5%, H, 5.0, N, 2.4; M^+ 585). ν_{max} (KBr)/ cm^{-1} 3629, 3568, 2323, 1740, 1700, 1646, 1336, 1607, 1474, 783, 500 and 409; ^1H NMR δ_H (400 MHz; solvent $CDCl_3$): 8.69 (1H, dd, *J = 4.8 Hz*, C_5H_4N), 7.93 (2H, dd, *J = 8.4 Hz*, C_6H_4), 7.74 (2H, dd, *J = 6.2 Hz*, C_5H_4N), 7.57 (2H, dd, *J = 8.8 Hz*, C_6H_4), 7.21 (1H, dd, *J = 6.6 Hz*, C_5H_4N), 4.74 (2H, t, *J = 1.8 Hz*, C_5H_4), 4.23 (2H, t, *J = 2.2 Hz*, C_5H_4), 4.11 (4H, s, COD-CH), 4.05 (5H, s, C_5H_5), 2.51 (4H, m, COD-CH_2), 1.84 (4H,

d, *J = 8.2 Hz*, COD-CH_2); ^{13}C NMR δ_C (101 MHz; solvent $CDCl_3$): 149.60 (C_5H_4N), 136.58 (C_5H_4N), 126.25 (C_6H_4), 126.77 (C_6H_4), 121.70 (C_5H_4N), 120.05 (C_5H_4N), 78.67 (COD), 69.63 (C_5H_5), 69.12 (C_5H_4), 66.49 (C_5H_4), 30.79 (COD); *m/z* (FAB) 585 (M^+, 1%), 548 (M-Cl, 3), 388 (2-Fc(C_6H_4)py, 60), 340 (60), 274 (10), 238 (3) and 115 (10).

7.4.19 (1,1'-Bis(2-pyridyl)ferrocene)(1,5-cyclooctadiene)rhodium perchlorate[40]

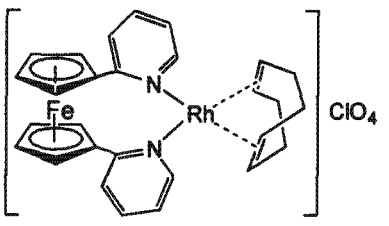

(1,1'-Bis(2-pyridyl)ferrocene)(1,5-cyclooctadiene)rhodium perchlorate was prepared according to the procedure for *7.4.4.* A white precipitate was observed to form immediately on addition of silver perchlorate (48.7 mg, 0.24 mmol) to a solution of chloro(l,5-cyclooctadiene)rhodium(I) dimer (58.0 mg, 0.12 mmol) in acetone (15 ml). 1,1'-Bis(2-pyridyl)ferrocene (80.0 mg, 0.24 mmol) was added to the supernatant, which was stirred at room temperature for a further 35 minutes. The reaction mixture was then concentrated and pentane added to precipitate the product. The product was collected by vacuum filtration as small dark red crystals (92.6 mg, 70%), mp 148-150 °C; (Found: C, 59.62%, H, 4.89, N, 2.21; M^+ 551.06569. $C_{28}H_{28}ClFeN_2O_4Rh$ requires C, 59.5%, H, 5.0, N, 2.4; M^+ 551.28874). ν_{max} (KBr)/ cm^{-1} 1596, 1555, 1494, 1419, 1283, 1120, 1086, 889, 814, 780, 746, 692, 624, 522, 447 and 420; ^1H NMR δ_H (400 MHz; solvent $CDCl_3$): 8.35 (2H, d, *J = 5.3 Hz*, C_5H_4N), 7.67 (2H, t, *J = 7.8 Hz*, C_5H_4N), 7.50 (2H, dd, *J = 6.7 Hz*, C_5H_4N), 7.08 (2H, dd, *J = 11.6 Hz*, C_5H_4N), 4.91 (4H, t, *J = 1.8 Hz*, C_5H_4), 4.50 (4H, s, COD-CH), 4.36 (4H, t, *J = 1.8 Hz*, C_5H_4), 2.81 (COD-CH_2), 2.00 (4H, br s, COD-CH_2); ^{13}C NMR δ_C (75 MHz; solvent $CDCl_3$): 156.97 (C_5H_4N), 136.51 (C_5H_4N), 131.90 (C_5H_4N), 128.39 (C_5H_4N), 120.30 (C_5H_4N), 75.21 (COD), 71.48 (C_5H_4), 68.73 (C_5H_4) and 30.02 (COD); *m/z* (FAB) 551 (M^+, 14%), 443 (M^+-COD, 17), 387 (7), 341 ($Fc(2\text{-}py)_2$, 11), 258 (23), 189 (19), 154 (37), 115 (58) and 89 (100).

7.4.20 (1,1'-Bis(4-pyridyl)ferrocene)(1,5-cyclooctadiene)rhodium perchlorate

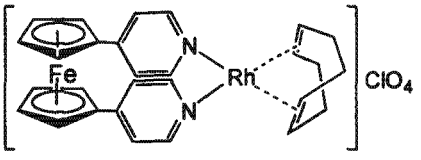

(1,1'-Bis(4-pyridyl)ferrocene)(1,5-cyclooctadiene)rhodium perchlorate was prepared according to the procedure for *7.4.4.* A white precipitate was observed to form immediately on addition of silver perchlorate (60.9 mg, 0.29 mmol) to a solution of chloro(l,5-cyclooctadiene)rhodium(I) dimer (72.5 mg, 0.15 mmol) in ethanol (15 ml). 1,1'-Bis(4-pyridyl)ferrocene (100.0 mg, 0.29 mmol) was added to the supernatant, which was stirred at room temperature for a further 40 minutes. The reaction mixture was then concentrated and pentane added to precipitate the product. The product

was collected by vacuum filtration as small dark red crystals (107.1 mg, 67%), mp 208-210 °C dec.; (Found: C, 59.32%, H, 4.86, N, 2.32; M^+ 551. $C_{28}H_{28}ClFeN_2O_4Rh$ requires C, 59.5%, H, 5.0, N, 2.4; M^+ 551). ν_{max} (KBr)/ cm^{-1} 3504, 3436, 3361, 2363, 1650, 1595, 1426, 1113, 1086, 841, 692, 617 and 543; ^1H NMR δ_H (400 MHz; solvent $CDCl_3$): 8.52 (4H, d, *J = 5.8 Hz*, C_5H_4N), 7.16 (4H, d, *J = 5.6 Hz*, C_5H_4N), 4.85 (4H, t, *J = 1.8 Hz*, C_5H_4), 4.52 (4H, t, *J = 1.8 Hz*, C_5H_4), 4.39 (4H, s, COD-CH), 2.89 (4H, m, COD-CH_2), 1.98 (4H, br s, COD-CH_2); ^{13}C NMR δ_C (101 MHz; solvent $CDCl_3$): 149.69 (C_5H_4N), 120.18 (C_5H_4N), 75.18 (COD), 72.24 (C_5H_4), 68.45 (C_5H_4) and 30.21 (COD); *m/z* (FAB) 551 (M^+, 7%), 442 (1), 387 (1), 342 ($Fc(4\text{-}py)_2$, 3), 279 (100), 258 (3), 223 (3), 207 (5), 185 (100) and 115 (10).

7.4.21 Chloro(1,5-cyclooctadiene)(1',2',3',4',5'-pentamethylazaferrocene)rhodium

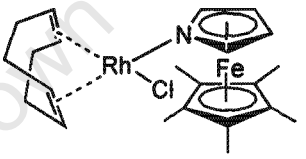

Chloro(1,5-cyclooctadiene)(1',2',3',4',5'-pentamethylazaferrocene)rhodium was prepared according to the procedure followed for *7.4.2.* 1',2',3',4',5'-Pentamethylazaferrocene (70.0 mg, 0.27 mmol) was added to a solution of chloro(I,5-cyclooctadiene)rhodium(I) dimer (67.1 mg, 0.14 mmol) in dichloromethane (10 ml). The reaction mixture was stirred for a further 37 minutes. The reaction mixture was then concentrated *in vacuo* and pentane added to precipitate the product. The product was collected *via* vacuum filtration as an orange powder (47.3 mg, 67%), mp 192-193 °C; (Found: C, 52.12%, H, 5.98, N, 2.65; M^+ 505. $C_{22}H_{31}ClFeNRh$ requires C, 52.4%, H, 6.2, N, 2.8; M^+ 504.75). ν_{max} (KBr)/ cm^{-1} 2907, 2872, 2832, 1738, 1704, 1650, 1575, 1473, 1446, 1371, 1324, 1113, 1066, 1018, 943, 869, 814, 767 and 468; ^1H NMR δ_H (400 MHz; solvent $CDCl_3$): 5.33 (2H, s, C_4H_4N), 4.53 (2H, s, C_4H_4N), 4.16 (2H, s, COD-CH), 3.81 (2H, s, COD-CH), 2.41 (4H, s, COD-CH_2), 2.08 (15H, s, CH_3) and 1.75 (4H, s, COD-CH_2); ^{13}C NMR δ_C (101 MHz; solvent $CDCl_3$): 88.96 (C_5Me_5), 82.64 (C_4H_4N), 75.38 (COD), 74.21 (C_4H_4N), 31.04 (COD), 30.45 (COD) and 11.50 (CH_3); *m/z* (FAB) 505 (M^+, 10%), 466 (2), 402 (2), 341 (3), 290 (4), 258 (100), 244 (8). 226 (4) and 207 (7).

7.4.22 Chloro(1,5-cyclooctadiene)(4-octyloxystilbene)rhodium[41]

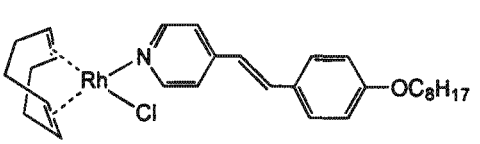

Chloro(1,5-cyclooctadiene(4-octyloxystilbene)rhodium was prepared according to the procedure followed for *7.4.2.* 4-Octyloxystilbene (70.0 mg, 0.23 mmol) was added to a solution of chloro(I,5-cyclooctadiene)rhodium(I) dimer (55.8 mg, 0.11 mmol) in dichloromethane (10 ml). The reaction mixture was stirred for a further 50 minutes. The reaction mixture was then

concentrated *in vacuo* and pentane added to precipitate the product. The product was collected *via* vacuum filtration as a light yellow powder (86.3 mg, 67%), mp 89-128 °C (lit. 85-130 °C). ^{1}H NMR δ_H (400 MHz; solvent $CDCl_3$): 8.60 (2H, d, *J = 6.6 Hz*, C_5H_4N), 7.45 (2H, d, *J = 8.4 Hz*, C_6H_4), 7.30 (2H, d, *J = 6.6 Hz*, C_5H_4N), 7.26 (1H, d, *J = 16.1 Hz*, CH=CH), 6.90 (2H, d, *J = 8.8 Hz*, C_6H_4), 6.78 (1H, d, *J = 16.1 Hz*, CH=CH), 4.22 (4H, br s, COD-CH), 3.98 (2H, t, *J = 6.6 Hz*, OCH_2), 2.50 (4H, m, COD-CH_2), 1.83 (4H, d, *J = 7.7 Hz*, COD-CH_2), 1.42 (2H, m, CH_2), 1.29 (10H, m, CH_2 x 5), 0.89 (3H, m, CH_3); ^{13}C NMR δ_C (101 MHz; solvent $CDCl_3$): 149.10 (C_5H_4N), 133.41 (C=C), 127.12 (C_6H_4), 120.42 (C=C), 119.72 (C_6H_4), 113.34 (C_5H_4N), 66.59 (COD), 30.17 (COD), 29.28 (OCH_2), 27.70 (CH_2 x 5), 21.01 (CH_2) and 12.43 (CH_3).

7.4.23 (1,5-Cyclooctadiene)-1,1'-bis(diphenylphosphino)ferrocene)rhodium perchlorate[42]

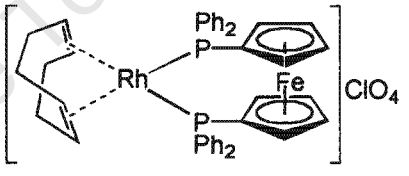

(1,5-Cyclooctadiene)-1,1'-bis(diphenylphosphino)ferrocene) rhodium perchlorate was prepared according to the procedure for *7.4.4*. A white precipitate was observed to form immediately on addition of silver perchlorate (37.4 mg, 0.18 mmol) to a solution of chloro(l,5-cyclooctadiene)rhodium(I) dimer (44.5 mg, 0.09 mmol) in acetone (15 ml). 1,1'-Bis(diphenylphosphino)ferrocene (100.2 mg, 0.18 mmol) was then added slowly to the supernatant, which was stirred at room temperature for a further 35 minutes. The reaction mixture was then concentrated and diethyl ether added to precipitate the product. The product was collected by vacuum filtration as an orange-gold powder (126.2 mg, 81%), mp 193-195 °C dec.; (Found: M^+ 765. $C_{42}H_{40}ClFeO_4P_2Rh$ requires M^+ 765.52). ν_{max} (KBr)/ cm^{-1} 2356, 2329, 2288, 1765, 1738, 1684, 1616, 1575, 1541, 1514, 1480, 1432, 1398, 1337, 1310, 1188, 1161, 1099, 1038, 998, 862, 821, 753, 699, 624, 543, 495 and 434; ^{1}H NMR δ_H (300 MHz; solvent $CDCl_3$): 7.86 (10H, dd, *J = 4.4 Hz*, C_6H_5), 7.59 (10 H, d, *J = 4.8 Hz*, C_6H_5), 4.41 (4H, s, COD-CH), 4.34 (4H, t, *J = 1.8 Hz*, C_5H_4), 4.28 (4H, t, *J = 1.8 Hz*, C_5H_4), 2.37 (4H, m, COD-CH_2), 2.16 (4H, d, *J = 8.1 Hz*, COD-CH_2); ^{13}C NMR δ_C (75 MHz; solvent $CDCl_3$): 134.21 (C_6H_5), 131.75 (C_6H_5), 129.10 (C_6H_5), 99.37 (COD-CH), 75.05 (C_5H_4), 74.10 (C_5H_4) and 30.51 (COD-CH_2); *m/z* (FAB) 765 (M^+, 20%), 733 (18), 634 (27), 578 (42), 395 (10), 321 (20), 258 (30), 185 (100), 149 (21) and 115 (10).

7.4.24 Chloro(1,5-cyclooctadiene)(ferrocenyldiphenylphosphine)rhodium

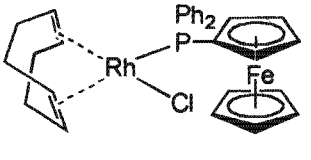

Chloro(1,5-cyclooctadiene)(ferrocenyldiphenylphosphine)rhodium was prepared according to the procedure followed for *7.4.2*. Ferrocenyldiphenylphosphine (100.0 mg, 0.27 mmol) was added to

a solution of chloro(l,5-cyclooctadiene)rhodium(I) dimer (66.7 mg, 0.13 mmol) in dichloromethane (10 ml). The reaction mixture was stirred for a further 36 minutes. The reaction mixture was then concentrated *in vacuo* and pentane added to precipitate the product. The product was collected *via* vacuum filtration as a mustard-yellow powder (107.8 mg, 65%), mp 156-158 °C; (Found: C, 57.97%, H, 5.13; M^+ 616.02563. $C_{30}H_{31}ClFePRh$ requires C, 58.4%, H, 5.1; M^+ 616.74827). ν_{max}/cm^{-1} (KBr): 3062, 2879, 2832, 2356, 2322, 1772, 1684, 1616, 1609, 1575, 1541, 1514, 1480, 1426, 1412, 1398, 1385, 1324, 1303, 1161, 1106, 1086, 1066, 1032, 1011, 998, 984, 957, 841, 814, 753, 699, 644, 543, 522, 488, 461 and 447; ^1H NMR δ_H (300 MHz; solvent C_6D_6): 7.79 (5H, t, *J = 5.0 Hz*, C_6H_5), 7.03 (5H, d, J = *5.7 Hz*, C_6H_5), 5.89 (4H, br s, COD-CH), 4.89 (2H, br s, C_5H_4), 4.31 (5H, s, C_5H_5), 4.14 (2H, br s, C_5H_4), 3.18 (4H, m, COD-CH_2), 2.16 (4H, d, *J = 8.4 Hz*, COD-CH_2); ^{13}C NMR δ_C (75 MHz; solvent $CDCl_3$): 126.86 (C_6H_5), 126.67 (C_6H_5), 122.87 (C_6H_5), 85.01 (COD-CH), 70.86 (C_5H_4), 70.82 (C_5H_4), 67.41 (C_5H_5) and 29.10 (COD-CH_2); ^{31}P NMR δ_P (121 MHz; solvent C_6D_6): 25.69 (PPh_2); *m/z* (FAB) 616 (M^+, 69%), 581 (M-Cl, 100), 579 (47), 551 (10), 501 (17), 470 (12), 433 (16), 393 (32), 370 ($FcPPh_2$, 86), 351 (12), 293 (10), 273 (12), 233 (8), 210 (M-$FcPPh_2$, 5), 186 (Ferrocene, 8), 154 (13) and 136 (12).

7.4.25 (1,5-Cyclooctadiene)bis(ferrocenyldiphenylphosphine)rhodium perchlorate

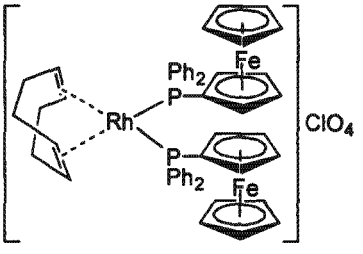

(1,5-Cyclooctadiene)bis(ferrocenyldiphenylphosphine)rhodium perchlorate was prepared according to the procedure for *7.4.4.* A white precipitate was observed to form immediately on addition of silver perchlorate (84.1 mg, 0.40 mmol) to a solution of chloro(l,5-cyclooctadiene)rhodium(I) dimer (100.0 mg, 0.20 mmol) in acetone (20 ml). Ferrocenyldiphenylphosphine (300.1 mg, 0.81 mmol) was then added slowly to the supernatant, which was stirred at room temperature for a further 40 minutes. The reaction mixture was then concentrated and diethyl ether added to precipitate the product. The product was collected by vacuum filtration as a brown crystalline solid (451.8 mg, 99%), 95-98 °C; (Found: C, 59.48%, H, 4.77; M^+ 950.9. $C_{52}H_{50}ClFe_2O_4P_2Rh$ requires C, 59.4%, H, 4.8; M^+ 950.5). ν_{max}/cm^{-1} (KBr): 3056, 2356, 2329, 1616, 1575, 1541, 1514, 1480, 1432, 1398, 1378, 1337, 1303, 1161, 1120, 1113, 1100, 1032, 998, 821, 746, 692, 624, 570, 481, 461, 454 and 434; ^1H NMR δ_H (300 MHz; solvent $CDCl_3$): 7.60 (10H, br s, C_6H_5), 7.07 (10H, br s, C_6H_5), 4.33 (4H, br s, C_5H_4), 4.15 (4H, br s, C_5H_4), 4.04 (10H, s, C_5H_5), 3.59 (4H, br s, COD-CH), 3.10 (4H, m, COD-CH_2), 2.18 (4H, d, *J = 8.5 Hz*, COD-CH_2); *m/z* (FAB) 950.9 (M^+, 5%),

843 (M-COD, 48), 763 (10), 723 (5), 657 (8), 581 (M-$FcPPh_2$, 75), 501 (29), 417 (39), 393 (79), 386 (98), 370 ($FcPPh_2$, 100), 321 (77), 293 (34), 233 (27), 210 (M-2 $FcPPh_2$, 11), 136 (43), 115 (45), 89 (82) and 77 (100).

7.5 Iridium complexes

7.5.1 Chloro(l,5-cyclooctadiene)iridium(I) dimer[43]

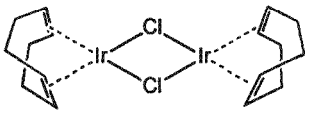

1,5-Cyclooctadiene (1.47 g, 1.70 ml, 13.61 mmol) was added to a dark suspension of iridium trichloride (1.50 g, 4.25 mmol) in ethanol/water 5:1 (20 ml). The reaction mixture was heated under reflux overnight. The product was observed as an orange-red crystalline suspension with the supernatant gradually changing colour from a dark solution to light orange. The product was collected by vacuum filtration and washed successively with pentane and methanol (404.5 mg, 28%), mp 192 °C dec.. ν_{max} (KBr)/ cm^{-1} 1698, 1471, 668, 530, 497 and 444; ^1H NMR δ_H (400 MHz; solvent C_6D_6): 4.32 (8H, s, COD-CH), 2.02 (8H, br s, COD-CH_2), 1.25 (8H, d, *J = 8.0 Hz*, COD-CH_2); ^{13}C NMR δ_C (101 MHz; solvent C_6D_6): 61.68 (COD) and 31.56 (COD).

7.5.2 Chloro(1,5-cyclooctadiene)(pyridine)iridium[44]

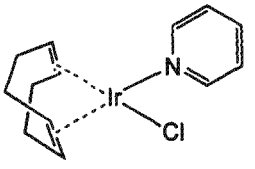

Pyridine (19.0 mg, 19.3 µl, 0.24 mmol) was added slowly to an orange solution of the chloro(l,5-cyclooctadiene)iridium(I) dimer (80.0 mg, 0.12 mmol) in tetrahydrofuran (15 ml). The solution was observed to change to bright yellow on addition of pyridine. The reaction mixture was further stirred under nitrogen at room temperature for 23 minutes and then concentrated *in vacuo*. Pentane was added to precipitate the product that was collected *via* vacuum filtration as a bright yellow powder (76.2 mg, 77%), mp 137-139 °C dec. (lit.[44] 136-138 °C dec.). ν_{max} (KBr)/ cm^{-1} 2365, 2344, 1696, 1601, 1473, 1208, 1067, 1000, 668, 492, 436 and 406;^1H NMR δ_H (400 MHz; solvent C_6D_6): 8.29 (2H, d, *J = 6.4 Hz*, C_5H_5N), 6.56 (1H, t, *J = 6.3 Hz*, C_5H_5N), 6.27 (2H, t, *J = 7.2 Hz*, C_5H_5N), 3.97 (4H, br s, COD-CH), 2.21-2.18 (4H, m, COD-CH_2), 1.47-1.41 (4H dd, *J = 11.8 Hz*, COD-CH_2); ^{13}C NMR δ_C (101 MHz; solvent C_6D_6): 150.37 (C_5H_4N), 136.29 (C_5H_4N), 124.65 (C_5H_4N), 68.00 (COD) and 31.95 (COD).

7.5.3 (1,5-Cyclooctadiene)bis(pyridine)iridium perchlorate[43,44]

Excess pyridine (94.2 mg, 96 µl, 1.20 mmol) was added slowly to an orange suspension of chloro(l,5-cyclooctadiene)iridium(I) dimer (100.2 mg, 0.15 mmol) in ethanol (15 ml). The

bright yellow solution was further stirred at room temperature under nitrogen for 26 minutes. Silver perchlorate (61.7 mg, 0.30 mmol) was added to the reaction mixture. A white precipitate of silver chloride was observed to precipitate almost immediately. The reaction mixture was filtered under vacuum to remove precipitated silver chloride. The filtrate was then concentrated and left to crystallise at 0 °C. The product was collected *via* vacuum filtration as a crystalline yellow powder (468.8 mg, 70%). ν_{max} (KBr)/cm^{-1} 3568, 3023, 1603, 1484, 1211, 1109, 1087, 762, 622, 489 and 436; ^{1}H NMR δ_H (300 MHz; solvent $CDCl_3$): 8.80 (4H, br s, C_5H_4N), 7.76 (2H, t, *J = 7.1 Hz*, C_5H_4N), 7.51 (4H, br s, C_5H_4N), 3.84 (4H, s, COD-CH), 2.49 (4H, br s, COD-CH_2), 1.82 (4H, d, *J = 7.7 Hz*, COD-CH_2); ^{13}C NMR δ_C (75 MHz; solvent $CDCl_3$): 149.88 (C_5H_4N), 138.77 (C_5H_4N), 126.92 (C_5H_4N), 70.74 (COD) and 31.28 (COD).

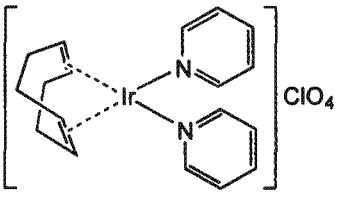

7.5.4 Chloro(1,5-cyclooctadiene)(4-phenylpyridine)iridium

Chloro(1,5-cyclooctadiene)(4-phenylpyridine)iridium was prepared according to the procedure followed for *7.5.2.* 4-Phenylpyridine (46.6 mg, 0.30 mmol) was added to a solution of chloro(I,5-cyclooctadiene)iridium(I) dimer (100.0 mg, 0.15 mmol) in tetrahydrofuran (15 ml). The reaction mixture was stirred for a further 30 minutes. and then concentrated *in vacuo*. Pentane was added to precipitate the product. The product was collected *via* vacuum filtration as a yellow crystalline solid (111.0 mg, 75%); (Found: C, 46.34%, H, 4.68, N, 2.74; M^+ 491.1. $C_{19}H_{21}ClIrN$ requires C, 46.4%, H, 4.4, N, 2.8; M^+ 491.6). ν_{max} (KBr)/ cm^{-1} 3674, 3646, 3627, 1750, 1733, 1634, 1609, 1483, 1436, 1414, 765 and 408; ^{1}H NMR δ_H (400 MHz; solvent C_6D_6): 8.39 (2H, d, *J = 5.8 Hz*, C_5H_4N), 7.12 (5H, br s, C_6H_5), 6.68 (2H, d, *J = 5.9 Hz*, C_5H_4N), 3.53 (4H, s, COD-CH), 2.23 (4H, m, COD-CH_2), 1.49 (4H, d, *J = 11.5 Hz*, COD-CH_2); ^{13}C NMR δ_C (101 MHz; solvent C_6D_6): 150.63 (C_5H_4N), 129.68 (C_6H_5), 129.08 (C_6H_5), 126.97 (C_6H_5), 122.46 (C_5H_4N), 68.90 (COD), 32.03 (COD); *m/z* (FAB) 491 (M^+, 8%), 456 (M-Cl, 44), 452 (26), 347 (6), 297 (24), 295 (22), 170 (9), 156 (ligand-H^+, 100), 115 (5) and 77 (6).

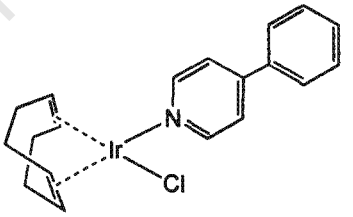

7.5.5 Chloro(1,5-cyclooctadiene)(4-phenylimine-4'-pyridine)iridium

Chloro(1,5-cyclooctadiene)(4-phenylimine-4'-pyridine)iridium was prepared according to the procedure followed for *7.5.2.* 4-Phenylimine-4'-pyridine (55.0 mg, 0.30 mmol) was added to a solution of chloro(I,5-

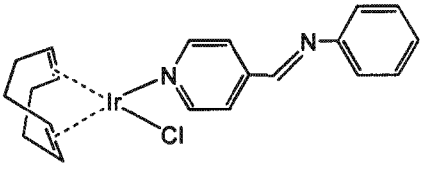

cyclooctadiene)iridium(I) dimer (100.0 mg, 0.15 mmol) in tetrahydrofuran (15 ml). The reaction mixture was stirred for a further 47 minutes and then concentrated *in vacuo*. Pentane was added to precipitate the product. The product was collected *via* vacuum filtration as an orange powder (87.8 mg, 57%), mp 197-200 °C dec.; (Found: C, 46.08%, H, 4.31, N, 5.19; M^+ 518.0. $C_{20}H_{22}ClIrN_2$ requires C, 46.3%, H, 4.2, N, 5.4; M^+ 518.2). ν_{max} (KBr)/ cm^{-1} 3629, 1700, 1696, 1653, 1560, 668, 412 and 410; ^1H NMR δ_H (300 MHz; solvent $CDCl_3$): 8.83 (2H, dd, *J = 6.6 Hz*, C_5H_4N), 8.45 (1H, s, N=CH), 7.83 (2H, dd, *J = 6.6 Hz*, C_5H_4N), 7.42 (2H, t, *J = 7.7 Hz*, C_6H_5), 7.33 (2H, d, *J = 7.2 Hz*, C_6H_5), 7.27 (1H, t, *J = 8.4 Hz*, C_6H_5), 3.78 (4H, br s, COD-CH), 2.32 (4H, m, COD-CH_2), 1.63 (4H, d, J = 7.4 Hz, COD-CH_2); ^{13}C NMR δ_C (75 MHz; solvent $CDCl_3$): 157.98 (N=C), 154.28 (C_5H_4N), 151.89 (C_5H_4N), 144.51 (C_6H_5), 129.38 (C_5H_4N), 127.65 (C_6H_5), 123.24 (C_6H_5), 122.06 (C_6H_5), 85.12 (COD) and 30.32 (COD); *m/z* (FAB) 518 (M^+, 8%), 479 (M-Cl, 55), 452 (7), 399 (15), 373, (M-COD, 11), 335 (7), 295 (28), 195 (7), 183 (Ligand-H^+, 100), 149 (19), 79 (py, 13) and 77 (47).

7.5.6 Chloro(1,5-cyclooctadiene)(4-ferrocenylpyridine)iridium

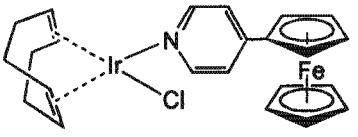

Chloro(1,5-cyclooctadiene)(4-ferrocenylpyridine)iridium was prepared according to the general procedure followed for *7.5.2.* 4-Ferrocenylpyridine (78.3 mg, 0.30 mmol) was added to a solution of chloro(I,5-cyclooctadiene)iridium(I) dimer (100.1 mg, 0.15 mmol) in tetrahydrofuran (12 ml). The reaction mixture was stirred for a further 40 minutes and then concentrated *in vacuo.* Pentane was added to precipitate the product. The product was collected *via* vacuum filtration as an orange-brown solid (92.4 mg, 51%), mp 179-182 °C dec.; (Found: C, 45.91%, H, 4.23, N, 2.27; M^+ 598.1. $C_{23}H_{25}ClFeIrN$ requires C, 46.1%, H, 4.2, N, 2.3; M^+ 598.2). ν_{max} (KBr)/ cm^{-1} 3568, 2317, 1845, 1700, 1636, 1614, 1499, 1457, 668 and 411; ^1H NMR δ_H (400 MHz; solvent C_6D_6): 8.38 (2H, d, *J = 5.9 Hz*, C_5H_4N), 6.66 (2H, d, *J = 6.1 Hz*, C_5H_4N), 4.21 (2H, t, *J = 1.8 Hz*, C_5H_4), 4.05 (2H, t, *J = 1.8 Hz*, C_5H_4), 3.67 (5H, s, C_5H_5), 2.24 (4H, m, COD-CH_2), 1.29 (4H, d, *J = 8.1 Hz*, COD-CH_2); ^{13}C NMR δ_C (101 MHz; solvent C_6D_6): 149.97 (C_5H_4N), 121.40 (C_5H_4N), 70.99 (C_5H_4), 70.24 (C_5H_5), 67.28 (C_5H_4), 67.26, (COD), 32.08 (COD); *m/z* (FAB) 598 (M^+, 10%), 578 (16), 564 (M-Cl, 43), 454 (6), 440 (26), 400 (29), 363 (7), 297 (14), 263 (ligand, 100), 198 (11), 121 (54) and 77 (44).

7.5.7 (1,5-Cyclooctadiene)bis(ferrocenylpyridine)iridium perchlorate

(1,5-Cyclooctadiene)bis(ferrocenylpyridine)iridium perchlorate was prepared according to the procedure for *7.5.3.* 4-Ferrocenylpyridine (0.18 g, 0.69 mmol) was added slowly to an orange suspension of chloro(I,5-cyclooctadiene)iridium(I) dimer (0.12 g, 0.17 mmol) in ethanol (15

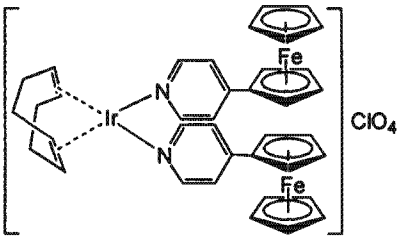

ml). The bright red solution was further stirred at room temperature under nitrogen for 24 minutes. Silver perchlorate (0.07 g, 0.34 mmol) was added to the reaction mixture. A white precipitate of silver chloride was observed to precipitate almost immediately. The reaction mixture was filtered under vacuum to remove precipitated silver chloride, the filtrate concentrated and left to crystallise at 0 °C. The product was collected *via* vacuum filtration as a fine pink-red powder (0.29 g, 94%), mp 170-174 °C dec.; (Found: C, 49.21%, H, 3.82, N, 2.67; M^+ 826.13734. $C_{38}H_{38}ClFe_2IrN_2O_4$ requires C, 49.3%, H, 4.1, N, 3.0; M^+ 826.615494). ν_{max} (KBr)/ cm^{-1} 3584, 2349, 1728, 1703, 1634, 1615, 1486, 1435, 1429, 1404, 1122, 667, 43 and 408; ^1H NMR δ_H (400 MHz; solvent $CDCl_3$): 8.78 (4H, d, *J = 5.9 Hz*, C_5H_4N), 7.75 (4H, d, *J = 6.1 Hz*, C_5H_4N), 5.17 (4H, t, *J = 1.8 Hz*, C_5H_4), 4.75 (4H, t, *J = 1.8 Hz*, C_5H_4), 4.19 (10H, s, C_5H_5), 2.77 (4H, m, COD-CH_2), 1.29 (4H, d, *J = 8.1 Hz*, COD-CH_2); ^{13}C NMR δ_C (101 MHz; solvent C_6D_6): 150.58 (C_5H_4N), 122.69 (C_5H_4N), 72.38 (C_5H_4), 70.02 (C_5H_5), 67.47, (COD), 67.08 (C_5H_4), 31.89 (COD); *m/z* (FAB) 827 (33), 826 (M^+, 9%), 608 (7), 580 (13), 440 (16), 400 (18), 263 (ligand, 100), 154 (25) and 77 (13).

7.5.8 Bis(carbonyl)chloro(4-pyridylimine-4'-phenylferrocene)iridium

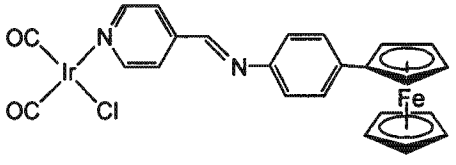

4-Pyridylimine-4'-phenylferrocene (87.2 mg, 0.24 mmol) was added to an orange solution of the iridium dimer (80.0 mg, 0.12 mmol) in dichloromethane (10 ml). The reaction mixture was further stirred under nitrogen for at least 10 minutes. Carbon monoxide was then bubbled through the reaction mixture for 15 minutes. The reaction mixture was concentrated *in vacuo* and hexane added to precipitate the product. The product was collected *via* vacuum filtration as a fine maroon powder (81.0 mg, 52%), mp 151-167 °C; (Found: C, 44.40%, H, 2.66, N, 3.95; M^+ 650. $C_{24}H_{18}ClFeIrN_2O_2$ requires C, 44.3%, H, 2.8, N, 4.3; M^+ 649.94). ν_{max}/cm^{-1} (KBr): 3447, 2926, 2067 (CO), 1991 (CO), 1619 (C=N), 1577, 1429, 1103, 846, 823, and 503; ^1H NMR δ_H (300 MHz; solvent $CDCl_3$): 8.88 (2H, d, *J = 6.7 Hz*, C_5H_4N), 8.60 (1H, s, N=CH), 8.00 (2H, d, *J = 6.7 Hz*, C_5H_4N), 7.57 (2H, d, *J = 8.5 Hz*, C_6H_4), 7.29 (2H, d, *J = 8.5 Hz*, C_6H_4), 4.69 (2H, t, *J = 1.8 Hz*, C_5H_4), 4.38 (2H, t, *J = 1.8 Hz*, C_5H_4) and 4.06 (5H, s, C_5H_5); ^{13}C NMR δ_C (75 MHz; solvent $CDCl_3$): 154.17 (N=C), 152.19 (C_5H_4N), 147.61 (C_5H_4N), 144.76 (C_6H_4), 139.07 (C_5H_4N), 126.89 (C_5H_4N), 122.38 (C_5H_4N), 121.49 (C_6H_4), 69.82 (C_5H_5), 69.43 (C_5H_4) and 66.67 (C_5H_4); *m/z* (FAB) 650 (M^+, 1%), 559 (M-Cl-2CO, 7), 473 (7), 468 (5), 432 (4), 367 ($Fc(C_6H_4)NCpy$, 4), 301 (2) and 245 (4).

7.6 Palladium complexes

7.6.1 Dichlorobis(pyridine)palladium

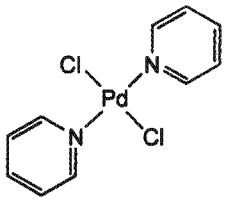

The reaction mixture was observed to change from a light brown solution to opaque yellow on addition of a solution of pyridine (54.0 mg, 55.0 µl, 0.68 mmol) in ethanol (5 ml) to a solution of sodium tetrachloropalladate(II) (100.0 mg, 0.34 mmol) in (1:2) ethanol/water (3 ml). The reaction mixture was further stirred at room temperature for 24 hours. A precipitate was observed during this time. The product was collected *via* vacuum filtration as a light yellow powder (88.1 mg, 77%). ν_{max} (KBr)/ cm^{-1} 3629, 1636, 1604, 1474, 769, 668 and 472; ^1H NMR δ_H (400 MHz; solvent $CDCl_3$): 8.84 (4H, dd, *J = 8.1 and 5.1 Hz*, C_5H_5N), 7.78 (2H, tt, *J = 7.7 Hz*, C_5H_5N), 7.34 (4H, t, *J = 7.7 Hz*, C_5H_5N); ^{13}C NMR δ_C (101 MHz; solvent $CDCl_3$): 153.65 (C_5H_5N), 138.96 (C_5H_5N), 124.95 (C_5H_5N)

7.6.2 Dichlorobis(4-phenylpyridine)palladium

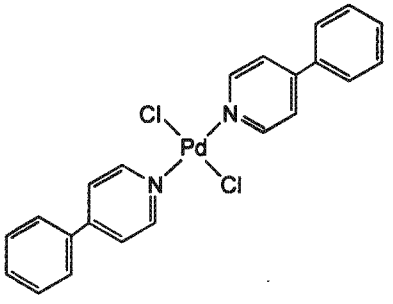

A light yellow precipitate was observed to occur immediately on addition of a solution of 4-phenylpyridine (0.21 g, 1.36 mmol) in dichloromethane (5 ml) to a solution of sodium tetrachloropalladate(II) (0.20 g, 0.68 mmol) in (1:2) ethanol/water (6 ml). The reaction mixture was further stirred at room temperature for 6 hours. The product was collected as a light yellow powder by vacuum filtration (0.27 g, 83%); (Found: C, 54.52%, H, 3.55, N, 5.58. $C_{22}H_{18}Cl_2N_2Pd$ requires C, 54.2%, H, 3.7, N, 5.7). ν_{max} (KBr)/ cm^{-1} 3626, 1760, 1699, 1634, 1609, 1480, 667, 503 and 431; ^1H NMR δ_H (solvent $CDCl_3$): ^1H NMR δ_H (300 MHz; solvent $CDCl_3$): 8.69 (4H, d, *J = 5.8 Hz*, C_5H_4N), 7.48 (4H, d, *J = 5.8 Hz*, C_5H_4N), 7.32 (10H, m, C_6H_5).

7.6.3 Dichlorobis(4-ferrocenylpyridine)palladium

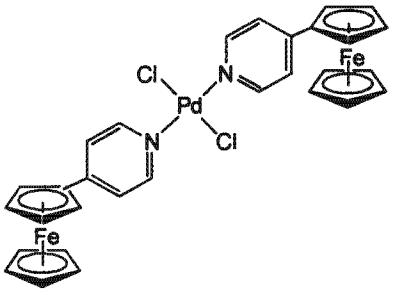

Dichlorobis(4-ferrocenylpyridine)palladium was prepared according to the procedure for *7.6.2*. A red precipitate was observed to occur immediately on addition of a solution of 4-ferrocenylpyridine (0.50 g, 1.9 mmol) in dichloromethane (5 ml) to a solution of sodium tetrachloropalladate(II) (0.28 g, 0.95 mmol) in (1:2) ethanol-water (6 ml). The reaction

mixture was further stirred at room temperature 8 hours. The product was collected as a red powder by vacuum filtration (0.56 g, 84%), mp 250-253 °C dec.; (Found: C, 50.76%, H, 3.52, N, 4.02; M^+ 703.92108. $C_{30}H_{26}Cl_2Fe_2N_2Pd$ requires C, 51.2%, H, 3.7, N, 4.0; M^+ 703.65268). ν_{max} (KBr)/ cm^{-1} 3568, 1700, 1636, 1611, 1499, 1215, 1107, 1039, 825 and 494; ^1H NMR δ_H (solvent $CDCl_3$): 8.59 (4H, d, *J = 6.7* Hz, C_5H_4N), 7.30 (4H, br s, C_5H_4N), 4.72 (4H, s, C_5H_4), 4.52 (4H, s, C_5H_4), 4.07 (10H, s, C_5H_5); *m/z* (FAB) 703.9 (M^+, 28%), 667 (M-Cl, 14 8), 613 (9), 482 (7), 460 (25), 371 (8), 329 (32), 307 (75), 289 (60), 263 (ligand, 77), 176 (58), 107 (70) and 89 (86).

7.6.4 Dichlorobis(3-ferrocenylpyridine)palladium

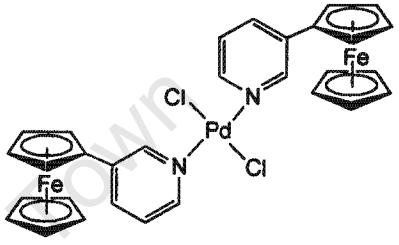

Dichlorobis(3-ferrocenylpyridine)palladium was prepared according to the procedure for *7.6.2.* A yellow precipitate was observed to occur immediately on addition of a solution of 3-ferrocenylpyridine (0.30 g, 1.2 mmol) in dichloromethane (5 ml) to a solution of sodium tetrachloropalladate(II) (0.17 g, 0.59 mmol) in (1:2) ethanol-water (6 ml). The reaction mixture was further stirred at room temperature for 6 hours. The product was collected as a fine mustard-yellow crystalline powder by vacuum filtration (0.35 g, 84%), mp 148-150 °C dec.; (Found: C, 50.86%, H, 3.64, N, 3.92; M^+ 703.92108. $C_{30}H_{26}Cl_2Fe_2N_2Pd$ requires C, 51.2%, H, 3.7, N, 4.0; M^+ 703.65268). ν_{max} (KBr)/ cm^{-1} 3626, 1699, 1634, 1615, 1495, 1106, 815, 667 and 498; ^1H NMR δ_H (300 MHz; solvent $CDCl_3$): 8.91 (2H, br s, C_5H_4N), 8.62 (2H, d, *J = 5.1 Hz*, C_5H_4N), 7.75 (2H, d, *J = 6.9 Hz*, C_5H_4N), 7.20 (2H, t, *J = 6.6 Hz*, C_5H_4N), 4.73 (4H, br s, C_5H_4), 4.46 (2H, br s, C_5H_4), 4.18 (10H, s, C_5H_5); ^{13}C NMR δ_C (75 MHz; solvent $CDCl_3$): 151.13 (C_5H_4N), 149.76 (C_5H_4N), 138.31 (C_5H_4N), 135.05 (C_5H_4N), 124.20 (C_5H_4N), 70.37 (C_5H_4), 70.28 (C_5H_5) and 67.16 (C_5H_4); *m/z* (FAB) 706 (55), 704 (M^+, 74%), 702 (30), 669 (M-Cl, 15), 633 (M-Cl, 8), 581 (7), 511 (13), 371 (30), 369 (M-ligand, 39), 263 (ligand, 100), 198 (29), 154 (38), 136 (37) and 89 (11).

7.6.5 Dichlorobis(2-ferrocenylpyridine)palladium[45]

Dichlorobis(2-ferrocenylpyridine)palladium was prepared according to the procedure for *7.6.2.* A brown two-layer solution was observed on addition of a solution of 2-ferrocenylpyridine (0.50 g, 1.9 mmol) in dichloromethane (5 ml) to a solution of sodium tetrachloropalladate(II) (0.28 g, 0.95 mmol) in (1:2) ethanol-water (6 ml). The reaction mixture was further stirred at room temperature for 7.5 hours. The two-layer reaction mixture was separated and the organic layer was concentrated. The product was precipitated on addition of pentane and

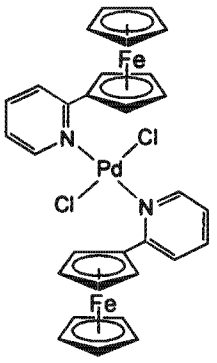

collected as dark red microcrystals by vacuum filtration (0.52 g, 78%), mp 108-110 °C; (Found: C, 51.56%, H, 3.78, N, 4.07; M^+ 703.92108. $C_{30}H_{26}Cl_2Fe_2N_2Pd$ requires C, 51.2%, H, 3.7, N, 4.0; M^+ 703.65268). ν_{max} (KBr)/ cm^{-1} 3626, 1760, 1703, 1634, 1605, 1495, 1435, 1106, 815, 667 and 408; ^1H NMR δ_H (300 MHz; solvent $CDCl_3$): 9.25 (2H, d, *J = 12.8 Hz*, C_5H_4N), 8.56 (2H, br s, C_5H_4N), 7.47 (2H, d, *J = 7.7 Hz*, C_5H_4N), 7.16 (2H, d, *J = 8.1 Hz*, C_5H_4N), 4.92 (4H, t, *J = 1.8 Hz*, C_5H_4), 4.39 (4H, t, *J = 1.8 Hz*, C_5H_4), 4.16 (10H, s, C_5H_5); ^{13}C NMR δ_C (75 MHz; solvent $CDCl_3$): 157.51 (C_5H_4N)152.22 (C_5H_4N), 139.08 (C_5H_4N), 125.67 (C_5H_4N), 119.68 (C_5H_4N), 70.94 (C_5H_4), 70.12 (C_5H_4) and 67.84 (C_5H_5); *m/z* (FAB) 704 (M^+, 22%), 666 (M^+-Cl, 3), 631 (M-Cl, 17), 565 (5), 510 (4), 370 (18), 368 (M-ligand, 19), 279 (35), 263 (ligand, 100), 198 (25), 154 (35), 136 (27) and 89 (13).

7.6.6 Dichlorobis(4-ferrocenylphenyl-4'-pyridine)palladium

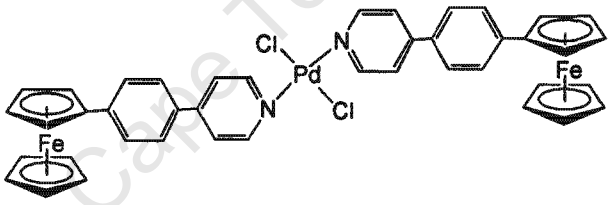

Dichlorobis(4-ferrocenylphenyl-4'-pyridine)palladium was prepared according to the procedure for *7.6.2.* 4-Ferrocenylphenyl-4'-pyridine (49.5 mg, 0.15 mmol) in dichloromethane (5 ml) was added to a solution of sodium tetrachloropalladate(II) (21.5 mg, 0.07 mmol) in (1:2) ethanol/water (3 ml). The reaction mixture was further stirred at room temperature for 8 hours. The product was collected as red-brown microcrystals by vacuum filtration (49.1 mg, 82%), mp 224-226 °C dec.; (Found: C, 59.25%, H, 4.38, N, 2.85; M^+ 856.1. $C_{42}H_{34}Cl_2Fe_2N_2Pd$ requires C, 58.9%, H, 4.0, N, 3.3; M^+ 855.8). ν_{max} (KBr)/ cm^{-1} 3585, 1750, 1699, 1634, 1615, 1495, 1456, 8189, 667 and 406; ^1H NMR δ_H (300 MHz; solvent $CDCl_3$): 8.84 (4H, d, *J = 4.1 Hz*, C_5H_4N), 7.56 (8H, br s, C_6H_4), 7.54 (4H, d, *J = 6.1 Hz*, C_5H_4N), 4.72 (4H, t, *J = 1.8 Hz*, C_5H_4), 4.41 (4H, t, *J = 1.8 Hz*, C_5H_4), 4.08 (10H, s, C_5H_5); ^{13}C NMR δ_C (75 MHz; solvent $CDCl_3$): 153.10 (C_5H_4N), 127.04 (C_6H_4), 126.75 (C_6H_4), 122.03 (C_5H_4N), 69.72 (C_5H_4), 69.59 (C_5H_4) and 66.67 (C_5H_5); *m/z* (FAB) 856 (M^+, 4%), 675 (13), 610 (4), 415 (24), 339 (ligand, 100), 278 (7), 149 (25) and 85 (60).

7.7Platinum complexes

7.7.1 Chloro(1,5-cyclooctadiene)(4-pyridylimine-4'-phenylferrocene)platinum chloride

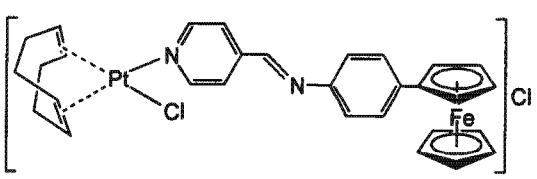

4-Pyridylimine-4'-phenylferrocene (23.1 mg, 0.06 mmol) was added to a solution of dichloro(1,5-cyclooctadiene)platinate (23.8 mg, 0.06 mmol) in pentane (6 ml). The reaction mixture was stirred at room temperature for 2 days after which a purple precipitate was observed. The product was collected *via* vacuum filtration as purple crystalline flakes (18.3 mg, 39%), mp 200-202 °C; (Found: C, 48.76%, H, 3.87, N, 3.39; M^+ 704.10948. $C_{30}H_{30}Cl_2FeN_2Pt$ requires C, 48.6%, H, 4.1, N, 3.8; M^+ 704.97134). ν_{max} (KBr)/ cm^{-1} 3503, 1685, 1624, 1577, 1473, 1406, 847, 668, 552 and 418; ^1H NMR δ_H (300 MHz; solvent $CDCl_3$): 8.74 (2H, d, *J = 5.9 Hz*, C_5H_4N), 8.52 (1H, s, N=CH), 7.76 (2H, dd, *J = 5.9 Hz*, C_5H_4N), 7.52 (2H, dd, *J = 8.6 Hz*, C_6H_4), 7.22 (2H, d, *J = 8.3 Hz*, C_6H_4), 5.59 (4H, br s, COD-CH), 4.66 (2H, t, *J = 1.8 Hz*, C_5H_4), 4.34 (2H, t, *J = 1.8 Hz*, C_5H_4), 4.04 (5H, s, C_5H_5), 2.72-2.67 (4H, m, COD-CH_2) and 2.27-2.23 (4H, d, *J = 8.3 Hz*, COD-CH_2); ^{13}C NMR δ_C (75 MHz; solvent $CDCl_3$): 153.71 (N=C), 150.85 (C_5H_4N), 148.54 (C_5H_4N), 143.24 (C_6H_4), 139.07 (C_5H_4N), 126.72 (C_5H_4N), 122.38 (C_5H_4N), 121.49 (C_6H_4), 69.89 (C_5H_5), 69.39 (C_5H_4) and 66.69 (C_5H_4) *m/z* (FAB) 704 (M^+, 1%), 519 (3), 460 (8), 410 (6), 366 (ligand, 68), 277 (95), 229 (20), 176 (24), 149 (25), 91 (37) and 77 (100).

7.7.2 Dichlorobis(pyridine)platinum[46]

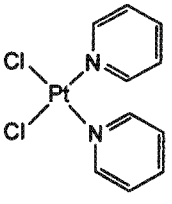

A solution of pyridine (95.0 mg, 0.10 ml, 1.20 mmol) in ethanol (5 ml) was added slowly to a solution of potassium tetrachloroplatinate(II) (0.25 g, 0.60 mmol) in (1:2) ethanol/water (6 ml). The reaction mixture was further stirred at room temperature for at least 24 hours. A precipitate was observed to form during this time. The product was collected as a white powder *via* vacuum filtration (0.18 g, 72%), mp 227-229 °C. ν_{max} (KBr)/ cm^{-1} 3608, 3087, 3023, 2322, 2317, 1843, 1634, 1616, 1607, 1575, 1557, 1482, 1436, 1242, 1207, 1156, 1075, 790, 767, 697, 427, 410 and 404; ^1H NMR δ_H (300 MHz; solvent $CDCl_3$): 8.76 (2H, d, C_5H_5N), 7.33 (2H, dd, C_5H_5N), 7.84 (1H, t, C_5H_5N); ^{13}C NMR δ_C (75 MHz; solvent $CDCl_3$): 152.90 (C_5H_5N), 126.314 (C_5H_5N), 138.52 (C_5H_5N).

7.7.3 Dichlorobis(4-phenylpyridine)platinum

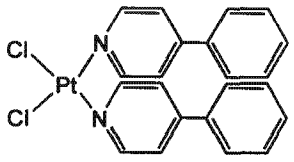

Dichlorobis(4-phenylpyridine)platinum was prepared according to the general procedure for *7.7.2*. A solution of 4-phenylpyridine (64.7 mg, 0.42 mmol) in ethanol (2 ml) was added to a solution of potassium tetrachloroplatinate(II) (86.5 mg, 0.21 mmol) in (1:2) ethanol/water (3 ml). The reaction mixture was stirred under nitrogen at room temperature for 2 days. A precipitate was observed to form during this time. The product was collected *via* vacuum filtration as a cream powder (90.8 mg, 75%), mp 235 °C dec. (Found: C, 46.19%, H, 3.26, N, 4.87. $C_{22}H_{18}Cl_2N_2Pt$ requires C, 45.8%, H, 3.1, N, 4.9). ν_{max} (KBr)/ cm^{-1} 3565, 3055, 2349, 2322, 1662, 1616, 1575, 1505, 1498, 1447, 1393, 1292, 1076, 1014, 842, 729, 693, 562, 497, 441, 435, 416, 410 and 404; ^1H NMR δ_H (300 MHz; solvent DMSO-*d*$_6$): 8.61 (4H, d, *J = 5.8 Hz*, C_5H_4N), 7.86 (8H, m, C_6H_5), 7.76 (2H, d, *J = 8.0 Hz*, C_6H_5), 7.66 (4H, d, *J = 5.8 Hz*, C_5H_4N); ^{13}C NMR δ_C (75 MHz; solvent DMSO-*d*$_6$): 149.89 (C_5H_4N), 129.09 (C_6H_5), 128.84 (C_6H_5), 126.99 (C_6H_5) and 126.86 (C_5H_4N).

7.7.4 Dichlorobis(4-phenylimine-4'-pyridine)platinum

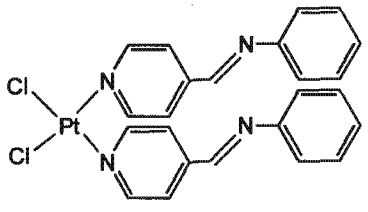

Dichlorobis(4-phenylimine-4'-pyridine)platinum was prepared according to the procedure for *7.7.2*. A solution of 4-phenylimine-4'-pyridine (0.44 g, 2.4 mmol) in ethanol (10 ml) was added to a solution of potassium tetrachloroplatinate(II) (0.50 g, 1.2 mmol) in (1:2) ethanol/water (12 ml). The reaction mixture was stirred under nitrogen at room temperature for 2 days. A precipitate was observed to form during this time. The product was collected *via* vacuum filtration as a mustard-yellow powder (0.53 g, 70%), mp 145-146 °C; (Found: C, 45.69%, H, 3.12, N, 8.62; M^+ 630.07145. $C_{24}H_{20}Cl_2N_4Pt$ requires C, 45.7%, H, 3.2, N, 8.9; M^+ 630.42326). ν_{max} (KBr)/ cm^{-1} 3611, 3054, 2322, 1662, 1645, 1623, 1616, 1575, 1557, 1495, 1429, 1061, 832, 765, 692, 668, 552, 435, 420, 410 and 403; ^1H NMR δ_H (300 MHz; solvent DMSO-*d*$_6$): 9.04 (4H, d, *J = 6.6 Hz*, C_5H_4N), 8.66 (2H, s, N=CH), 8.05 (4H, d, *J = 7.3 Hz*, C_6H_5), 7.83 (4H, d, *J = 5.8 Hz*, C_5H_4N), 7.44 (2H, dd, *J = 7.6 Hz*, C_6H_5), 7.36 (2H, t, C_6H_5); ^{13}C NMR δ_C (75 MHz; solvent DMSO-*d*$_6$): 156.95 (N=C), 153.70 (C_5H_4N), 152.12 (C_5H_4N), 150.10 (C_5H_4N), 129.02 (C_6H_5), 123.84 (C_6H_5)121.06 (C_6H_5), and 120.78 (C_6H_5); *m/z* (FAB) 630 (M^+, 10%), 558 (M-2 Cl, 27), 469 (30), 375 (33), 195 (4), 183 (ligand, 100) and 77 (32).

7.7.5 Dichlorobis(4-ferrocenylpyridine)platinum

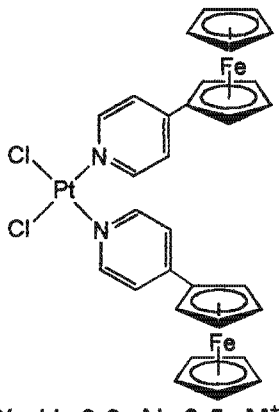

Dichlorobis(4-ferrocenylpyridine)platinum was prepared according to the general procedure for 7.7.2. A solution of 4-ferrocenylpyridine (15.4 mg, 0.06 mmol) in ethanol (2 ml) was added to a solution of potassium tetrachloroplatinate(II) (12.1 mg, 0.03 mmol) in (1:2) ethanol/water (2 ml). The reaction mixture was stirred under nitrogen at room temperature for 24 hours. A precipitate was observed to form during this time. The product was collected *via* vacuum filtration as an pink-red powder (16.7 mg, 72%), mp 228-230 °C dec.; (Found: C, 45.42%, H, 3.54, N, 3.15; M^+ 793. $C_{30}H_{26}Cl_2Fe_2N_2Pt$ requires C, 45.5%, H, 3.3, N, 3.5; M^+ 792.27). ν_{max} (KBr)/ cm^{-1} 3629, 1701, 1696, 1653, 1617, 1521, 1437, 833, 501, 423, 416, 410, 406 and 403; ^1H NMR δ_H (300 MHz; solvent $CDCl_3$): 8.56 (4H, d, *J = 5.3 Hz*, C_5H_4N), 7.25 (4H, br s, C_5H_4N), 4.69 (4H, br s, C_5H_4), 4.51 (4H, br s, C_5H_4), 4.02 (10H, s, C_5H_5); ^{13}C NMR δ_C ($CDCl_3$): 152.98 (C_5H_4N), 125.23 (C_5H_4N), 73.15 (C_5H_5), 70.64 (C_5H_4) and 69.96 (C_5H_4); *m/z* (FAB) 793 (M^+, 4%), 521 (96), 398 (12), 342 (20), 279 (52), 263 (4-Fcpy, 24) and 223 (21).

7.7.6 Dichlorobis(4-ferrocenylphenyl-4'-pyridine)platinum

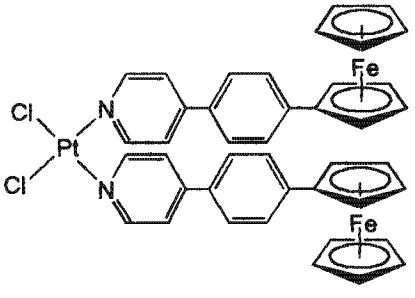

Dichlorobis(4-ferrocenylphenyl-4'-pyridine)platinum was prepared according to the general procedure for 7.6.2. A solution of 4-ferrocenylphenyl-4'-pyridine (50.0 mg, 0.15 mmol) in dichloromethane (5 ml) was added to a solution of potassium tetrachloroplatinate(II) (30.6 mg, 0.07 mmol) in (1:2) ethanol/water (3 ml). The reaction mixture was stirred under nitrogen at room temperature for 6 hours. A two-layer reaction mixture was obtained with a dark red organic layer and colourless aqueous layer. The layers were separated and the solvent removed *in vacuo*, yielding dark red crystals (43.0 mg, 65%), mp 239-241 °C dec.; (Found: C, 53.08%, H, 3.64, N, 2.85; M^+ 944.04473. $C_{42}H_{34}Cl_2Fe_2N_2Pt$ requires C, 53.4%, H, 3.6, N, 3.0; M^+ 944.38395). ν_{max} (KBr)/ cm^{-1} 1601, 1121, 1105, 1073, 1030, 1002, 887, 854, 815, 524, 504, 444 and 425; ^1H NMR δ_H (300 MHz; solvent $CDCl_3$): 8.89 (4H, dd, *J = 5.9 Hz*, C_5H_4N), 7.62 (4H, dd, *J = 6.0 Hz*, C_5H_4N), 7.54 (8H, s, C_6H_4), 4.70 (4H, t, *J = 1.8 Hz*, C_5H_4), 4.40 (4H, t, *J = 1.8 Hz*, C_5H_4), 4.07 (10H, s, C_5H_5); ^{13}C NMR δ_C (75 MHz; solvent $CDCl_3$): 152.82 (C_5H_4N), 126.96 (C_6H_4), 126.80 (C_6H_4), 122.55 (C_5H_4N), 69.82 (C_5H_5), 69.62 (C_5H_4) and 66.73 (C_5H_4); *m/z* (FAB) 944 (M^+, 5%), 908 (M^+-Cl, 3), 871 (3), 675 (10), 610 (5), 533 (15), 415 (9), 340 (63), 339 (ligand, 100), 307 (14), 261 (6), 176 (12), 154 (51) and 89 (34).

7.8 Cobaloxime complex

7.8.1 (Methyl)(4-pyridylimine-4'-phenylferrocene)cobaloxime

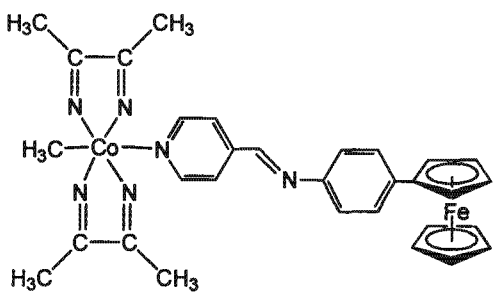

The cobaloxime complex was prepared by a general procedure involving displacement of pyridine from methylpyridinecobaloxime[47]. Dowex 50W-X4 strongly acidic ion-exchange resin (527.6 mg) was added to a solution of methylpyridine-cobaloxime (261.7 mg, 0.82 mmol) in methanol-water 7:1 (80 ml). The mixture was stirred and heated at 50-55 °C for an hour. The orange-red solution was hot-filtered, concentrated and left to crystallise. The orange-red crystals of {Co}(Me)(H_2O) (112.7 mg, 0.44 mmol, 54% yield) were then dehydrated by heating to 60 °C *in vacuo* in order to remove the coordinated water molecule and form the light-sensitive dimer [{Co}(Me)]$_2$ (105.2 mg, 0.44 mmol) as dark red needles. 4-Pyridylimine-4'-phenylferrocene (61.4 mg, 0.17 mmol) was added to a suspension of the dimer (40.0 mg, 0.08 mmol) in dichloromethane (12 ml). The dark red solution was further stirred under nitrogen for 22.6 hours. The reaction mixture was concentrated and hexane added to precipitate the product that was collected *via* vacuum filtration. The product was obtained as small maroon crystalline flakes (67.6 mg, 67%), mp 249-251 °C; (Found: C, 61.48%, H, 5.12, N, 13.52; M^+ 604.14481. $C_{31}H_{33}CoFeN_6$ requires C, 61.6%, H, 5.5, N, 13.9; M^+ 604.42263). ν_{max} (KBr)/ cm^{-1} 3553, 2361, 1685, 1624, 1617, 1576, 1235 and 511; ^{1}H NMR δ_H (300 MHz; solvent $CDCl_3$): 8.73 (2H, d, *J = 6.6 Hz*, C_5H_4N), 8.50 (1H, s, N=CH), 7.78 (2H, d, *J = 6.5 Hz*, C_5H_4N), 7.51 (2H, d, *J = 8.5 Hz*, C_6H_4), 7.20 (2H, d, *J = 8.6 Hz*, C_6H_4), 4.66 (2H, t, *J = 1.8 Hz*, C_5H_4), 4.35 (2H, t, *J = 1.9 Hz*, C_5H_4), 4.05 (5H, s, C_5H_5), 2.14 (12H, s, N=C-CH_3) and 0.86 (3H, s, Co-CH_3); ^{13}C NMR δ_C (75 MHz; solvent $CDCl_3$): 154.17 (N=C), 151.89 (C_5H_4N), 146.01 (C_5H_4N), 143.26 (C_6H_4), 139.05 (C_5H_4N), 127.00 (C_5H_4N), 122.38 (C_5H_4N), 121.48 (C_6H_4), 69.88 (C_5H_5), 69.42 (C_5H_4) and 66.70 (C_5H_4); *m/z* (FAB) 604 (M^+, 2%), 533 (4), 366 (56), 305 (20), 277 (43), 227 (24) and 77 (64).

7.9 Catalytic studies

7.9.1 Polymerisation of phenylacetylene[48,49,32]

A typical polymerisation was carried out in a 2-necked 50 ml round bottom flask. The catalyst (0.02 mmol) was added to a solution of phenylacetylene (0.55 g, 0.60 ml, 5.44 mmol) in methanol (15 ml). The reaction mixture was stirred under N_2 (g) atmosphere at room

temperature (maintained at 25 °C) for 24 hours at atmospheric pressure. During this time a yellow precipitate of polyphenylacetylene was formed. The polyphenylacetylene was collected by vacuum filtration, washed with methanol and dried *in vacuo*. Care was taken not to heat the samples as this resulted in some isomerisation of the polymer. Polymers formed were analysed by NMR and infrared spectroscopy, thermal analysis and gel permeation chromatography.

7.9.2 Carbonylation of nitrobenzene[50,51,52]

A typical experiment was conducted in a 200 ml steel autoclave. The autoclave was fitted with an overhead stirrer, a thermocouple to monitor the reaction temperature internally, pressure gauges to monitor the pressure of the reaction vessel internally and pressure release valves. Hydrogen gas was introduced through an inlet valve and samples were removed through a separate outlet valve. A mixture of the catalyst (0.29 mmol), iron powder (17.0 mmol, 0.949 g), iodine (0.68 mmol, 0.173 g), pyridine (10.54 mmol, 0.83 g, 0.85 ml) and nitrobenzene (0.14 mol, 16.9 g, 14.2 ml) in ethanol (0.55 mol, 32.3 ml) (where ethanol served as both solvent and reagent) was introduced to the reaction vessel under nitrogen. The mixture was initially flushed with carbon monoxide and then heated to either 150 or 180 °C and pressurised to 4 MPa carbon monoxide pressure while stirring vigorously. The reaction was allowed to progress for a total of two hours and monitored by removal of samples at various time intervals as the reaction progressed. Samples were analysed by gas chromatography.

7.9.2.1 Gas chromatography instrument conditions

Analysis of samples was carried out using gas chromatography. Samples were filtered through a 0.4 μm teflon microfilter prior to injection. Gas chromatography was carried out using a Carlo Erba Strumentazione Fractovap 4200 series dual column modular gas chromatograph fitted with a Phenomenex Zebron ZB-1 capillary column (30 m x 0.25 mm x 0.5 μm). Nitrogen was used as carrier gas (1.7 $kg.cm^{-3}$). A flame ionisation detector was used with a hydrogen flow rate of 0.4 $kg.cm^{-3}$. Samples were injected into the column with a split ratio set at 0.17 min^{-1}. The temperature programme was set with an isothermal run at 120 °C for the determination of the carbonylation products with injector and detector temperatures set at 220 and 240 °C respectively. Analysis and identification of these products was carried out by comparison of retention times with commercially available or independently prepared samples as well as by injection of samples containing added standard solutions. Furthermore, quantitative determinations were based on response factors and corresponding peak areas, where the relative response factor for a given product was calculated using *Equation 7.1*.

Relative response factor = Response factor of sample / Response factor of reference [7.1]

7.9.3 Hydrogenation of 1-hexene and cyclohexene

A typical experiment was carried out in a Schlenck tube designed to accommodate pressures slightly above atmospheric. The catalyst (0.02 mmol) was added to a solution of the alkene (1.0 mmol), either cyclohexene or 1-hexene, in dichloromethane (10 ml). Octane (1.0 mmol) was added as an internal standard to aid monitoring of the reaction. Hydrogenation of cyclohexene was conducted in a 250 ml reaction vessel and 1-hexene hydrogenation in a 70 ml reaction vessel. The reaction mixture was degassed by the freeze-thaw method and flushed with hydrogen gas several times to ensure maximal introduction and interaction of reaction mixture with hydrogen gas. The solution was then stirred vigorously at a constant rate under a hydrogen gas atmosphere at atmospheric pressure and room temperature, which was maintained at 24 °C, for a total of 24 hours. The reaction mixture was monitored by removal of samples at various time intervals as the reaction progressed. Samples were analysed with gas chromatography.

7.9.3.1 Gas chromatography instrument conditions

Analysis of the samples was carried out using gas chromatography. Samples were filtered through a 0.4 μm teflon microfilter prior to injection. Gas chromatography was carried out using a Carlo Erba Strumentazione Fractovap 4200 series dual column modular gas chromatograph fitted with a Phenomenex Zebron ZB-1 capillary column (30 m x 0.25 mm x 0.5 μm). Nitrogen was used as carrier gas (1.7 $kg.cm^{-3}$). A flame ionisation detector was used with a hydrogen flow rate of 0.4 $kg.cm^{-3}$. Samples were injected into the column with a split ratio set at 0.17 min^{-1}. The temperature programme was set with an isothermal run at 50 °C for the determination of samples from both 1-hexene and cyclohexene hydrogenations, with injector and detector temperatures set at 220 and 240 °C respectively. Analysis and identification of hydrogenation products was carried out by comparison of retention times with commercially available samples as well as by injection of samples containing added standard solutions. Furthermore, quantitative determinations were based on response factors and corresponding peak areas as described in *Equation 7.1*. In all cases an internal standard, octane was included in order to verify results.

7.10 Biological studies

7.10.1 Cytotoxicity determinations

The cytotoxicity of a range of rhodium, iridium, platinum and palladium complexes was determined. Cell lines used for cytotoxicity determinations included WHCO1, an oesophageal cancer cell line and ME180, a cervical cancer cell line. The cell lines used were prepared in a given media with WHCO1 cells in DMEM (Dulbecco's Modified Eagle Media), 10 % FCS (Foetal Calf Serum, also called Foetal Bovine Serum or FBS) and pen/strep (a mixture of penicillin and streptomycin used to prevent bacterial contamination). ME180 cells were prepared in a media of McCoy's 5A, 5 % FCS and pen/strep.

The plating cells used were rinsed and lifted with trypsin, neutralised with an equal volume of media and counted using a haemocytometer. An appropriate volume of cell suspension was spun down at 10 000 rpm for 5 minutes, supernatant decanted and resuspended at 1 000 cells/ 90 µl. Cells were plated in CellStar 96 well plates, with 90 µl/ well (4 wells for each compound) and incubated at 37 °C in an atmosphere of 95 % air and 5 % CO_2 for a period of 24 hours.

Each compound tested was resuspended in DMSO in a concentration of 25 mg/ml. Dilutions were made several times including a dilution of stock into media (once into DMEM and once into McCoy's 5A). The respective diluted compounds investigated (10 µl) were added to each well of the well plate with final concentrations of 50, 10 and 1 µg/ml respectively, in 0.2 % DMSO followed by addition of 10 µl of 2 % DMSO to each of 4 wells, giving a 0.2 % DMSO final concentration. Cells were then incubated at 37 °C in an atmosphere of 95 % air and 5 % CO_2 for 48 hours.

Cell morphology and number were observed and recorded at 24 and 48 hours respectively. The media present in the wells was then discarded and methanol (100 µl) added to each well and left to stand for 10 minutes in order to fix the cells. The methanol was discarded and crystal violet solution (100 µl), a protein stain, was added to each well and left to stand for 20 minutes before rinsing the wells thoroughly with distilled water. Distilled water was introduced once more to each well and left to stand for an hour before discarding the water and repeating the process.

The plate was read on a multiwell plate reader at 595 nm. Samples were analysed by subtracting the baseline obtained from wells without cells and only containing media and

plotted on a bar chart taking into account solvent control as a reference. The extent of cell death was determined relative to the percentage of solvent control.

7.10.2 Determination of IC_{50} values

WHCO1, the oesophageal cancer cell line, was used for the determination of selected IC_{50} values with a media of DMEM, 10 % FCS and pen/strep. As before, the plating cells were rinsed and lifted with trypsin, neutralised with an equal volume of media and counted using a haemocytometer. An appropriate volume of cell suspension was spun down at 10 000 rpm for 5 minutes, supernatant decanted and resuspended at 1000 cells/ 90 µl. Cells were plated in CellStar 96 well plates, 90 µl/ well (4 wells for each compound), and incubated at 37 °C in an atmosphere of 95 % air and 5 % CO_2 for 24 hours.

The compounds investigated were prepared in a series of 11 dilutions from 1 to 50 µl with a final DMSO concentration of 2 % in media and 0.2 % in each well. The cell morphology and number was observed and recorded and MTT reagent (10 µl) added to each well followed by incubation for 4 hours in a TC incubator. A solubilisation solution (100 µl) was added to each well and the cells incubated overnight. The plate was then read on a multiwell plate reader at 595 nm. Samples were analysed by subtracting the baseline obtained from wells without cells and only containing media, and plotted on a bar chart taking into account solvent control as a reference. The extent of cell death was determined relative to the percentage of solvent control.

References:

1. B. S. Furniss, A. J. Hannaford, P. W. G. Smith and A. R. Tatchell, *Vogel's Textbook of Practical Organic Chemistry*, Longman Scientific and Technical, England (5th edition), 1989.
2. D. D. Perrin and W. L. F. Amarego, *Purification of laboratory chemicals*, Permagon Press, New York (3rd edition), 1988.
3. J. C. Ruble and G. C. Fu, *J. Org. Chem.*, 1996, **61**, 7230; C. E. Garret and G. C. Fu, *J. Am. Chem. Soc.*, 1998, **120**, 7479.
4. *COLLECT*, data collection software, Nonius B. V. Delft, The Netherlands, 2000.
5. Z. Otwinowski and W. Minor in C. W. Carter, J. Sweet and R. M. Sweet (Eds.), *Macromolecular Crystallography Part A*, Academic Press, New York, 1997, vol. **276**, p 307.

6. G. M. Sheldrick, *SHELX97, Programme for Solving Crystal Structures*, University of Göttingen, Germany, 1997.
7. G. M. Sheldrick, *SHELX97, Programme for the Refinement of Crystal Structures*, University of Göttingen, Germany, 1997.
8. M. N. Burnett and C. K. Johnson, *ORTEP-III*, Oak Ridge Thermal Ellipsoid Programme for Crystal Structure Illustrations, Oak Ridge National Laboratory, ORNL-6895, 1996.
9. A. L. Spek, *PLATON*, University of Utrecht, The Netherlands, 1997.
10. L. J. Barbour, *X-Seed*, University of Missouri-Columbia, USA, 1999.
11. R. W. Fish and M. Rosenblum, *J. Org. Chem.*, 1965, **30**, 1253.
12. Y.-H. Han, M. J. Heeg and C. H. Winter, *Organometallics*, 1994, **13**, 3009.
13. J. G. Mason and M. Rosenblum, *J. Am. Chem. Soc.*, 1960, **82**, 4206.
14. B. J. Coe, C. J. Jones, J. A. McCleverty, D. Bloor and G. Cross, *J. Organomet. Chem.*, 1994, **464**, 225.
15. V. Weinmayr, *J. Am. Chem. Soc.*, 1954, **77**, 3012.
16. C. Imrie, C. Loubser, P. Engelbrecht, C. W. McCleland, M. Tolom and V. O. Nyamori, *J. Chem. Soc., Perkin Trans. 1*, 1999, **17**, 2513.
17. T. Lanez and P. L. Pauson, *J. Chem. Soc., Perkin Trans. 1*, 1990, 2417.
18. S. P. Gubin and E. G. Perevalova, *Dokl. Akad. Nauk SSSR*, 1962, **143**, 1351.
19. S. Miyano, N. Abe and A. Abe, *Chem. Pharm. Bull.*, 1970, **18**, 511.
20. C. S. Barnes, E. J. Halbert, R. J. Goldsack and J. G. Wilson, *Aust. J. Chem.*, 1973, **26**, 1031.
21. M. M. Bhadbhade, A. Das, J. C. Jeffery, J. A. McCleverty, J. A. Navas Badiola and M. D. Ward, *J. Chem. Soc., Dalton Trans.*, 1995, 2769.
22. P. D. Beer, O. Kocian and R. J. Mortimer, *J. Chem. Soc., Dalton Trans.*, 1990, 3283.
23. T. M. Miller, K. J. Ahmed and M. S. Wrighton, *Inorg. Chem.*, 1989, **28**, 2347.
24. *Handbook of Grignard Reagents*, Eds. G. S. Silverman and P. E. Rakita, Marcel Dekker Inc., New York, 1996.
25. O. Carugo, G. De Santis, L. Fabbrizzi, M. Licchelli, A. Monichino and P. Pallavicini, *Inorg. Chem.*, 1992, **31**, 765.
26. K. Schlögl and M. Fried, *Monatsh. Chem.*, 1963, **94**, 537.
27. A. N. Nesmeyanov, V. A. Sazonara and A. V. Gerasmento, *Dokt. Akad. Nauk SSSR*, 1962, **147**, 634.
28. W.-Y. Wong, W.-T. Wong and K.-K. Cheung, *J. Chem. Soc., Dalton Trans.*, 1995, 1379.
29. M. D. Rausch and D. J. Ciappenelli, *J. Organomet. Chem.*, 1967, **10**, 127.
30. J. G. P. Delis, P. W. N. M. van Leeuwen, K. Vrieze, N. Veldman, A. L. Spek, J. Fraanje and K. Goubitz, *J. Organomet. Chem.*, 1996, **514**, 125.

31. C. Imrie, P. Engelbrecht, C. Loubser, C. W. McCleland, V. O. Nyamori, R. Bogardi, D. C. Levendis, N. Tolom, J. van Rooyen and N. Williams, *J. Organomet. Chem.*, 2002, **645**, 65.
32. S.-I. Lee, S.-C. Shim and T.-J. Kim, *J. Polym. Sci. Part A: Polym. Chem.*, 1996, **34**, 2377.
33. G. P. Sollot, H. E. Mertwoy, S. Portnoy and J. L. Snead, *J. Org. Chem.*, 1963, **28**, 1090.
34. J. A. McCleverty and G. Wilkinson, *Inorg. Synth.*, 1966, **8**, 211.
35. B. T. Heaton, C. Jacob and J. T. Sampanthar, *J. Chem. Soc., Dalton Trans.*, **1998**, 1403.
36. R. Uson, L. A. Oro, D. Carmona and M. Esteban, *J. Organomet. Chem.*, 1981, **220**, 103.
37. J. Chatt and L. M. Venanzi, *J. Chem. Soc.*, 1957, 4735.
38. P. Fougeroux, B. Denise, R. Bonnaire and G. Pannetier, *J. Organomet. Chem.*, 1973, **60**, 375.
39. R. Uson, L. A. Oro, C. Claver and M. A. Garralda, *J. Organomet. Chem.*, 1976, **105**, 365.
40. K. Tani, T. Mihana, T. Yamagata and T. Saito, *Chem. Lett.*, 1991, 2047.
41. D. W. Bruce, D. A. Dunmur, M. A. Esteruelas, S. E. Hunt, R. Le Lagadec, P. M. Maitlis, J. R. Marsden, E. Sola and J. M. Stacey, *J. Mater. Chem.*, 1991, **1**, 251.
42. P. Kalck, C. Randrianalimanana, M. Ridmy, A. Thorez, H. T. Dieck and J. Ehlers, *New. J. Chem.*, 1988, **12**, 679; B. Longato, G. Pilloni, R. Graziani and U. Casellato, *J. Organomet. Chem.*, 1991, **407**, 369.
43. R. H. Crabtree and G. E. Morris, *J. Organomet. Chem.*, 1977, **135**, 395.
44. G. Zassinovich, G. Mestroni and A. Camus, *J. Organomet. Chem.*, 1975, **91**, 379.
45. A. Kasahara, T. Izumi and M. Maemura, *Bull. Chem. Soc. Jpn.*, 1977, **50**, 1878.
46. C. Tessier and F. D. Rochon, *Inorg. Chim. Acta*, 1999, **295**, 25.
47. P. J. Toscano, T. F. Swider, L. G. Marzilli, N. Bresciani-Pahor and L. Randaccio, *Inorg. Chem.*, 1983, **22**, 3416.
48. F. D. Kleist and N. R. Byrd, *J. Polym. Sci.: Part A-1*, 1969, **7**, 3419.
49. C. I. Simionescu, V. Percec and S. Dumitrescu, *J. Polym. Sci.: Polym. Chem. Ed.*, 1977, **15**, 2497.
50. J. Skupińska, G. Smółka, W. Kaźmierowicz and J. Ilmużyńska, *React. Kinet. Catal. Lett.*, 1995, **54**, 59.
51. F. Ragaini and S. Cenini, *J. Mol. Cat. A: Chemical*, 1996, **109**, 1.
52. J. Skupińska and M. Karpińska, *J. Mol. Cat. A: Chemical*, 2000, **161**, 69.

Appendices

X-ray crystallographic data is provided in the form of structure factor tables and tables of data on diskette,

- Appendix 1 – X-ray data for complex **[3.6]**
- Appendix 2 – X-ray data for complex **[3.15]**
- Appendix 3 – X-ray data for complex **[3.16]**
- Appendix 4 – X-ray data for complex **[3.44]**

Acknowledgements

I would like to thank the following for their contributions to this thesis,

⌘ Professor John R. Moss, Dr Christopher Imrie and Associate Professor Alan T. Hutton for their support, advice and encouragement throughout this project.

⌘ The National Research Foundation, University of Cape Town and University of Port Elizabeth for funding this project.

⌘ The technical staff at both the Universities of Cape Town and Port Elizabeth, in particular Mr H. Marchant (UPE), Mr K. Achleitner, Mr P. Benincasa, Mrs D. Brooks, Mr N. Hendricks, Mr G. Hesselink and Mr P. Roberts (UCT).

⌘ Dr Hong Su for the X-ray crystal structures, Dr D. Hendricks for the biological assays and Dr P. Boshoff for the mass spectrometry.

⌘ My colleagues at UCT and UPE, both past and present: Ms. S. Baird, Mr E. R. T. Elago, Dr P. Engelbrecht and Mr V. O. Nyamori (UPE) and Dr P. Beagley, Dr M. Blackie, Dr M. Haumann, Ms C. Lawrence, Dr R. Meijboom, Mr M. E. Ndlovu and Mr M. Overett (UCT). Special thanks go to Dr Haumann for help with the autoclave, to Drs Beagley and Meijboom for proof reading parts of this thesis.

⌘ My family (my mother, Hansa, my sisters Sharmila and Prishana) and friends for their constant love, support and above-all, encouragement. This thesis is dedicated to you – you don't have to read this one.

⌘ God for making all things possible.